Johanna Flock

Redox-Active Pyridine Ligand Systems and Their Versatile Application in Low Valent Main Group Chemistry

DISSERTATION

zur Erlangung des akademischen Grades einer

Doktorin der technischen Wissenschaften

eingereicht an der

Technischen Universität Graz

Betreuer: DI Dr. techn. Assoc. Prof. Roland Fischer
Institut für Anorganische Chemie

Graz, April 2014

Eidesstattliche Erklärung

Ich erkläre an Eides statt, dass ich die vorliegende Arbeit selbständig verfasst, andere als die angegebenen Quellen/Hilfsmittel nicht benutzt, und die den benutzten Quellen wörtlich und inhaltlich entnommenen Stellen als solche kentlich gemacht habe.

Graz, am..... .....

(Unterschrift)

Statutory Declaration

I declare that I have authored this thesis independently, that I have not used other than the declared sources/resources, and that I have explicitly marked all material which has been quoted either literally or by content from the used sources.

....

date (signature)

Danksagung

An dieser Stelle möchte ich all jenen danken, die mich bei der Erstellung dieser Dissertation sehr unterstützt haben.
Roland Fischer danke ich herzlich für die Betreuung meiner Dissertation, sowie den stetigen Anregungen und der Möglichkeit, frei und selbständig zu arbeiten. Dieses Vertrauen hat mich stets motiviert und zum Gelingen dieser Arbeit sehr beigetragen.
Großer Dank gilt Michaela Flock, die mir immer mit Rat und Tat zur Seite stand und mich in den richtigen Momenten motiviert und mir dadurch großen Mut verschafft hat. Frank Uhlig danke ich für die Möglichkeit am Institut zu arbeiten, für das Vertrauen und jegliche Unterstützung bei Weiterbildungen und Forschungsaufenthalten.
Weiters will ich Michal Zalibera für die gute Zusammenarbeit bei den ESR Messungen danken, als auch Michaela Flock für die theoretischen Berechnungen, Monika Filzwieser für die Elementaranalyse und Astrid Falk und Barbara Seibt für jegliche Hilfe am Institut. Bei meinen Kolleginnen Stefan Müller, Melanie Wolf, Patricia Handel und Petra Wilfling möchte ich mich herzlich für die Geduld, die offenen Ohren und die Aufmunterungen bedanken.
Mein besonderer Dank gilt meiner Familie, die immer an mich geglaubt hat. Meinen lieben Freunden will ich für die lustigen Zeiten und die lieben Gespräche vielmals danken.
Schließlich und keineswegs zuletzt will ich meinem Verlobten Markus Guldenschuh herzlichst danken. Er stand mir immer zur Seite, hat immer an mich geglaubt und fand immer die richtigen aufmunternden warmen Worte, die mich motivierten und ermutigten. Vielen lieben Dank für deine vorbehaltlose Unterstützung, dein Dasein und deine Liebe!

Johanna Flock
Graz, April 2014

Abstract

Stabilizing reactive metal centers is a promising field in main group chemistry. Highly reactive main group elements provide remarkable properties regarding their reactivity and catalytic behaviors. The ligand design is decisive for the synthetic strategy, the stabilization of the metal center and the reactivity of the complexes. Redox-active pyridine ligand systems gain more and more attention in modern coordination chemistry. However in main group chemistry, these ligand systems are less investigated. In this PhD thesis, the redox-active diiminopyridine ligand 2,6-[ArN=CH]$_2$(NC_5H_3) (Ar= Dipp) (DIMPY) and the single armed iminopyridine ligand 2-[ArN=CH](NC_5H_4) (Ar= Dipp) (SIMPY) are studied regarding their ability to form radical anions while reacting them with alkali metals. Furthermore, it is proven that these ligand systems, as well as their saturated amine analogs, provide highly interesting coordination modes towards heavier group 14 elements in low oxidation states. Also a P homolog of the SIMPY ligand system was prepared to stabilize low valent group 14 elements. The stabilization by this kind of P-based ligands is barely known for group 14 elements. Their coordination behavior should differ compared to the imino relatives and represents novel aspects in main group chemistry. Examples of Ge and Sn compounds stabilized by 2,6-[ArN=CH]$_2$(NC_5H_3) (Ar= Dipp) were synthesized, which formally possess an oxidation state of zero. Synthesizing and investigating these species give a new insight in the astonishing field of low oxidation state main group chemistry.

Kurzfassung

Die Stabilisierung von reaktiven Metallzentren ist ein vielversprechendes Thema in der Hauptgruppenelementchemie, da reaktive Hauptgruppenelemente bisher unbekannte katalytische Fähigkeiten aufweisen. Das stabilisierende Ligandensystem ist ausschlaggebend für die Synthese, Stabilität und Reaktivität der Hauptgruppenelementkomplexe. Redox-aktive Pyridinliganden erhalten in der modernen Koordinationschemie immer mehr Aufmerksamkeit, sind jedoch in Bezug auf die Stabilisierung von Hauptgruppenelementen kaum erforscht. In dieser Doktorarbeit werden die Fähigkeiten des Diiminopyridinliganden, 2,6-$[ArN{=}CH]_2(NC_5H_3)$ (Ar= Dipp) (DIMPY), und des Iminopyridinliganden, 2-$[ArN{=}CH](NC_5H_4)$ (Ar= Dipp) (SIMPY), in Bezug auf die Bildung von Radikalanionen mit Alkalimetallen erforscht. Des Weiteren werden diese Ligandensysteme, als auch deren gesättigte aminoanalogen und P-analogen Systeme eingesetzt, um reaktive höhere Gruppe 14 Elemente in niederen Oxidationsstufen zu stabilisieren. Gruppe 14 Elemente in niederen Oxidationsstufen haben die erstaunliche Eigenschaft kleine Moleküle, wie H_2, NH_3, P_4 und Olefine, zu aktivieren und sich somit wie ein Übergangsmetallkomplex zu verhalten. Höchst interessante Ge und Sn Verbindungen wurden erhalten, in denen das Gruppe 14 Element in der Oxidationsstufe 0 stabilisiert wurde. Die Erforschung der Eigenschaften dieser seltenen Ge^0 und Sn^0 Komplexe ermöglichen neue Einblicke in das spannende Feld der Hauptgruppenelementchemie.

Contents

List of Abbreviations

bp	Boiling Point
CV	Cyclic Voltammogram
d	Density
DAMPY	Diaminopyridine Ligand, 2,6-[ArN-CH_2]$_2$(NC_5H_3) (Ar= Dipp)
DFT	Density Functional Theory
DIMPY	Diiminopyridine Ligand, 2,6-[ArN=CH]$_2$(NC_5H_3) (Ar= Dipp)
Dipp	Diisopropylphenyl substituent
EPR	Electron Paramagnetic Resonance
HOMO	Highest Occupied Molecular Orbital
IR	Infrared
LUMO	Lowest Unoccupied Molecular Orbital
MeDIMPY	Methyl substituted Diiminopyridine Ligand, 2,6-[ArN=CMe]$_2$(NC_5H_3) (Ar= Dipp)
Mes*	2,4,6-Tri-*tert*-butylphenyl substituent
mp	Melting Point
MW	Molecular Weight
NHC	N-heterocyclic Carbene
NMR	Nuclear Magnetic Resonance
PA	Proton Affinities
PAPY	Phosphaalkenepyridine Ligand, 2-[ArP=CH](NC_5H_4) (Ar= Mes*)
RT	Room Temperature
SAMPY	Singleaminopyridine Ligand, 2-[ArN-CH_2](NC_5H_4) (Ar= Dipp)
SIMPY	Singleiminopyridine Ligand, 2-[ArN=CH](NC_5H_4) (Ar= Dipp)
UV	Ultra Violett

Chapter 1

Introduction

Pyridine ligand systems, especially those bearing imino functionalities, are known to be redox active and non-innocent compounds.[1–3] In transition metal chemistry, the diimino pyridine ligand system 2,6-[ArN=C(H or Me)]$_2$(NC_5H_3) coordinates metal centers and the resulting complexes show great ability in olefin polymerization or as Ziegler-Natta catalysts.[1–10] Recently, also main group derivatives were synthesized as well as lanthanide complexes representing the chemical non innocence of the ligand system.[11–13] Thereby alkylating the ligand system 2,6-[ArN=CMe]$_2$(NC_5H_3) (Ar= Dipp) (MeDIMPY) with for example Me_3Al leads to alkylations at the imino functionality and at all positions of the pyridine ring.[14–16] Further reactions involve the enamine formation of the methyl group or dimerization via C-C bond formation at the backbone of the ligand system.[11,13,17] Recently, also the radical anions of these ligand systems were studied, mainly for 2-[ArN=CH](NC_5H_4) (Ar= Dipp) (SIMPY).[18–25] This PhD thesis presents the versatile application of the imino pyridine ligand systems as well as their saturated amine analogs to form rare and highly interesting complexes with group 1 and 14 elements .

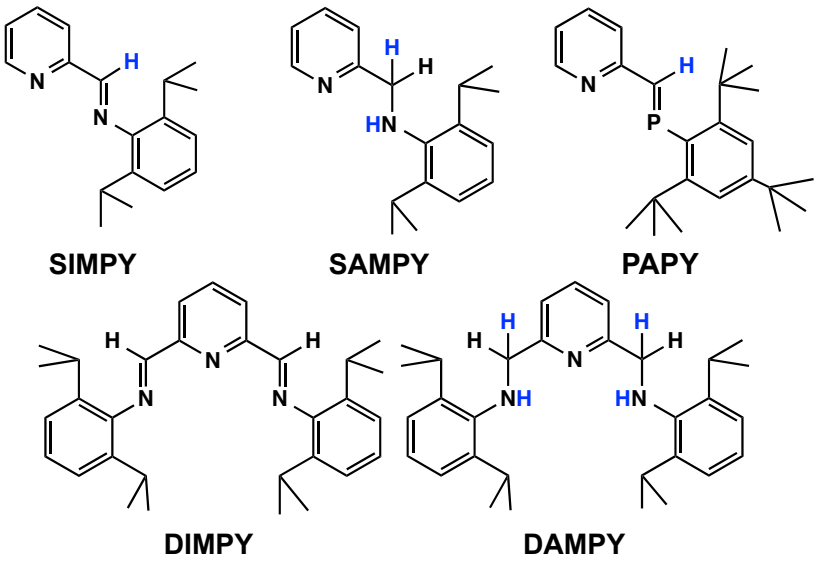

Figure 1.1: Pyridine ligand system used in this PhD thesis to stabilize reactive metal centers. The blue colored hydrogen atoms at the ligand backbone or at the amino functionality are eliminated by reactants to form unusual and highly interesting low valent group 14 complexes, even in the oxidation state of zero.

Part of this PhD thesis focuses on the ability of the α-imino pyridine ligand systems SIMPY, 2-[ArN=CH](NC_5H_4) (Ar= Dipp), and DIMPY, 2,6-[ArN=CH]$_2$(NC_5H_3) (Ar= Dipp) to form monoanionic salts while reacting it with alkali metals (Li - Cs). These monoanionic species are studied regarding the delocalization of the radical at the ligand center. Furthermore, the influence of the alkali metal (Li - Cs) towards the radical center is observed via EPR and solid state structure analysis and supported by DFT calculations.

The main work focuses on the synthesis of low valent group 14 complexes. Therefore, the diimino and monoimino pyridine ligand systems 2,6-[ArN=CH]$_2$(NC_5H_3) (Ar= Dipp) (DIMPY) and 2-[ArN=CH](NC_5H_4) (Ar= Dipp) (SIMPY) were synthesized as well as their saturated amine analogs (as shown in Figure 1.1). Apart of the big chapter of imino and amino pyridine ligand systems, also phosphaalkene derivatives are studied. The monophosphaalkene ligand system 2-[ArP=CH](NC_5H_4) (Ar= Mes*) (PAPY) is reacted with group 14 elements. Compared to the imino congener, the phosphaalkene pyridine ligand system shows a completely different reaction behavior. Thereby, a very rare example of a stannylstannylene $RSn^{I}Sn^{III}PAPY_2R$ (R=$N(SiMe_3)_2$) species was isolated. For the aminopyridine ligand systems as

well as the SIMPY ligand, a new phenomenon is studied regarding their reaction behavior to eliminate the H atom at the ligand backbone. This new phenomenon provides interesting low valent group 14 complexes, even in the oxidation state of zero which have been inaccessible up to this point.

Low valent main group compounds are coordinatively unsaturated species and therefore extremely reactive.[26,27] In literature, these complexes are known to mimic transition metal centers.[28,29] Group 14 elements in the oxidation state +2, owing to their singlet ground state, possess a lone pair of electrons which acts as twofold σ donor and a vacant π orbital which acts as a π acceptor. Therefore, they can activate small molecules as for example H_2, NH_3 and C_2H_4 under mild conditions and show a catalytic potential for future applications.[28,29] The reactivity of group 14 elements in the formal oxidation state of zero is not studied yet. Due to the fact that E^0 species possess two lone pairs of electrons, they formally act only as σ donors (as shown in Figure 1.2). Therefore, the reactivity compared to oxidation state +2 compounds should differ. These species can be compared to transition metals coordinated either in 16 electron or 18 electron complexes. In transition metal chemistry $16e^-$ and $18e^-$ compounds differ regarding their catalytic behavior. Synthesizing and investigating unprecedented low valent group 14 compounds, particularly E^0 species and their reaction behavior, has an important impact in understanding low valent main group chemistry.

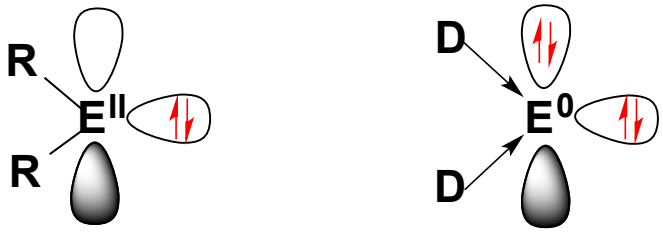

Figure 1.2: A simple consideration comparing E^{II} and E^0 compounds: Low valent group 14 complexes in the oxidation state of +2 (left) possess two electrons in the σ orbital and two electrons in the vacant π orbital (singlet state). For E^0 species the ligand system is only donating and therefore two lone pairs are formed. (right)

In this PhD thesis, the versatile reactivity of pyridine ligand systems involving imino, amino and phosphaalkene functionalities towards group 1 and 14 elements is studied. The low valency of main group 14 elements provides high reactivity. Diverse electronical and structural properties are observed for these metal centers depending on the ligand design and their properties. Investigations of redox-active ligand systems complexing group 14 elements lead to unusual bonding motifs. These unexpected reactions give new insights in low valent main group chemistry.

Chapter 2

Literature

2.1 Redox-active Pyridine Ligand Systems

The term 'redox-active' describes a well defined redox process taking place at the ligand center itself.[1] The increasing interest for such redox-active ligand systems can be explained by the fact that these multifunctional ligands have a significant impact in catalytic reactions of transition metals.[1–4] Diiminopyridine ligand systems, for example, can accept or donate negative charge to the coordinated metal. The DIMPY ligand system was studied regarding it's redox potential which ranges depending on the substituent at the backbone of the ligand system.[30] A series of differently substituted DIMPY ligands exhibit a reversible reduction ranging from -2.35 to -2.83 V.[30] Thereby, a fine-tuning of the redox potential of the metal center and it's Lewis acidity is possible, which determines the catalytic behavior of the transition metal complex.[16,31]

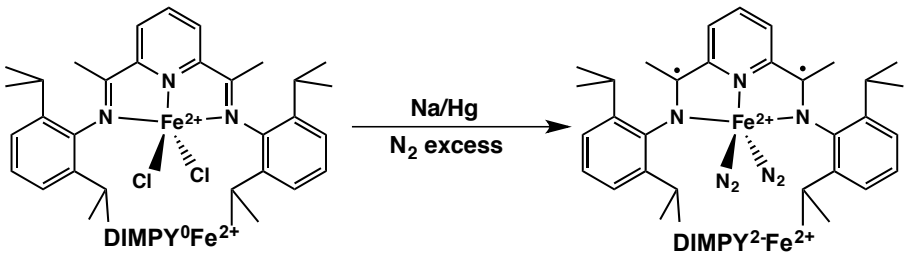

Figure 2.1: A highly reactive precatalyst is formed by the reduction of the $DIMPY^{0}Fe^{2+}Cl_2$ complex in presence of dinitrogen and Na/Hg.[2,8]

An example of a reactive precatalyst is shown in Figure 2.1. Various iron and cobalt catalysts that effect multi-electron redox chemistry were synthesized and investigated recently.[2,4,8] This is possible due to the presence of the redox-active diiminopyridine ligand DIMPY. The diiminopyridine ligand DIMPY participates in the redox reactions, which enables the metal to mediate multiple electron processes.[2,8,32–34] The di(dinitrogen) precatalyst [DIMPY^{2-}Fe^{2+}(N$_2$)$_2$] is formed reducing the iron^{II} complex [DIMPY^{0}Fe^{2+}Cl$_2$] in presence of dinitrogen with sodium amalgam (Figure 2.1). Versatile organic transformations catalyzed by [DIMPY^{2-}Fe^{2+}(N$_2$)$_2$] were studied, namely [2+2] cycloaddition reaction, olefin isomerization and hydrosilylation of unfunctionalized alkenes.[2,32,34] The chemical non innocence of the DIMPY ligand system was further proven by the reaction with lanthanide metals.[4,13] The MeDIMPY ligand was reacted with a lanthanide tetramethylaluminates [Ln(AlMe$_4$)$_3$] complex, yielding organolanthanide imino–amido–pyridine complexes due to alkane elimination processes.[13]

2.1.1 The DIMPY Ligand Coordinating Main Group Elements

The redox-activity of the DIMPY ligand system was employed in main group chemistry for alkali and alkaline earth metals and mainly group 13 elements.[4] Various reaction were investigated for the MeDIMPY ligand and transition to an enamine based ligand system.[4]

Figure 2.2 shows the MeDIMPY ligand reacting with for example MeLi, LiCH$_2$SiMe$_3$ or Li metal in polar solvents. The reaction with MeLi leads to an alkylation of the pyridenyl functionality (Me$_3$DIMPYLi(Et$_2$O)), and - by warming up to room temperature - a mixed methyl/enamine ligand system coordinating the lithium metal is formed. Another interesting reaction is the synthesis of a MeDIMPYLi$_3$ trianion. However, the reaction does not only afford MeDIMPYLi$_3$; another ligand featuring an enamine functionality could be isolated.[31] Further reactions with magnesium alkyls with MeDIMPY were studied, resulting in similar alkylations at the pyridine ring system.[12] The alkylation reactions at the pyridine ring systems were also intensively studied for the reaction with R$_3$Al reagents.[4,14,15] Interestingly, a convenient way to synthesize diamino pyridine ligands was found through selective alkylation of MeDIMPY by AlMe$_3$ followed by hydrolysis.[35]

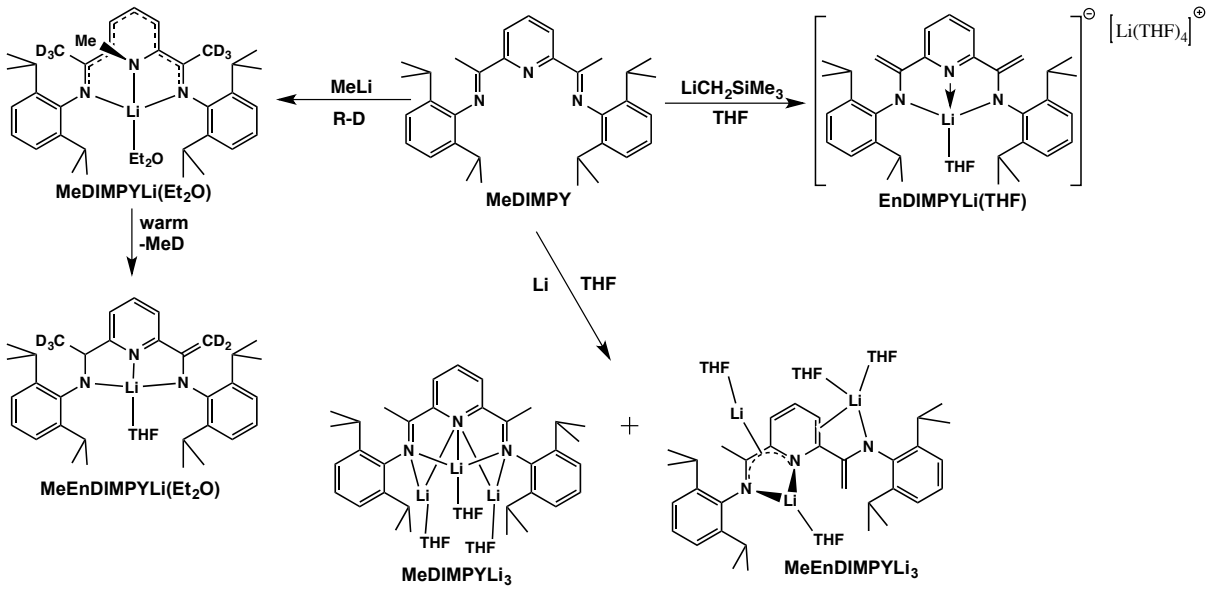

Figure 2.2: The MeDIMPY ligand reacts with numerous alkali reagents to give unusual enamine ligand based systems. This enamine formation proves the chemical non/innocence of the diiminopyridine ligand MeDIMPY.[4]

Ragogna and coworkers proved that the substitution at the ligand backbone of diiminopridine ligands matters regarding the coordination mode towards the element center.[36] The reaction of PI_3 with MeDIMPY gives a complex mixture of products involving enamine tautomers. Reacting PI_3 with -H or -Ph substituted DIMPY ligands leads to $RDIMPYP^+$ cations (R= H, Ph).[36] Further highly reactive DIMPY main group element complexes in low oxidation states were synthesized which are exclusively cationic and isoelectronic to the $RDIMPYP^+$ cations.[17,37–39,39,40] For example, $DIMPYAs^+$ cation,[37] the $DIMPYIn^+$ cation[39] and $DIMPYCh^{2+}$ dications[38] (Ch= S^{2+}, Se^{2+}, and Te^{2+})[41] were isolated.

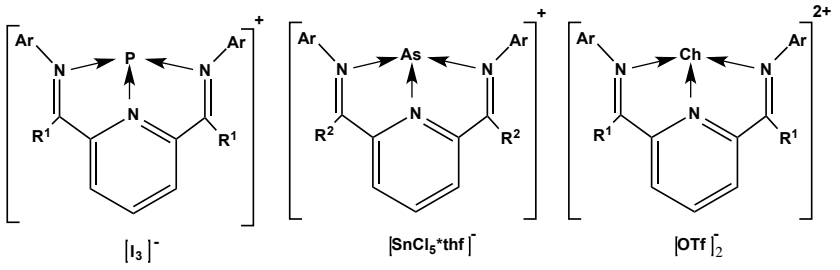

Figure 2.3: DIMPY main group element complexes are mainly cationic.[36–38]

Recently, a dianionic PhDIMPY^{2-}AlH complex was synthesized reacting the PhDIMPY complex with a "$AlCl_2H$" solution.[42] This aluminum complex reacts with anilines to give the N-H-activated products (PhDIMPYH$^-$)AlH-(NHAr). Heating the N-H activated product releases H_2 and affords an (MeDIMPY$^-$)Al(NHAr) as shown in Figure 2.4.[42] This interesting finding proves the redox-activity of the DIMPY ligand system as well as addition reactions which are usually known for transition metal complexes and now are also observed for main group elements. Examples for Group 14 ele-

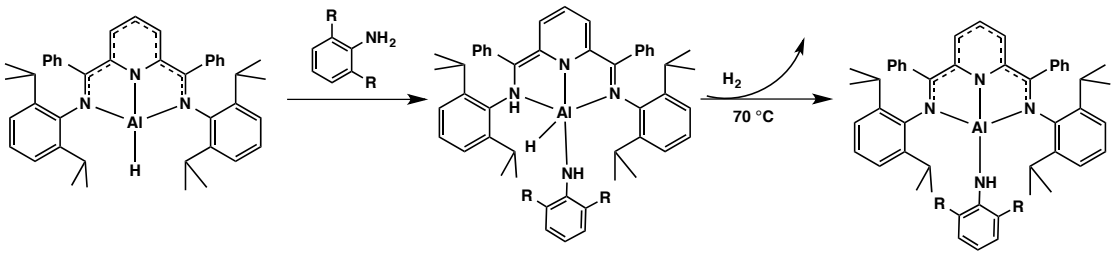

Figure 2.4: The dianionic (PhDIMPY^{2-})AlH complex reacts with anilines to give the N-H-activated products. After heating the reaction solution, H_2 is released.[42]

ments are the Sn^{II} and Pb^{II} complexes coordinated by a pentadentate DIMPY bishydrazine ligand[43] and the [MeDIMPYSn^{II}Cl]$^+$ cation stabilized by (2,6-[ArN=C(Me)]$_2$(NC_5H_3) (Ar= C_6H_3-2,6-^{i}Pr$_2$).[40]

2.1.2 The SIMPY Ligand

The SIMPY ligand system (N-2,6-diisopropyl-phenylimino-2-pyridine) can be assigned to α,α'-diimines due to their conjugated NCCN fragment. α,α'-diimines are well known in literature to coordinate transition metals, as well as main group elements and lanthanides.[24,44–46] Thereby, they provide unusual reactivity as well as unique structural motives. While the SIMPY ligands were initially used in the neutral state as ligands for late transition metals,[47–50] recent studies focused on their application as radical anions and dianions. The SIMPY ligand system can address three different redox states and shows therefore versatile coordination and redox properties.[25]

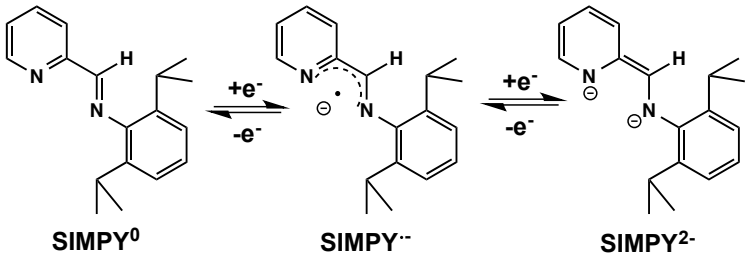

Figure 2.5: The SIMPY ligand system can address three different oxidation states.[25]

The electrochemical properties of the SIMPY ligand were determined using cyclic voltammetry and a reversible one electron reduction process at 2.57 V was observed.[25] The SIMPY ligand is able to react with moderately Lewis acidic ions such as alkali and alkaline earth metals,[25,51,52] highly electrophilic main group element ions (Al^{III}, Ga^{III}),[18–21] first row transition metal ions (Cr, Mn, Fe, Co, Ni, and Zn)[22,23,53] and lanthanides[24,54–56] and form monoanionic or dianionic salts. The reaction of (e.g.) the ytterbocene $(C_5H_4Me)_2Yb(THF)$ with two equivalents of SIMPY forms the Yb^{III} complex $[Yb^{III}(C_5H_4Me)2,6^{i}PrC_6H_3NCH(C_5H_4N)\bullet^{-}]_2$ containing two radical anions.[56] Further investigations of the reaction of $(\eta5\text{-}C_9H_7)_2Yb^{II}(THF)_2$ with a series of α-iminopyridines showed that the redox chemistry of the obtained complexes can be controlled sterically with no change of the metal oxidation state.[54] The reaction of first row transition metal dichloride precursors (Cr, Mn, Fe, Co, and Zn) with two equivalents of SIMPY and two equivalents Na gave neutral complexes bearing a divalent metal center and two monoanionic π

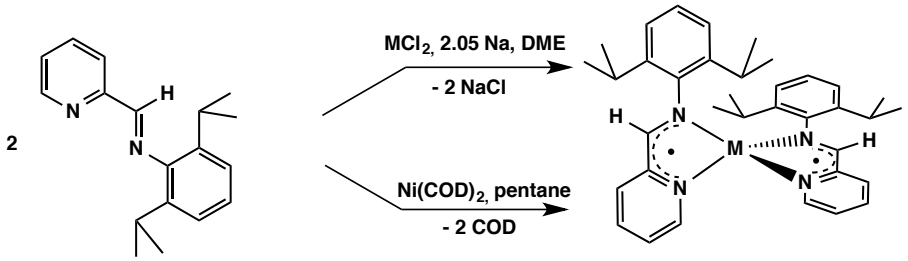

Figure 2.6: The synthesis of SIMPY radical anions with 1st row transition metals: Corresponding dichloride precursors were reduced in presence of sodium metal yielding a divalent metal center coordinated by two monoanionic radicals.[23]

radicals of the SIMPY ligand.[23] Further studies concentrated on the Electron Paramagnetic Resonance (EPR) and Electron Nuclear Double Resonance (ENDOR) of the neutral complex $Zn^{2+}(SIMPY\bullet^{-})_2$ and its monocationic analog $[ZnSIMPY(SIMPY\bullet)*THF]^{+}$ in comparison with DFT calculations.[22] Berben and her working group investigated that redox processes similar to those of transition metals are also achievable for Al^{III} and Ga^{III} ions via the reaction with these electrophilic metal centers with the SIMPY ligand. In case of Al^{III}, the neutral complex $SIMPYAlCl_3$, the monoanionic $(SIMPY\bullet^{-})_2AlX$ (X= Cl, CF_3SO_3) and the dianionic $[(SIMPY^{-})_2Al]^{-}$ were isolated and their electronic and magnetic properties were studied.[18] [2] In contrast to aluminum, the $(SIMPY\bullet^{-})_2GaX$ (X= Cl, OH, TEMPO) and $[(SIMPY^{-})_2Ga]^{-}$ can be transferred only via an overall two electron process.[21] Recently, also the reactions of SIMPY with Na and K were studied.[25] The alkali metals were reacted with SIMPY (1:1 or 2:1) to give either dimeric π radical monoanionic potassium salts $[K(sol)_2SIMPY_2]$ (sol= THF, Et_2O) or the doubly reduced $[Na_4(Et_2O)_4(SIMPY)_2]$ complex. Interestingly, it was not possible to isolate the dianionic $SIMPY^{2-}$ in case of K and the monoanionic complex in case of Na.

Neutral SIMPY complexes with main group elements are less investigated. An example of a group 14 SIMPY derivative is the reaction of a MeOSIMPY ligand [2-[MeC=N(C_6H_3-2,6-$^{i}Pr_2$)]-6-(MeO)C_6H_3N] with Ge and Sn halogenides.[57] The addition of $SnCl_2$ and $GeCl_2$ afforded the ionic $[MeOSIMPYGe^{II}Cl]^{+}[Ge^{II}Cl_3]^{-}$ and $[MeOSIMPYSn^{II}Cl]+[Sn^{II}Cl_3]^{-}$ complexes, respectively, as the result of spontaneous dissociation of ECl_2 (E = Ge, Sn). The treatment of the ligand MeOSIMPY with $GeCl_4$ and $SnBr_4$ gives the $Ge^{IV}$and

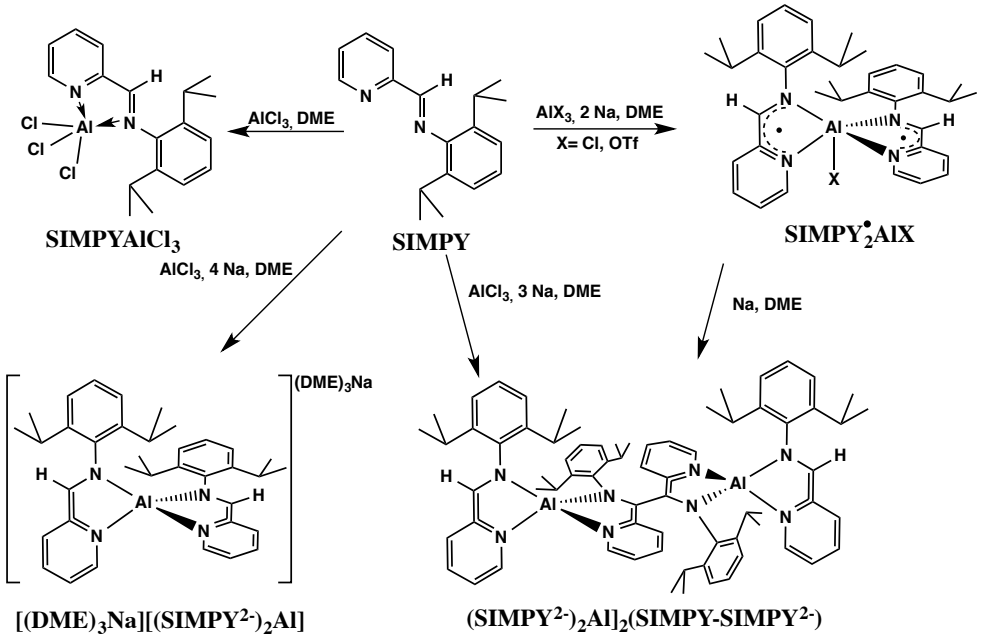

Figure 2.7: The synthesis of SIMPY radical anions with aluminum: Depending on the amount of Na, different SIMPY aluminum complexes are obtained. The redox-activity is shown in case of the special arrangement of a dimeric aluminum complex via C-C coupling[18]

Sn^{IV} complexes MeOSIMPYGeCl_4 and MeOSIMPYSnBr_4, respectively, and no dissociation processes were observed.[57] Berben and coworkers synthesized a related $SIMPY_2Si$ complex where the silicon atom is in the oxidation state of +4.[52] Further reactions with N-tert-butyl pyridine-2-aldimines were studied.[58] The ligand system 6-methyl-2-iminopyridine was reacted with two equiva-

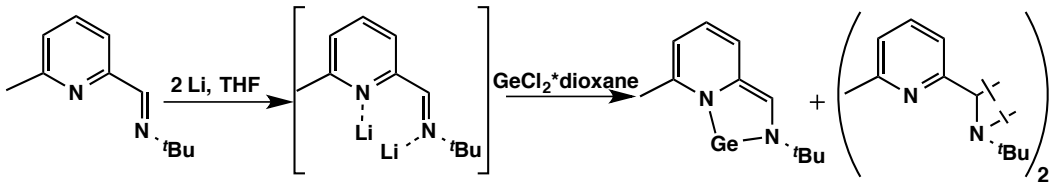

Figure 2.8: The related SIMPY 6-methyl-2-iminopyridine was first reacted with Li metal, then with $GeCl_2$ dioxane to give a germylene, which is only stable at low temperatures. The byproduct is formed due to decomposition of the germylene.[58]

lents of Li metal under subsequent addition of $SiCl_4$, $GeCl_2$*dioxane and $SnCl_2$ at low temperatures of -20°C.[58] The desired low valent Si and Sn complexes were not obtained and the low valent Ge complex was only stable at lower temperatures. Byproducts were isolated, where CH activation occurred. The

CH activation leads to C-C bond formations between two ligands, and dimers are formed. This also happens in case of the reaction of SIMPY with "GaI" or Me_3Al species.[17,18] Gudat and his working group synthesized a $SIMPYP^+$ cation by reacting the SIMPY ligand with PI_3.[59]

2.1.3 The Aminopyridine Ligand Systems

The DAMPY ligand is an extremely rigid, tridentate diamide ligand system which is built by a neutral pyridine donor between two amide functionalities. The SAMPY ligand is a bidentate ligand with one amide functionality in contrast to DAMPY. These ligands have a quite different electronic and steric environment compared to iminopyridine ligand systems.[13] These differences are based on the fact that iminopyridine ligand systems are neutral donors and aminopyridine ligands are anionic and therefore negatively charged. The DAMPY ligand system (2,6-$[ArN\text{-}CH_2]_2(NC_5H_3)$ (Ar = C_6H_3-2,6-$^i Pr_2$)) was involved in transition metal chemistry isolating $DAMPYZrR_2$ (R= Me, Cl, NMe_2, CH_2Ph, C_4H_6)[60,61] complexes, Ti^{IV} compounds[62] and Th complexes.[63]

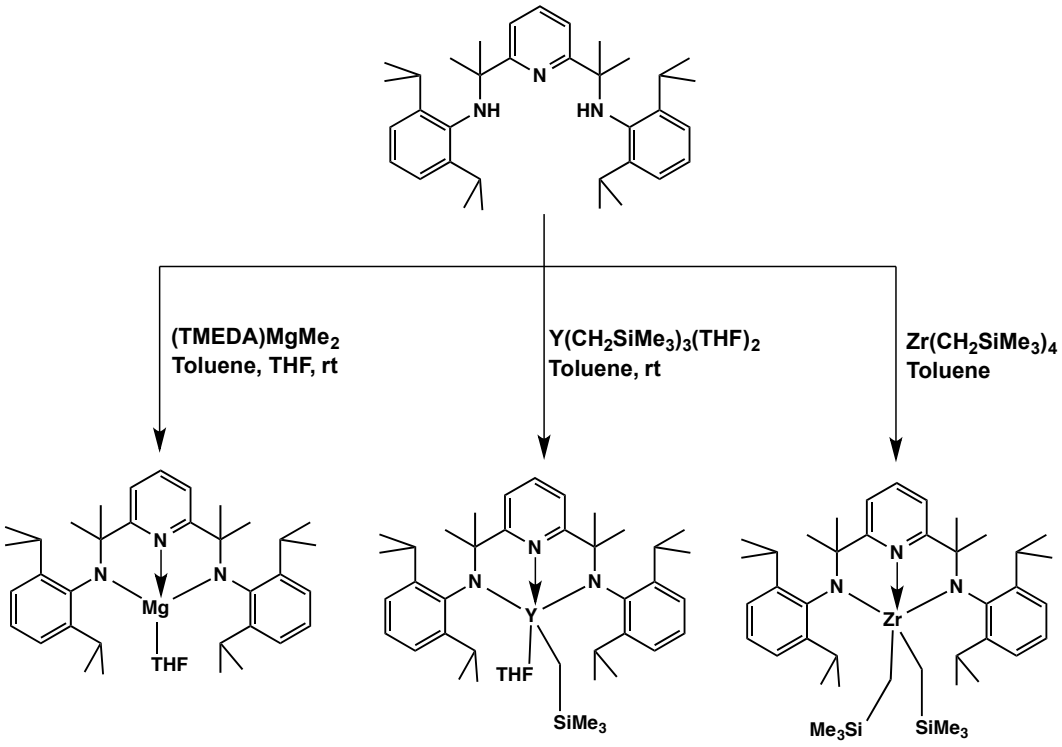

Figure 2.9: The synthesis of DAMPY Mg, Y and Zr complexes.[35]

Other examples of related DAMPY compounds are shown in Figure 2.9. This DAMPY ligand system was synthesized via the reaction of the corresponding DIMPY ligand system with $AlMe_3$ followed by hydrolysis.[35] The obtained DAMPY ligand was then reacted with metal alkyls by alkane elimination and gave the desired magnesium, yttrium and zirconium complexes.[35] A new class of complex mixed ligand systems with imino amido functionalities coordinates lanthanide metals have also been synthesized.[13] Further related ligands are the tetraamines, which form heavier benzannulated N-heterocyclic bisgermylenes, bisstannylenes or bisplumbylenes.[64,65]

For the SAMPY ligand system various Zr, Hf and Al complexes were synthesized.[66] Treatment of the corresponding iminopyridine ligands with $AlMe_3$ followed by hydrolysis yielded a series of substituted SAMPY derivatives. Reacting these ligands with tetrabenzylzirconium or tetrakis(dimethylamido)zirconium or -hafnium gave the corresponding transition metal complexes.[66] Recently, related SAMPY nickel complexes were synthesized which can catalyze ethylene polymerization under moderate pressure and ambient temperature.[67] Effective catalyst precursors for ethylene polymerization are also a series of (arylimido)vanadium(V) dichloride complexes containing (2-anilidomethyl)pyridine ligands of the type $V(NAr)Cl_2[2\text{-}(ArN)CH_2(C_5H_4N)]$ [Ar=2,6-$Me_2C_6H_3$).[68] Westerhausen and coworkers synthesized magnesium, tin and zinc complexes with the related SAMPY ligands (2-pyridylmethyl)(trialkylsilyl)amines.[51] Further addition of dimethylzinc to a toluene solution of the methylzinc (2-pyridylmethyl)(triisopropylsilyl)-amide at raised temperatures yields the C-C coupling product [1,2-dipyridyl-1,2-bis(triisopropylsilylamido)ethane]-bis(methylzinc). Further C-C cou-

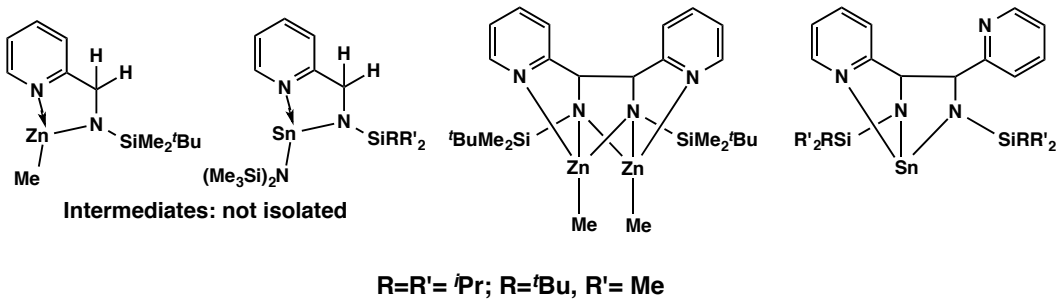

Figure 2.10: The synthesis of Sn and Zn complexes and their unexpected C-C coupling products.[51]

plings of Zn halide complexes and Sn complexes were studied.[51] The transamination reaction of (2-pyridylmethyl)(trimethylsilyl)amine with tin^{II}bis[bis(trimethylsilyl)amide] gives the [bis(trimethylsilyl)amido]tin^{II} (2-pyridylmethyl)(triisopropylsilyl)amide complex. Again a C-C coupling product is formed due to elimination of tin metal and elimination of hexamethyldisilazane.[51]

2.1.4 The Phosphaethenyl Pyridine Ligand System (PAPY)

The reactivity of imino based ligand systems differs compared to phosphaalkene based ligand systems. The major differences can be explained by three effects.[69] Phosphorus is reluctant to give sp and sp^2 hybridization. This is caused by the weak overlap of 3s and 3p atomic orbitals on the phosphorus atom. In classical sp^2 N=C based systems, the angle between RN=C is 120°, in contrast to RP=C around 100°.

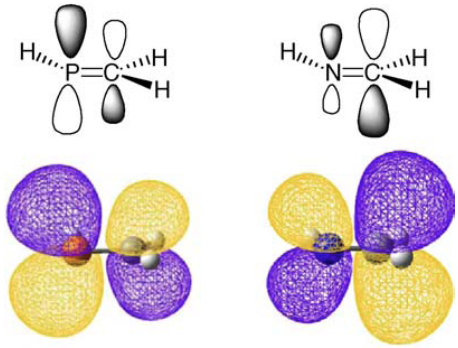

Figure 2.11: A comparison between the LUMOs of $HPCH_2$ and $HNCH_2$ illustrating the accepting capacity of low coordinate phosphorus ligands.[69]

The second major effect is the electronegativity difference in the of N=C and P=C-based systems. Phosphorus (2.1) is more electropositive than nitrogen (3.0) according to the Pauling scale. Therefore, the donor properties of N alkene based ligand systems are stronger than in case of P based alkene ligand systems. A third effect is based on the fact that the π system-based P=C bond bears a significant positive charge at the phosphorus atom (NBO calculations). In N=C compounds this is reversed and the nitrogen atom bears a substantial negative charge. As a consequence, most of these low coordinate P=C deriva-

tives are less stable and only isolable protecting the P=C bond with steric encumbered groups.[69]

Reactive phosphaalkene ligands were mainly applied in transition metal chemistry.[69–73] Related pyridine ligand systems (PNP pincer ligands) were synthesized which either involve R_2P/PR_2 donor functionalities[74] or P=C groups.[75] Comparing both, the PNP pincer ligands with PR_2 donors represent the more applied system. An example for the phosphaethene pyridine ligand is the tridentate ligand 2,6-bis(1-phenyl-2-phosphaethenyl)pyridine coordinating a Fe^{I} metal.[76] A related bis-phosphaalkenyl based PNP-pincer was synthesized coordinating Cu^{I} metal.[77] The bidentate PAPY ligand system was applied in palladium chemistry for olefin polymerization.[78] A further example is the coordination towards a cationic Ir^{III} complex.[79]

Main group element compounds were synthesized, but there were mainly R_2P/PR_2 donor ligands deployed.[80,81] For the PAPY ligand system no main group complex is known so far. Related species are, for example, various phosphorus NHC analog systems such as 1,3-diphospha-2-metallapentanes [ML_n ($P(Ph)C_6H_4PPh$)] [L_n= rac-SnR_2 or $SnMe_2$].[82] Similar compounds were synthesized for Si, Ge and Sn.[83] Furthermore, a 1-sila-2,5- diphosphacyclopent-3-ene was reported.[84] In 2004, Schoeller *et al.* studied heavier group 14 elements stabilized by 1,4-diphosphabuta-1,3-diene by quantum chemical calculations and compared the results with the NHC homologues.[85]

2.2 Low Valent Heavier Main Group 14 Compounds

Recently, new approaches in main group element chemistry are observed due to their fascinating behavior to mimic transition metals.[28] In fact, compounds of main grow elements like germanium and tin, activate small molecules such as H_2, NH_3 and C_2H_4 under mild conditions and therefore show a catalytic potential for future applications. In the last 30 years, fascinating compounds

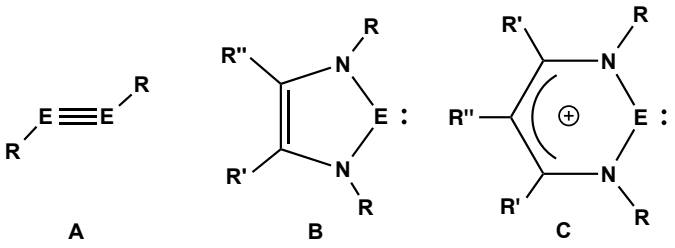

Figure 2.12: The E≡E low valent compound **A** with a formal oxidation state of +1 and the heavier NHC analogues **B** and **C** with a formal oxidation state of +2 display the possibility to activate small molecules such as H_2, NH_3 and olefins under mild conditions. E= Si, Ge, Sn and Pb.

which were previously supposed to be unstable were synthesized. These kinds of species are, for example, multiple bond compounds (**A**) and N-heterocyclic (NHC) analogues **B** and **C** containing heavier group 14 elements, as shown in Figure 2.12. Low valent main group compounds are coordinatively unsaturated species and therefore extremely reactive. The central atom E^{II} for a low valent group 14 compound is divalent. This divalent group 14 element E^{II} possesses a lone pair of electrons and a vacant orbital. To stabilize such reactive main group element centers, the ligand design is decisive. The steric protection by bulky ligands reveals a group 14 element in divalent state with a coordination number of two due to the coordiantion two bulky ligands. Another effect is the electronic stabilization where a divalent group 14 element can reveal higher coordination numbers due to additional donor groups. Depending on the heteroatom stabilizing E^{II} in divalent state, different stabilizing effects occur. Amino based ligands R_2N (R= $N(SiMe_3)_2$) show great stability towards low valent E^{II} (E= Ge, Sn or Pb) elements.[86] They are stable at room temperature as long as they remain under inert gas atmosphere; some even can be distilled in vacuo.[87–89] However, the similar alkane derivatives do not show

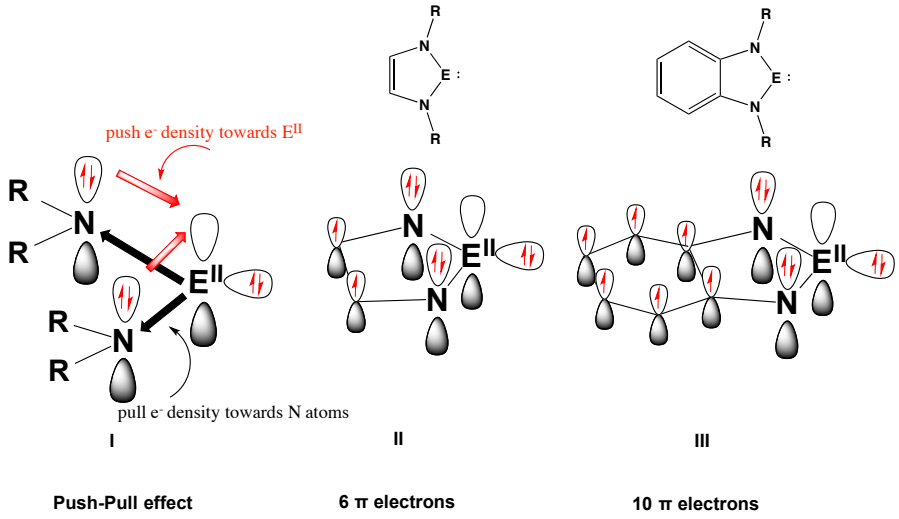

Figure 2.13: The stabilization of divalent E^{II} species is based on the inductive and the mesomeric effect. (**I**) Another effect is the cyclization and the resulted aromaticity in the ring system (**II** and **III**).[86]

this stability. The remarkable stability of N based ligands can be explained by two effects, the inductive and the mesomeric effect.[86] The inductive effect is caused by the reduction of σ-electron density at E^{II} by the more electronegative N atom. The mesomeric effect is based on the phenomenon of π-electron donation of the free electron pairs at the nitrogen atoms towards E^{II}. Another effect is the cyclization. The E^{II} atom is incorporated into an unsaturated imidazole or benzimidazole ring system (**II** and **III**). This applies additional thermodynamic stability in the low valent group 14 complex (Figure 2.13). The thermodynamic stability can be explained by the formed cyclic delocalization of the 6 π-electron or 10 π-electron system which leads to aromaticity in the ring system.[86]

As a result of these great stabilization properties, the majority of E^{II} complexes, which were isolated until now, contain N based ligand systems.[27] This is also the case for low valent group 13 complexes in which the aluminum or gallium atom can be found in the oxidation state of +1.[27,90] Also S and O containing ligands are reported, as for example the *ortho*-benzodithiol ligand in case of S.[86] The most prominent N based ligand systems are N,N bidentate ligands forming N-heterocyclic carbenes (NHCs) and their heavier analogs, shown in Figure 2.14. Since the isolation of the first stable imidazol-2-ylidene in 1991 by Arduengo *et al.*,[91] N-heterocyclic carbenes (NHCs) have gained immense atten-

tion. NHCs display unique properties due to their reactive carbon center and their excellent σ donating properties. Therefore, they are very useful in complexing transition metals.[92,93] This led to the formation of various organometallic catalysts which are very effective in, for example, olefin metathesis, Heck and Suzuki coupling, aryl amination reactions, hydrosilylation reactions, and many more.[92,93] In the last decade working groups were also interested in stabilizing heavier group 14 elements E (E= Si, Ge, Sn and Pb) by N,N-bidentate ligands.[27,29] This led to the formation of fascinating types of compounds. The cationic species of type **B** and **C** also exist coordinating by the corresponding halogenid as anion. The heavier NHC type compounds, as shown in Figure 2.14, have an oxidation state of +2 and display fascinating reaction behavior due to the bifunctionality at the element center. This results in promising properties of heavier NHC carbenes in activating small molecules. Typical synthetic methods to obtain heavier NHC analogs are salt elimination reactions followed by reduction of the mostly halogenated intermediate.

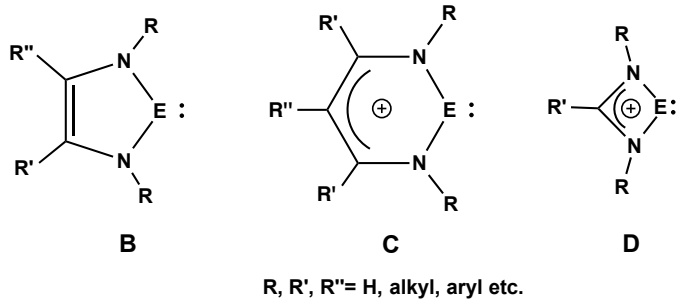

Figure 2.14: General types of heavier NHC analogs. E= Si, Ge, Sn and Pb. (acc. Driess and Jones[27]).

Further low valent group 14 species are found in multiple bonded species. Research on multiple bond formation of heavier carbon analogs led to various spectacular low oxidation state compounds after as shown in Figure 2.15. Very interesting reviews on multiple bond formation of main group compounds were published by Y. Wang and G. H. Robinson,[94] P. P. Power and R. C. Fischer,[95] a profound book was written by V. Lee and A. Sekiguchi.[26] For type

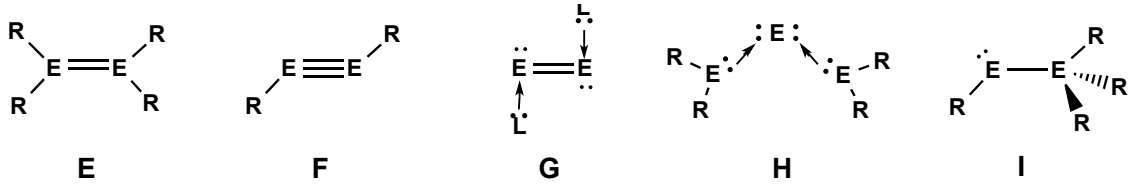

Figure 2.15: Generalization of neutral types of low oxidation state heavier group 14 compounds containing multiple bonds. Type **E**: Oxidation state +2. Type **F**: Oxidation state +1 (E= Si, Ge, Sn and Pb). Type **G**: Formal oxidation state 0 and Type **H**: Centered element with an oxidation state 0 (E= Si, Ge and Sn). Type **I**: Bimetallic complex with divalent and tetravalent E.[94]

E, the so called *dimetallenes* with an oxidation state of +2, species for all heavier carbon analogues were synthesized.[96,97] In solution however, these compounds frequently dissociate into monomers. The oxidation state of +1 is observed for type **F**, the E≡E triple bond compounds. In 2000, Power *et al.* isolated the first RPb≡PbR structure, a spectacular breakthrough in multiple bond chemistry of heavier main group elements.[98] Other discoveries involving E≡E triple bonds of heavier congeners followed.[26,99,100]

Recently, an astonishing novel type of group 14 compounds was developed, where the group 14 elements are in the formal oxidation state of zero.[94,101,102] For main group elements, this is a completely new approach. A metal in an oxidation state of zero is formally stabilized only via donor-acceptor interactions. This means that the E^0 element possesses two lone pairs of electrons. E^0 compounds are classified as so called "tetrylones" compared to tetrylenes - the E^{II} complexes. Tetrylenes are bonded covalently towards a dianionic ligand. Hence, tetrylenes possess a vacant π orbital and one lone pair of electrons as discussed in chapter 1. Frenking and coworkers determined the degree of E^0 species by the calculations of 1^{st} and 2^{nd} proton affinities (Figure 2.16).[103–108]

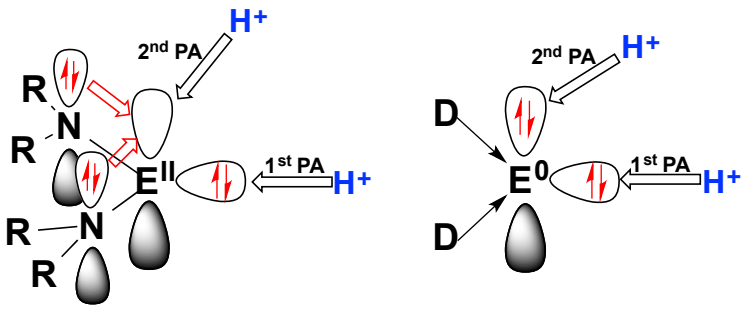

Figure 2.16: The first and second proton affinities (PA) determine the difference between tetrylenes E^{II} complexes and tetrylones E^0 compounds. The PA's are depending on orbital geometries and especially the 2^{nd} PA differs due to the fact that higher values are observed for E^0 species which can stabilize the second H^+ better due to the second lone pair of electrons.[103–108]

Due to the differences in the bonding situation, the frontier orbitals of E^0 and E^{II} complexes differ significantly. In case of E^{II} complexes, the HOMO is represented by a σ donor type orbital and for E^0 compounds the HOMO represents a π donor type orbital due to the two lone pairs of electrons. Hence, the reactivity of tetrylenes and tetrylones differs because the reactivity is determined by the frontier orbitals. In case of the first and second proton affinities, these differences are observed. Protonating a tetrylene or tetrylone once does not show a significant difference. In case of the first proton affinity, the values are similar due to the interaction of the H^+ atom with one lone pair of electrons which both species possess. However, the value of the 2^{nd} proton affinity is depending much more on the orbital geometry. The second H^+ atom is better stabilized by a π donor type orbital with two lone pairs of electrons than by a tetrylene with a σ donor type orbital possessing one lone pair of electrons. The stabilization of the second proton in case of tetrylenes depends on the stabilizing effect of the ligand system. If a delocalization of electrons are observed as for amino based ligand systems a second protonation is possible. However, higher 2^{nd} proton affinities are investigated for tetrylones.[103–108]

In general, group 14 compounds with multiple bonds in an oxidation state of two, one or zero, can be classified by a simple generalization of five neutral types shown in Figure 2.15. Group 14 elements in zero oxidation state are found in compounds where, for example, the dinuclear Si=Si core is coordinated by two Lewis base carbene ligands (L:), (L: = :C[N(2,6-^{i}Pr$_2$C$_6$H$_3$)CH]$_2$) (type **G**).[101] Later, the respective Ge=Ge and Sn=Sn complexes were isolated.[109,110] Computational results showed that the bonding situation in the carbodiphosphoranes ($R_3P{=}C{=}PR_3$) and "carbodicarbenes" (NHC:C:NHC) is well described by a central E^0 atom complexed by two donor ligands.[103–108] The computational studies were experimentally confirmed by the isolation of the bis(benzimidazolin-2-ylidene)carbon^0 complex[111] and are further supported by other bent allenes.[112–114] Similarly, the bent central structural motif in the heavier group 14 allenes $R_2E{=}E{=}ER_2$ (type **H**),[115–120] trisila-,[115] 1,3-disila-2-germa-,[116] 1,3-digerma-2-sila,[117] trigerma-,[118] and tristanna-allene[120] is readily rationalized by donor-acceptor interactions between two heavier tetrylene fragments and a central E^0 atom. Further examples of main group elements in the formal oxidation state of zero are provided by metalloid main group clusters E_nR_m (n>m).[121,122]

More recently, a novel type of heavier group 14 compound has been developed in which the tetrel elements silicon[123] and germanium[124] are in the formal oxidation state of zero and are thus the first experimentally realized examples of silylones and germylones. Furthermore, there is experimental evidence for a certain degree of E^0 character in some N-heterocyclic stannoles (Figure 2.17).[125,126]

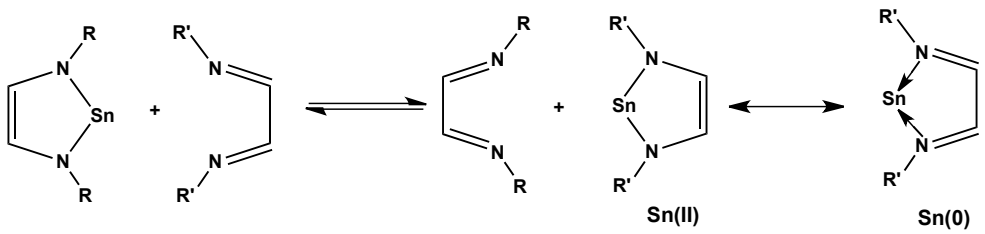

Figure 2.17: Sn-transfer reaction between diazastannoles and diazadienes. This indicates a certain degree of Sn^0 character. (acc. Gudat *et al.*[125])

Examples of transition metal complexes of germanium, tin, and lead compounds where the tetrel has a formal oxidation state of zero are provided by the compounds $[L_2EM(CO)_5]$ (L = pyridine or 2,2'-bipyridine, 2,2'-bipyrimidine, 1,10-phenantroline; M = Cr, Mo, W).[127] In transition metal chemistry, dative

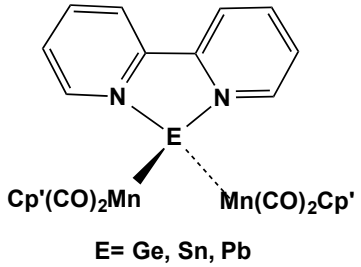

Figure 2.18: The stabilization of group 14 elements in a formal oxidation state of zero by transition metal complexes and 2,2'-bipyridines.[127]

ligand coordination and the resulting stabilization of the central atom in an oxidation state of zero is a common bonding motif. Typical donor functionalities are for example CO, PR_3 and NHCs which provides donor and acceptor properties. Besides donor properties, the acceptor properties are very important for the stabilization of a metal in zero oxidation state. The metal is additionally stabilized *via* the backbonding from the metal towards the ligand system.

Apart from unsaturated multiple bond species, $RE\text{-}ER_3$ (E= Ge, Sn, Pb; R= alkyl or aryl group) complexes (type **I**) gain more and more attention.[128–132] These dimetallic compounds bear a divalent and a tetravalent heavier group 14 element with direct metal to metal bonding. These compounds were only existing as unstable transition states of (e.g.) dimetallenes (type **E**) and verified through trapping reactions.[133–136] Until now, only a few stable compounds have been isolated. The first structural characterized compound with a $RSn\text{-}SnR_3$ bonding motif was synthesized via the reaction of a halogenatedSn^{II} precursor $[(C_5H_4N)(Me_3Si)_2CSnCl]$ with $[Li(THF)_3Sn(SiMe_3)_3]$in Et_2O. Further examples include Ar'GeGe(^{t}Bu)$_3$ (Ar' = $C_6H_3Mes_2$-2,6; Mes = $C_6H_2Me_3$-2,4,6), Ar*SnSn(Ph)$_2$Ar*and Ar*SnSn(Me)$_2$Ar* (Ar*=$C_6H_3Trip_2$-2,6; Trip= $C_6H_2{}^iPr_3$-2,4,6).[129,137–139] These dimetallic compounds are stable due to the steric encumbering ligands. E-E (E= Sn, Pb) bond fragments are also found stabilized in organic ring structures[130,140] and employed by additional coordination of the E atom.[131,132,141] A rearrangement of dimeric dimetallenes of type **E** to corre-

sponding RE-ER_3 species in solution was studied.[139] However, due to large substituents of these dimers, structure RE-ER_3 is disfavored because it places three large substituents at one E atom. If one of the two organic substituents at each E atom is relatively small, rearrangement of that substituent to the other E atom is possible, though.[139]

2.3 Activation of Small Molecules

Recently, highly interesting reviews were published regarding the activation of small molecules by heavier low valent group 14 compounds.[28,142] Due to the activation of small molecules, low valent main group complexes mimic transition metal centers. The activation of small molecules is depending on the presence of open coordination sites and valence orbitals separated by modest energies ($\leq$4 eV).[28] These characteristics were found in many transition metal species and recently in low valent main group complexes. Numerous investigations display the behavior of E$\equiv$E triple bond compounds to activate small molecules. The addition of ethylene and butadiene to the relatively stable disilyne RSi$\equiv$SiR (R= SiMe(Si^tBu_3)$_2$) afforded the [2+2] and [2+4] addition products.[143] Further discoveries showed addition products of the stable disilyne RSi$\equiv$SiR (R= Si^iPr[$CH(SiMe_3)_2$]$_2$) with cis and trans but-2-ene.[144]

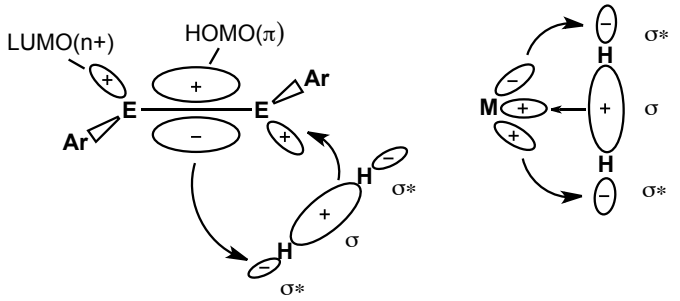

Figure 2.19: The interaction of the frontier orbital of triple bond main group compounds Ar E$\equiv$EAr(Ar= C_6H_3-2,6(C_6H_3-2,6-$^iPr_2$)$_2$(Dipp)) (E= Ge, Sn) with H_2 (left) and the comparison with a transition metal (right). The activation of H_2 by main group element compounds is very similar to the activation by transition metals. (acc. Power *et al.*[28])

In 2005, Power *et al.* were the first to react H_2 with the Ge and Sn alkyne ArE≡EAr (Ar= C_6H_3-2,6(C_6H_3-2,6-Pr^i_2)$_2$). For the Ge congener, the hydrogenated products Ar(H)GeGe(H)Ar, Ar$(H)_2$GeGe$(H)_2$Ar and Ge$(H)_3$Ar were isolated.[145] The ArSn≡SnAr compound exclusively gives ArSn(μ-H_2)SnAr. This phenomenon is explained by the interaction of frontier orbitals with H_2 as shown in Figure 2.19. The π HOMO orbital of the E≡E species donates electrons into the σ* orbital of H_2 and then a electron donation of the σ orbital of H_2 follows into the π*-LUMO of ArE≡EAr. This interaction enables the oxidative addition of H_2 due to the weakening of the H-H bond. Further calculations were published studying the activation of H_2 by germylenes and stannylenes at a level of density functional theory.[146] More recently ArSn≡SnAr (Ar= C_6H_3-2,6(C_6H_3-2,6-Pr^i_2)$_2$ or C_6H-2,6-(C_6H_2-2,4,6Pr^i_3)-3,5Pr^i_2) was reacted reversibly with ethylene at room temperture and one atmosphere pressure to obtain a double cycloadduct. This structure displays the first example of a reversible interaction between a very reactive group 14 species and a relatively unreactive substrate molecule under mild conditions.

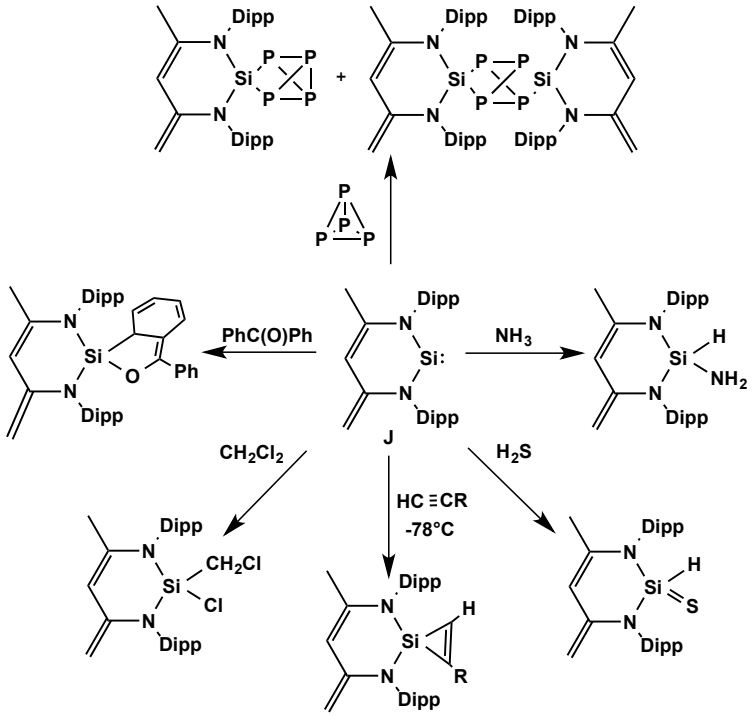

Figure 2.20: The silylene 4 reacts with various inorganic and organic compounds to yield the corresponding products. Reactions with: a) white phosphorus, b) ammoniac, c) hydrogen sulfide, d) multiple bonds, e) organohalides and f) benzophenone. (acc. Driess *et al.*[147])

Recently, Bertand *et al.* published a review covering the behavior of singlet carbenes mimicing the reactivity of transition metal centers.[29] In this review, the activation of CO, H_2, NH_3 and P_4 is discussed as well as the ability of carbene analogs to stabilize highly reactive species as it is possible for transition metal complexes. The activation depends on the HOMO-LUMO gap of the low valent main group complex. The smaller the HOMO-LUMO gap ($\leq$4 eV), the more likely an activation reaction takes place. The activation of H_2 was accomplished with the germylenes Ar_2Ge: and stannylenes Ar_2Sn: (Ar= C_6H_3-2,6(C_6H_3-2,6-^{i}Pr$_2$)$_2$ or C_6H_3-2,6-(C_6H_2-2,4,6-Me$_3$)$_2$) under relatively mild conditions. However, sometimes arene elimination of the bulky aryl substituent occurs.[29,148] The activation of ammonia by these heavier carbene analog species was studied.[148] Furthermore, the first example of a germaketene reacting a diaryl germylene with CO was investigated.[28,29]

Further studies were performed regarding the conversion of white phosphorus to the red allotrope by a stable silylene.[29] Recent developments display the reactivity of silylene **J**, which inserts into P_4 to yield the strained polycyclic silaphosphanes.[29] Further reactions of silylene **J** led to spectacular synthetic results as the first examples of (e.g.) sila-ketones, sila-esters.[147] The diversity of the reaction behavior of the low oxidation state compounds can be seen by this fascinating activation of small molecules. However, the reaction behavior of Ge and Sn congeners are not as well investigated as those of the silylenes.

Chapter 3

Results and Discussion

3.1 Iminopyridines and 1^{st} Main Group Elements

2-Iminopyridine and 2,6-iminopyridine ligand systems provide unusual reactivity as well as unique structural motives due to their conjugated NCCN fragment.[24,47–50] A part in this PhD thesis is the synthesis of highly reactive radical monoanionic 1^{st} row alkali salts using the SIMPY and DIMPY ligands. In collaboration with Michal Zalibera and the Institute of Physical Chemistry, we investigated SIMPY$\bullet^{-}$ and DIMPY$\bullet^{-}$ radical anions. The question was where the electron is stabilized within the SIMPY and DIMPY alkali metal complexes. Furthermore the alkali metals could have an influence towards the radical anion regarding their diverse coordination environment in the solid state.* Therefore EPR measurements were performed in solution and in solid state to determine the sterical and electronic influence of the diverse structures depending on the alkali metal. Furthermore our study focuses on the delocalization of the radical itself, due to the fact that in case of SIMPY two α-iminopyridine ligands are donating the alkali metal. In case of DIMPY two imino bonds are involved coordinating the alkali metal and a distribution of the negative charge all over the ligands due to their conjugated system seems possible. This is studied by EPR measurements and by DFT calculations.

* M. Zalibera, J. Flock, P. Cias, G. Gescheid, R. C. Fischer; *manuscript in preparation*, **2013**.

The SIMPY ligand N-2,6-diisopropyl-phenylimino-2-pyridine was synthesized according to literature.[59] Two equivalents of SIMPY with lithium metal give a dark red solution of monoanionic $Li^{+}(SIMPY^{\bullet -})(SIMPY)$ (**1**) after 12 hours reaction time at room temperature in Et_2O. Due to the 2:1 ratio of the ligand SIMPY to lithium metal, only one ligand site is reduced and the other ligand coordinates as neutral ligand to complete the coordination sphere of the lithium metal in solid state. An etheric solvent for the reaction with metallic lithium is preferred due to faster conversions in contrast to aromatic or aliphatic solvents. After removing the solvent, a dark red powder was obtained, which was recrystallized in Et_2O at -30°C to give dark red cubic crystals suitable for X-ray analysis.

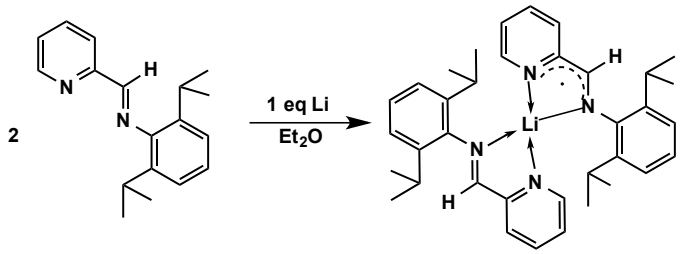

Figure 3.1: Reaction of two equivalents SIMPY with one equivalent of Li metal, gives the monomeric $Li^{+}(SIMPY^{\bullet -})(SIMPY)$ complex **1**.

Similar reaction conditions were chosen for the monoanionic salts of Na (**2**) and K (**3**). Two equivalents of SIMPY were dissolved in benzene and one equiv-

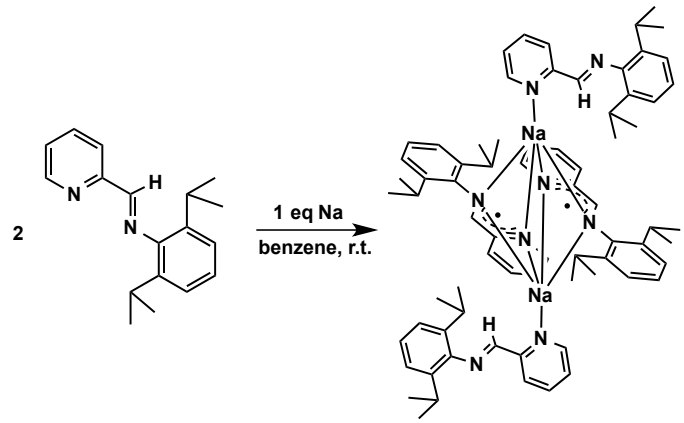

Figure 3.2: Reaction of two equivalents SIMPY with one equivalent of Na metal, gives the dimeric $Na^{+}(SIMPY^{\bullet -})(SIMPY)$ complex **2**

alent of the metal was added. Color change was immediate as the solution went from clear yellow to a dark red. Crystals of the monoanionic complex $Na^+(SIMPY\bullet^-)(SIMPY)$ (**2**) were grown out of a concentrated solution in benzene at room temperature. In case of $K^+(SIMPY\bullet^-)(SIMPY)$ (**3**) no solid state structure could be obtained.

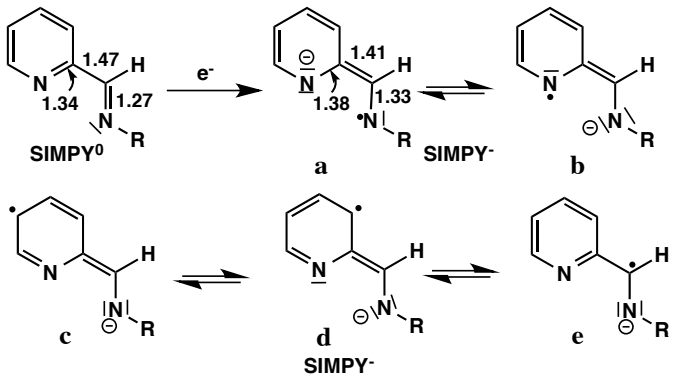

Figure 3.3: The one electron reduction of the neutral SIMPY ligand system $SIMPY^0$ leads to five resonance structures **a, b, c, d** and **e**.

In Figure 3.3 the one electron reduction of the neutral SIMPY ligand $SIMPY^0$ is displayed. The reduction process leads to five possible resonance structures **a, b, c, d** and **e**. The bond lengths which are mainly effected are displayed as well. The conjugated ligand system changes significantly with an elongation of the C_{im} – N_{im} bond with an average value of 0.06 Å. Consequently, the C_{im} – C_{py} distance in the backbone of the ligand system gets shortened by about 0.06 Å and the C_{py} - N_{py} bond length is effected too with an elongation of about 0.04 Å. The resonance structure **e** is very interesting concerning the C-C coupling reactions reported in literature.[17,51] The reaction of two of these radical species where the electron is stabilized at the backbone of the ligand system gives the rare C-C coupling products as for example the $[SAMPY_2GaI_2]_2$ complex.[17,51] The rich and unique chemistry of this redox active SIMPY ligand is based on the manifold possibilities to change the conjugated ligand system either by reduction or by oxidation processes. The resonance structures shown in Figure 3.3 help to understand the bonding situation in the $Li^+(SIMPY\bullet^-)(SIMPY)$ complex (**1**) and the $Na^+(SIMPY\bullet^-)(SIMPY)$ complex (**2**). This complex bonding motif will be discussed comparing the solid state structures of **1** and **2**.

Compound **1** crystallizes in the monoclinic crystal group $P2_1$ containing two crystallographic independent molecules in the unit cell (compound **1** and **1'**). The lithium complex **1** possesses a four-coordinated lithium metal center (as shown in Figure 3.4). The compound can be categorized as pseudo tetrahedral complex with N1-Li-N2 angle of 86.4(2)° for the one electron reduced ligand and with N3-Li-N4 of 80.0(2)° for the neutral ligand coordinating the lithium metal center. The Li–N distances are ranging from 2.002(5) and 2.133(4) Å. In

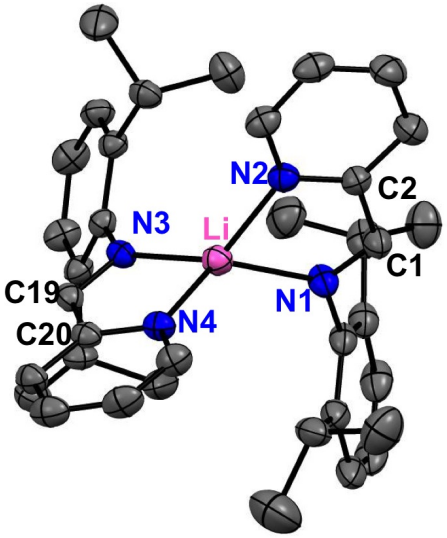

Figure 3.4: Solid-state structure of **1**. Anisotropic displacement parameters are depicted at the 50% probability level. Hydrogen atoms are omitted for clarity.

case of the monoanionic ligand the Li – N bonds have similar bond lengths with 2.002(5) and 2.008(4) Å, respectively. These are shorter compared to the Li – N bonds of the neutral ligand. The Li – N distances of the coordinated neutral ligand differ regarding the Li – N_{im} bond of the coordinating imino group with 2.133(4) Å and the Li – N_{py} of the pyridine functionality with 2.075(5) Å. These differences can be explained by the fact that in the neutral ligand a stronger pyridine donor gives a shorter Li - N bond length compared to the weaker imino Li - N_{im} distance. Regarding the resonance structures in Figure 3.3, the aromaticity in the pyridine ring is broken which leads to similar Li - N bond lengths Li – N_{py} and Li – N_{im} for the monoanionic ligand fragment. In literature, comparable compounds with two α-iminopyridine ligands involved in a complex are, for example, the monoanionic $(SIMPY\bullet)_2AlX$ (X= Cl, CF_3SO_3) complexes,[18] the heavier Ga analogues $(SIMPY\bullet^-)_2Ga^+X$ (X= Cl, OH, TEMPO),[21] the $(SIMPY\bullet^-)_2Mg^{+2}(THF)$ complex[52] and the monoanionic potas-

sium salts [$K^+(sol)_2(SIMPY^{\bullet -})_2$] (sol= THF, Et_2O).[25] Typical bond lengths of the conjugated monoanionic complexes are for the imino bond C_{im} – N_{im} in a range of 1.331 to 1.367 Å and for the C_{im} – C_{py} distance in the backbone of the ligand system in a range of 1.385 to 1.432 Å.[18,21,25,52] These are consistent with the bond lengths of the isolated $Li^+(SIMPY^{\bullet -})(SIMPY)$ (**1**) complex. The imino bond C1 – N1 is 1.336(3) Å long, which agrees well with the known complexes and is elongated compared to the imino bond C19 – N3 of the neutral ligand with 1.289(4) Å coordinating the lithium metal center in complex **1**. For the C_{im} – C_{py} distance a C1 – C2 bond length of 1.410(4) Å is observed, which is in good agreement with the known monoanionic complexes and shortened in contrast to the neutral ligand with a C19 – C20 bond length of 1.487(4) Å. Furthermore, the aromatic system in the pyridine ring is disturbed. This is observed by the C_{py} - N_{py} distance which is in the neutral $SIMPY^0$ C2 - N2 1.339(3) Å. By the one electron reduction the bond lengths in the pyridine ring change as can also be seen looking at the resonance structures in Figure 3.3. Therefore, the C2 - N2 distance is elongated with 1.388(4) Å. In case of the second neutral SIMPY ligand coordinating the Li atom the C2 - N2 distance is similar to the SIMPY ligand with 1.340(3) Å.

Table 3.1: Bond lengths [Å] and angles [°] of the SIMPY ligand and compounds $Li^+(SIMPY^{\bullet -})(SIMPY)$ **1** and $Na^+(SIMPY^{\bullet -})(SIMPY)$ **2**.

Bond lengths and angles	**SIMPY**	**1**	**1′**	**2**
M – N1	-	2.002(5)	2.002(5)	2.515(2)
M – N2	-	2.008(5)	2.004(5)	2.488(2)
M – N3	-	2.133(5)	2.103(5)	2.500(2)
M – N4	-	2.075(5)	2.123(5)	2.729(2)
Na – N5	-	-		2.416(4)
C1 – N1	1.270(2)	1.336(3)	1.324(3)	1.337(3)
C1 – C2	1.473(3)	1.410(4)	1.408(3)	1.410(3)
C2 - N2	1.339(3)	1.388(4)	1.395(4)	1.389(3)
C19 – N3	-	1.289(3)	1.280(3)	-
C19 – C20	-	1.487(4)	1.468(4)	-
C20 - N4	-	1.340(3)	1.354(3)	-
N1-M-N2	-	86.4(18)	87.09(2)	68.15(6)
N3-M-N4	-	80.0(2)	79.62(2)	64.67(6)

The dimeric complex **2** crystallizes in the triclinic space group $P\bar{1}$ and has an inversion center in the middle of the Na_2N_4 fragment. The sodium metals are fivefold coordinated by four nitrogen atoms of ligands $SIMPY^{\bullet -}$ and by an

additional pyridenyl nitrogen N_{py} of the neutral ligand. An octahedral complex is formed, by the monoanionic ligand systems coordinating two sodium metals. The Na – N distances vary from 2.500(2) to 2.729(2) Å and are in between the distances of the lithium complex **1** and the monoanionic potassium salts $[K^+(sol)_2(SIMPY^{\bullet -})_2]$ (sol= THF, Et_2O),[25] as expected. The Li – N bond lengths are ranging from 2.002(5) and 2.133(4) Å and the K – N distances of the monoanionic potassium salts $[K^+(sol)_2(SIMPY^{\bullet -})_2]$(sol= THF, Et_2O)[25] are between 2.795(2) and 3.020(2) Å. The M – N bond lengths represent a trend resulting in shorter M – N distances for the coordination towards the small Li atom and increasing the M – N bond lengths regarding their heavier homologues Na and K as expected for the bigger ionic radii. Assuming that the alkali metal has an influence over the radical anion located at the ligand site seems possible regarding this trend in the solid state structures. For the re-

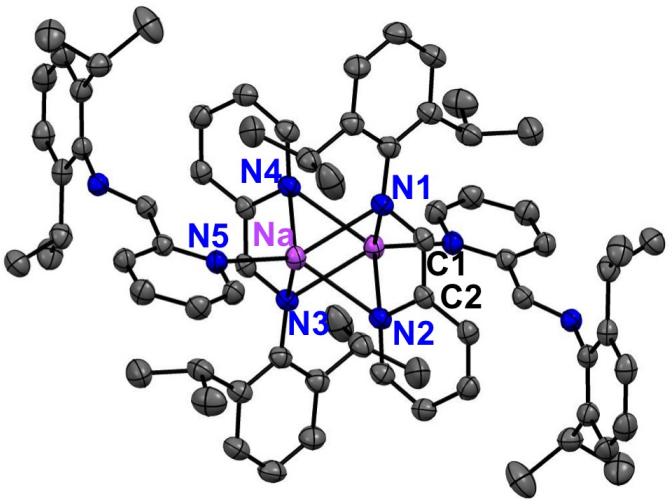

Figure 3.5: Solid-state structure of **2**. Anisotropic displacement parameters are depicted at the 50% probability level. Hydrogen atoms are omitted for clarity.

duced ligand $SIMPY^{\bullet -}$ the imino bond C1-N1 is with 1.337(3) Å slightly elongated compared to compound **1** and is in good agreement with the literature known complexes.[18,21,25,52] The same applies for the C1 – C2 distance at the backbone of the ligand system with 1.410(3) Å, which is in the typical range for a monoanionic conjugated $SIMPY^{\bullet -}$ fragment. This shows that the radical is delocalized over one ligand site resulting in the typical bond length variations for the conjugated α-iminopyridinyl radical anion affecting the C_{im} – N_{im} bond to be elongated and the C_{im} – C_{py} bond to be shortened. Furthermore, the aromaticity in the pyridine ring is disturbed which effects the C2 - N2 distance

with an elongation of about 0.06 Å. This correlates with the lithium complex **1** and other related species reported in literature.[18,21,25,52]

The EPR investigations of the $Li^+(SIMPY\bullet^-)(SIMPY)$ complex were performed with a solid sample as well as with its solution in THF. The spectrum of the solid shows a single isotropic Lorentzian line with ΔB_{pp} = 0.19 mT centered at the g = 2.0031(1) (Figure 3.6). These signal characteristics are typical for an organic radical in solid state, where the high concentration of unpaired spins in a small volume leads to the exchange narrowing of the EPR line. On the contrary, the spectrum of a diluted $Li^+(SIMPY\bullet^-)(SIMPY)$ solution shows a rich and complicated hyperfine splitting pattern (Figure 3.6). Based on the EPR measurements we can conclude that the radical of the $Li^+(SIMPY\bullet^-)(SIMPY)$ structure is located at the ligand center. Furthermore it seems that in solution only one ligand radical anion is bound to the Li metal while the second neutral SIMPY ligand is not coordinating. Therefore a transfer of the electron - a self exchange L•ML to LML• - from one to the other ligand is not possible.

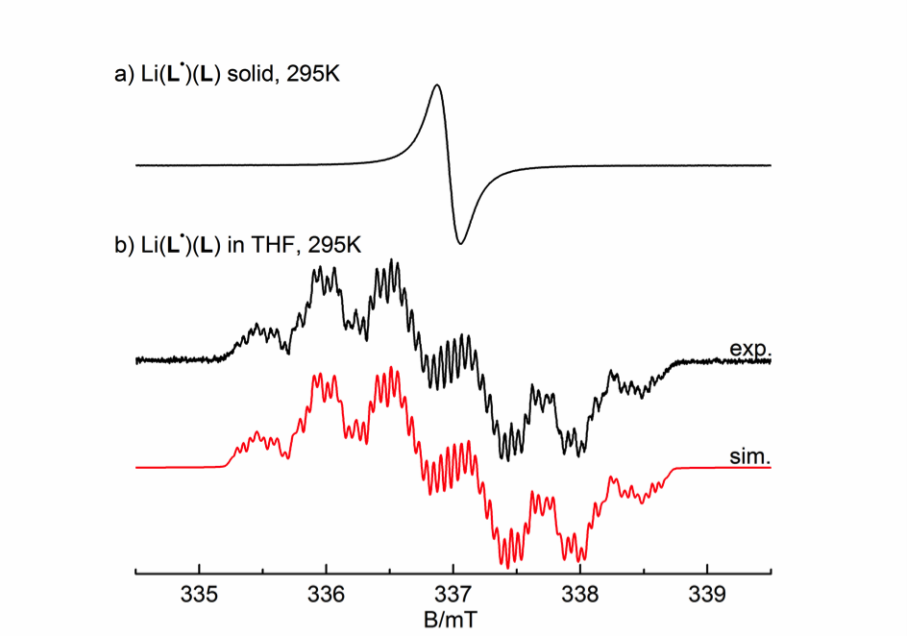

Figure 3.6: a) EPR spectrum of the solid $Li^+(SIMPY\bullet^-)(SIMPY)$ complex recorded at 295K, g = 2.0031(1) ΔB_{pp} = 0.19 mT; b) EPR spectrum obtained after dissolving of the $Li^+(SIMPY\bullet^-)(SIMPY)$ complex in dry degassed THF at 295K together with the simulation. g = 2.0031(1).

Furthermore a detailed study on the interaction of the SIMPY$\bullet^{-}$ with different alkali metals was performed. Therefore, (SIMPY$\bullet^{-}$)Li^{+}, (SIMPY$\bullet^{-}$)Na^{+} and (SIMPY$\bullet^{-}$)K^{+} complexes were studied by EPR measurements in the solid state, in different solvents as pentane, benzene and THF and at different temperatures ranging from room temperature down to 175 K.

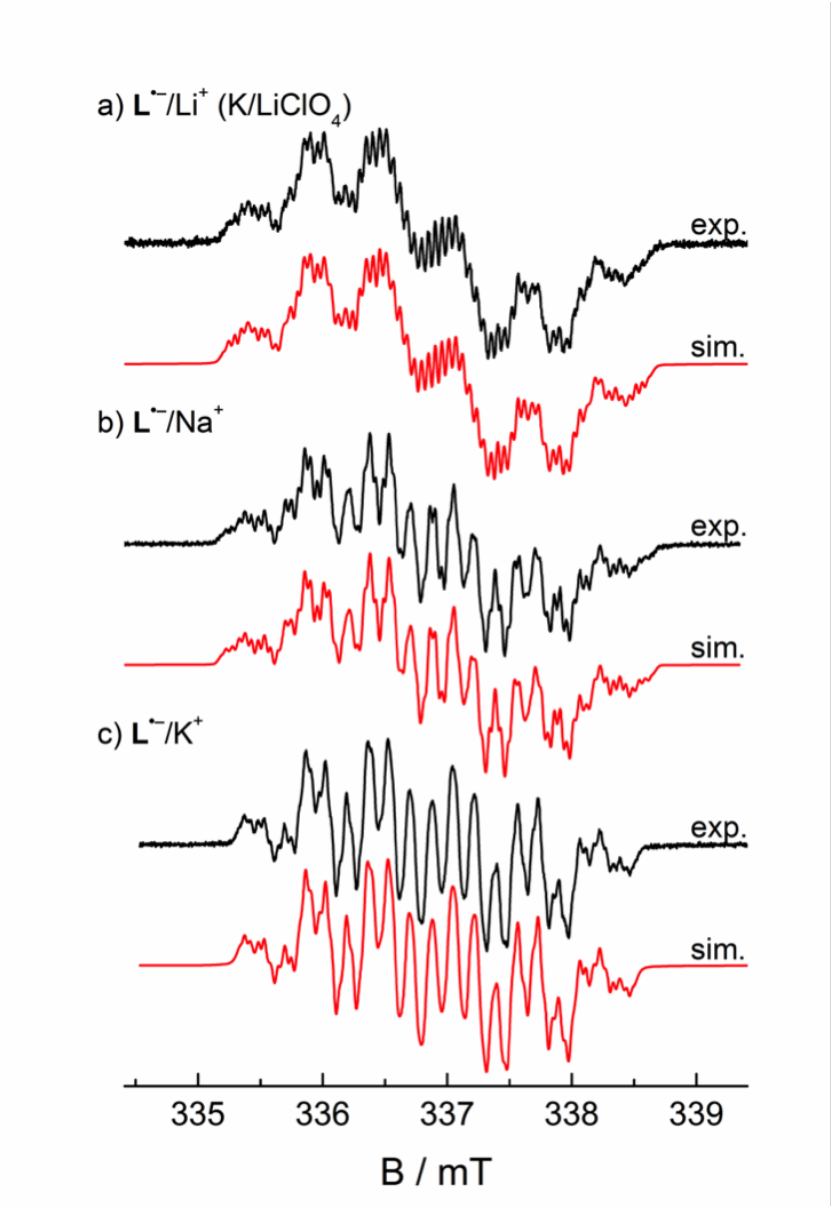

Figure 3.7: a) EPR spectrum obtained after reduction of L with K mirror in dry degassed THF with excess of $Li(ClO_4)$ at 295K (black) and simulation (red); b) EPR spectrum of (SIMPY$\bullet^{-}$)Na^{+} (black) and simulation (red); c) EPR spectrum of (SIMPY$\bullet^{-}$)K^{+} (black) and simulation (red). g = 2.0031.

An ion pairing phenomenon could be responsible for the differences of SIMPY•⁻ coordinated to different counter ions. For this study (SIMPY•⁻)Li^+, (SIMPY•⁻)Na^+ and (SIMPY•⁻)K^+ were compared with each other. One additional sample was prepared by the reduction of SIMPY with K in the presence of an excess amount of $LiClO_4$. This should proof if an ion exchange is possible regarding the presumably weaker donor-acceptor interactions of the bigger counter ion K towards the coordinating ligand. In the (SIMPY•⁻)Li^+ complex a tighter bonding towards the monoanionc SIMPY•⁻ fragment is expected than in the (SIMPY•⁻)K^+ complex. If this is true, an ion exchange from the (SIMPY•⁻)K^+ complex to form the (SIMPY•⁻)Li^+ complex should occur when $LiClO_4$ is present in the reaction solution. The EPR spectra clearly show an influence due to the presence of the corresponding cations (in Figure 3.7a: by the excess of Li^+, even though the reduction was performed with K). Simulation of the spectrum in Fig. 3.7c could be obtained considering only the hyperfine couplings with the N and H nuclei. In other words, the hfc from ^{39}K is too small or the ion pair too loose to influence the spectral pattern. On the other hand, for the simulation of the spectra in Fig. 3.7a,b the interaction with the corresponding cation (Figure 3.7a: Li^+, Figure 3.7b: Na^+) had to be considered. The smaller the cation, the more it influences the SIMPY•⁻ radical anion.

Therefore it seems plausible that an ion exchange takes place in the sample K/$LiClO_4$. Due to the weak interaction of K^+ with SIMPY•⁻, an ion exchange with $LiClO_4$ is feasible. The influence of Li^+ towards SIMPY•⁻ is demonstrated in the EPR spectrum of Figure 3.7a and leads to identical spectra observed for the (SIMPY•⁻)Li^+ complex Figure 3.7c. This proofs that an ion exchange from the (SIMPY•⁻)K^+ complex to form the (SIMPY•⁻)Li^+ complex occurred in presence of $LiClO_4$. This tight interaction of Li^+ towards SIMPY•⁻was also studied at low temperatures. Ion pairing is an entropic phenomenon and as such is favored with raising the temperature. The ratios between the tight ion pair (with hyperfine coupling of the electron spin to the counterion nuclear spin) and loose ion pair (without this coupling) are usually temperature sensitive and the shape of the spectrum is influenced by temperature. Figure 3.8 shows the EPR spectra of the (SIMPY•⁻)Li^+ at various temperatures. No significant changes in the spectra were observed (except of line broadening) by

varying the temperature and the (SIMPY•$^{-}$)Li^{+} can thus be regarded as a tight ion pair.

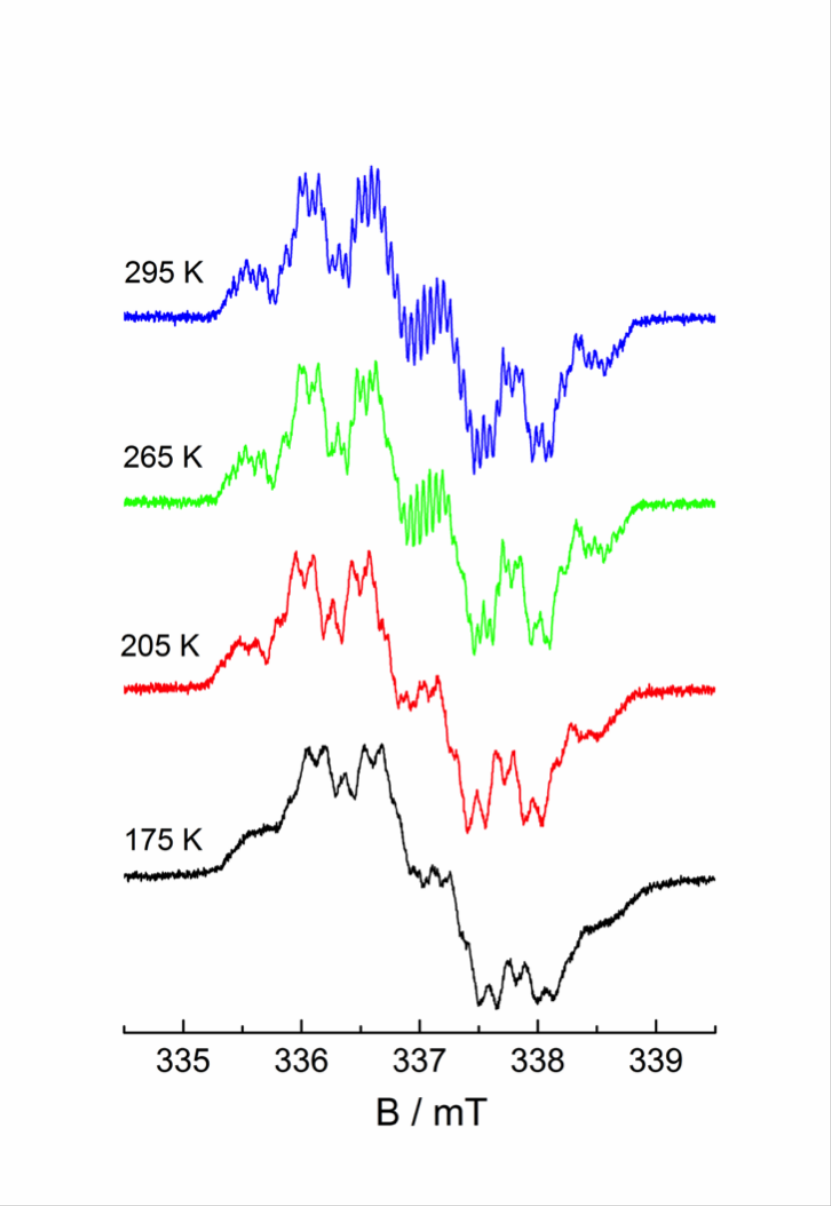

Figure 3.8: EPR spectra of (SIMPY•$^{-}$)Li^{+}(SIMPY) dissolved in THF at various temperatures.

The synthesis of the monoanionic DIMPY salts were also synthesized with alkali metals. The DIMPY ligand system was prepared according to literature procedures.[9] The equimolar reaction of the DIMPY ligand with alkali metals M (Li (4), Na (5), K (6), Rb (7), Cs (8)) gives dark red solutions in THF at room temperature. After 12 hours reaction time, a complete consumption of the alkali metals was assured and the solvent was reduced *in vacuo*. The concentrated dark red solution was kept at -30°C to obtain dark red cubic crystals for **6** ,**7** and **8**. In case of the reaction with Li and Na, no solid state structures could be obtained. In literature the reaction of Li metal with a related ligand MeDIMPY was performed, but exclusively yielding in the trianionic MeDIMPYLi_3 complex and a trianionic enamine derivative.[31] In the cause of this study, monoanionic DIMPY salts with heavier alkali metals K, Rb and Cs are obtained and the solid state structure analysis is presented in this PhD thesis.

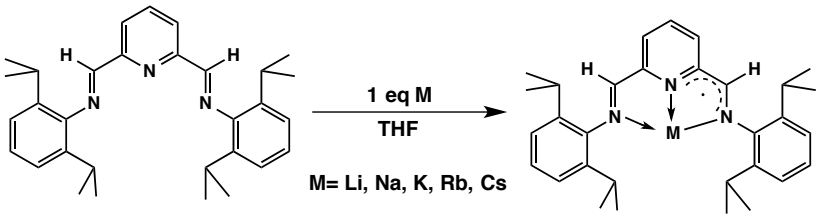

Figure 3.9: Synthesis of monoanionic DIMPY salts with alkali metals M= Li, Na, K, Rb, Cs.

The one electron reduction of the DIMPY ligand can be rationalized by five resonance structures (Figure 3.10).

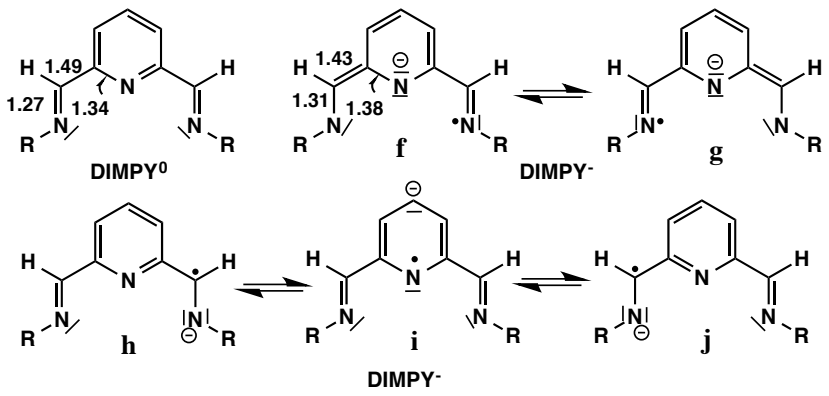

Figure 3.10: Different resonance structures of the radical anion (DIMPY•⁻) and the bonding situation for a neutral DIMPY ligand and average values for monoanionic (DIMPY•⁻)M^+ complex.

Transferring one electron of a strong Lewis acidic metal, as demonstrated with the alkali metals, changes the conjugated ligand system. Those bond lengths, which are mainly effected by the one electron reduction with alkali metals K, Rb and Cs are displayed in Figure 3.10. Similar to the SIMPY ligand system, the C_{im} - N_{im} bond is elongated by 0.05 Å compared to the neutral ligand DIMPY and the C_{im} - C_{py} bond at the backbone of the ligand system is shortened by 0.06 Å as the resonance structures **f** and **g** show. Furthermore, the C_{py} - N_{py} distances are effected with an elongation of about 0.04 Å and the aromaticity of the pyridine ring is removed as can be seen in the resonance structures **f**, **g** and **i**. Additionally, these effects are also noticed for the other ligand site which indicates a distribution of the radical all over the ligand system. This complex bonding motif will be further discussed comparing the solid state structures of compounds **6** , **7** and **8**.

The solid state structures of compounds **6** , **7** and **8** are shown in Figures 3.11 and 3.12 and the bond lengths and angles are given in Table 3.2. Interestingly, dimeric $(DIMPYM)_2$ structures are observed, where the metal center is additionally stabilized by the π interaction with aromatic diisopropylphenyl group of the second DIMPYM fragment.

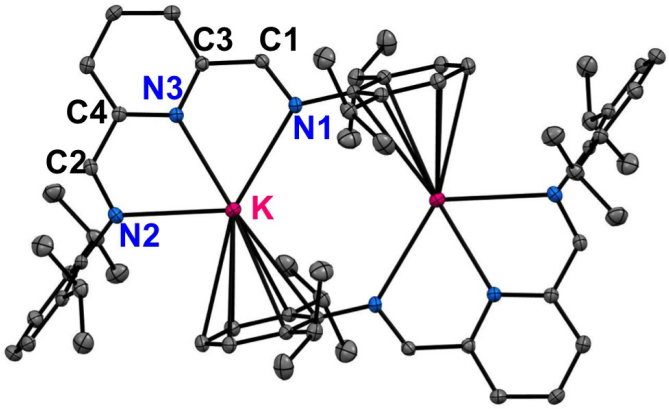

Figure 3.11: Solid state structures of compound **7**. Anisotropic displacement parameters are depicted at the 50% probability level. Hydrogen atoms are omitted for clarity.

The $(DIMPY^{\bullet -})K^{+}$ complex crystallizes in the orthorhombic space group P*bcn* and has an inversion center in the middle of the K_2N_2 fragment. The K atom is coordinated by three N atoms with bond lengths ranging from 2.638(1) Å to 2.907(1) Å and by the η_6-complexation of the diisopropyphenyl group with

about 3.202(1) Å. The K atom is not symmetrically centered in the middle of the ligand regarding the K - N1 distance with 2.907(1) Å and the K - N2 distance with 2.862(1) Å, but in plane with the DIMPY ligand fragment. The C_{im} - N_{im} bonds are elongated, but one ligand site is much more effected with C1 - N1 of 1.313(2) Å compared to C2 - N2 with 1.296(2) Å. This is also observed for the C_{im} - C_{py} distance at the backbone, which is shortened with C1-C3 of 1.437(2) Å and C2-C4 of 1.451(2) Å. The C_{py} - N_{py} are shortened too with C3 - N3 of 1.374(2) Å and C4 - N3 of 1.368(2) Å. The angles observed in the (DIMPY•$^-$)K^+ complex are for N1-K-N2 123.13(4)° and for N1-K-N3 61.94°.

Table 3.2: Bond lengths [Å] and angles [°] of compounds (DIMPY•$^-$)K^+ **6**, (DIMPY•$^-$)Rb^+ **7** and (DIMPY•$^-$)Cs^+ **8**.

Bond lengths and angles	**6**	**7**	**8**
M – N1	2.907(1)	3.030(1)	3.152(2)
M – N2	2.862(1)	2.803(1)	3.095(2)
M – N3	2.638(1)	2.985(1)	2.972(2)
C1 – N1	1.313(2)	1.317(2)	1.308(3)
C1 – C3	1.437(2)	1.430(2)	1.429(3)
C2 – N2	1.296(2)	1.289(2)	1.280(3)
C2 – C4	1.451(2)	1.458(2)	1.456(3)
C3 – N3	1.374(2)	1.375(2)	1.382(3)
C4 – N3	1.368(2)	1.370(2)	1.380(3)
M - O1	-	2.903(2)	3.317(3)
N1-M-N2	123.13(4)	115.36(3)	108.61(5)
N1-M-N3	61.94(4)	58.98(4)	55.69(5)

In literature, only a few comparable compounds were reported, which bear the related monoanionic MeDIMPY salt. Frequently, paramagnetic MeDIMPY species were reported as intermediates, but could not be isolated.[4,12] Solid state structures were isolated of the paramagnetic (MeDIMPY•)$AlMe_2$ complex[15] and of the (MeDIMPY•)$_2$Mn(PF_6)[149] complex. A significant change in the bond lengths of the conjugated ligand system is also noticed.[15,149] The C_{im} - N_{im} bond lengths vary from 1.331 to 1.321Å and the C_{im} - C_{py} bond lengths at the backbone range from 1.418 to 1.442 Å.[4,15,149] These bond lengths are in good agreement with the obtained bond lengths for (DIMPY•$^-$)K^+ complex.

For M= Rb and Cs, also dimeric complexes are obtained crystallizing in the triclinic space group $P\bar{1}$ (Figure 3.12). The alkali metal is coordinated by three

N atoms, by the η_6-complexation of diisopropyl group and by one O atom of the solvent THF. The additional donation of one THF molecule per alkali metal Rb or Cs can be explained by the bigger coordination sphere compared to the smaller K atom. This leads also to larger M - N distances ranging for the (DIMPY•⁻)Rb^+ complex from 2.803(1) Å to 3.030(1) Å and for the (DIMPY•⁻)Cs^+ complex from 2.972(2) Å to 3.152(2) Å. Furthermore, the Rb and Cs atoms are not in plane with the DIMPY ligand fragment. Another effect is the observation of smaller angles the bigger the alkali metal gets. For Rb, angles of 115.36(3)° for M1-Rb-M2 and 58.98(4)° for M1-Rb-M3 are present in the complex. For the (DIMPY•⁻)Cs^+ complex, smaller angles are noticed for M1-Cs-M2 with 108.61(5)° and for M1-Cs-M3 with 55.69(5)°. The M - O1 distance is 2.903(2) Å for Rb and 3.317(3) Å for Cs. For the reduced (DIMPY•⁻) ligand the bonding motif is similar to the known complexes in literature[4,15,149] and to the (DIMPY•⁻)K^+ complex. The C_{im} - N_{im} bond distances are elongated with 1.317(2) Å for Rb and with 1.308(3) Å for Cs and simultaneously a shortening of the C_{im} - C_{py} distances with 1.430(2) Å (Rb) and 1.429(3) Å (Cs) takes place. Again one ligand site is more effected than the other. The less effected bond lengths vary around 1.28 Å for C_{im} - N_{im} distances and around 1.46 Å for the C_{im} - C_{py} distances and agree well with literature known complexes.[4,15,149]

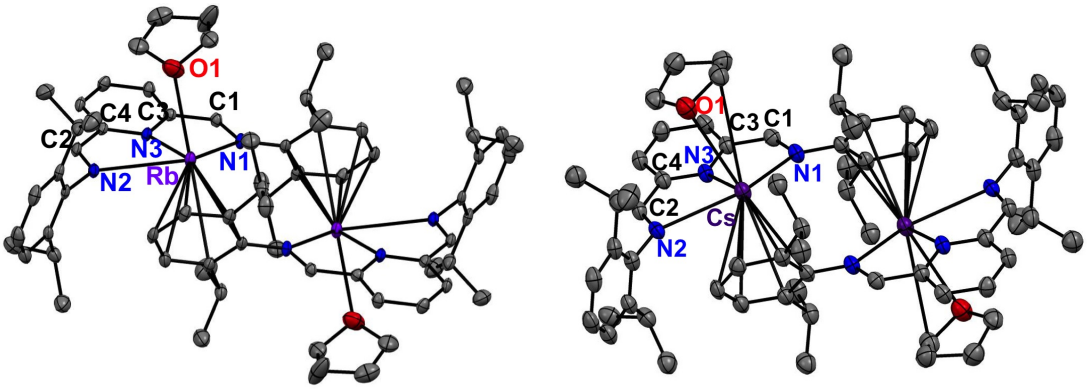

Figure 3.12: Solid state structures of compounds **7** and **8**. Anisotropic displacement parameters are depicted at the 50% probability level. Hydrogen atoms are omitted for clarity.

EPR measurments were performed for all (DIMPY•⁻)M^+ complexes, but due to the complex bonding situation in the DIMPY ligand, explained by the five resonance structures, no simulations were successful yet.

3.2 Synthesis of Unexpected Low Valent Main Group Complexes Using the SAMPY Ligand

A series of highly interesting low valent group 14 compounds were synthesized, which were stabilized by N,N bidentate ligands.[27] However, the stabilization using aminopyridine ligands is less investigated. Westerhausen and coworkers were the first to react a related aminopyridine ligand system with main group elements Mg and Sn.[51] In this PhD thesis the aminopyridine ligand SAMPY (2-[ArN-CH_2]$_2$(NC_5H_4) (Ar = C_6H_3-2,6-^{i}Pr$_2$)) reacts with Ge^{II}, Sn^{II} and Pb^{II}bis[bis(trimethylsilyl)amide] (E($N(SiMe_3)_2$)$_2$) *via* a transamination reaction.[†150] The E($N(SiMe_3)_2$)$_2$ compounds (E= Ge, Sn, Pb) were first synthesized by Lappert and coworkers.[96] By the time these E^{II} species were isolated, these low valent systems were considered as curiosity. Nowadays these E^{II} complexes are classified as effective E^{II} source and helpful in the preparation of low valent heavier group 14 compounds.

The SAMPY ligand (2-[ArN-CH_2]$_2$(NC_5H_4) (Ar = C_6H_3-2,6-^{i}Pr$_2$))[66] and the E[$N(SiMe_3)_2$]$_2$ (E = Ge, Sn, Pb)[96] were prepared according to literature procedures. The transamination reaction of the SAMPY ligand with E[$N(SiMe_3)_2$]$_2$ affords the heteroleptic SAMPY$E^{II}N(SiMe_3)_2$ complexes (E= Ge, Sn, Pb). In case of E=Ge, one equivalent of Ge[$N(SiMe_3)_2$]$_2$ was reacted with one equivalent of SAMPY ligand in diethyl ether at room temperature. During the reaction hexamethyldisilazane is formed as byproduct due to the elimination of the hydrogen at the amino functionality. The transamination reaction needs a long reaction time to proceed with a minimum of 5 days to yield the yellow SAMPY$Ge^{II}N(SiMe_3)_2$ complex **9**. Compared to E= Sn and Pb, the reaction time is increased. The equimolar reaction of Sn[$N(SiMe_3)_2$]$_2$ and Pb[$N(SiMe_3)_2$]$_2$ with the SAMPY ligand gives the yellow-greenish SAMPY$Sn^{II}N(SiMe_3)_2$ **10** and SAMPY$Pb^{II}N(SiMe_3)_2$ **11** complexes after 24 hours in THF. Reacting the substrates in etheric solvents increases the reaction time in contrast to aliphatic solvents. The obtained complexes were recrystallized in diethyl ether at -30 °C. The reaction to yield SAMPY$Pb^{II}N(SiMe_3)_2$ **11** has to be performed at -30°C and the addition of Pb($N(SiMe_3)_2$)$_2$ has to occur drop wise due to the

[†] Preliminary studies, Amra Suljanovic, PhD Thesis: Design and Synthesis of Polysilazanes, **2011**, TU Graz.

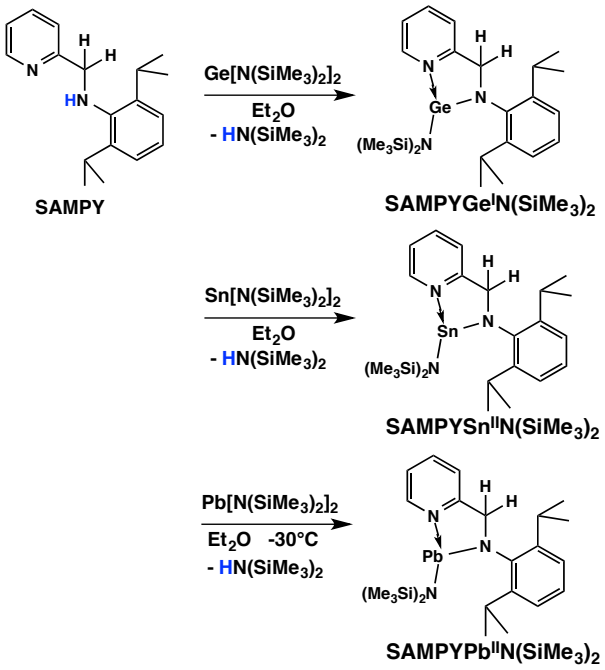

Figure 3.13: The equimolar reation of the SAMPY ligand with $E[N(SiMe_3)_2]_2$ gives the complexes $SAMPYE^{II}N(SiMe_3)_2$ **9**, **10** and **11**.

high reactivity of $Pb(N(SiMe_3)_2)_2$. Compounds $SAMPYSn^{II}N(SiMe_3)_2$ **10** and $SAMPYPb^{II}N(SiMe_3)_2$ **11** decompose slowly in solution resulting in precipitated Sn and Pb metal and SIMPY ligand (the reaction mechanism will be discussed subsequently). Hence, in reaction solution several byproducts are present additionally to the starting material SAMPY and although recrystallization was investigated for various solvents, it was not possible to obtain high yields of 100% purified samples of **9**, **10** and **11**. Compounds **9**, **10** and **11** were fully characterized by elemental analyses, multinuclear NMR studies and solid state structure analysis. In the ^1H NMR a low field shifting of the ^{i}Pr groups occurs due to the coordination environment of the group 14 element. The SAMPY ligand shows a septet of the C**H**$(CH_3)_3$ proton at 3.58 ppm and and a doublet of CH(C**H**$_3)_3$ at 1.25 ppm (Figure 3.14) in C_6D_6. Depending on the group 14 element the C**H**$(CH_3)_3$ proton signal ranges from 3.65 (for E= Sn), 3.67 (for E= Ge) to 4.10 ppm (for E= Pb). The same low field shifting is observed for the protons of CH(C**H**$_3)_3$ giving a set of doublets varying from 1.27 to 1.38 ppm. Furthermore, the heavier the group 14 element the broader are the signals revealed (or the less they are resolved) in the ^1H NMR spectra. For the germanium complex **9**, a clearly defined ^1H spectrum

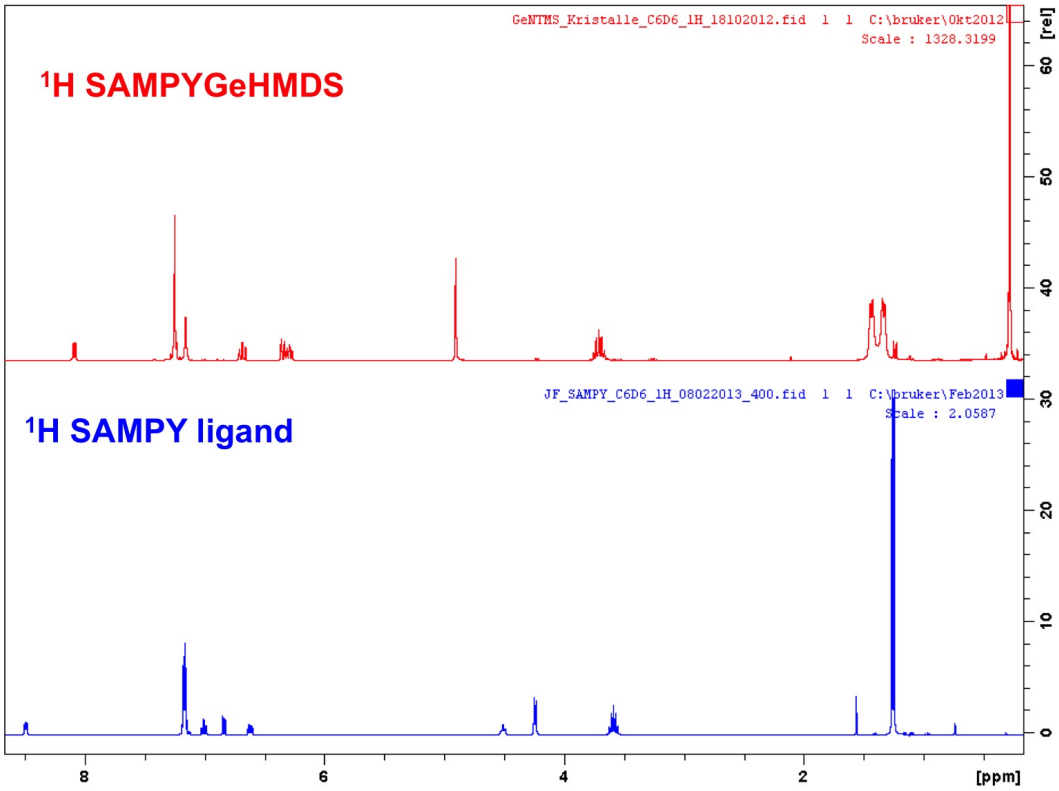

Figure 3.14: NMR spectra of the SAMPY ligand (blue) and the heteroleptic SAMPYGe^{II}N(SiMe$_3$)$_2$ complex **9**.

was obtained regarding the septet of the C**H**(CH$_3$)$_3$ and the two doublets of CH(C**H**$_3$)$_3$ (Figure 3.14). In case of compounds **10** and **11** broadened signals were observed. This is caused by the dynamic coalescence effect which is based on an inversion around the group 14 element E (E= Ge, Sn, Pb). The heavier the group 14 element, the more this effect appears which is mainly temperature dependent. The rotation barrier around the group 14 element E can be influence by temperature and is high for the small Ge atom and gets higher the heavier the group 14 element gets. Hence, the broadened signals for the SAMPYSn^{II}N(SiMe$_3$)$_2$ **10** and SAMPYPb^{II}N(SiMe$_3$)$_2$ **11** complexes are caused due to high rotation barriers around the group 14 element. Regarding the aromatic signals, a high field shifting is observed as displayed in Figure 3.14, comparing the SAMPY ligand with compound **9**. ^{29}Si NMR shows one signal at -2.46 ppm for SAMPYGe^{II}N(SiMe$_3$)$_2$, -2.91 ppm for SAMPYSn^{II}N(SiMe$_3$)$_2$ and -4.90 ppm for SAMPYPb^{II}N(SiMe$_3$)$_2$. The lighter the group 14 element the more the signal is shifted to the low field. Compared to the starting material E(N(SiMe$_3$)$_2$)$_2$ the signals were slightly shifted to the higher field.[96] The ^{119}Sn

NMR displays a chemical shift at 79.78 ppm for the SAMPYSn^{II}N(SiMe$_3$)$_2$ complex **10**.

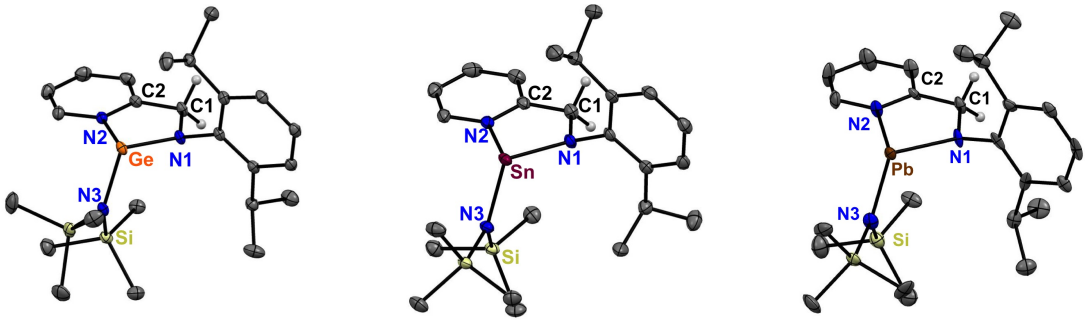

Figure 3.15: Solid state structures of compounds SAMPYGe^{II}N(SiMe$_3$)$_2$ **9**, SAMPYSn^{II}N(SiMe$_3$)$_2$ **10** and SAMPYPb^{II}N(SiMe$_3$)$_2$ **11**. Anisotropic displacement parameters are depicted at the 50% probability level. Hydrogen atoms are omitted for clarity except at the CH_2 group.

The germanium compound **9** crystallizes in the space group $P\bar{1}$ and the Ge atom is coordinated by three nitrogen atoms. Ge - N1 and Ge - N2 are covalent bonds with a distance of 1.913(1) and 1.946(9) Å and the pyridenyl N_{py} donates towards the Ge atom with 2.083(1) Å (as listed in Table 3.4) . The Ge - N distances are in a typical range for single bonds varying from 1.910 - 2.042 Å[151] and the donor-acceptor interaction is elongated as expected. A five-membered ring system is formed with an angle of N1-Ge-N2 with 79.87(4)°. The Ge atom is in a trigonal pyramidal environment and the N(SiMe$_3$)$_2$ functionality possesses an angle N1-Ge-N3 of 107.72(4)°. At the ligand backbone, the amino bond is in a range of a typical single bond with C1 - N1 of 1.446(2) Å as well as the C1 - C2 single bond with 1.498(2) Å.

Table 3.3: Bond lengths [Å] and angles [°] of compounds SAMPYGe^{II}N(SiMe$_3$)$_2$ **9** **9**, SAMPYSn^{II}N(SiMe$_3$)$_2$ **9** **10** and SAMPYPb^{II}N(SiMe$_3$)$_2$ **9** **11**.

Bond lengths and angles	**9**	**10**	**11**
E – N1	1.931(1)	2.128(3)	2.235(7)
E – N2	2.083(1)	2.270(2)	2.393(7)
E – N3	1.946(9)	2.140(2)	2.243(8)
C1 - N1	1.446(2)	1.445(4)	1.437(1)
C1 – C2	1.498(2)	1.499(5)	1.497(1)
N1-E-N2	79.87(4)	74.72(9)	72.10(3)
N1-E-N3	107.72(4)	107.42(9)	103.24(3)

The tin compound **10** crystallizes in the triclinic space group $P\bar{1}$ and shows similar bonding trends as compound **9**. As expected the Sn - N distances are longer than the Ge - N bonds. The Sn atom is threefold coordinated by two covalent bonded nitrogens and one donor-acceptor interaction of the pyridenyl N_{py}. The Sn - N bonds are ranging from 2.128(3) to 2.270(2) Å. These Sn - N bonds are in good agreement with literature known Sn - N distances ranging from 2.121 to 2.397 Å.[151] The starting material $Sn(N(SiMe_3)_2$ bears Sn - N bond lengths of 2.09(1) Å.[152] These are slightly shortened compared to the Sn - N3 distance of 2.140(2) Å. The C1 - N1 bond length is 1.445(4) Å and the C1 - C2 distance is 1.499(5) Å and both agree well with the bond lengths of compound **9**. The heavier the group 14 element gets, the smaller are the angles in the corresponding complexes. For Sn, the N1-Sn-N2 angle is 74.72(9)° and the N1-Sn-N3 angle is 107.42(9) ° and for E= Pb angles are observed with 72.10(3)° for N1-Pb-N2 and 103.24(3)° for N1-Pb-N3. The lead compound **11** crystallizes in the triclinic space group $P\bar{1}$ bearing two molecules in the unit cell. The Pb metal is threefold coordinated by nitrogen atoms with the Pb - N distances ranging from 2.235(7) Å to 2.393(7) Å. The Pb - N distances are, as expected, elongated compared to the lighter group 14 elements Ge and Sn. In the starting material $Pb(N(SiMe_3)_2$, Pb - N bond lengths of 2.24(2) Å[152] are observed which are in good agreement with the Pb - N3 distance of 2.243(8) Å. The bonding situation is similar to the heteroleptic complexes **9** and **10**. Therefore the distances C1 - N1 with 1.437(1) and C1 - C2 with 1.497(1) are in good agreement with the complexes discussed previously.

Interestingly, the reaction does not stop with the heteroleptic low valent group 14 complexes. In case of the heteroleptic germylene, an intramolecular elimination of the benzylic hydrogen at the backbone of the ligand system is observed (Figure 3.16). The $N(SiMe_3)_2$ functionality bonded to the germanium atom reacts with one hydrogen of the CH_2 group at the ligand backbone. Therefore, the ligand system itself is involved in the synthesis of a highly interesting germylene **12**. Due to elimination of one hydrogen, an iminopyridine ligand system is obtained coordinating the Ge atom. The bonding situation can be described by two resonance structure as shown in Figure 3.16. In one case an iminopyridine ligand is coordinating the Ge atom *via* donor-acceptor interactions. This bonding motif involves a neutral ligand system SIMPY coordinating towards a Ge atom in a formal oxidation state of zero forming a rare ex-

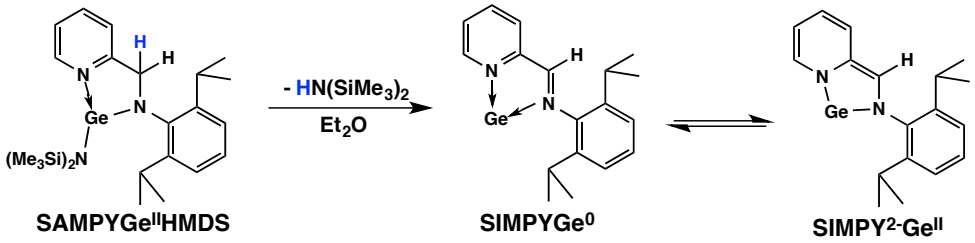

Figure 3.16: The intramolecular elimination of $N(SiMe_3)_2$ in the SAMPYGe^{II}N$(SiMe_3)_2$ compound 9 gives access to a highly interesting germylene the (SIMPY)Ge complex **12**.

ample of a germylone. The other resonance structure displays a Ge atom in the oxidation state of +2 bonded two a ligand dianion $SIMPY^{2-}$. The dianionic ligand is formed by the loss of the aromaticity in the pyridine ligand system and rearranging a C=C double bond at the backbone. This bonding motif involves a stabilization *via* cyclization, hence an aromatic system containing 10 π electrons is observed. This aromatic system results in a well stabilized germylene. In literature, a similar bonding situation was observed for N-heterocyclic stannylenes which was discussed in chapter 2.[125] By addition of a diimino ligand, a Sn-transfer reaction between diazastannoles and diazadienes was investigated *via* NMR studies. This indicated a certain degree of Sn^0 character in solution.[125]

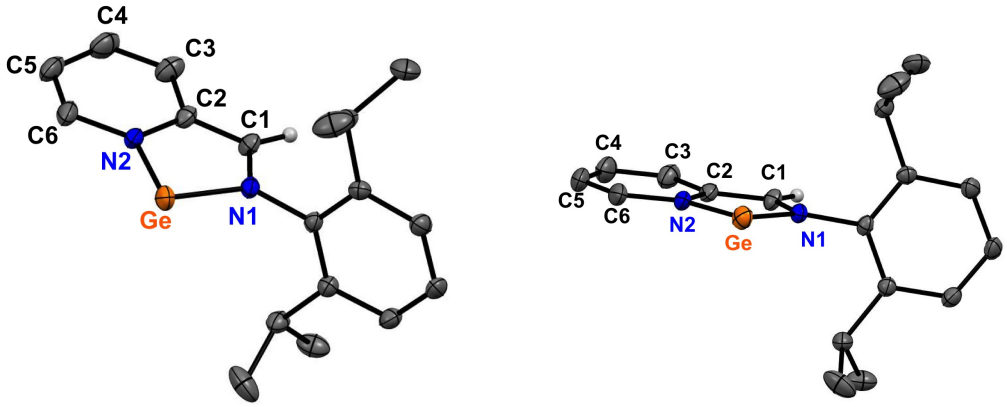

Figure 3.17: Solid state structure of the (SIMPY)Ge complex **12**. Anisotropic displacement parameters are depicted at the 50% probability level. Hydrogen atoms are omitted for clarity except at the N=CH group.

To determine the bonding situation in the germanium complex **12**, the solid state structure of the (SIMPY)Ge complex **12** is compared with the solid state structures of the SIMPY ligand and the SAMPYGeN(SiMe$_3$)$_2$ complex **9** (Table 3.4). Compound **12** crystallizes in the in the triclinic space group $P\bar{1}$ and pos-

Table 3.4: Bond lengths [Å] and angles [°] of compounds SAMPYGe^{II}N(SiMe$_3$)$_2$ **9**, SIMPYGe **12** and **12'**.

Bond lengths and angles	**SIMPY**	**9**	**12**	**12'**
Ge – N1	-	1.931(1)	1.873(4)	1.843(3)
Ge – N2	-	2.083(1)	1.903(4)	1.917(4)
C1 - N1	1.270(2)	1.446(2)	1.376(4)	1.370(5)
C1 – C2	1.473(3)	1.498(2)	1.374(5)	1.380(7)
C2 - C3	1.390(3)	1.394(2)	1.429(6)	1.417(6)
C3 - C4	1.390(3)	1.383(2)	1.351(6)	1.346(8)
C4 - C5	1.378(3)	1.397(2)	1.419(8)	1.428(6)
C5 - C6	1.381(3)	1.377(2)	1.349(7)	1.358(7)
C6 - N2	1.333(3)	1.352(2)	1.392(5)	1.376(6)
N2 - C3	1.339(3)	1.341(2)	1.397(6)	1.389(6)
N1-Ge-N2	-	79.87(4)	82.58(1)	83.82(1)

sesses two independent molecules in the unit cell (**12** and **12'**). The Ge atom is coordinated by two nitrogen atoms with bond lengths for Ge - N1 with 1.873 Å and for Ge - N2 with 1.903 Å. The Ge - N distances are shortened compared to a typical Ge - N single bonds varying from 1.910 - 2.042 Å[151] The angle of N1-Ge-N2 is 82.58(1) ° and is similar to the heteroleptic SAMPYGeN(SiMe$_3$)$_2$ complex **9** with 79.87(4) °. In case of compound **12**, the ligand system changed dramatically from an aminopyridine ligand to an iminopryidine ligand system. The main effected bond lengths are the amide bond C1 - N1 and the C - C$_{py}$ bond at the backbone of the ligand system. The C1 - N1 distance of the heteroleptic germylene bearing an amide bond is 1.446(2) Å and the C1- N1 distance of the aromatic germylene is shortened with 1.376(4) Å. However, the C1 - N1 distance of the uncoordinated SIMPY ligand is still much shorter with 1.270(2) Å. Therefore, the iminobond of complex **12** is very elongated which indicates a delocalization of π electrons in the five membered ring. This can be also explained by the C1 - C2 bond length in the backbone of the ligand system which is shortened too with 1.374(5) Å and similar to the C1 - N1 distance confirming the aromaticity in the five membered ring system. Compared to the C1 - C2 distance of the heteroleptic SAMPYGeN(SiMe$_3$)$_2$ with 1.498(2) Å and the SIMPY ligand with C1 - C2 of 1.473(3) Å, the C1 - C2 distance of **12** is shortened

by 0.1 Å. Furthermore, the pyridine ligand distances do not show the typical bond length of around 1.39 for C -C distance and 1.35 Å for the C - N_{py} bond lengths regarding the complex SAMPYGeN(SiMe$_3$)$_2$ **9** and the SIMPY ligand. In complex **12** the bond lengths for C - C range from 1.35 Å to 1.43 Å. The C - N_{py} distances are elongated too with 1.39 Å. Hence, the aromaticity in the pyridine ring is disturbed confirming the resonance structure of the SIMPY^{2-}Ge^{II} as shown in Figure 3.16.

In case of the compounds SAMPYSn^{II}N(SiMe$_3$)$_2$ **10** and SAMPYPb^{II}N(SiMe$_3$)$_2$ **11**, the intramolecular elimination reaction of HN(SiMe$_3$)$_2$ occurs, but the afforded (SIMPY)Sn and SIMPYPb complexes are not stable and decompose. The

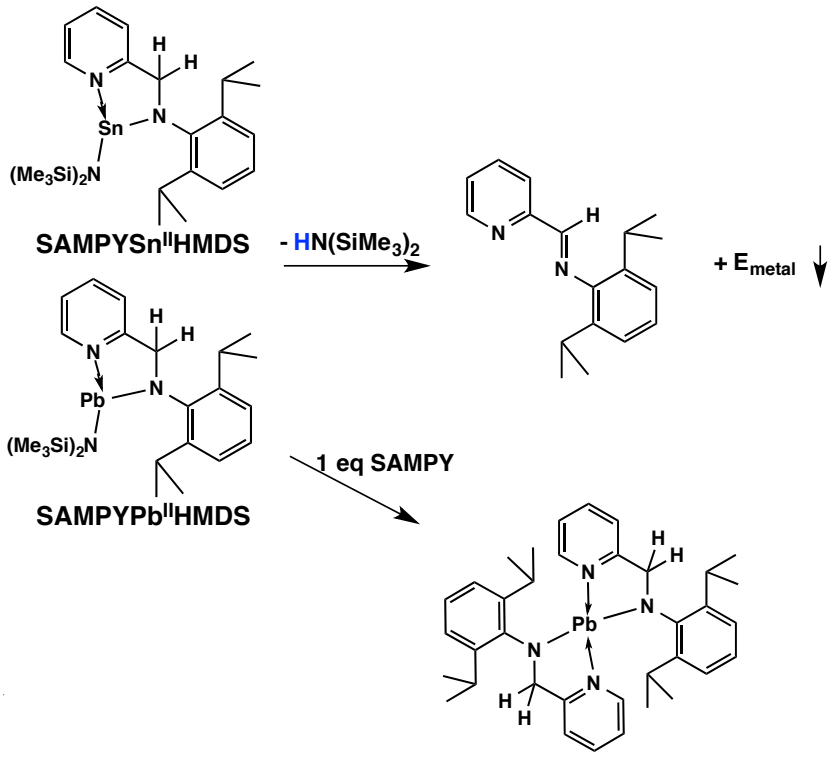

Figure 3.18: The intramolecular elimination of HN(SiMe$_3$)$_2$ in the SAMPYE^{II}N(SiMe$_3$)$_2$ compounds **10** and **11** gives only decomposition products SIMPY ligand and Sn or Pb metal. (E= Sn or Pb)

decomposition products are SIMPY ligand and precipitated Sn and Pb metal. The decomposition indicate that the two resonance structures as discussed for the (SIMPY)Ge complex are present in the (SIMPY)Sn and (SIMPY)Pb complexes, too. In case of the heavier group 14 elements the degree of the oxidation state zero character is higher and the complexes much more labile. Hence,

decomposition occurs. Furthermore, in case of Pb another very stable complex is obtained namely the $SAMPY_2Pb$ complex **13**, as shown in Figure 3.18. This compound is the thermodynamically favored product due to a high steric bulk protecting the Pb^{II} element. Complex **13** is formed in high yields reacting the two equivalents of SAMPY ligand with $Pb(N(SiMe_3)_2)_2$ in diethyl ether at room temperature. After stirring over night a yellow precipitate is formed, filtrated and washed with pentane. The $SAMPY_2Pb$ complex **13** was fully characterized by ^{1}H and ^{13}C NMR, elemental analysis and solid state structure analysis. In the ^{1}H and ^{13}C NMR spectra a similar trend is observed, shifting the diisopropyl group protons towards low field. Unfortunately no ^{207}Pb NMR resonance was observed for the Pb complexes.

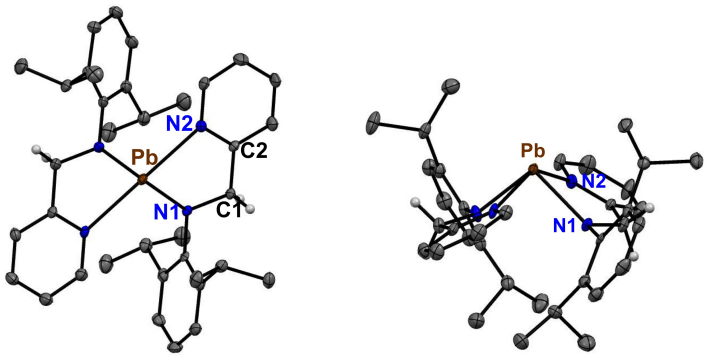

Figure 3.19: Solid state structures of compound **13**. Anisotropic displacement parameters are depicted at the 50% probability level. Hydrogen atoms are omitted for clarity except foe the CH_2 group. Selected bond lengths [Å] and angles [°]: Pb - N1, 2.251(3) ; Pb - N2, 2.571; Pb - N3, 2.240(2); Pb - N4, 2.547(3); C1 - N1, 1.447(5); C1 - C2, 1.498(5); N1-Pb-N2, 68.81(1)°

Compound **13** crystallizes in the triclinic space group $P\bar{1}$ and shows similar bonding trends as compound **11**. The complex bears a pyramidal in geometry and the Pb center is coordinated by our N atoms. The Pb - N bonds range from 2.240(2) Å to 2.571 Å and are in good agreement with compound **11**. The N1-Pb-N2 angle is shortened with 68.81(1)° due to the fourfold coordination towards the Pb center. The C1-N1 and C1-C2 distances are in good agreement with the previously discussed $(SAMPY)EN(SiMe_3)_2$ complexes (E= Ge, Sn, Pb).

A ^{1}H NMR study was performed investigating the formation of the heteroleptic SAMPYGe^{II}N(SiMe$_3$)$_2$ **9** and the (SIMPY)Ge complex **12**. Therefore, the SAMPY ligand was reacted with Ge(N(SiMe$_3$)$_2$)$_2$ in C_6D_6 at room temperature and ^{1}H NMR spectra were recorded after 1 hour, 3 days, 2 weeks and 4 weeks, as shown in Figure 3.20. As indicated the transamination reaction to form complex **9** needs minimum 5 days in etheric solvents. In aromatic solvents as C_6D_6 even longer reaction times are observed. However, after 3 days

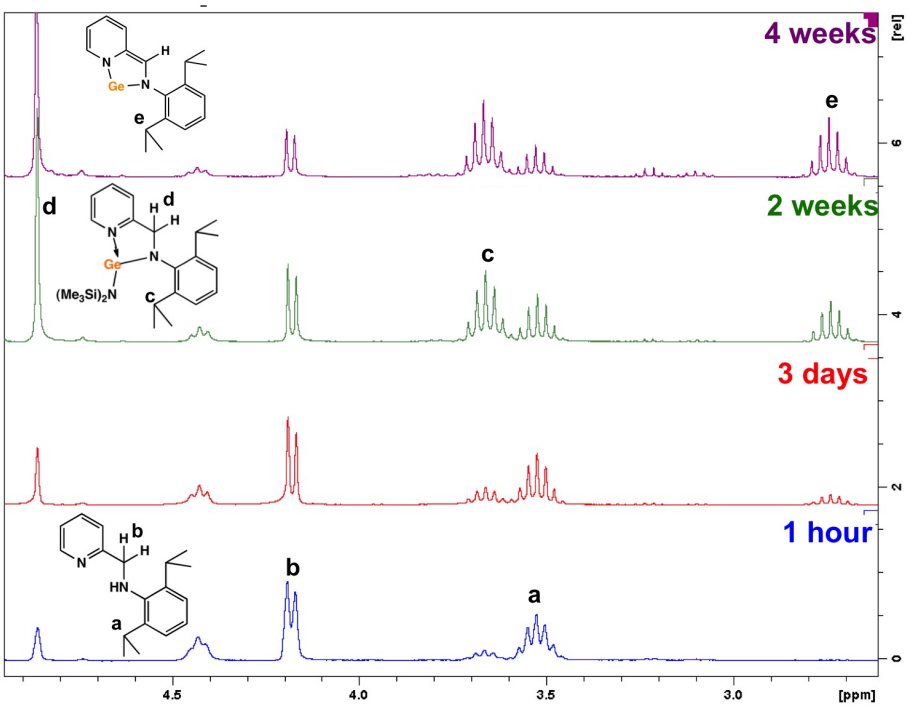

Figure 3.20: The reaction of SAMPYGe^{II}N(SiMe$_3$)$_2$ **9** takes minimum 5 days until the product is formed. Simultaneously, a highly interesting germylene the (SIMPY)Ge complex **12** is observed.

a second septet **c** of the C**H**(CH$_3$)$_3$ proton and a second proton **d** for the C**H**$_2$ functionality appear in the spectra for the SAMPYGe^{II}N(SiMe$_3$)$_2$ compound **9**. After 2 weeks, the conversion of SAMPY to the heteroleptic complex **9** proceeded with about 77%. Simultaneously, a third septet **e** of the C**H**(CH$_3$)$_3$ proton for the (SIMPY)Ge complex **12** is displayed in the ^{1}H NMR. After four weeks the ratio of the SAMPY ligand is further decreased, but still present in reaction solution. Hence, more (SIMPY)Ge complex **12** is formed in expense of the SAMPYGe^{II}N(SiMe$_3$)$_2$ compound **9**. Even though the reaction was stirred for four weeks, three components were still present in reaction solution. For a better conversion, reaction conditions were varied, as shown in Figure 3.21.

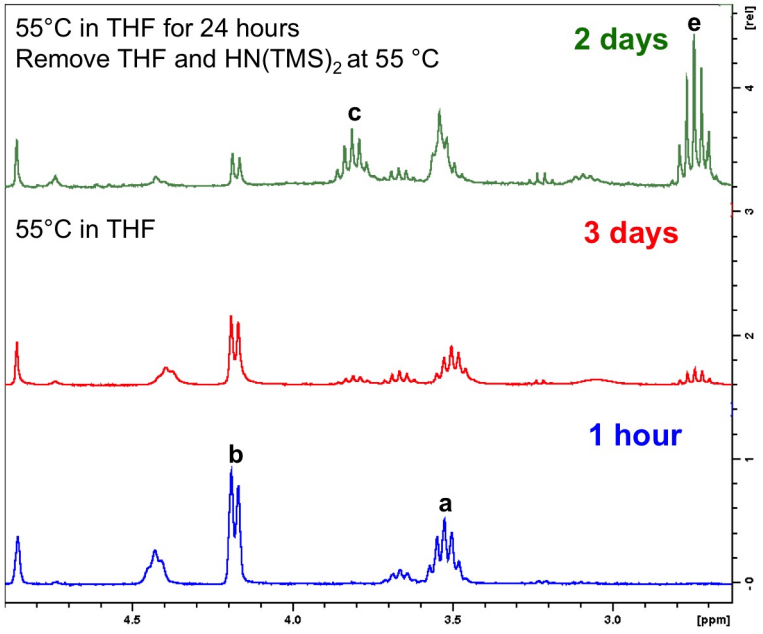

Figure 3.21: NMR study at 55 °C after one hour (blue), after three days (red) and after two days with removal of all volatile components and further stirring at 55 °C.

The reaction was performed in THF at 55°C. However, better conversions were not observed. Interestingly, reacting the SAMPY ligand with $Ge(N(SiMe_3)_2)_2$ in THF for 24 hours at 55°C and removing the solvent as well as the byproduct hexamethyldisilazane under continuous stirring of the concentrated substrates, give high conversions to the (SIMPY)Ge complex **12**. The reason for better conversions is the removal of the base hexamethyldisilazane. In presence of the base, a thermodynamical equilibrium prevents a full conversion of the first step, the transamination reaction. The transamination presumably is the rate limiting step. Hence, a driving force has to be implemented to obtain a full conversion to the (SIMPY)Ge complex **12**.

Therefore, the SAMPY ligand system was lithiated and a highly reactive precursor was generated. Subsequent addition of $Ge(N(SiMe_3)_2)_2$ forms $LiN(SiMe_3)_2$ and the SAMPY$Ge^{II}N(SiMe_3)_2$ compound **9**. Further elimination of $HN(SiMe_3)_2$ leads to the (SIMPY)Ge complex **12** as shown in Figure 3.22. The lithiation of the SAMPY ligand is a very complex reaction. In etheric solvents the dissolved lithiated SAMPYLi precursor decomposes even at low temperatures (-30°C) forming a red solution. The color change from clear yellow to a dark red is observed after a few minutes and indicates the presence of radi-

cal species of SAMPYLi, which were intensively studied for the imino ligand SIMPY with alkali metals in chapter 3.1. In literature, the SAMPY ligand was

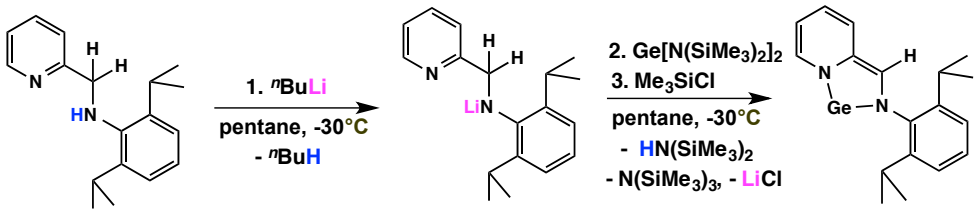

Figure 3.22: New synthetic pathway to obtain a full conversion and high yields of the (SIMPY)Ge complex **12**.

lithiated in hexane to yield a highly reactive slightly yellow powder at -30°C.[153] Reacting the SAMPY ligand at -30°C with ^{n}BuLi in pentane, precipitates a yellowish powder after 10 minutes stirring. Simultaneously, the yellow reaction solution turns slightly reddish. After 30 minutes stirring at -30°C, the upper solution containing radical byproducts was separated and a yellow powder was obtained still retaining at low temperatures. Subsequently, $Ge(N(SiMe_3)_2)_2$ dissolved in pentane was slowly added *via* a cannula at -30°C. After 1 hour reaction time the solution was warmed up to room temperature and stirred over night. A brown-orange solution was obtained. The separation of the byproduct $LiN(SiMe_3)_2$ was tried *via* recrystallization in various solvents, but unsuccessful. Therefore, Me_3SiCl was added to the reaction solution yielding $N(SiMe_3)_3$ and LiCl. The LiCl precipitated and was separated from the reaction solution *via* a filter cannula. Further purification was achieved *via* recrystallization in pentane obtaining the (SIMPY)Ge complex **12** pure and in high yields with 62%. Another great advantage of this synthetic pathway is that the reaction time is significantly reduced. Instead of minimum 5 days reaction time, the (SIMPY)Ge complex **12** complex can be synthesized in one working day.

As shown in Figure 3.23, only the (SIMPY)Ge complex is observed in reaction solution with the new synthetic pathway. Furthermore, the ^{1}H NMR spectra clearly indicate that a conversion from an aminopyridine ligand system by the loss of the C$\mathbf{H}_2$ functionality with a signal at 4.45 ppm to an imino functionality with a hydrogen signal at 7.84 ppm took place. The septet of the C$\mathbf{H}(CH_3)_3$ proton was shifted from 3.58 ppm to 2.7 ppm and the doublet of $CH(C\mathbf{H}_3)_3$ was shifted from 1.25 ppm to 0.8 ppm high field. The doublet of $CH(C\mathbf{H}_3)_3$ groups do show a splitting due to the coordination of the Ge atom resulting in

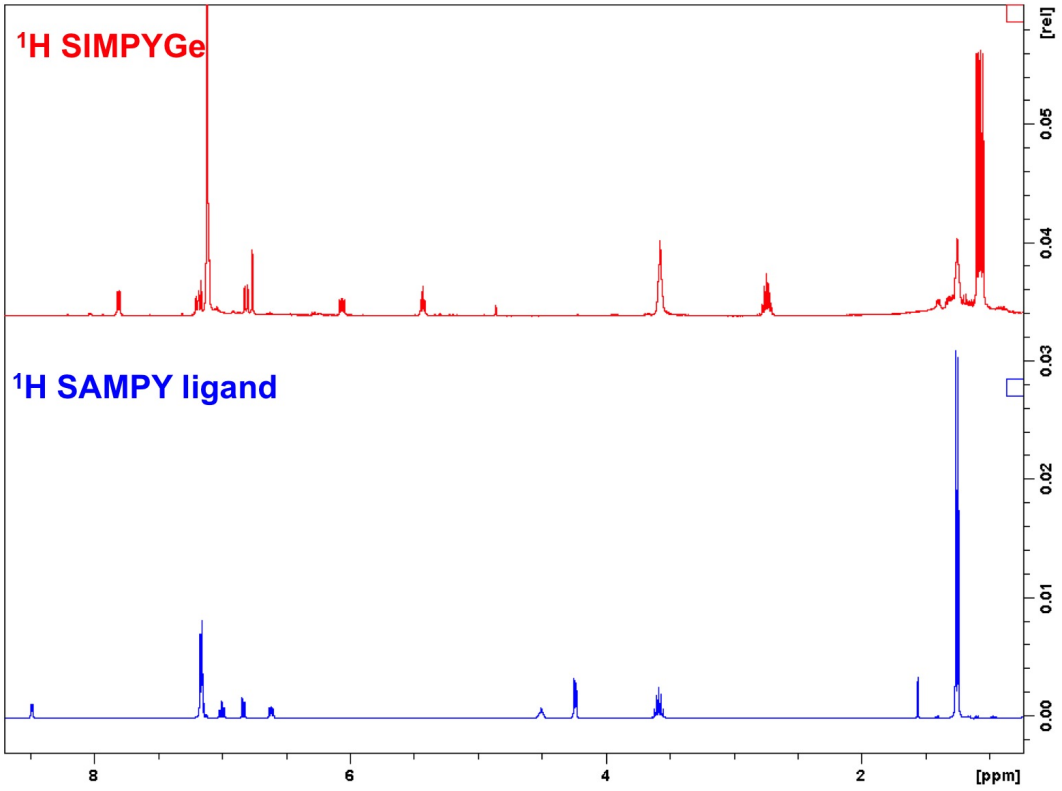

Figure 3.23: The ^{1}H NMR of the obtained (SIMPY)Ge complex **12** compared to the ^{1}H NMR of the SAMPY ligand.

a set of doublets. Furthermore, the pyridine ring signals in the aromatic regions are also shifted high field.

To gain insights in the electronic properties of compound **12**, a cyclic voltammogram (CV) was performed.‡ Therefore, the complex **12** was compared to the SIMPY ligand as shown in Figure 3.24. The samples were dissolved in a 0.1 M tetrabutylammonium perchlorate (TBAP)/CH_2Cl_2 solution. The measurements succeeded using a Pt disk working electrode and 100 mVs^{-1} scan rate. The potentials are referred vs. the ferrocenium/ferrocene (Fc^+/Fc) redox couple. The CV of the (SIMPY)Ge complex **12** shows an irreversible oxidation peak with a peak potential around –0.03 V vs. Fc^+/Fc (Figure 3.24a). The reference CV of the SIMPY ligand also shows an irreversible oxidation process, but it occurs close to the anodic limit of the available potential window (the cathodic voltammetry of SIMPY was studied in by Roesky and coworkers[25]). The oxidation the (SIMPY)Ge complex **12** is likely followed by chemical reac-

‡ Performed and analyzed by Dr. Michal Zalibera, Department of Physical Chemistry, TU Graz

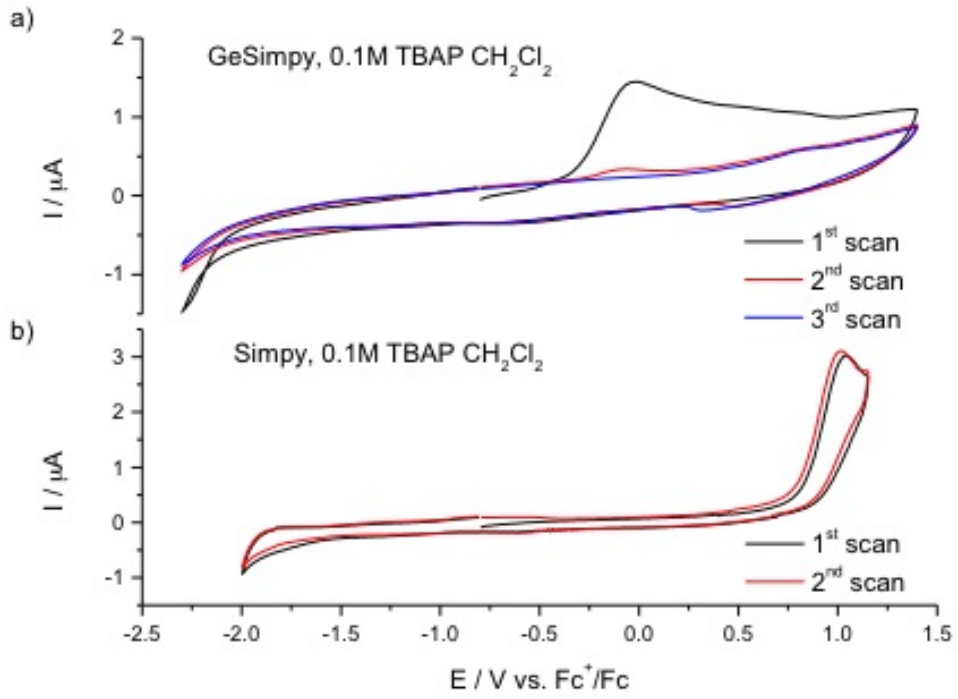

Figure 3.24: a) CV recorded for the sample **12** in 0.1 M tetrabutylammonium perchlorate (TBAP)/CH_2Cl_2 solution. Three successive cycles are shown; b) CV of the SIMPY ligand recorded under the same conditions.

tions that block the surface of the electrode, as no signal could be observed in the 2^{nd} and 3^{rd} scan. The electron transfer probably occurs at the Ge central atom as the oxidation of the ligand occurs at much more positive potentials, when compared to the ligand alone.

To further investigate compound **12**, a theoretical study was performed.[§] Therefore, the solid state structures of the SAMPYGe^{II}N(SiMe$_3$)$_2$ and the (SIMPY)Ge complexes were geometry optimized at a density functional level using the hybrid MPW1PW91 functional together with a double-zeta basis set (SDD). Furthermore, the transition states between those species were calculated. In Figure 3.25, the calculated reaction pathway of (SIMPY)Ge is displayed. The calculated pathway confirms the experimental results observed by ^{1}H NMR studies. The heteroleptic germylene (**I**) represents the intermediate of the reaction forming the (SIMPY)Ge complex. Subsequently, the aminohydrogen is transferred to the -N(SiMe$_3$)$_2$ substituent displayed in the transition state

[§] Theoretical studies in collaboration with M. Flock. Institute of Inorganic Chemistry, TU Graz

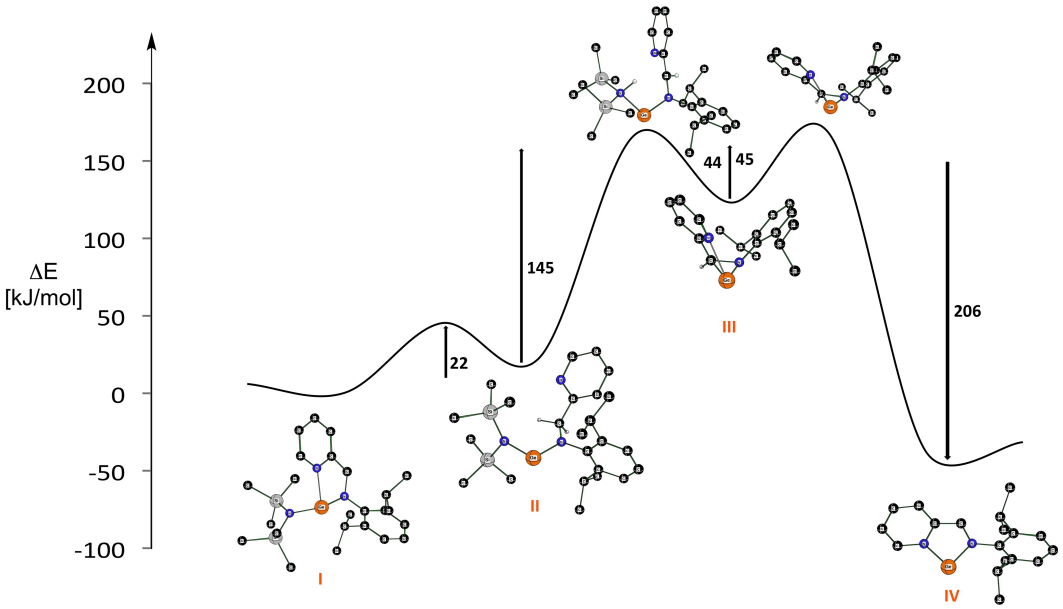

Figure 3.25: The calculated reaction pathway of the (SIMPY)Ge complex **12** (MPW1PW91/SDD).

II. The intramolecular elimination of the aminohydrogen forms $HN(SiMe_3)_2$ and the thermodynamically favored (SIMPY)Ge complex **IV** is obtained.

Regarding the frontier orbitals of complex **12** calculated with MPW1PW91/6-311G*, untypical orbital arrangements are observed for the germylene (Figure 3.26). A classical germylene displays typically a σ-donor-type orbital as the HOMO orbital. In case of compound **12**, a π-donor-type orbital is observed instead. The σ-donor-type orbital is lower in energy with -6.94 eV (HOMO-2 at -6.94 eV). Hence, the π-donor-type orbital (HOMO at -4.74 eV) is of course much more involved in the reaction chemistry (as for example the activation of small molecules) than the σ-donor-type orbital (HOMO-2). This can lead to different observations in the reaction chemistry as known for classical low valent group 14 compounds. In literature, Frenking and coworkers did determine *via* quantum chemical calculations that the less investigated class of tetrylones (E^0) do show a π-donor-type orbital as HOMO compared to tetrylenes (E^{II}) which show a σ-donor-type orbital.[103–105] This can be explained by the fact, that two lone pairs of electrons are located at the Ge^0 element in contrast to the Ge^{II} element bearing only one lone pair of electrons. The oxidation state is determined by the bonding situation at the element center. The stabilization of a dianionic ligand system bears an E^{II} element as observed for many

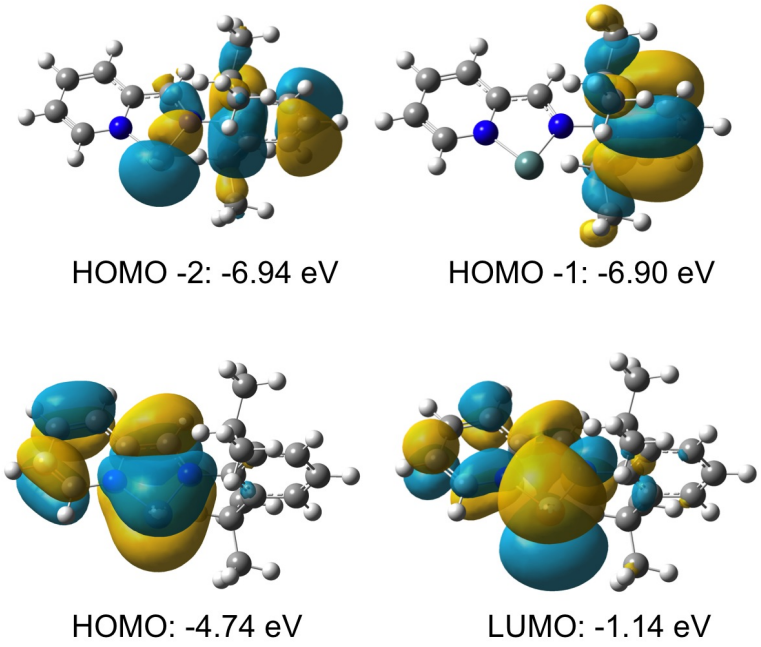

Figure 3.26: The frontier orbitals of complex **12** calculated with MPW1PW91/6-311G*.

tetrylenes in, for example, heavier NHC congeners.[27] In case of E^0 species only donor-acceptor interactions stabilize the formal oxidation state zero complex and a tetrylone with two lone pairs of electrons is formed. Furthermore, the HOMO displays the 10 π aromaticity in the ring system. A HOMO-LUMO gap of 3.70 eV was calculated and the LUMO shows a π-acceptor-type orbital. Due to these interesting findings in the calculated frontier orbitals, the activation of small molecules by the (SIMPY)Ge complex **12** seems possible. In literature, it is known that the activation of small molecules is depending on small energy separations ($\leq$4 eV) of the frontier orbitals. Furthermore, new insights in main group chemistry were obtained by reacting compound **12** with small molecules as H_2, NH_3 or P_4 due to the fact that a certain degree of a Ge^0 species is observed theoretically.

The activation of small molecules was performed by reacting the (SIMPY)Ge complex **12** with ammonia-borane BH_3NH_3 (H_2 source), CO_2, PhC$\equiv$CPh, P_4, S_8, BH_3, AdaC$\equiv$P and H_2O in THF at room temperature. Surprisingly, the (SIMPY)Ge complex **12** is so stable that no reactions occur with NH_3BH_3, CO_2, PhC$\equiv$CPh, P_4 and AdaC$\equiv$P at all. The reaction solutions were stirred at room temperature for several days. Furthermore, heating and ultrasonication were

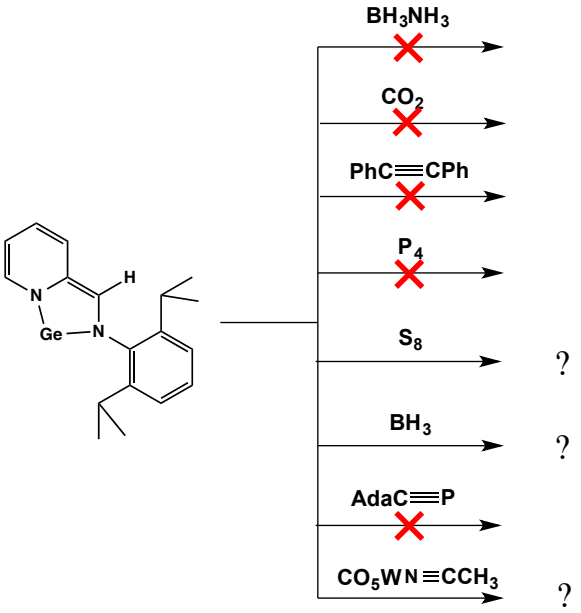

Figure 3.27: Various reactions of small molecules with the (SIMPY)Ge complex **12** were carried out in THF at room temperature.

performed, too. However, no activation of small molecules was observed. This can be explained by the 10 π cyclization which stabilizes the germylene very effectively. Hence, a dramatic change has to be made to disturb the aromaticity and is therefore thermodynamically not favored. Another reason could be that the energy separation of the frontier orbitals with 3.7 eV is not small enough for the activation of small molecules. The reaction with S_8 gives the SIMPY ligand system in solution and an insoluble precipitate which is presumably germanium sulfide GeS. Reacting the (SIMPY)Ge with BH_3 gives a bright red solution with a dark brown precipitate. NMR spectra could not be obtained which indicates radical species. Unfortunately, no solid state structures could be obtained. The reaction with H_2O gives again an insoluble powder which prevented the recrystallization and further characterization.

3.2.1 Synthesis of Group 13 Complexes Using the SAMPY Ligand

Low valent group 13 complexes are of high interest in main group chemistry.[4,90,94,95,154] Group 13 elements (M= Al, Ga) prefer the oxidation state +3 based on stabilizing effects. The oxidation state of +1 is not thermodynamically favored. The isolation of kinetically stable Al^{I} and Ga^{I} species bears many difficulties. However, working groups reported the synthesis of Al^{I} and Ga^{I} complexes stabilized by N,N bidentate ligands.[4,90,154] Furthermore, research groups were interested in synthesizing multiple bond species containing group 13 elements. However, multiple bond compounds as for example dimetallenes are less investigated.[94,95] Stable and isolatable group 13 dimetallenes were only reported for the heavier elements Ga, In and Tl. The multiple bond species ArM=MAr (M=Ga, In and Tl) have to be stabilized by bulky aryl substituents as C_6H_3-2,6-(C_6H_3-2,6-$^{i}Pr_2)_2$ (Ar), but when the ligand system got bulkier only monomeric species were obtained. The corresponding ArAl=AlAr complex could not be isolated.[95] Compounds with triple bond character are rare. Well investigated species are the Na_2[ArMMAr] dianions (M= Al, Ga) and Na_2[Ar'GaGaAr'] (Ar'= C_6H_3-2,6(C_6H_2-2,4,6- $^{i}Pr_3)_2$).[95]

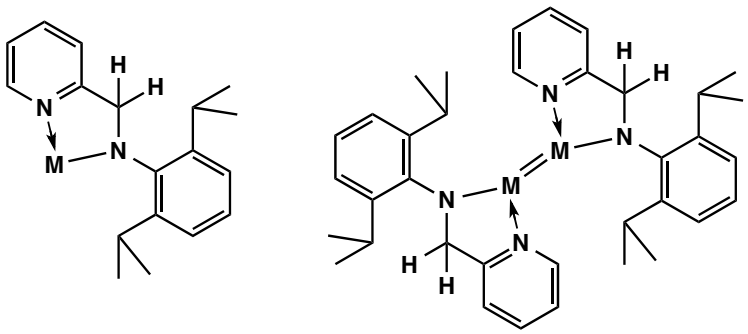

Figure 3.28: Target molecules in this PhD thesis are low valent group 13 complexes stabilized by the SAMPY ligand.

In this PhD thesis target molecules are Al^I and Ga^I species stabilized by the SAMPY ligand system as shown in Figure 3.28. The SAMPY ligand does not possess two bulky aryl substituents in comparison to the sterically encumbered terphenyl systems and bears only one diisopropylphenyl group for steric protection. However, the pyridenyl functionality represents an effective protection due to donor-acceptor interactions. Less bulkiness, but additional stabilization *via* the donor functionality could also lead to multiple bond species of Al and Ga.

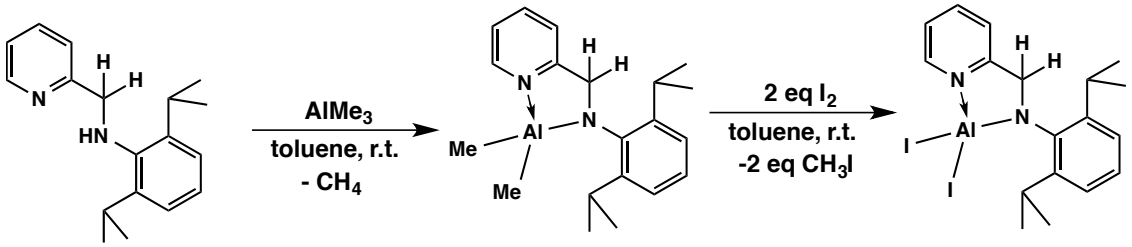

Figure 3.29: The synthesis of (SAMPY)Al precursors.

The synthesis of (SAMPY)Al precursors are shown in Figure 3.29. This straight forward synthetic method was also implemented by Roesky and coworkers synthesizing β-diketiminatoaluminumdiiodide $LAlI_2$ (L= CH[(CMe)(2,6-$^i Pr_2C_6H_3N$)]$_2$).[90] Reduction of the diiodide precursor with 2 eq of K metal at room temperature gave a monomeric Al^I complex. The halogenated (SAMPY)AlI_2 precursor can be reduced with alkali metals, Li- or K-selectrides or further reducing agents to give a low valent Al^I compound. As displayed in Figure 3.29 the SAMPY ligand was first reacted with $AlMe_3$ to give the (SAMPY)$AlMe_2$ complex **14** *via* methane elimination. The reaction is carried out in toluene at room temperature and forms a bright yellow greenish solution. After stirring over night, all volatile components were removed *in vacuo* and an off white powder was obtained in high yields as confirmed by NMR measurments. Crystals were grown out of a concentrated solution in toluene. Compound **14** was fully characterized by ^1H and ^{13}C NMR, elemental analysis and *via* solid state structure analysis.

The reaction conditions to form the aluminum diiodide complex **15** were varied. At first an in situ reaction was performed. After the addition of $AlMe_3$ to the SAMPY ligand in toluene and stirring over night, two equivalents of I_2 dis-

solved in toluene were added at -30°C. The yellow greenish solution turned dark red. After 30 minutes the dark red solution turned again yellow greenish and the solution was warmed up to room temperature and stirred over night. All volatile components were reduced *in vacuo* and the obtained white powder was recrystallized in toluene at -30°C. The ^{1}H and ^{13}C NMR spectra indicate that complex **15** was formed, but that byproducts were formed as well. Mixtures of the desired product **15** with a mixed species (SAMPY)AlMeI and a ligand exchange product $(SAMPY)_2AlI$ **16** were observed. Also variations of temperature, reaction time, addition rate of I_2 and various attempts to recrystallize the obtained powder could not yield pure **15**. Furthermore, it was tried to obtain compound **15** *via* a two step reaction. First synthesizing $(SAMPY)AlMe_2$ **14**, reduce all volatile components and then the addition of two equivalents of iodide followed. This attempt gives the ligand exchange product **16** in high yields of about 36%. The formation of $(SAMPY)_2AlI$ **16** can be explained by a ligand exchange reaction between two $(SAMPY)AlI_2$ complexes. The two $(SAMPY)AlI_2$ compounds redistribute into AlI_3 and the corresponding $(SAMPY)_2AlI$ complex **16**. The $(SAMPY)_2AlI$ complex **16** was fully characterized by ^{1}H and ^{13}C NMR, elemental analysis and solid state structure analysis. The ^{1}H and ^{13}C NMR of compounds **14** and **16** do show a low field shifting of the diisopropyl functionalities as typically observed for metal coordinated SAMPY complexes.

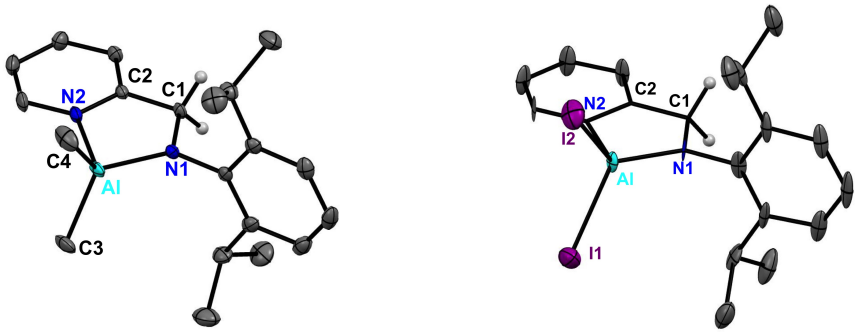

Figure 3.30: Solid state structure of the (SAMPY)$AlMe_2$ complex **14** and the (SAMPY)AlI_2 complex **15**. Anisotropic displacement parameters are depicted at the 50% probability level. Hydrogen atoms are omitted for clarity except at the CH_2 group.

In Figure 3.30 the isolated solid state structures of compound **14** and **15** are shown and the bond lengths and angles are given in Table 3.5. The complexes **14** and **15** crystallize in the monoclinic space group $P2_1/c$. The Al center is four-fold coordinated and the complexes can be described as pseudo tetrahedral. The N1-Al-N2 angles are 84.98(4)° regarding compound **14** and 88.95(4)° for compound **15**. The N1-Al-X1 (X1 represents either a methyl group or I atom) is 118.49(5)° for compound **14** and slightly higher with 121.05(3)° for complex **15**. In case of compound **14**, two nitrogen atoms of the SAMPY ligand and two methyl groups are covalently bonded to the Al^{III} atom. The bond lengths are for Al - N1 1.843(9) Å and for Al - N2 1.976(9) Å which are in typical range of Al - N distances varying from 1.806(3) Å to 1.977(4) Å in literature.[155–157] In case of the coordinated methyl groups a bond lengths of Al - C (or Al - X in Table 3.5) around 1.96 Å is observed. This value agrees very well with literature known Al - C distances ranging from 1.928(6) to 2.051(5) Å.[155–157]

Table 3.5: Bond lengths [Å] and angles [°] of compounds (SAMPY)$AlMe_2$ **14**, (SAMPY)AlI_2 **15** and $(SAMPY)_2AlI$ **16**.

Bond lengths and angles	**14**	**15**	**16**
Al – N1	1.843(9)	1.809(8)	1.838(5)
Al – N2	1.976(9)	1.923(8)	2.058(5)
Al - X1	1.956(1)	2.492(3)	2.610(5)
Al - X2	1.973(2)	2.487(3)	-
C1 - N1	1.447(1)	1.439(1)	1.469(5)
C1 – C2	1.504(1)	1.503(1)	1.497(6)
N1-Al-X1	118.49(5)	121.05(3)	91.14(5)
N1-Al-N2	84.98(4)	88.95(4)	82.52(5)

In case of the (SAMPY)AlI_2 complex **15**, Al - N distances of Al - N1 with 1.809(8) Å and an expected elongated donor-acceptor interaction Al - N2 is observed with 1.923(8) Å. These values agree well with literature known Al - N distances[155–157] and with the (SAMPY)$AlMe_2$ complex **14**. The Al - I bond lengths are elongated as expected with Al - I1 of 2.492(3) Å and Al - I2 of 2.487 Å compared to the Al - C distances of complex **14**. The C1 - N1 distances around 1.45 Å as well as the C1 - C2 bond lengths around 1.50 Å of the SAMPY ligand are similar and bear values as expected for the ligand system. Compound **16** crystallizes in the monoclinic space group C2/c and the Al^{III}

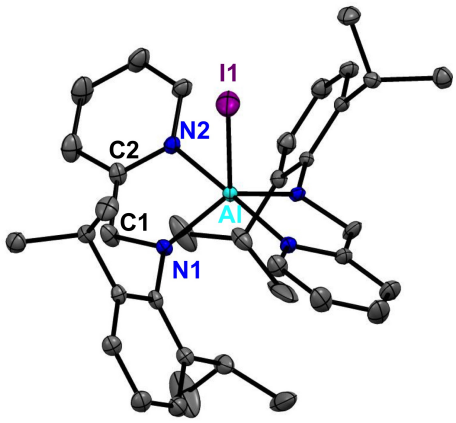

Figure 3.31: Solid state structure of the $(SAMPY)_2AlI$ complex **16**. Anisotropic displacement parameters are depicted at the 50% probability level. Hydrogen atoms are omitted for clarity.

atom is fivefold coordinated bearing a pyramidal environment. The asymmetric unit possesses only one SAMPY ligand coordinating AlI and the second SAMPY ligand is symmetry generated. Therefore bond lengths are only given for one ligand system in Table 3.5. The I atom is nearly perpendicular to the (SAMPY)Al unit and has an angle N1-Al-I1 of 91.14°. The angle N1-Al-N2 is 82.52(5)° and shortened compared to complexes **14** and **15**. The Al^{III} atom is bonded covalently to two N atoms with a distance of Al - N1 with 1.838(5) Å. The Al - N_{py} distances are elongated as expected with 1.497(6) Å. These bond lengths agree well with the Al - N distances of complexes **14** and **15** and with literature known complexes.[155–157] The Al - I1 distance is 2.610(5) Å and elongated compared to the Al - I distances of complex **15**. This can be explained by the different environments the Al center is coordinated. In complex **15**, the Al center is in a pseudo tetrahedral environment and fourfold coordinated. In

compound **16**, more substituents are coordinating the Al atom which leads to the longer Al - I1 distance in the pyramidal environment. The C1 - N1 and C1 - C2 distances are in the expected range and agree well with compounds **14** and **15**. No reduction reactions were accomplished due to the impurities involved in the (SAMPY)AlI_2 complex **15**. Due to the ligand exchange reaction leading to complex **16**, the SAMPY ligand system is not suitable to synthesize Al^{I} species.

The synthesis of the low valent Ga^{I} complex was performed *via* the lithiation of the SAMPY ligand. The lithiation of the SAMPY ligand was extensively dis-

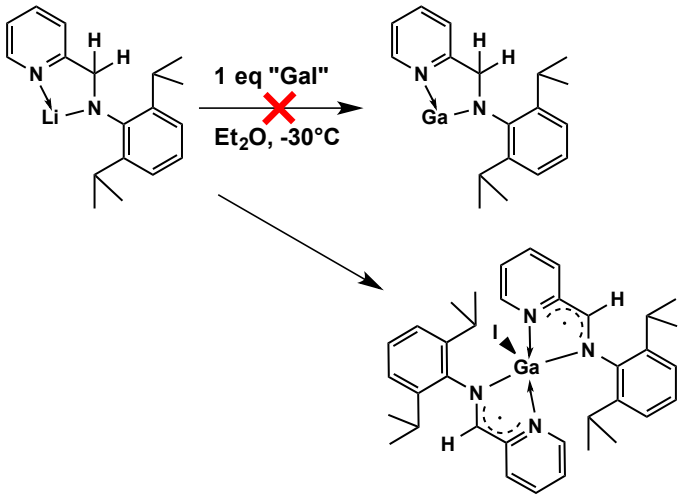

Figure 3.32: The equimolar reaction of SAMPYLi with "GaI" gives not the desired SAMPYGa complex. A redox process leads to the radical species (SIMPY•)$_2$GaI.

cussed in chapter 3.2. The SAMPY ligand was dissolved in pentane, cooled to -30°C and ^{n}BuLi was added slowly. The yellow powder was rapidly transferred in the dry box where it was kept at -30°C. When the yellow powder is warmed up to room temperature, the SAMPYLi complex decomposes by forming a red solid. At -30°C "GaI" was added to the SAMPYLi dissolved in THF. After 30 minutes at low temperatures, a dark green solution is formed and stirred over night. ^{1}H and ^{13}C NMR only showed the SAMPY ligand system in reaction solution. Therefore, EPR measurements were performed confirming a radical species. Dark green cubic crystals were collected after recyrstallization in THF at -30°C. The solid state structure analysis confirms the radical complex (SIMPY•$^{-}$)$_2$$Ga^{+}$I complex **17**. Related complexes were reported as the (SIMPY•)$_2$GaX (X= Cl, OH, TEMPO) complexes obtained *via* the reaction

of two equivalents SIMPY ligand with 3 equivalents $GaCl_3$ in presence of 3 equivalents Na metal.[21] The solid state structure is displayed in Figure 3.33. Compound **17** crystallizes in the monoclinic space group I2/a and bears a trig-

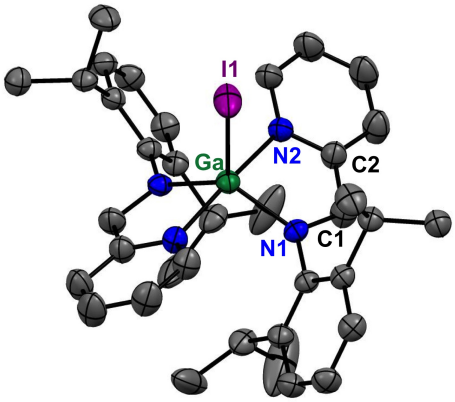

Figure 3.33: The solid state structure of compound **17**. Selected bond lengths and angles: Ga - N1, 1.907(4) Å; Ga - N2, 2.130(4) Å; Ga - I1, 2.567(4) Å; C1 - N1, 1.417(4) Å; C1 - C2, 1.467(3) Å; N1-Ga-N2, 80.88(4)°; N1-Ga-I1, 116.17(4)°. Anisotropic displacement parameters are depicted at the 50% probability level. Hydrogen atoms are omitted for clarity.

onal pyramidal in geometry. The asymmetric unit bears only the SIMPYGaI unit and the other SIMPY ligand is symmetry generated. Therefore only one ligand site is discussed. The Ga atom is fivefold coordinated with Ga - N distances of Ga - N1 with 1.907(4) Å and Ga - N2 with 2.130(4) Å. The Ga - N distances of literature known complexes are ranging from 1.775(2) to 1.958(2) Å and agree well with complex **17**. The Ga - I1 distance is 2.567(4) Å. Due to the monoanionic ligand, the imino bond C_{im} - N_{im} is elongated with 1.417(4) Å and the C_{im} - C_{py} bond is shortened with 1.467(3) Å and is in good agreement with the $(SIMPY^{\bullet -})_2Ga^{+}X$ (X= Cl, OH, TEMPO)[21] and related species.[18,25,52] EPR measurements were performed for compound $(SIMPY^{\bullet -})_2Ga\ ^{+}I$ **17** and a signal at g= 2.0027(1) was observed. This finding is in good agreement with the literature known complexes $(SIMPY^{\bullet -})_2Ga^{+}X$ (X= Cl, OH, TEMPO).[21]

3.3 Synthesis of Low Valent Group 14 Complexes Using Iminopyridine Ligand Systems

The synthesis of low valent group 14 compounds is very challenging. The synthetic route as well as the ligand systems are crucial for the successful isolation of group 14 elements in low oxidation states.[26,27] The purity of these compounds as well as the amount and the yield are important, particularly when further reactions are planned as the activation of small molecules. Several routes lead to low valent group 14 complexes which are stabilized by N, N bidentate ligand systems.[26,27] N, N bidentate ligand systems stabilizing low valent group 14 complexes showed a fascinating reaction chemistry in context of activating small molecules.[27,29] The SAMPY and the SIMPY ligand system have great potential to stabilize low valent group 14 complexes. As presented previously in chapter 3.2, the SAMPY ligand was used to stabilize Ge, Sn and Pb in low oxidation states. The synthetic route involved transamination reactions as well as lithiation of the SAMPY ligand and subsequent transmetalliation *via* salt elimination and gave highly interesting low valent main group complexes. The (SIMPY)Ge complex **12** bears a very interesting bonding motif, namely an iminopyridine ligand coordinating towards a Ge atom, which contains a certain degree of an oxidation state zero species. Could it be possible to synthesize this species and related heavier group 14 element complexes using directly the SIMPY and DIMPY ligand systems?

A possible reaction pathway is shown in Figure 3.34 for the SIMPY ligand system. Iminopyridine ligands have the ability to donate or accept negative charge as shown by the resonance structures in Figure 3.3 discussed in chapter 3.1. Hence, they can donate towards E^{II} species as $E^{II}(N(SiMe_3)_2)_2$ or $E^{II}X_2$ (E= Ge, Sn, Pb; X= Cl, Br, I, CF_3SO_3) to give iminopyridine group 14 complexes. These stabilized iminopyridine group 14 complexes act as precursors for highly reactive group 14 element compounds. The iminopyridine precursors can be reacted with various reducing agents as alkali metals, Li- and K-selectrides and other mild reducing agents to presumably give the desired group 14 complexes. In case of the reaction with alkali metals, salt elimination is the driving force to obtain low valent group 14 complexes stabilized by iminopyridine ligand systems. In case of Li or K-selectrides, a possible in-

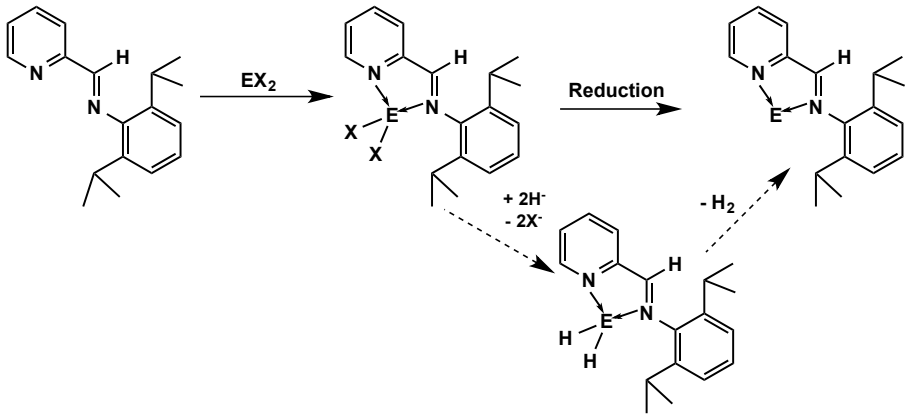

Figure 3.34: The synthetic route to obtain low valent group 14 complexes using iminopyridine ligands (an example is given for the SIMPY ligand). The (SIMPY)EX_2 precursors react with alkali metals or mild reducing agents to give low valent group 14 complexes.

termediate are labile (SIMPY)EH_2 complexes which release H_2 to form low valent group 14 complexes (Figure 3.34). In this chapter iminopyridine precursors are synthesized, isolated and fully characterized based on the SIMPY and DIMPY ligand systems. Various different iminopyridine precursors were synthesized varying the leaving groups within the complex. The leaving groups in the iminopyridine precursors are Cl^-, Br^-, I^- or OTf^- (OTf= CF_3SO_3). Depending on the leaving groups, differences in the complexes are investigated regarding the respective spectroscopical observations and solid state structure analysis. Therefore, a different reactivity concerning the reduction reactions could result. The successful reduction of the complex is depending the leaving group which determines the E - X bond strength towards the element center. Therefore, several iminopyridine precursors are synthesized and subsequently reacted with various reducing agents.

3.3.1 The SIMPY Ligand + $E(N(SiMe_3)_2)_2$: Unusual Elimination at the Ligand Backbone

The synthetic goal was to obtain group 14 complexes where loose donor-acceptor interactions of the ligand system SIMPY towards the group 14 element center are present. Further reductions with mild reducing agents as for example phenylsilane $PhSiH_3$ could lead to highly reactive group 14 complexes due to formation of H_2 as shown in Figure 3.34. However, these complexes were not observed. The reaction of the SIMPY ligand with $E(N(SiMe_3)_2)_2$ (E= Ge, Sn, Pb) forms $SIMPY_2E$ complexes where the low valent group 14 complex is coordinated by the C atom at the backbone of the ligand system as shown in Figure 3.35. Therefore, an elimination reaction at the backbone of the ligand systems takes place forming hexamethyldisilazane as a byproduct. The elimination of the hydrogen at the backbone is a new phenomenon regarding the SIMPY ligand system. In literature, elimination of the H atom at the CH_2 functionality of the SAMPY ligand system was investigated leading to C-C coupling reactions.[51]

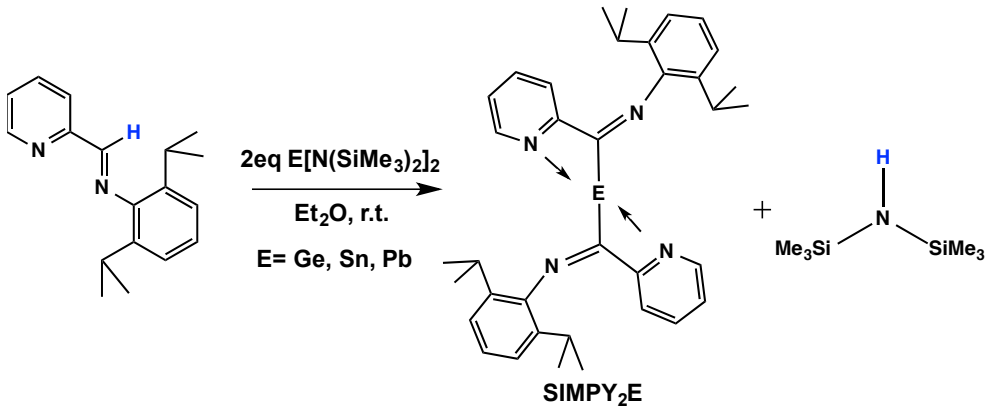

Figure 3.35: Two equivalents of the SIMPY ligand react with one equivalent of $E(N(SiMe_3)_2)_2$ (E= Ge, Sn, Pb) to give $SIMPY_2E$ complexes.

The reaction of two equivalents SIMPY with $E(N(SiMe_3)_2)_2$ (E= Ge, Sn, Pb) in diethyl ether gives the $SIMPY_2Ge$ complex **18**, the $SIMPY_2Sn$ complex **19** and the $SIMPY_2Pb$ complex **20** at room temperature (Figure 3.35). These complexes are obtained due to the elimination of the H atom at the backbone of the ligand

system, forming $HN(SiMe_3)_2$ as a byproduct.[¶] Although the stoichiometric ratio was varied (1:1) to give the heteroleptic $(SIMPY)EN(SiMe_3)_2$ complexes, the $SIMPY_2E$ species were always the final product. The reaction depends on the pK_a value of the H atom at the ligand backbone. In the Bordwell tables, pK_a values of protons next to imino functionalities are ranging from 20 to 26.[158] Therefore, the H atom is acidic enough to react with $E(N(SiMe_3)_2)_2$ (E= Ge, Sn, Pb). However, the reaction time varies depending on the group 14 element. In case of E= Ge, full conversion was achieved after one week of reaction time forming a dark red solution. In case of E= Sn or Pb, the conversion to $SIMPY_2E$ complexes was never completed. The starting materials were always present in reaction solution and could not be separated *via* recrystallization due to similar polarities. Therefore, a driving force has to be implemented for the reactions with $Sn(N(SiMe_3)_2)_2$ and $Pb(N(SiMe_3)_2)_2$. A base, as for example $KN(SiMe_3)_2$ could react with the SIMPY ligand, eliminating the proton at the backbone to give the SIMPYK salt and KH as byproduct. NMR tube reactions did show better conversions, but a full conversion was not observed. Therefore, an even stronger base has to be reacted with the SIMPY ligand system. This is not part of this PhD thesis and will be investigated in future work. The complexes were characterized by heteronuclear NMR spectroscopy and a solid structure could be isolated in case of $SIMPY_2Pb$.

[¶] Preliminary studies by Elisabeth Verwüster, Master Thesis, Department of Inorganic Chemistry, TU Graz

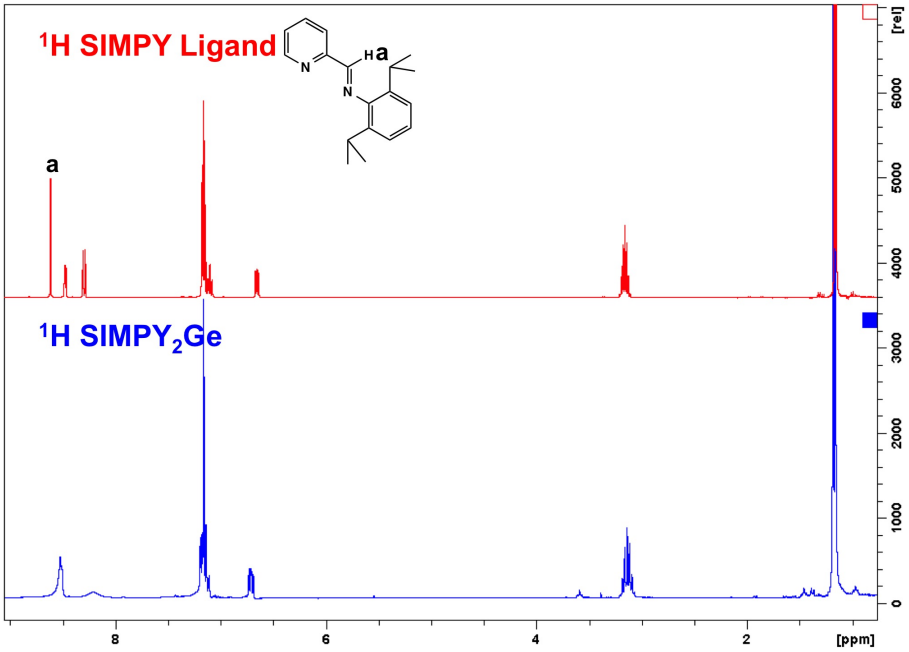

Figure 3.36: The comparsion of the ^{1}H NMR spectra of the SIMPY ligand with the reaction solution of the SIMPY$_2$Ge complex **18**. The **H**C=N proton **a** in the SIMPY$_2$Ge NMR (blue) is vanished, as displayed.

A comparsion of the ^{1}H NMR spectra of the SIMPY$_2$Ge complex **18** and the SIMPY ligand are displayed in Figure 3.36. An important signal in the SIMPY ligand ^{1}H NMR is the **H**C=N proton at 8.75 ppm. This signal is missing in the SIMPY$_2$Ge spectrum. Therefore, a full conversion could be obtained. Interestingly, the diisopropyl groups displaying a septet of the C**H**(CH$_3$)$_3$ proton at 3.10 ppm and and a doublet of CH(C**H**$_3$)$_3$ at 1.20 ppm are only slightly effected. As discussed in chapter 3.2, the diisopropyl substituents of the (SIMPY)Ge complex were much more effected and shifted towards high field. This can be explained by the fact that the C atom is covalently bonded to the element center and the N atom of the imino bond C=N isn't. Hence, the diisopropyl substituents are less effected by the electronic environment of the Ge atom. Furthermore, the signals in the aromatic region are slightly broadened. In case of E= Sn and Pb, similar spectra are observed. These effects correlate with the measured ^{13}C NMR spectra for compounds **18**, **19** and **20**.

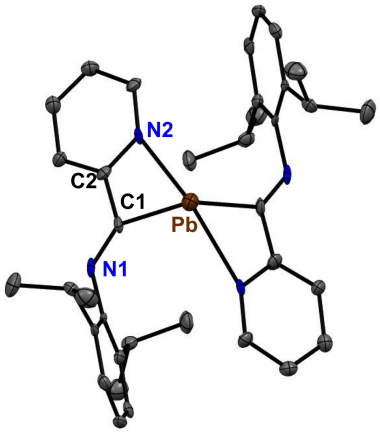

Figure 3.37: The solid state structure of compound **20**. Selected bond lengths and angles: Pb-C1, 2.356(2) Å; Pb - N2, 2.561(2) Å; C1 - C2, 1.428(1) Å; C2 - N2, 1.338(1) Å; C1 - N1, 1.322(1) Å; C1-Pb-N2, 55.02(2)°. Anisotropic displacement parameters are depicted at the 50% probability level. Hydrogen atoms are omitted for clarity.

Compound **20** crystallizes in the tetragonal space group $P\bar{4}2_1c$ and the asymmetric unit contains the SIMPYPb fragment. The other SIMPY ligand site is symmetry generated. Therefore, only one ligand fragment will be discussed. The Pb atom is in a pseudo pyramidal environment and is fourfold coordinated by two C atoms and two N atoms. The Pb - C bond is covalent and has a bond length of 2.356(2) Å. In literature, covalent Pb - C single bond lengths range from 2.240(11) Å to 2.431(11) Å for an E^{II} species which is in good agreement with the observed distance.[159,160] The donor-acceptor interaction Pb - N2 is 2.561(2) Å long which agrees well with donor-acceptor interactions Pb - N ranging from 2.406(2) Å to 2.631(4) Å known in literature.[159,160] The SIMPY

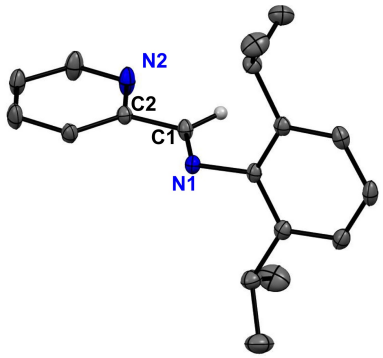

Figure 3.38: The solid state structure of the SIMPY ligand. Selected bond lengths: N1- C1, 1.270(2) Å; C2 - N2, 1.339(2) Å; C1 - C2, 1.473(3) Å. Anisotropic displacement parameters are depicted at the 50% probability level. Hydrogen atoms are omitted for clarity except the HC=N proton.

ligand system crystallizes in the tetragonal space group $P\bar{4}2_1c$ as shown in Figure 3.38. The imino bond N1 - C1 is 1.270(2) Å long. In complex **20** the N1 - C1 bond length is elongated with 1.322(1) Å although no direct coordination is observed. However, coordination towards the Pb center changes the ligand system. The C1 - C2 in the backbone is shortened with 1.428(1) Å compared to the neutral SIMPY ligand with C1 - C2 of 1.473(3) Å. The C2 - N2 distance in the pyridine ring remains more or less the same. The C1-Pb-N2 angle is very sharp with 55.02(2)°. This sharp angle corresponds with the shortened C1 - C2 distance in the backbone of the ligand system.

3.3.2 The SIMPY Ligand and E^{II} Halogenides

A common synthetic route to obtain low valent group 14 complexes is the synthesis of halogenated precursors and their subsequent salt elimination.[27,90,95] This reaction pathway led to various highly interesting low valent group 14 complexes.[27,90,95] The synthesis, isolation and characterization of (SIMPY)EX_2 salts is discussed in this PhD thesis. Furthermore, reduction reactions with various reducing agents were performed for these (SIMPY)EX_2 complexes. In literature, a related MeOSIMPY ligand reacts with $E^{II}X_2$ to give an ion pair $[MeO(SIMPY)EX]^+[EX_3]^-$.[57] Interestingly, ion paring was not observed in case of the unmodified SIMPY ligand.

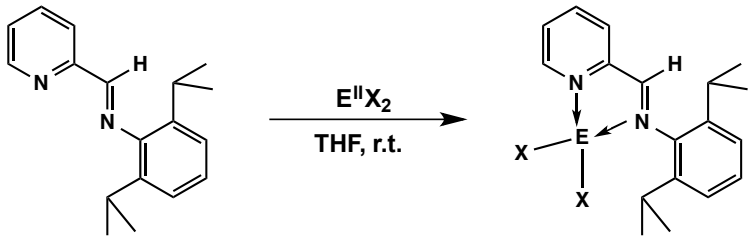

Figure 3.39: The equimolar reaction of the SIMPY ligand with EX_2 (E= Ge, Sn; X= Cl, Br, I, OTf) (OTf= CF_3SO_3) gives (SIMPY)EX_2 complexes.

The equimolar reaction of the SIMPY ligand with either GeX_2*dioxane (X= Cl, Br) or SnX_2 (X= Cl, Br, I, OTf) (OTf= CF_3SO_3) in THF at room temperature gives the neutral (SIMPY)EX_2 complexes after 15 minutes reaction time. The reaction solution turned from yellow to orange in case of the (SIMPY)$GeCl_2$ **21**, the (SIMPY)$GeBr_2$ **22** and the (SIMPY)$SnCl_2$ **23** complexes. In case of the (SIMPY)$SnBr_2$ **24** and the (SIMPY)SnI_2 **25** complexes dark red reaction solutions were obtained and for the (SIMPY)$SnOTf_2$ complex **26** a dark yellow solution was investigated. After stirring at room temperature, the solvent was reduced to give colored powders in high yields around 99%. Complexes **21**, **22**, **23**, **24** and **25** were fully characterized *via* heteronuclear NMR spectroscopy, elemental analysis and solid state structure analysis. Complex (SIMPY)$SnOTf_2$ **26** was fully characterized by heteronuclear NMR spectroscopy and elemental analysis, but no solid state structure could be isolated.

The (SIMPY)EX_2 complexes are only soluble in etheric solvents, especially in THF. Therefore, the ^{13}C and ^{119}Sn NMR spectra were recorded in a mixture

of C_6D_6 and THF to obtain sufficiently concentrated solutions. The ^{1}H NMR of the SIMPY ligand shows significant signals for the **H**C=N proton at 8.75 ppm, for the C**H**$(CH_3)_3$ proton a septet at 3.10 ppm and for CH(C**H**$_3)_3$ a doublet at 1.20 ppm. The SIMPY ligand donates negative charge towards the vacant π orbital of the E^{II} fragment. The SIMPY ligand is a neutral donor. Due to the coordination towards an E^{II} atom the **H**C=N proton is shifted towards low field as shown in Table 3.6. The signals range from 8.84 ppm for complex (SIMPY)$GeCl_2$ **21** to 9.94 ppm for (SIMPY)$SnBr_2$ **24**. It can be concluded that the heavier the group 14 element and the heavier the halogen the more the signal is shifted to low field. Interestingly, the **H**C=N proton of the (SIMPY)SnI_2 is a little less shifted to low field at 9.21 ppm compared to the (SIMPY)$SnBr_2$ **24** at 9.94 ppm.

Table 3.6: Comparison of ^{1}H and ^{119}Sn NMR signals of the SIMPY ligand and of the compounds (SIMPY)$GeCl_2$ **21**, (SIMPY)$GeBr_2$ **22**, (SIMPY)$SnCl_2$ **23**, (SIMPY)$SnBr_2$ **24**, (SIMPY)SnI_2 **25** and (SIMPY)$SnOTf_2$ **26**.

Compound	**H**C=N	C**H**$(CH_3)_3$	CH(C**H**$_3)_3$	^{119}**Sn**
SIMPY	8.75	3.10	1.20	-
21	8.84	3.18	1.23	-
22	8.85	3.17	1.22	-
23	9.18	3.13	1.27	-216.3
24	9.94	2.94	1.12	-80.07
25	9.21	3.00	1.08	317.2
26	9.43	2.65	1.24	-27.75

The shifting of the diisopropyl substituent is inconclusive. For the complexes (SIMPY)$GeCl_2$ **21**, (SIMPY)$GeBr_2$ **22** and (SIMPY)$SnCl_2$ **23**, a low field shifting is observed. In case of the complexes (SIMPY)$SnBr_2$ **24**, (SIMPY)SnI_2 **25** and (SIMPY)$SnOTf_2$ **26**, a high field shifting for the C**H**$(CH_3)_3$ ranging from 3.00 ppm to 2.65 ppm is investigated. For the CH(C**H**$_3)_3$ protons, a low field shifting for the complexes (SIMPY)$SnBr_2$ **24** and (SIMPY)SnI_2 **25** is observed, but for the (SIMPY)$SnOTf_2$ complex **26** a low field shifting with 1.24 ppm is the case. Furthermore, for the (SIMPY)$SnOTf_2$ complex **26** broadend signals in the ^{1}H spectrum are investigated. The ^{13}C NMR spectra correlate with the trends observed in the ^{1}H NMR spectra. The ^{119} Sn NMR shows signals for (SIMPY)$SnCl_2$ **23** at -216.3 ppm, for the (SIMPY)$SnBr_2$ **24** at -80.07 ppm, for (SIMPY)SnI_2 **25** at 317.2 ppm (very broad signal) and for the (SIMPY)$SnOTf_2$ complex **26** at -27.75 ppm. The ^{119} Sn signals of $SnCl_2$ and $SnBr_2$ in THF are at

-236.0 ppm and -70.7 ppm, respectively.[161] These signals correspond well with the observed (SIMPY)Sn chlorides and bromides signals. For SnI_2, only signals in DMF or DMSO are known displaying signals at -152 and 586 ppm,[161] respectively and therefore no comparison can be made. In case of the (SIMPY)EX_2 complexes, the trend is the heavier the halogen bonded towards the Sn^{II} center the more the signals are shifted to low field.

The (SIMPY)GeX_2 complexes **21** and **22** crystallize in the monoclinic space group $P2_1/n$ and display a pseudo tetrahedral geometry (Figure 3.40 and Table 3.7). The Ge center is fourfold coordinated by two N atoms and by two halogen atoms, chloride and bromide. The donor-acceptor interactions of the Ge - N distances are ranging from 2.170(2) Å to 2.490(8) Å. In case of the pyridenyl N_{py} - Ge distances, shorter bond lengths are observed due to the stronger donation of the pyridine ring towards the Ge atom. The imino group C=N is a weaker donor and affords the longer donor-acceptor interactions. The halogen atoms influence the Ge - N distances. The heavier the halogen, the shorter the E - N distances are within the complex.

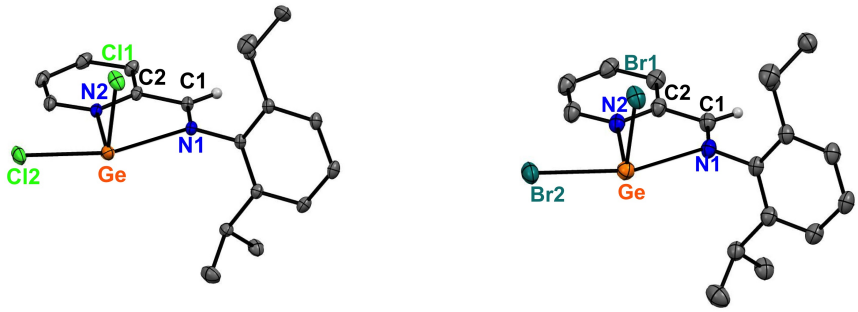

Figure 3.40: Solid state structure of the (SIMPY)$GeCl_2$ complex **21** and the (SIMPY)$GeBr_2$ complex **22**. Anisotropic displacement parameters are depicted at the 50% probability level. Hydrogen atoms are omitted for clarity except at the HC=N functionality.

In case of the Ge - X distances, bond lengths of 2.272(3) Å for Ge - Cl1 and 2.404(3) Å for Ge - Cl2 are observed. The Ge - Br distances are elongated as expected. Interestingly, the halogen atom which is oriented in nearly perpendicular fashion towards the (SIMPY)Ge plane bears shortened Ge - X1 bond lengths compared to the one being in plane. The difference between Ge - Cl and Ge - Br bonds is about 0.2 Å as shown in Table 3.7 which indicates that if a second functionality could get near the coordinations sphere of the GeX_2 frag-

ment, ion pairing can happen by expulsion of the X2 atom. This presumably is the case for the related complex $[MeO(SIMPY)GeCl]^+[GeCl_3]^-$ although the authors do neglect that the methoxy group is involved in the ion pairing process.[57] The difference in bond lengths Δ (E-X2)-(E-X1) is given in Table 3.7 and indicates that if an additional donor molecule or functional group is present, the X2 atom gets squeezed out of the complex forming an anion EX_3, as is the case in the related complex $[MeO(SIMPY)GeCl]^+[GeCl_3]^-$.[57] The Δ (E-X2)-(E-X1) difference is very large for bromide complexes $(SIMPY)GeBr_2$ complex **22** with 0.178 Å and $(SIMPY)SnBr_2$ **24** 0.152 Å which indicates that an ion pairing could be very favored. In case of the $(SIMPY)SnI_2$ complex **25** a Δ (E-X2)-(E-X1) difference of 0.095 Å is observed which could suggest a less favored ion pairing process by the presence of an additional donor functionality.

Table 3.7: Comparison of the bond lengths [Å] and angles [°] of the SIMPY ligand and of the compounds $(SIMPY)GeCl_2$ **21**, $(SIMPY)GeBr_2$ **22**, $(SIMPY)SnCl_2$ **23**, $(SIMPY)SnBr_2$ **24** and $(SIMPY)SnI_2$ **25**.

Bond lengths and angles	**21**	**22**	**23**	**24**	**25**
E – N1	2.490(8)	2.437(2)	2.565(2)	2.552(1)	2.517(6)
E – N2	2.175(8)	2.170(2)	2.364(2)	2.376(2)	2.342(5)
E - X1	2.272(3)	2.432(4)	2.441(6)	2.596(3)	2.902(1)
E - X2	2.404(3)	2.610(4)	2.564(6)	2.748(3)	2.997(1)
C1 - N1	1.271(1)	1.272(3)	1.268(2)	1.273(2)	1.264(8)
C1 – C2	1.469(1)	1.465(3)	1.469(3)	1.465(2)	1.465(1)
N1-E-X1	83.23(2)	82.14(4)	121.05(3)	82.96(3)	90.86(1)
N1-E-N2	71.21(3)	67.31(5)	88.95(4)	67.58(5)	67.81(2)
Δ (E-X2)-(E-X1)	0.132	0.178	0.123	0.152	0.095

The $(SIMPY)SnCl_2$ complex **23** and the $(SIMPY)SnBr_2$ complex **24** crystallize in the monoclinic space group $P2_1/n$ and the $(SIMPY)SnI_2$ complex **25** in the triclinic space group $P\bar{1}$. Similar to their lighter congeners, they show a pseudo tetrahedral complex. As expected, the Sn - N distances are elongated compared to the Ge - N bond lengths due to the bigger atomic radius of the Sn atom. The Sn - N donor-acceptor interactions vary from 2.342(5) Å to 2.565(2) Å. Similar trends of the $(SIMPY)GeX_2$ complexes are applied for the $(SIMPY)SnX_2$ compounds. Consistently, the pridenyl N_{py} is the stronger donor giving the shorter Sn - N bonds than the imino functionality. Furthermore, the heavier the halogen atom gets, the shorter the Sn - N reveal. The Sn - X distances are as expected longer for the heavy halogens and shorter for the chlorine atom. The

Sn - I bond lengths are 2.902(1) Å for Sn - I1, 2.997 Å for Sn - I2 and the Sn - Cl distances are shortened with Sn - Cl1 of 2.441(6) Å and Sn - Cl2 of 2.564(6) Å. The Sn - Br bond lengths are in between the Sn - Cl and Sn - I distances.

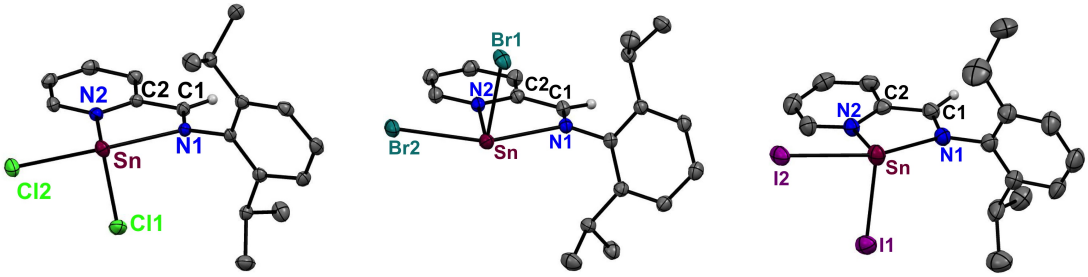

Figure 3.41: Solid state structures of compounds **23**, **24** and **25**. Anisotropic displacement parameters are depicted at the 50% probability level. Hydrogen atoms are omitted for clarity except at the HC=N functionality.

The synthesis and the isolation of the (SIMPY)EX_2 precursors were successful. The final goal was the synthesis of low valent group 14 complexes bearing a similar bonding motif as described for the (SIMPY)Ge complex **12**. Therefore the precursors (SIMPY)EX_2 were reacted with various reducing agents as alkali metals to give low valent (SIMPY)E. The germanium precursors were reacted with two equivalents of Na and K metal as well as C_8K. Additionally, mild re-

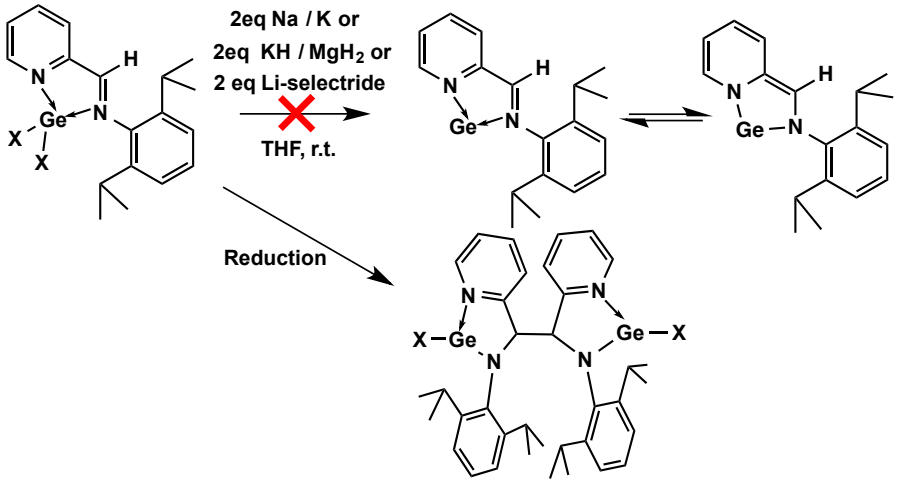

Figure 3.42: The reaction of the (SIMPY)GeX_2 complexes with reducing agents like Na, K, KH, MgH_2 and L-selectride does not give the desired germylene. Instead the $SIMPY_2GeX$ complexes are formed *via* a C-C coupling reaction.

ducing agents as Li-/K-selectrides, KH and MgH_2 were used as well to form the (SIMPY)E complexes *via* the formation of labile intermediates (SIMPY)EH_2

with subsequent elimination of H_2. The reactions were performed in etheric solvents as THF and temperatures were varied ranging from room temperature to -78°C. After stirring the reaction solution over night, dark orange solutions were obtained. However, the (SIMPY)Ge complex was not the observed product after the reduction of the (SIMPY)GeX_2 precursors. Instead, a ((SIMPY)GeX)$_2$ dimer was synthesized as shown in Figure 3.42. The dimer was found to be the main product in all reduction reactions which were performed using the (SIMPY)GeX_2 precursors. However, byproducts were formed which could not be characterized due to the fact that they were presumably radical species which decomposed fast in reaction solution forming SIMPY ligand and a dark precipitate. The dimer was isolated for the chlorine substituted SIMPY complex. The reaction mechanism to form **27** can be explained by the fact that highly reactive radical species are formed during the reaction process. As discussed in chapter 3.1, it is known that a radical is stabilized at the backbone of the ligand system. Therefore, C-C coupling reactions occur by the combination of two radical SIMPY ligand fragments forming a neutral dimer. In case

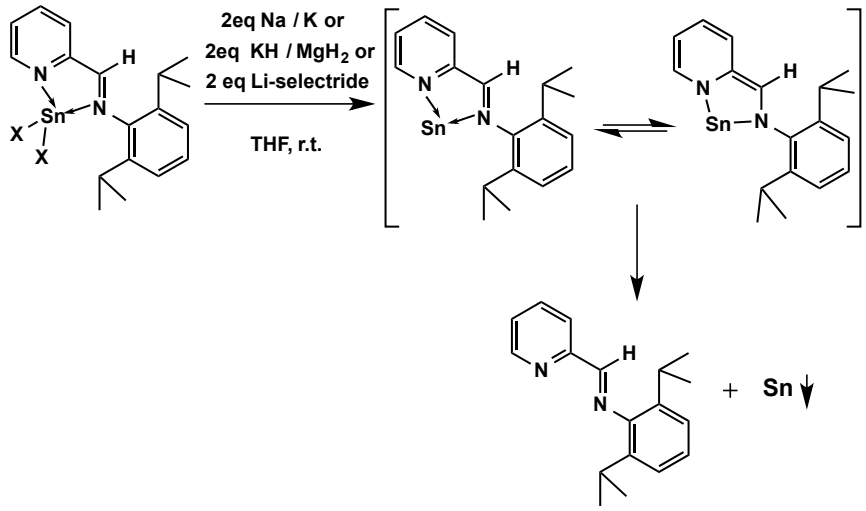

Figure 3.43: The reaction of the (SIMPY)SnX_2 complexes with reducing agents like Na, K, KH, MgH_2 and L-selectride does not give the desired stannylene. Instead the SIMPY ligand is formed and Sn metal precipitates.

of the (SIMPY)SnX_2 precursors, reductions were performed with Na, K metals as well as C_8K. Mild reducing agents such as L- and K- selectrides, KH, MgH_2 and $PhSiH_3$ were used as reducing agents as well. However, the desired stannylene was not observed, no matter which solvents or temperature ranges were applied. The reduction reactions led to SIMPY ligand and precipitated Sn

metal. This can be explained by the fact that the SIMPY ligand is less stabilizing for the low valent Sn element. Comparing Ge and Sn, the Ge element more likely remains in an oxidation state of +2 than the bigger Sn atom which is easily reduced to give Sn^0 metal. This indicates that donor-acceptor interactions are present forming the labile (SIMPY)Sn complex. Therefore, the (SIMPY)Sn complex decomposes immediately forming SIMPY ligand and Sn metal.

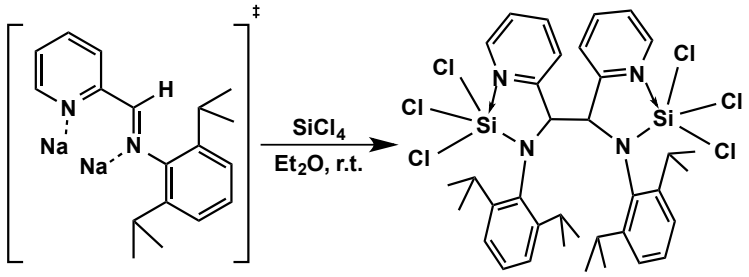

Figure 3.44: The reaction of the $SIMPYNa_2$ intermediate with $SiCl_4$ gives a $SIMPY_2SiCl$ complex *via* a C-C coupling reaction.

Another attempt to synthesize the desired low valent group 14 complexes, was to generate an $SIMPYNa_2$ intermediate (prepared according to literature procedures)[25] followed by the addition of either $SiCl_4$, $SnCl_2$ or $PbCl_2$. In case of the E^{II} precursors $SnCl_2$ and $PbCl_2$, the reaction with $SIMPYNa_2$ could yield directly the (SIMPY)E (E= Sn or Pb) complex. In case of tetravalent $SiCl_4$, a $SIMPYSiCl_2$ precursor could be generated which would yield by further reduction the SIMPYSi compound. However, the desired products were not observed. The reaction of $SIMPYNa_2$ with $SiCl_4$ in THF gave a bright orange solution. After stirring over night, all volatile components were reduced *in vacuo*. The bright orange powder was recrystallized in THF at -30°C to give clear cubic crystals. A similar product was observed as for the reduction reaction with (SIMPY)$GeCl_2$. After single crystal X-ray analysis, the cubic crystals were analyzed as the $(SIMPYSiCl_3)_2$ dimer **28**. The reaction mechanism is presumably similar. A radical anion is formed stabilized at the backbone of the ligand system. The reaction of two radical species (SIMPY•)$SiCl_3$ gave the observed dimer $(SIMPYSiCl_3)_2$ **28** as main product. This C-C coupling reactions are only observed for the lighter group 14 elements Si and Ge. In case of Sn and Pb, the reduction to give Sn and Pb metal is favored. Hence, the reaction of $SIMPYNa_2$ resulted in the precipitation of Sn or Pb metal and SIMPY ligand system even at low temperatures.

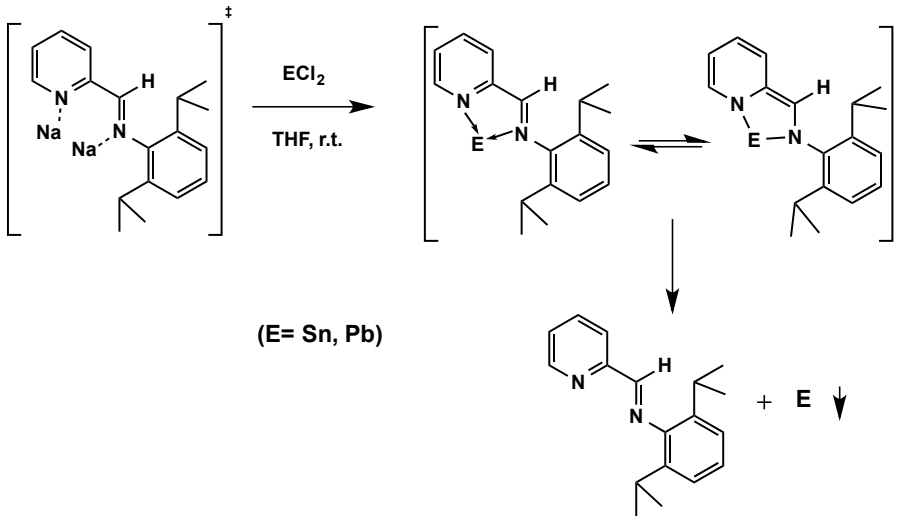

Figure 3.45: The reaction of the $SIMPYNa_2$ intermediate with $SnCl_2$ or $PbCl_2$ does not yield the desired stannylene or plumbylene. Instead the SIMPY ligand is formed and Sn or Pb metal precipitates.

The slightly yellow $((SIMPY)GeCl)_2$ complex **27** and the transparent $(SIMPYSiCl_3)_2$ dimer **28** were fully characterized by heteronuclear NMR, elemental analysis and solid state structure analysis. Due to the C-C coupling no SIMPY ligand is present. Instead a SAMPY ligand system is formed which can be confirmed by NMR spectroscopy and solid state structure analysis. The ^1H NMR spectra do not show the low field shift of the **H**C=N group at around 9 ppm. Instead, a signal at 4.46 ppm for the $((SIMPY)GeCl)_2$ complex **27** and a signal at 4.65 ppm for the $(SIMPYSiCl_3)_2$ dimer **28** is observed which correlates with a related SAMPY ligand system. The diisopropyl group shifts as expected to the low field with signals at 3.64 for the C**H**$(CH_3)_3$ and at 1.39 ppm for the CH(C**H**$_3)_3$ protons for complex **27**. Compound **28** displays similar shifts with signals at 3.77 ppm for the C**H**$(CH_3)_3$ and 1.40 ppm for the CH(C**H**$_3)_3$ protons. These findings are in agreement with the ^{13}C NMR spectra where signals are observed for the C-C atoms at 67.16 ppm (((SIMPY)$GeCl)_2$ complex **27**) and at 65.91 ppm ($(SIMPYSiCl_3)_2$ dimer **28**). Originally, the C=N signal is observed at around 164 ppm. The ^{29} Si NMR spectra of complex $(SIMPYSiCl_3)_2$ **28** displays a signal at -19.09 ppm. This is a relatively highly shifted high field signal for a silicon compound. This high field shift can be explained by the fact that a silicon trichloride is coordinated via two N atoms. One Si - N distance is a donor-acceptor interaction and one is a covalent Si - N bond. Hence, the Si

atom is fivefold coordinated by substituents bearing negative charges and creating a high field shift at -19.09 ppm.

The $((SIMPY)GeCl)_2$ complex **27** crystallizes in the monoclinic space group C2/c. The Ge atoms Ge1 and Ge2 are threefold coordinated and display a pseudo trigonal pyramidal geometry. The (SIMPY)GeCl fragments are slightly

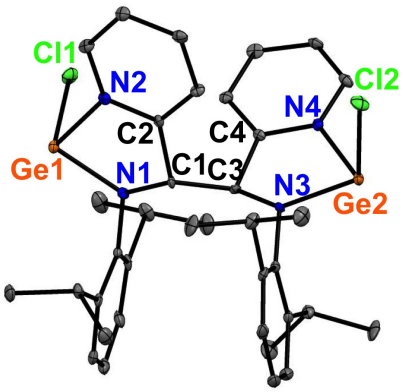

Figure 3.46: Solid state structure of compound **27**. Anisotropic displacement parameters are depicted at the 50% probability level. Hydrogen atoms are omitted for clarity.

different regarding the bond lengths and angles. The Ge1 - N1 and Ge2 - N3 distances are 1.884(4) Å and 1.898(5) Å, respectively, and represent covalent Ge - N bonds. The donor-acceptor interactions Ge1 - N2 and Ge2 - N4 are elongated with about 0.2 Å. The Ge - N distances are in good agreement with literature known Ge - N distances[151] and with the previously discussed $SAMPYGeN(SiMe_3)_2$ and $(SIMPY)GeX_2$ complexes. The Ge1 - Cl1 distance with 2.346(2) Å and Ge2 - C2 with 2.325(1) Å agree with Ge - Cl bonds of complex $(SIMPY)GeCl_2$ and literature known compounds ranging from 2.215(2)[57] to 2.404(3) Å. The angles observed in the complex are N1-Ge1-Cl1 and N3-Ge-Cl2 around 102° and N1-Ge1-N2 and N3-Ge2-N4 around 80 ° which agree with the heteroleptic $SAMPYGeN(SiMe_3)_2$ complex **9**. The solid state structure demonstrates further that the SIMPY ligand system changed due C-C coupling to a related SAMPY ligand system. The C1 - C3 distance is 1.560(7) Å connecting the two (SIMPY)GeCl fragments. The former imino bonds C1 - N1 and C3 - N3 are elongated with 1.473(7) Å and 1.460(6) Å, respectively, compared to the SIMPY ligand. Therefore, they represent amino bonds in complex **27**. The C1 - C2 and C3 - C4 distances in the backbone of the ligand system are

1.527(7) and 1.511(8) Å. These bond lengths agree well with the heteroleptic SAMPYGeN($SiMe_3$)$_2$ complex **9** discussed in chapter 3.2.

Table 3.8: Comparison of the bond lengths [Å] and angles [°] of the SIMPY ligand and of the compounds ((SIMPY)GeCl)$_2$ **27**, (SIMPY$SiCl_3$)$_2$ **28** and the SAMPYGeN($SiMe_3$)$_2$ complex.

Bond lengths and angles	SIMPY	27	28	SAMPYGeN($SiMe_3$)$_2$
E1 – N1	-	1.884(4)	1.743(1)	1.931(1)
E1- N2	-	2.039(4)	1.955(2)	2.083(1)
E2 - N3	-	1.898(5)	1.740(2)	-
E2 – N4	-	2.035(4)	1.956(2)	-
E1 - Cl1	-	2.346(2)	2.089(7)	-
E2 - Cl2	-	2.325(1)	2.098(7)	-
C1 - N1	1.270(2)	1.473(7)	1.482(2)	1.446(2)
C1 – C2	1.473(3)	1.527(7)	1.504(2)	1.498(2)
C3 - N3	-	1.460(6)	1.481(2)	-
C3 - C4	-	1.511(8)	1.501(2)	-
C1 - C3	-	1.560(7)	1.579(2)	-
N1-E1-Cl1	-	103.83(1)	120.92(5)	-
N1-E1-N2	-	80.59(1)	83.83(7)	79.87(4)
N3-E-Cl2	-	101.23(1)	121.69(6)	-
N3-E2-N4	-	80.91(2)	84.18(7)	-

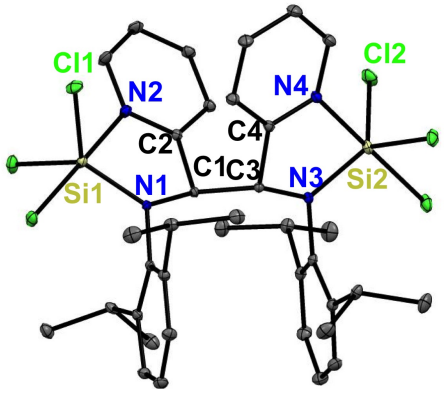

Figure 3.47: Solid state structure of compound **28**. Anisotropic displacement parameters are depicted at the 50% probability level. Hydrogen atoms are omitted for clarity.

Compound (SIMPY$SiCl_3$)$_2$ **28** crystallizes in the tetragonal space group Pbca. The Si atoms Si1 and Si2 are fivefold coordinated by three chlorine atoms and two nitrogen atoms bearing a pyramidal environment. The Si - N distances are ranging from shorter covalent bonds with 1.740(2) Å to 1.956(2) Å for the

donor-acceptor interactions of the pyridinyl N_{py}. These findings agree well with the comparable $SIMPY_2Si$ complex of Berben and coworkers with covalent Si - N bond lengths ranging from 1.740(1) to 1.726(1) Å.[52] The Si - Cl bonds are around 2.09 Å and shortened compared to the Ge - Cl bonds as expected. The C1 - N1 and C3 - N3 distances are around 1.48 Å and agree with the bond lengths of the dimer **27** and the $SAMPYGeN(SiMe_3)_2$ complex **9**. This applies also for the C1 - C2 and C3 - C4 distances with 1.50 Å and the C-C coupling bond length C1 - C3 with 1.579(2) Å.

3.3.3 The Synthesis of Group 14 Element Precursors Stabilized By The DIMPY Ligand and Their Reduction Reactions

The reduction reactions of the (SIMPY)EX_2 precursor were not successful. The SIMPY ligand system could not stabilize the low valent Sn and Pb elements and in case of Si and Ge, C-C coupling reactions occurred. The DIMPY ligand system has an additional imino functionality which bears an additional donor group to stabilize the labile group 14 elements. This additional protecting group could make a huge difference in isolating low valent group 14 elements. The synthetic route is similar to the one synthesizing low valent (SIMPY)E complexes. In the first step DIMPY group 14 element precursors have to be isolated bearing a leaving group as for example Cl, Br, I or OTf (OTf= CF_3SO_3). Then a reduction reaction follows with alkali metals or mild reducing agents. In this chapter DIMPY group 14 element precursors will be synthesized and fully characterized. Furthermore, reduction reactions will be performed to obtain low valent group 14 elements stabilized by the DIMPY ligand system.

In literature, the MeDIMPY ligand was reacted with two equivalents of $GeCl_2$*dioxane or $SnCl_2$ to give the ion pair $[MeDIMPYECl]^+[ECl_3]^-$ (E= Ge, Sn).[40] Another example of reacting EX_2 salts (E= Ge, Sn; X= Cl) with a related MeOSIMPY ligand was reported by Jambor and coworkers[57] which leads to the isolation of further ion pairs. As discussed in chapter 3.3.2, the reaction of the SIMPY ligand with EX_2 salts does not yield ion pairs. In case of the DIMPY ligand system an auto-ionization and therefore the formation of ion pairs is expected due to the second imino functionality. An auto-ionization results when a strong Lewis base is present in reaction solution to coordinate, for example EX_2 salts, as the iminopyridine ligand system DIMPY. In literature, reactions of main group elements with the DIMPY ligand are rare. The reaction of the DIMPY ligand with EX_2 salts are unknown and will be studied for GeX_2 and SnX_2 salts with various counter ions (X= Cl, Br, I or OTf). This study gives new insights in main group element chemistry regarding the tridentate ligand system DIMPY.

The reaction of one equivalent DIMPY with two equivalents of EX_2 gives the ion pairs $[DIMPYEX]^+[EX_3]^-$ (E= Ge, Sn; X= Cl, Br, I) as shown in Figure 3.48. The DIMPY ligand acts as Lewis base and the repulsion of a halogen atom occurs forming the anion $[EX_3]^-$. Hence, the cation $[DIMPYEX]^+$ is observed where the DIMPY ligand coordinates as neutral ligand towards the group 14 element center. The ion pair $[DIMPYEX]^+[EX_3]^-$ bears the group 14 elements in the oxidation state of +2 and is comparable with the ion pair $[MeDIMPYECl]^+[ECl_3]^-$ (E= Ge, Sn).[40] In case of E= Ge, two equiva-

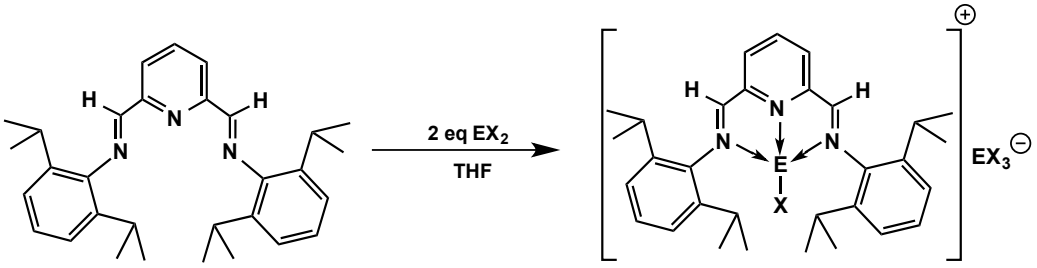

Figure 3.48: The reaction of two equivalents EX_2 (E= Ge, Sn; X= Cl, Br, I) with the DIMPY ligand system gives the ion pair $[DIMPYEX]^+[EX_3]^-$.

lents $GeCl_2$*dioxane or $GeBr_2$*dioxane were reacted with one equivalent of DIMPY in THF at room temperature to obtain the $[DIMPYGeCl]^+[GeCl_3]^-$ complex **29** and the $[DIMPYGeBr]^+[GeBr_3]^-$ complex **30**, respectively. An color change was immediate as the solution turned from yellow to bright orange (**29**) or dark orange (**30**). After stirring for several minutes, the solvent was reduced and an orange powder was obtained. In case of E= Sn, one equivalent DIMPY was reacted with two equivalents of $SnCl_2$ to give the orange $[DIMPYSnCl]^+[SnCl_3]^-$ complex **31**, with two equivalents of $SnBr_2$ to yield the red $[DIMPYSnBr]^+[SnBr_3]^-$ complex **32** and with two equivalents of SnI_2 to obtain the dark red $[DIMPYSnI]^+[SnI_3]^-$ complex **33**. After stirring for several minutes at room temperature, the solvent THF was reduced. The colored powders were obtained in high yields.

Apart from halogens, triflate groups CF_3SO_3 (OTf) are promising counter ions. Therefore, the DIMPY ligand system was reacted with $Sn(OTf)_2$ to give the $DIMPYSnOTf_2$ complex **34**. Interestingly, no auto-ionization occurred. The triflate groups are presumably too tightly bonded towards the Sn atom and the formation of a $Sn(OTf)_3^-$ anion is thermodynamically not favored compared

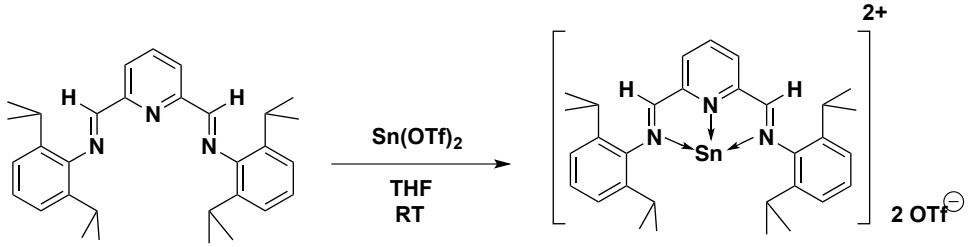

Figure 3.49: The equimolar reaction of the DIMPY ligand with $Sn(OTf)_2$ (OTf= CF_3SO_3) gives the DIMPYSn$(OTf)_2$ complex.

to the related halogen species. The reaction was carried out in THF at room temperature. After stirring for several minutes, a bright orange solution was observed. The solvent was reduced and a bright orange powder was obtained.

The $[DIMPYGeCl]^+[GeCl_3]^-$ complex **29**, the $[DIMPYSnCl]^+[SnCl_3]^-$ complex **31**, the $[DIMPYSnBr]^+[SnBr_3]^-$ complex **32** and the $DIMPYSnOTf_2$ complex **34** were fully characterized by heteronuclear NMR spectroscopy, elemental analysis and solid state structure analysis. The $[DIMPYGeBr]^+[GeBr_3]^-$ complex **30** and the $[DIMPYSnI]^+[SnI_3]^-$ complex **33** were fully characterized as well by heteronuclear NMR spectroscopy and elemental analysis, but no solid state structures were obtained.

Table 3.9: Comparison of ^1H and ^{119}Sn NMR signals of the DIMPY ligand and of the compounds $DIMPYGeCl]^+[GeCl_3]^-$ **29**, $[DIMPYGeBr]^+[GeBr_3]^-$ **30**, $[DIMPYSnCl]^+[SnCl_3]^-$ **31**, $[DIMPYSnBr]^+[SnBr_3]^-$ **32**, $[DIMPYSnI]^+[SnI_3]^-$ **33** and $DIMPYSnOTf_2$ **34**.

Compound	**H**C=N	C**H**$(CH_3)_3$	CH$(CH_3)_3$	^{119}**Sn NMR**
DIMPY	8.55	3.12	1.18	-
29	8.61	3.15	1.25/1.16	-
30	8.61	3.15	1.25/1.16	-
31	8.12	3.12	1.02/0.95	-445.2/-57.9
32	8.61	3.21	1.33/1.23	98.2/-405.8
33	8.40	3.02	1.09	-
34	8.18	3.52	1.27	-46.4

Important ^1H NMR signals are shown in Table 3.10. The DIMPY ligand signals are compared to the signals of the ion pairs $[DIMPYEX]^+[EX_3]^-$. As discussed in chapter 3.3.2 in case of the (SIMPY)EX_2 complexes, a low field shifting is observed for the **H**C=N signal. In case of the complexes $[DIMPYGeCl]^+[GeCl_3]^-$ complex **29**, $[DIMPYGeBr]^+[GeBr_3]^-$ complex **30** and $[DIMPYSnBr]^+[SnBr_3]^-$

complex **32** a low field shifting with a signal at 8.61 ppm is observed. For the complexes $[DIMPYSnCl]^+[SnCl_3]^-$ complex **31**, $[DIMPYSnI]^+[SnI_3]^-$ complex **33** and $DIMPYSnOTf_2$ complex **34** a high field shifting is investigated ranging from 8.12 to 8.40 ppm. For the $CH(C\mathbf{H}_3)_3$ protons of the diisopropyl group, mainly a low field shifting is displayed in the ^1H NMR spectra ranging from 1.16 to 1.33 ppm. Furthermore, the doublet is split to give a doublet of doublets in case of **29**, **30**, **31** and **32**. For the complexes bearing big leaving groups as $[DIMPYSnI]^+[SnI_3]^-$ complex **33** and $DIMPYSnOTf_2$ complex **34**, only one very broad doublet is investigated. All the other signals of these two complexes are broadened as well. For complexes $[DIMPYSnCl]^+[SnCl_3]^-$ **31** and $[DIMPYSnI]^+[SnI_3]^-$ **33** again a high field shifting for the $CH(C\mathbf{H}_3)_3$ protons is displayed in the ^1H NMR spectra. Regarding the $C\mathbf{H}(CH_3)_3$ only for complexes $[DIMPYSnBr]^+[SnBr_3]^-$ complex **32** and $DIMPYSnOTf_2$ complex **34** a low field shifting is observed. Therefore, these signals are shifting inconclusively as noticed for the $(SIMPY)EX_2$ complexes in chapter 3.3.2 as well.

The ^{119}Sn NMR shows signals for the $[DIMPYSnCl]^+$ cation at -445.2 ppm and for the anion $[SnCl_3]^-$ at -57.9 ppm which correlates with literature known complexes.[40] For the $[DIMPYSnBr]^+[SnBr_3]^-$ complex **32** a signal was found at 98.2 ppm for the cation and at -405.8 ppm for the anion. These shifts differ from the chloride complex **31** due to the heavier bromine atoms. In case of the $[DIMPYSnI]^+[SnI_3]^-$ complex **33**, no ^{119}Sn signals could be observed which can be explained by the fact that even in the ^1H NMR spectra very broadened signals were investigated. Therefore, a very broadened signal is presumably expected in the ^{119}Sn NMR spectrum and was not detected.

The $[DIMPYGeCl]^+[GeCl_3]^-$ complex **29** crystallizes in the monoclinic space group $P2_1/c$ and the cation $[DIMPYGeCl]^+$ as well as the anion $[GeCl_3]^-$ are present in the unit cell (Figure 3.50, Table 3.10). The cation $[DIMPYGeCl]^+$ bears a pseudo trigonal pyramidal environment where the Ge1 atom is fourfold coordinated by three nitrogen atoms and one chlorine atom. The Ge - N distances are ranging from 2.077(4) Å to 2.314(6) Å. The short Ge - N3 distance with 2.077(4) Å is observed for the strong donor-acceptor interaction from the pyridenyl N_{py} towards the Ge center. The elongated Ge - N2 bond lengths with 2.314(6) Å can be explained by the non-symmetrical coordination of the Ge element within the DIMPY complex bearing two different imino N_{im}

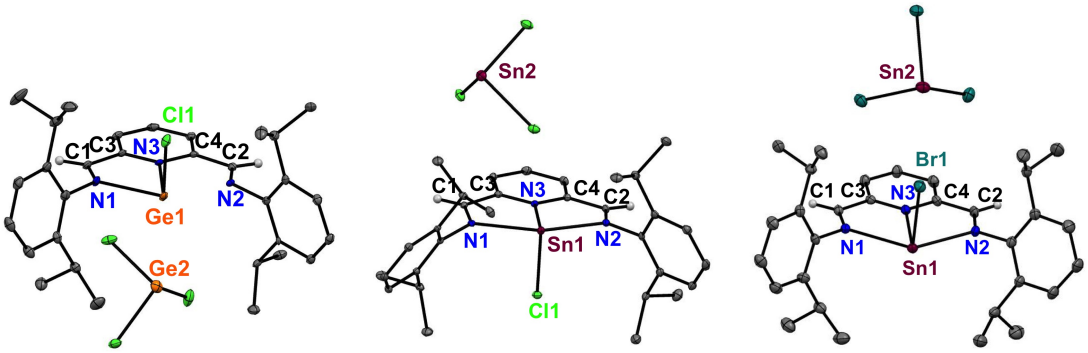

Figure 3.50: Solid state structures of compounds **29**, **31** and **32**. Anisotropic displacement parameters are depicted at the 50% probability level. Hydrogen atoms are omitted for clarity except at the HC=N functionality.

- Ge distances. The N_{im} - Ge interactions are, as observed in the (SIMPY)EX_2 complexes, weaker than the pyridinyl N_{py} - Ge donor-acceptor interactions. The Ge - N distances agree well with the (SIMPY)GeX_2 (X= Cl, Br) and literature known complexes ranging from 2.071(1)[40] Å to 2.490(8) Å. The Ge atom is planar within the DIMPY ligand plane with an angle N1-Ge-N3 of 146.42(2)° and an angle N1-Ge-N3 of 73.84(2)°. The chlorine atom is nearly perpendicular to the DIMPYGe plane with an angle N1-Ge-Cl1 of 85.99(1)°. The Ge - Cl1 distance is 2.228(2) Å and is in good agreement with the (SIMPY)EX_2 complexes and complexes known in literature ranging from 2.215(2) to 2.404(3) Å.[40,57] The DIMPY ligand bond lengths are as expected for a neutral ligand coordinating an element center which are slightly elongated. The imino bonds C1 - N1 and C2 - N2 are slightly different with 1.270(6) Å and 1.277(6) Å, respectively. This is in agreement with the slightly different C - C distances in the backbone of the ligand system. The C1 - C3 distance is 1.473(8) Å and the C2 - C4 is 1.464(8) Å long which agrees with the fact that the Ge atom is unsymmetrically coordinated by the DIMPY ligand within the complex. The Ge2 atom in the anion $[GeCl_3]^-$ is coordinated by three chlorine atoms bearing a trigonal pyramidal environment. The Ge - Cl distances are around 2.30 Å are in good agreement with literature known complexes.[40,57]

The $[DIMPYSnCl]^+[SnCl_3]^-$ complex **31** crystallizes in the triclinic space group $P\bar{1}$ and the $[DIMPYSnBr]^+[SnBr_3]^-$ complex **32** crystallizes in the monoclinic space group $P2_1/c$ (Figure 3.50, Table 3.10). The cation $[DIMPYSnX]^+$ as well as the anion $[SnX_3]^-$ are present in the crystal lattice bearing a distorted trigonal pyramidal environment for the Sn centers, respectively. In the

Table 3.10: Comparison of the bond lengths [Å] and angles [°] of compounds $[DIMPYGeCl]^+[GeCl_3]^-$ **29**, $[DIMPYSnCl]^+[SnCl_3]^-$ **31**, $[DIMPYSnBr]^+[SnBr_3]^-$ **32** , $DIMPYSnOTf_2$ **34** and **34′**.

Bond lengths and angles	**29**	**31**	**32**	**34**	**34′**
E – N1	2.255(6)	2.453(2)	2.453(4)	2.515(6)	2.450(6)
E – N2	2.314(6)	2.414(2)	2.457(4)	2.502(5)	2.773(6)
E – N3	2.077(4)	2.303(2)	2.280(3)	2.317(5)	2.360(5)
E - X1	2.228(2)	2.452(7)	2.601(3)	2.381(5)	2.248(5)
C1 – N1	1.270(6)	1.274(3)	1.265(5)	1.261(8)	1.279(9)
C1 – C3	1.473(8)	1.478(3)	1.466(7)	1.483(9)	1.468(9)
C2 – N2	1.277(6)	1.274(3)	1.270(5)	1.279(8)	1.263(8)
C2 – C4	1.464(8)	1.474(3)	1.464(7)	1.462(9)	1.469(9)
N1-E-X1	85.99(1)	85.30(5)	86.39(9)	79.89(2)	80.16(2)
N1-M-N2	73.84(2)	68.74(6)	68.22(1)	68.84(2)	69.22(2)
N1-M-N3	146.42(2)	136.70(6)	136.56(1)	137.83(2)	133.91(2)

cation $[DIMPYSnX]^+$, the Sn1 atom is fourfold coordinated by three nitrogen atoms and one halogen atom. The Sn - N distances are ranging from 2.280(3) Å to 2.457(4) Å and show a similar bonding motif as discussed for the $[DIMPYGeCl]^+[GeCl_3]^-$ complex **29**. The shorter Sn - N distances are observed for the stronger N_{py} - Sn donor-acceptor interactions. For the $[DIMPYSnCl]^+$ cation **31**, the Sn - N3 distance is 2.303(2) Å and for the cation $[DIMPYSnBr]^+$ **32** the Sn - N3 distance is shortened with 2.280(3) Å. Regarding the imino N_{py} - Sn distances, they are much more alike in compound $[DIMPYSnBr]^+$ **32** with bond lengths Sn - N1 2.453(4) Å and 2.457(4) Å as compared to complex **31** with distances Sn - N1 2.453(2) Å and 2.414(2) Å. The Sn atoms in the cationic species are planar with the DIMPY ligand and the halogen atom is perpendicular to this DIMPYSn plane. The Sn - Cl1 distance is 2.452(7) Å and the Sn - Br1 bond length is elongated as expected with 2.601(3) Å and are in good agreement with the Sn - X bond lengths of the $(SIMPY)EX_2$ complexes showing the same trend. The angles observed in the complexes are similar with average values of N1-Sn-N2 with 68.5° and N1-Sn-N3 angle with 136.7°. Compared to complex $[DIMPYGeCl]^+[GeCl_3]^-$ **29** smaller angles are observed for the Sn complexes due to the bigger atomic radius of the Sn atom. The angle N1-Sn-Cl1 is 85.30(5)° and N1-Sn-Br is 86.39(9)° and are similar to the N1-Ge-Cl1 angle of the germanium complex **29**. The DIMPY ligand system displays a similar bonding situation as in complex $[DIMPYGeCl]^+[GeCl_3]^-$ **29**. The imino bond

lengths are around 1.27 Å and the C-C distances in the backbone are around 1.47 Å.

The DIMPYSnOTf$_2$ complex **34** crystallizes in the monoclinic space group P2$_1$/n bearing two independent molecules in the unit cell **34** and **34'** (Figure 3.51, Table 3.10). The Sn atom in complex **34** shown in Figure 3.51 at the left, is fivefold coordinated by three nitrogen atoms and two oxygen atoms. It bears a trigonal bipyramid in geometry. In case of **34'** (Figure 3.51, right), a much more unsymmetrical complex is observed due to an additional coordination of the solvent molecule THF. The Sn - N distances are much more elongated than in

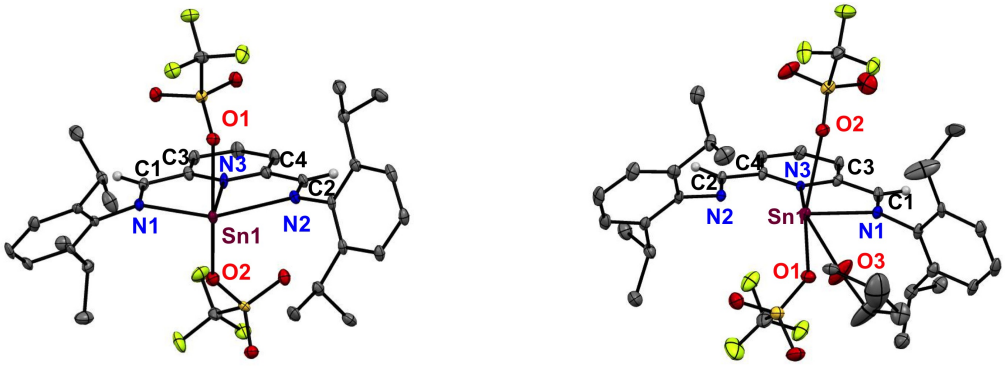

Figure 3.51: Solid state structures of compounds **34** and **34'**. Anisotropic displacement parameters are depicted at the 50% probability level. Hydrogen atoms are omitted for clarity except at the HC=N functionality.

the complexes known from literature[40,57] and discussed previously. The Sn - N distances are ranging from 2.317(5) Å to 2.773(6) Å. The shorter Sn - N$_{py}$ distances are 2.317(5) Å for **34** and 2.360(5) Å for **34'** and are longer than in the [DIMPYEX]$^+$[EX$_3$]$^-$ complexes. The Sn - N$_{im}$ distances are quite different for the symmetrical complex **34** with Sn - N1 2.515(6) Å and Sn - N2 with 2.502(5) Å and for the asymmetrical **34'** bond lengths with Sn - N1 of 2.450(6) Å and Sn - N2 of 2.773(6) Å. This can be explained by the different coordination environment in complex **34'** due to the additional donor molecule THF. This agrees also with the fact that the OTf groups reveal different Sn - O distances. In complex **34**, the Sn - O1 distance is 2.381(5) Å and the Sn - O2 distance is similar with 2.394(5) Å. In case of complex **34'**, the Sn - O1 distance is 2.248(5) Å and the Sn - O2 bond lengths is elongated with 2.614(5) Å due to the asymmetrical environment. The Sn - O3 distance of the solvent molecule THF is even longer with 2.726(5) Å. The N1-Sn-O1 angles are smaller than the angles observed in the ion pairs with an average value of 80°. The N1-Sn-N2 angles are

similar with around 69° and the N1-Sn-N3 is only similar for the symmetrical complex **34** with 137.83(2)°. In complex **34'** the N1-Sn-N3 angle is much smaller with 133.91(2)°. The DIMPY ligand fragment is a neutral donor and the bonding situation agrees well with the DIMPY ligand distances discussed previously.

The synthesis of DIMPY group 14 element precursors were successful. Therefore, reduction reactions are established to give low valent (DIMPY)E complexes (E= Ge and Sn). For the reduction various reducing agents as alkali metals Na and K and mild reducing agents KH, MgH_2 and L- and K-selectrides were used. Interstingly, different results were obtained for the reduction reactions depending on the leaving groups. In case of the

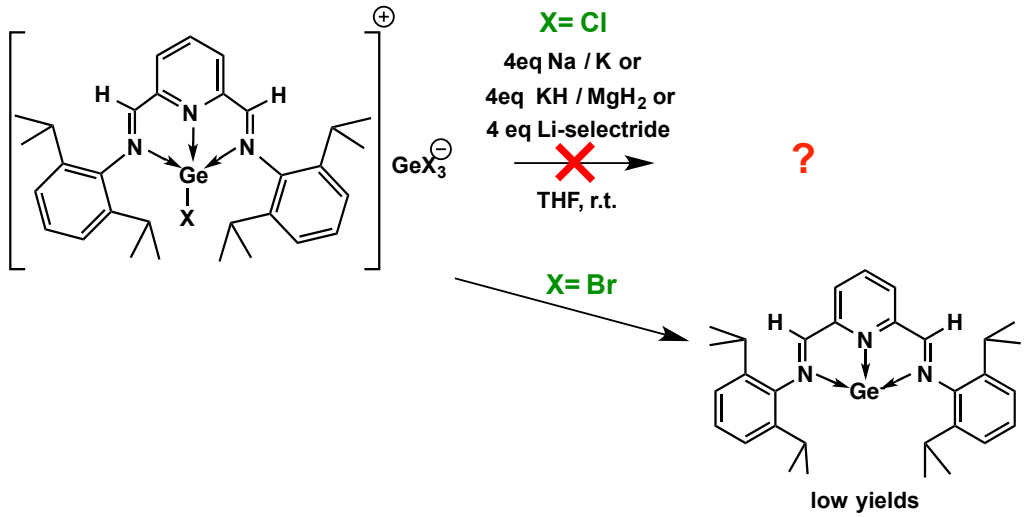

Figure 3.52: The reaction of the [DIMPYGeX][GeX_3] complexes with reducing agents like Na, K, KH, MgH_2 and L-selectride gives only in case of x= Br the desired dark green (DIMPY)Ge complex, but in low yields.

$[DIMPYGeX]^+[GeX_3]^-$ complexes, the reduction reactions were performed in THF at room temperature as well as at low temperatures of -30°C. In case of the $[DIMPYGeCl]^+[GeCl_3]^-$ complex **29**, red solutions were obtained after warming up to room temperature and stirring over night. According to NMR studies several products are observed, which could not be characterized. No matter which reducing agent was used, no main product could be isolated. In case of the $[DIMPYGeBr]^+[GeBr_3]^-$ complex **30**, dark green solutions were obtained. Again several products were observed *via* NMR spectroscopy. However, it was possible to crystallize one product and characterize it as the de-

sired dark green (DIMPY)Ge complex. Due to low yields, the synthetic route to give the (DIMPY)Ge complex was not satisfying. Despite from low yields of the (DIMPY)Ge complex around 10%, a brown byproduct was present which could not be separated from the desired germylene. Low valent group 14 complexes are very labile and for example column chromatography could therefore not be performed. Recrystallization was unsuccessful, too. Therefore, another synthetic route had to be established to yield the (DIMPY)Ge complex in high yields without any byproducts. The complete characterization as well as the novel synthetic pathway to isolate the (DIMPY)Ge complex will be discussed in the next chapter 3.4. Very recently while writing this PhD thesis, a related (MeDIMPY)Ge complex was synthesized.[162] The synthetic route to obtain the related (MeDIMPY)Ge complex,[162] was similar to the attempts discussed previously. The ionpair $[MeDIMPYGeCl]^+[GeCl_3]^-$ was reduced with C_8K in toluene and the (MeDIMPY)Ge complex[162] was obtained in high yields around 65%. The main differences compared to the reactions discussed above are the solvent and the MeDIMPY ligand. The MeDIMPY ligand could be the major issue why the (MeDIMPY)Ge complex[162] was obtained in high yields and the (DIMPY)Ge complex was not. The DIMPY ligand possesses H atoms at the backbone of the ligand system which are reactive too and could be presumably responsible for several byproducts.

In case of the $[DIMPYSnX]^+[SnX_3]^-$ complexes, the reduction reactions were performed by various reducing agents as alkali metals and mild reducing agents and at different temperatures (at room temperature and at -30°). After stirring over night and warming up to room temperature, Sn metal precipitated out of the reaction solutions. Furthermore, the DIMPY ligand was formed. Although a tridentate ligand is present, the low valent Sn element could not be stabilized. The driving force to reduced the Sn^{II} element to give Sn^0 metal is much more favored than giving a low valent DIMPYSn complex. Interestingly, in case of the reduction with $[DIMPYSnBr]^+[SnBr_3]^-$ complex **32**, a dark green solution was obtained. The ^1H NMR did only show the DIMPY ligand in reaction solution, but no Sn metal was precipitated. Presumably, a radical species is formed. Unfortunately this species could not be isolated. The differences in the reduction reactions of the $[DIMPYEX]^+[EX_3]^-$ complexes depend on the leaving groups. As discussed in the solid state structure analysis, the E - X distances differ regarding the halogen atom. However, the E - N dis-

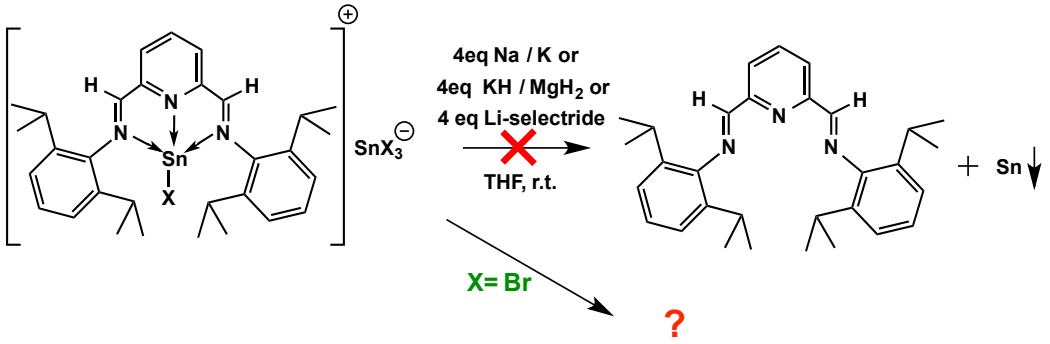

Figure 3.53: The reaction of the [DIMPYSnX][SnX_3] complexes with reducing agents like Na, K, KH, MgH_2 and L-selectride does not give the desired DIMPYSn complex. Instead DIMPY ligand and Sn metal is formed.

tances stay more or less the same compared to the Sn - N distances in complexes $[DIMPYSnCl]^+[SnCl_3]^-$ **31** and $[DIMPYSnBr]^+[SnBr_3]^-$ **32** (Table 3.10). Hence, the reducing agent can react with the elongated bond lengths of the E - Br species much more easily than with the much more stronger bonded E - Cl complexes. This results in the isolation of the DIMPYGe complex regarding the reduction reaction of $[DIMPYGeBr]^+[GeBr_3]^-$ complex **30** and the different findings for the reductions with the $[DIMPYSnBr]^+[SnBr_3]^-$ complex **32**.

However, the synthetic pathway to obtain low valent (DIMPY)E complexes was not successful. Although the DIMPY ligand is a strong tridentate ligand system, the low valent group 14 complexes could neither be stabilized or nor isolated in high yields. Therefore, another synthetic route has to be established bearing the interesting bonding motif as in the (SIMPY)Ge complex **12**. The (SIMPY)Ge complex **12** was synthesized using an aminopyridine ligand system SAMPY. The next chapter 3.4 will present interesting and unexpected reactions of the DAMPY ligand system with group 14 elements.

3.4 The Synthesis of Unexpected Low Valent Group 14 Complexes Using the DAMPY Ligand

Tridentate ligand systems bearing a pyridine donor functionality as DIMPY and DAMPY ligand systems were successfully applied in transition metal chemistry.[4,60–63] They can be easily modified with different aryl substituents on the imino or amino nitrogen atoms and therefore stabilize reactive metal centers effectively.

In case of the DIMPY ligand, the synthesis of low valent group 14 complexes was difficult to perform as discussed in chapter 3.3.3. The DIMPYGe complex could be isolated, but in low yields with additional byproducts. The (DIMPY)Sn complex, could not be isolated. In chapter 3.2, the SAMPY ligand system reacts with $Ge(N(SiMe_3)_2)_2$ to give the (SIMPY)Ge complex **12** *via* an elimination of the H atom at the backbone of the ligand system. The (SIMPY)Ge complex **12** bears an interesting bonding motif with a certain degree of the Ge atom in a formal oxidation state of zero - a germylone. Group 14 elements in the oxidation state of zero are rare in literature.[94,101,102,109,110,115–120] In main group chemistry, this novel complexes are a completely new approach due to the fact that the main group element is only stabilized via donor-acceptor interactions. Hence, a group 14 element possesses two lone pairs of electrons. The reaction chemistry of these complexes are unknown and should differ compared to E^{II} complexes. Due to the interesting findings using the SAMPY ligand system, the reactions of the DAMPY ligand system with group 14 elements was performed.[102,150 ||] Main group complexes stabilized by the DAMPY ligand system are rare. In case of group 14 complexes no examples are known.

[||] Preliminary studies, Amra Suljanovic, PhD Thesis: Design and Synthesis of Polysilazanes, **2011**, TU Graz

The DAMPY ligand reacts with two equivalents of $E(N(SiMe_3)_2)_2$ (E= Ge, Sn, Pb) in diethyl ether at room temperature to yield an intermediate the bistetrylene DAMPY[$E^{II}(N(SiMe_3)_2]_2$ *via* a transamination reaction as shown in Figure 3.61. After further stirring at room temperature, an elimination reaction of the benzylic H atoms at ligand system occurs, to give the desired (DIMPY)E complexes. Therefore, it is possible to synthesize highly interesting (DIMPY)E complexes out of the DAMPY ligand system. The synthesis of the desired (DIMPY)E complexes can only be performed due to an intramolecular ligand based redox process taking place at the backbone of the DAMPY ligand system. This further indicates that also the DAMPY ligand does possess a redox-activity as known for the DIMPY ligand system. No matter in which ratio the

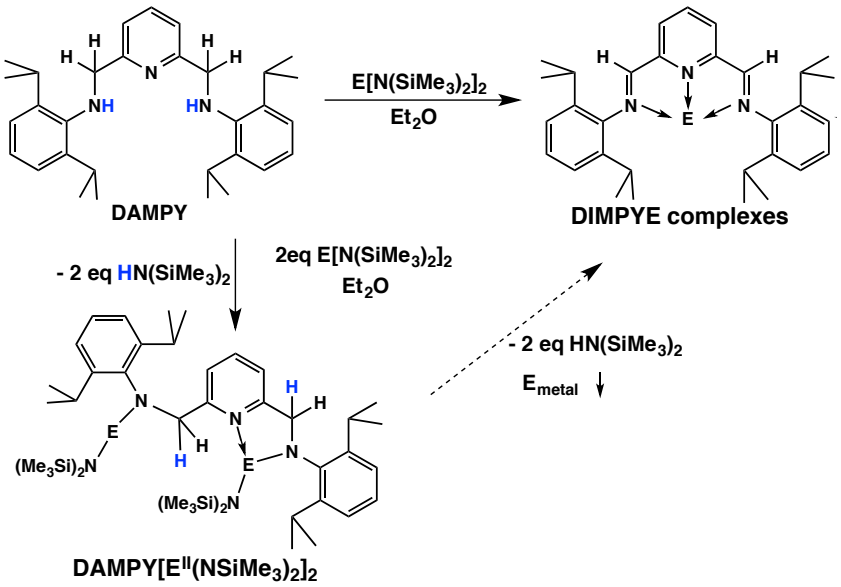

Figure 3.54: The reaction of the DAMPY ligand system with two equivalents $E(N(SiMe_3)_2)_2$ (E= Ge, Sn, Pb) yield highly interesting DIMPYE complexes *via* a transamination reaction in the first step and an elimination reaction of the H atoms at the backbone of the ligand system in the second step.

reaction of the DAMPY ligand and $E(N(SiMe_3)_2)_2$ (E= Ge, Sn, Pb) was carried out (e.g. 1:1), a DIMPY ligand stabilizing a group 14 element was always the main product. Hence, it can be rationalized that the (DAMPY)E complex, which could be a reasonable product of a transamination reaction with one equivalent DAMPY and one equivalent $E(N(SiMe_3)_2)_2$ (E= Ge, Sn, Pb), is not favored. It was never investigated in solution, although an intensive NMR study was performed.

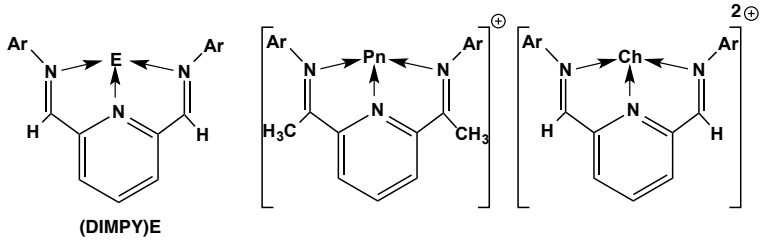

Figure 3.55: The neutral (DIMPY)E complexes are isoelectronic to the cationic group 15 (+I) and group 16 (+II) analogues.[36,37,41]

The neutral (DIMPY)E complexes are isoelectronic to the cationic $[DIMPYP]^{+}$,[36] $[DIMPYAs]^{+}$[37] and $[DIMPYCh]^{2+}$[41] (Ch= S, Se, Te) complexes as shown in Figure 3.55. Considering the bonding situation in the (DIMPY)E complexes, the E atom is in the formal oxidation state of zero due to donor-acceptor interaction stabilizing the E^0 atom. In literature, E^0 species are rare and were very recently reported.[94,101,109,110,115–120] Furthermore the known E^0 complexes are exclusively coordinated by two N-heterocyclic carbene ligands or related donor molecules. Hence, the (DIMPY)E complexes represent the first examples of a neutral, mononuclear, group 14 complex with Ge, Sn and Pb in a formal oxidation state of zero stabilized by only one donor molecule. During writing this PhD thesis, a related (MeDIMPY)Ge^0 complex[162] was published which bears a similar bonding motif compared to the (DIMPY)E complexes. The related (MeDIMPY)Ge^0 complex[162] was synthesized *via* a different synthetic route as discussed in chapter 3.3.3. The ionpair $[MeDIMPYGeCl]^{+}[GeCl_3]^{-}$ was reduced with C_8K in toluene and the (MeDIMPY)Ge complex[162] was obtained in high yields around 65%.

The bonding motif can be described by four resonance structures shown in Figure 3.56. According to resonance structure **I**, the (DIMPY)E complexes can be considered as a group 14 element E in the oxidation zero which is coordinated by the DIMPY ligand *via* donor-acceptor interactions. A similar bonding situation was used to describe the related (MeDIMPY)Ge^0 complex,[162] some N-heterocyclic stannylenes[125,126] and the transition metal complexes $[L_2EM(CO)_5]$ (L = pyridine or L = 2,2′-bipyridine, 2,2′-bipyrimidine, 1,10-phenantroline; M = Cr, Mo, W).[127] Alternatively, the (DIMPY)E complexes can be described as a tetrylene - bearing an E^{II} atom - according to resonance forms **II** and **III**, where

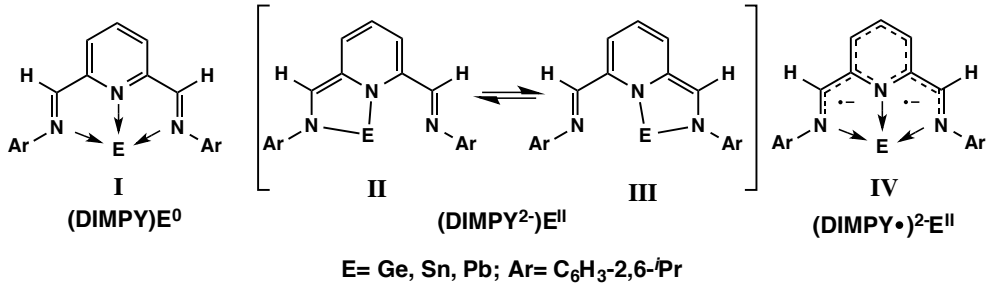

Figure 3.56: Possible resonance structures for the (DIMPY)E complexes.

two covalent E - N bonds form at the expense of the aromaticity of the pyridine ring. Finally, **IV** represents a bonding situation, in which a E^{II} center interacts with a doubly reduced ligand $DIMPY^{2-}$, where the latter can either exist as a closed shell singlet or as open shell singlet or triplet diradicals. The bonding situation within the (DIMPY)E complexes will be studied by NMR- and EPR- measurements, solid state structure analysis and in case of E= Sn with Mössbauer spectroscopy. At first the synthesis of the (DIMPY)E complexes will be discussed in detail.

In case of E= Ge, the same trend is observed for the reaction with the SAMPY ligand in chapter 3.2. The transamination reaction is the rate limiting step and does need a long time to proceed for the reaction with the DAMPY ligand. $Ge(N(SiMe_3)_2)_2$ was reacted with the DAMPY ligand system in diethyl ether at room temperature to give a slightly greenish solution after 48 hours reaction time. To gain insight in the reaction mechanism, the solution was cooled to - 30°C to isolate the intermediate of the first reaction step - the bisgermylene $DAMPY(Ge^{II}N(SiMe_3)_2)_2$ **35**. Interestingly, an intermediate was isolated, but it was not the bisgermylene. The reaction afforded the $DAMPYNHGeN(SiMe_3)_2$ complex **36** as shown in Figure 3.57. One equivalent $Ge(N(SiMe_3)_2)_2$ reacted with the DAMPY ligand to give a heteroleptic germanium complex which possesses an additional amino group turned away from the central atom. Compound **36** is comparable to the heteroleptic $SAMPYGeN(SiMe_3)_2$ complex **9**. The conversion to yield the bisgermylene $DAMPY(Ge^{II}N(SiMe_3)_2)_2$ **35** is so slow that the $DAMPYNHGeN(SiMe_3)_2$ complex **36** was the main product after 48 hours stirring. Still, to form a (DIMPY)E complex the intermediate $DAMPYGe^{II}(N(SiMe_3)_2$ **35** has to be present in reaction solution and was con-

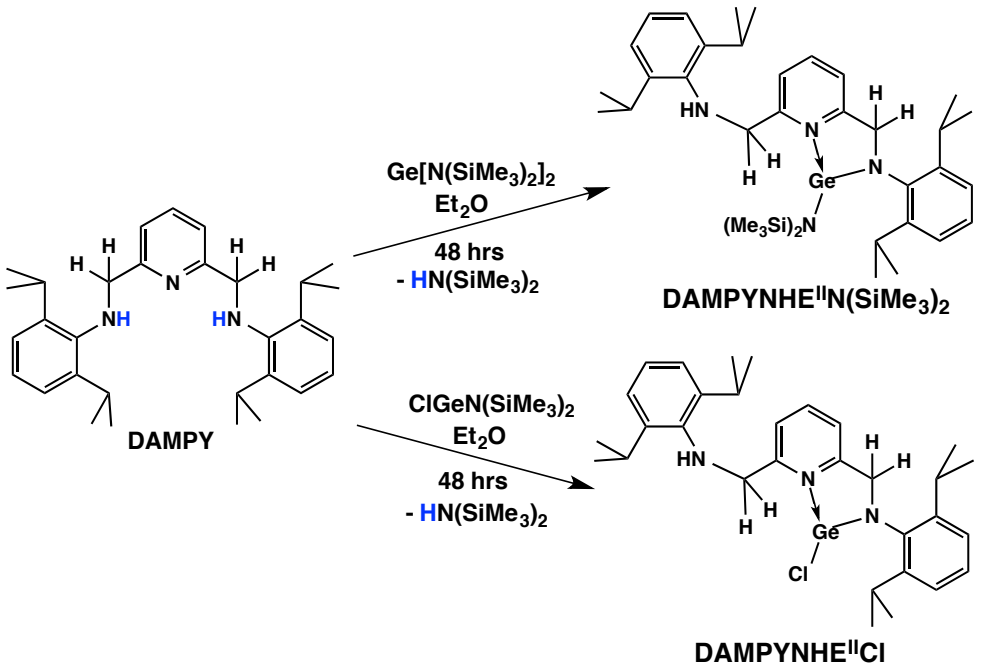

Figure 3.57: The reaction of the DAMPY ligand system with $Ge(N(SiMe_3)_2)_2$ gives the $DAMPYNHGeN(SiMe_3)_2$ complex **36** *via* a transamination reaction. Another reaction with $ClGeN(SiMe_3)_2$ yielded a related DAMPYNHGeCl complex **37**.

firmed by ^1H NMR spectroscopy, but could not be isolated and characterized by solid state structure analysis.

A heteroleptic germanium complex bearing a chlorine functionality was achieved by the reaction of the DAMPY ligand with $ClGe(N(SiMe_3)_2$[96] yielding the DAMPYNHGeCl complex **37** *via* a transamination reaction as shown in Figure 3.57. The DAMPYNHGeCl complex **37** reveals the same bonding motif as compound $DAMPYNHGeN(SiMe_3)_2$ **36**. A Ge^{II} atom is bonded covalently to one nitrogen atom and the pyridenyl N_{py} donates towards the element center. The second amino functionality is turned away from the Ge^{II} atom. Compound **36** and **37** were isolated *via* recrystallization at -30°C in diethyl ether as light green cubic crystals. The yield is low due to the presents of several byproducts in solution. The low reactivity of $Ge(N(SiMe_3)_2)_2$ towards the DAMPY ligand is problematic, because byproducts are always present and can't be separated due to similar polarities of the compounds. When the reaction of the DAMPY ligand with two equivalents $Ge(N(SiMe_3)_2)_2$ was further stirred a dark green solution was obtained. All volatile components were removed *in vacuo* and the dark green powder was recrystallized in diethyl ether

at -30°C. Dark green cubic crystal were isolated in low yields and were characterized as the desired (DIMPY)Ge complex **38**.

Faster conversions were obtained for E= Sn and Pb. In case of E= Sn, the reaction of one equivalent of the DAMPY ligand with two equivalent of $Sn(N(SiMe_3)_2)_2$ in diethyl ether at room temperature yielded the intermediate $DAMPY(Sn^{II}N(SiMe_3)_2)_2$ **39** after 12 hours as shown in Figure 3.58. After

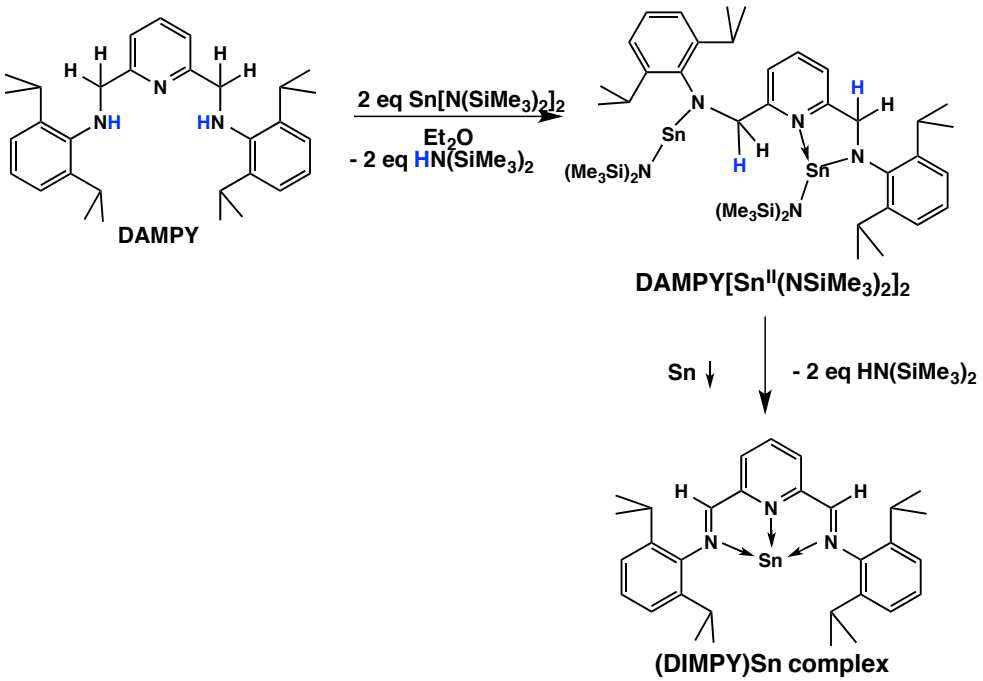

Figure 3.58: The reaction of the DAMPY ligand system with two equivalent $Sn(N(SiMe_3)_2)_2$ gives the $DAMPY(Sn^{II}N(SiMe_3)_2)_2$ complex **39** *via* a transamination reaction. Due to intramolecular eliminations of two equivalents $H(N(SiMe_3)_2$, the(DIMPY)Sn complex **40** is formed.

further stirring over night, a dark purple solution was obtained. All volatile components were removed and the purple powder was recrystallized in diethyl ether at -30°C. Cubic purple crystals were characterized as the desired (DIMPY)Sn complex **40**. The DIMPYSn complex **40** is stable in solid state, however decomposes into elemental Sn and the DIMPY ligand in polar aprotic solvents. Hence, the DIMPYSn complex could not be isolated purely in high yields. Besides the DIMPY ligand and Sn metal, traces of the starting materials and the intermediate $DAMPY(Sn^{II}N(SiMe_3)_2)_2$ **39** are present in reaction solution and in the recrystallized powder. Attempts to separate the (DIMPY)Sn complex from it's byproducts failed due to the labile nature of the (DIMPY)Sn

complex. A ^{1}H NMR study was performed to gain further insights in the synthesis of the (DIMPY)Sn complex **40**. Every hour an ^{1}H NMR was recorded for three days in deuterated THF. As shown in Figure 3.59, the C**H**$_2$ group signal at 4.1 ppm vanishes and at 9.1 ppm a signal for the **H**C=N functionality rises which indicates the formation of the (DIMPY)Sn complex **40**. Furthermore it

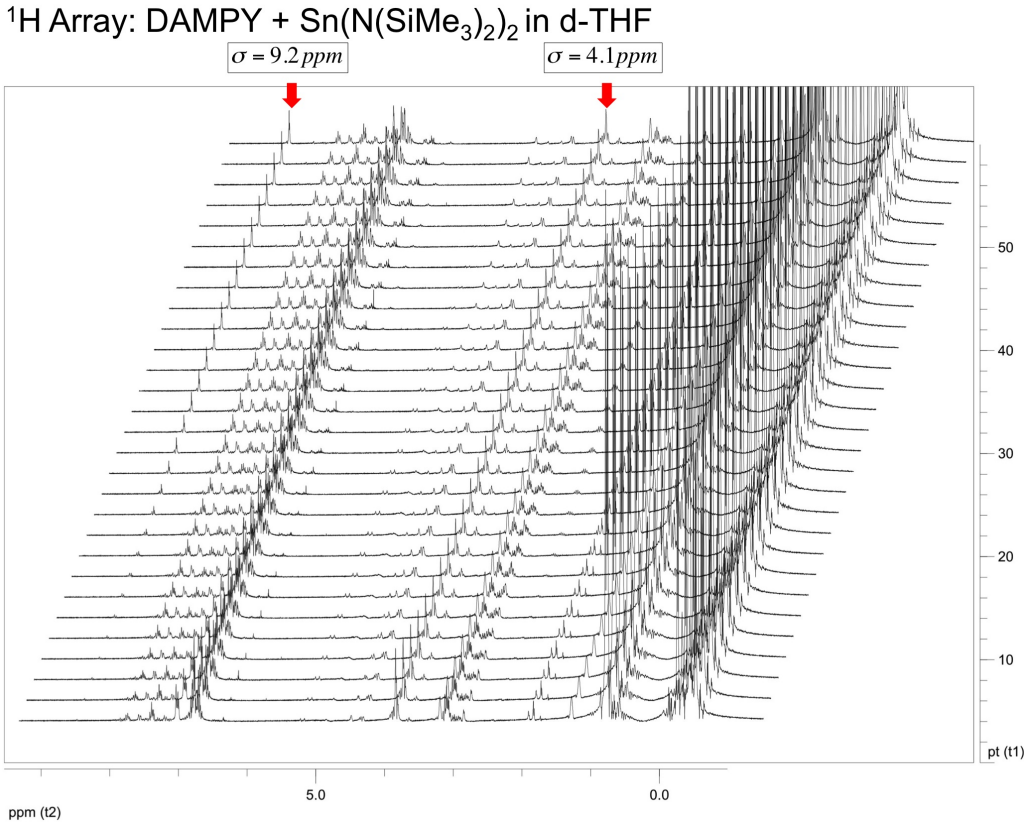

Figure 3.59: ^{1}H NMR array of the reaction of the DAMPY ligand system with Sn(N(SiMe$_3$)$_2$)$_2$. After one day reaction time a signal rises at 9.2 ppm for the **H**C=N functionality which indicates the formation of the (DIMPY)Sn complex. At 4.1 ppm the C**H**$_2$ group vanishes.

can be seen, that byproducts are always present in reaction solution.

In case of E= Pb, the DAMPY ligand was reacted with two equivalents Pb(N(SiMe$_3$)$_2$)$_2$ in diethyl ether as shown in Figure 3.60. After five minutes the solution turned dark red. After additional stirring, Pb metal precipitated and DIMPY ligand was dissolved in the reaction solution confirmed by NMR spectroscopy. This indicated the formation of a very labile (DIMPY)Pb complex **41**. Due to the lability of the (DIMPY)Pb complex **41**, the solution was performed at low temperatures of -80°C. Warming up to room temperature yielded again

the precipitation of Pb metal and the formation of the DIMPY ligand. Therefore, attempts were carried out to transfer the reaction solution directly to the freezer to crystallize the labile complex, but the (DIMPY)Pb complex **41** could not be isolated.

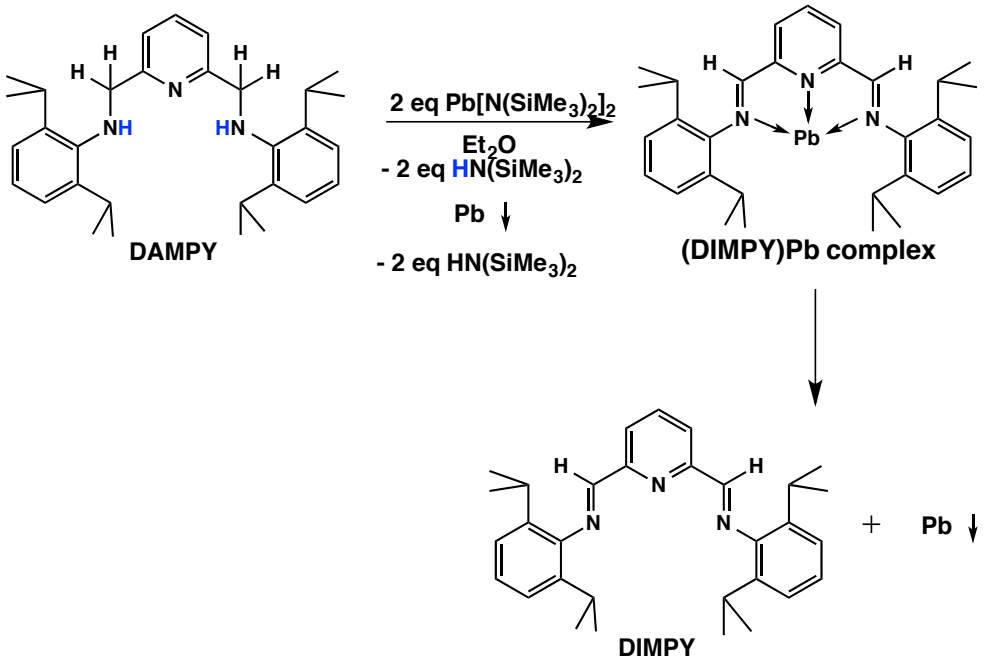

Figure 3.60: The reaction of the DAMPY ligand system with two equivalent $Pb(N(SiMe_3)_2)_2$ gives the labile (DIMPY)Pb complex **41** *via* a transamination reaction and a subsequent intramolecular eliminations of two equivalents $H(N(SiMe_3)_2$. However, the complex (DIMPY)Pb **41** is unstable and forms DIMPY ligand and Pb metal.

Impurities of the target molecules (DIMPY)Ge **38** and (DIMPY)Sn **40** posed the same problem as for the (SIMPY)Ge complex **12** in chapter 3.2. In this particular case, a driving force was implemented to accelerate the transamination reaction. It worked very well and therefore, the same reaction conditions were carried out for the DAMPY ligand system. As reported in literature, the $DAMPYLi_2$ complex is very labile even in solid state and decomposes rapidly by warming up to room temperature.[63] Furthermore, the $DAMPYLi_2$ complex is not stable in etheric solvents even at low temperatures. Therefore, the solvent of choice for the lithiation of the DAMPY ligand is either pentane or hexane. Hence, the DAMPY ligand was lithiated with two equivalents of ^{n}BuLi in pentane at -80°C. After 10 minutes reaction time, the product $DAMPYLi_2$ precipitates out of a greenish solution as a yellow powder. To obtain higher yields,

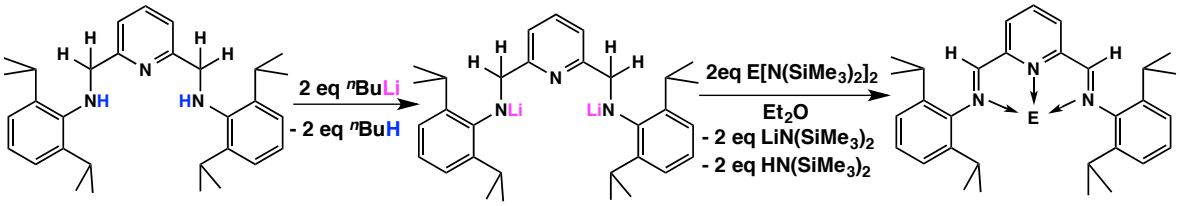

Figure 3.61: New synthetic route to obtain (DIMPY)E complexes: The reaction of the DAMPY ligand system with two equivalents of ^{n}BuLi gives the labile DAMPYLi$_2$ complex. Then two equivalents of E(N(SiMe$_3$)$_2$)$_2$ (E= Ge, Sn) are added and give the (DIMPY)E complexes in high yields without any byproducts.

the reaction solution was warmed up to -30°C for 10 more minutes. Then the greenish solution was separated from the yellow powder and a cooled solution of E(N(SiMe$_3$)$_2$)$_2$ (E= Ge, Sn) in diethyl ether was added at -80°C. The reaction solution turns in case of E= Ge dark green and in case of E= Sn deep purple after stirring over night and warming up to room temperature. To eliminate the byproduct LiN(SiMe$_3$)$_2$, Me$_3$SiCl was added to give LiCl and N(SiMe$_3$)$_3$. All volatile components were removed *in vacuo*. Pentane was added to the obtained powder, LiCl was separated via filtration and the pentane solution was concentrated. After recrystallization in pentane, the complexes (DIMPY)Ge **38** and (DIMPY)Sn **40** were isolated in high yields around 65% without any byproducts. Complexes (DIMPY)Ge **38** and (DIMPY)Sn **40** as well as their intermediates were fully characterized by heteronuclear NMR, elemental analysis and solid state structure analysis. In case of the (DIMPY)Sn complex **40** further characterizations were performed as solid state NMR measurements, Mössbauer spectroscopy and theoretical DFT studies.

The most effected ^{1}H NMR signals of compounds DAMPYNHGeN(SiMe$_3$)$_2$ **36**, DAMPYNHGeCl **37**, (DIMPY)Ge **38**, DAMPY(Sn^{II}N(SiMe$_3$)$_2$)$_2$ **39** and (DIMPY)Sn **40** are given in Table 3.14 and are compared to the signals of the DAMPY ligand. The DAMPY ligand has significant signals at 4.25 ppm for the C**H**$_2$ group, at 3.54 ppm for the C**H**(CH$_3$)$_3$ protons and at 1.25 ppm for the CH(C**H**$_3$)$_3$ protons. In case of the germanium complexes DAMPYNHGeN(SiMe$_3$)$_2$ **36** and DAMPYNHGeCl **37**, these significant signals are shifted towards high field and split due to the unsymmetrical coordination environment within the complexes. Therefore, signals at 4.78 and 4.76 ppm are observed for the C**H**$_2$ group in case of complex DAMPYNHGeN(SiMe$_3$)$_2$

Table 3.11: Comparison of ^{1}H NMR signals of the DAMPY ligand and of the compounds DAMPYNHGeN(SiMe$_3$)$_2$ **36**, DAMPYNHGeCl **37**, (DIMPY)Ge **38**, DAMPY(Sn^{II}N(SiMe$_3$)$_2$)$_2$ **39** and (DIMPY)Sn **40**.

Compound	**H**C=N	C**H**$_2$	C**H**(CH$_3$)$_3$	CH(C**H**$_3$)$_3$
DAMPY	-	4.25	3.54	1.25
36	-	4.78/4.76	3.65/3.25	1.34/1.23
37	-	4.43/4.19	3.21/3.17	1.28/1.10
38	8.12	-	3.12	1.15
39	8.61	5.70/5.38/5.01/4.78	4.07/3.84/3.42/3.17	1.37/1.21/1.08
40	8.40	-	2.86	1.15/1.07

36 and for DAMPYNHGeCl **37** signals are investigated at 4.43 ppm and 4.19 ppm. The diisopropyl group is effected too with a shift towards high field. DAMPYNHGeN(SiMe$_3$)$_2$ **36** reveals signals at 3.65 ppm and 3.25 ppm and DAMPYNHGeCl **37** also shows a set of two septets at 3.21 ppm and 3.17 ppm for the C**H**(CH$_3$)$_3$ protons. The signal of the CH(C**H**$_3$)$_3$ protons are split into two doublets and show signals at 1.34 and 1.23 ppm for DAMPYNHGeN(SiMe$_3$)$_2$ **36** and signals at 1.28 ppm and 1.10 ppm for the DAMPYNHGeCl **37** compound. The intermediate DAMPY(Sn^{II}N(SiMe$_3$)$_2$)$_2$ **39** is a highly unsymmetrical compound. It bears two different amide ligand fragments bonded towards two differently coordinated Sn atoms, one revealing an additional pyridenyl N$_{py}$ donation and one turned away from the center of the molecule. Hence, the C**H**$_2$ protons are split into four signals shifted towards low field at 5.70 ppm, 5.38 ppm, 5.01 ppm and 4.78 ppm. This is also the case for the C**H**(CH$_3$)$_3$ protons showing four septets at 4.07 ppm, 3.84 ppm, 3.42 ppm and 3.17 ppm. The CH(C**H**$_3$)$_3$ protons are observed at 1.37 ppm, 1.21. ppm and 1.08 ppm. The complex DAMPY(Sn^{II}N(SiMe$_3$)$_2$)$_2$ **39** displays two singlets in the solution state ^{119}Sn NMR corresponding to two differently coordinated Sn^{II} atoms. A peak at 489.4 ppm is assigned to the Sn atom coordinated by two nitrogen atoms turned away from the center and a peak at -195.7 ppm is assigned to the Sn atom coordinated by three nitrogen atoms including the additional pyridenyl N$_{py}$ donation.

The ^{1}H NMR of complexes (DIMPY)Ge **38** and (DIMPY)Sn **40** are displayed in Figure 3.62 and compared to the ^{1}H NMR of the DAMPY ligand. As shown in

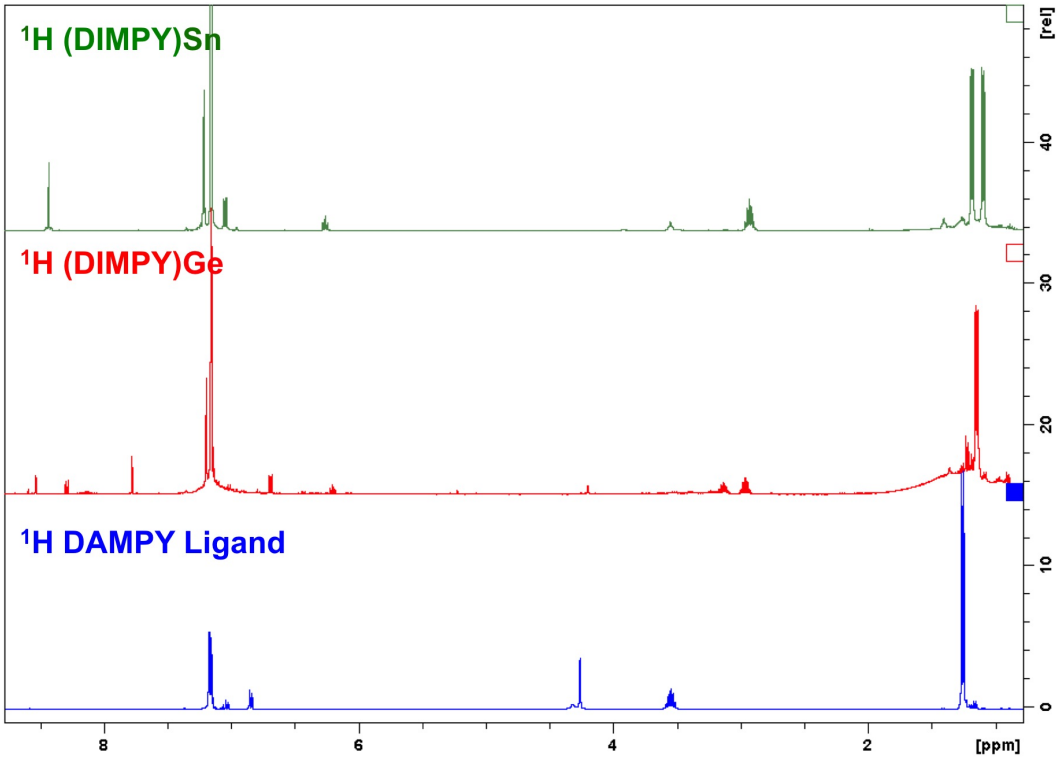

Figure 3.62: The comparison of the ^{1}H spectra of the DAMPY ligand with the complexes (DIMPY)Ge **38** and (DIMPY)Sn **40**.

Figure 3.62, the protons of the C**H**$_2$ group are vanished in case of the ^{1}H NMR spectra of the (DIMPY)Ge **38** and (DIMPY)Sn **40** complexes. Instead, an imino functionality **H**C=N appears in the low field with a signal of 7.78 ppm for (DIMPY)Ge **38** and with a signal of 8.49 ppm for (DIMPY)Sn **40**. The C**H**$(CH_3)_3$ protons from the diisopropyl group are shifted to high field resulting from the coordination of the ligand towards the metal center. The C**H**$(CH_3)_3$ signals are at 2.97 ppm for the (DIMPY)Ge **38** and at 2.89 ppm for the (DIMPY)Sn **40** compound. The signal of the CH(C**H**$_3)_3$ protons is shifted towards high field as well. Furthermore, a splitting of the doublet is induced due to the coordination environment of the group 14 element. The (DIMPY)Ge complex **38** shows a doublet of doublets in the high field at 1.15 ppm and and the (DIMPY)Sn complex **40** reveals a doublet of doublets at 1.15 ppm and 1.07 ppm. In literature, it was studied that the in-plane diiminopyridine hydrogens are shifted in the NMR spectra when paramagnetic species were observed.[163,164] Hence, the in-plane diiminopyridine hydrogens are diagnostic for the electronic state of a

DIMPY complex coordinating a metal center.[163,164] In case of [DIMPYFe]L^- the in-plane ^{1}H signals are temperature independent.[163,164] This is in contrast to the pentacoordinated [DIMPYFe]L_2 complexes which reveal a strong temperature dependence of the in-plane proton resonances. These significant findings are observed due to paramagnetic contributions to NMR shifts which would arise from orbital mixing with excited triplet states.[163,164] If the (DIMPY)E complexes would bear a bonding situation, in which a E^{II} center interacts with a doubly reduced ligand $DIMPY^{2-}$, as shown in the resonance structure **IV**, this findings should be investigated by NMR studies.[163,164] However, complexes (DIMPY)Ge **38** and (DIMPY)Sn **40** neither display a temperature dependence of the in-plane ^{1}H NMR shifts nor are these significantly shifted. Hence, both temperature dependent and independent paramagnetic contributions to NMR shifts which would arise from orbital mixing with excited triplet states can be ruled out and therefore the (DIMPY)Ge **38** and (DIMPY)Sn **40** cannot be considered as in resonance structure **IV**. This was also confirmed by EPR measurements. To rule out the presence of radical species, EPR measurements were performed for the complexes (DIMPY)Ge **38** and (DIMPY)Sn **40**. No resonances were observed in the EPR spectra in solution and solid state in a temperature range between 77 K and room temperature. Hence, a resonance structure **IV** where a E^{II} center interacts with a doubly reduced ligand $DIMPY^{2-}$, can be excluded.

The ^{1}H NMR spectra furthermore clearly rule out the existence of E-H bonds in (DIMPY)Ge **38** and (DIMPY)Sn **40** complexes and further support the unusual nature of this species. These findings correspond with the ^{13}C NMR spectra. Complex (DIMPY)Sn **40** shows a broad signal in the ^{119}Sn NMR spectrum at 64 ppm with a line width of 236 Hz. However, two highly anisotropic resonances are detected in solid state ^{119}Sn NMR. The isotropic chemical shifts 56.9 ppm (A) and 50.2 ppm (B) indicated by asterisks in Figure 3.63, are identified by recording the spectra at two different magic angle spinning rates (13.0 and 15.0 kHz) (referenced to Ph_4Sn, δ = -121.1 ppm). The occurrence of two ^{119}Sn resonances with almost identical spectroscopic parameters for complex (DIMPY)Sn **40** could arise from two slightly different crystallographic sites as cocrystallized solvent molecules were removed *in vacuo* prior to recording the NMR spectra.[102] Another reason could be the slight asymmetrical environment of the Sn atom which is also confirmed by the solid state structure analysis. The

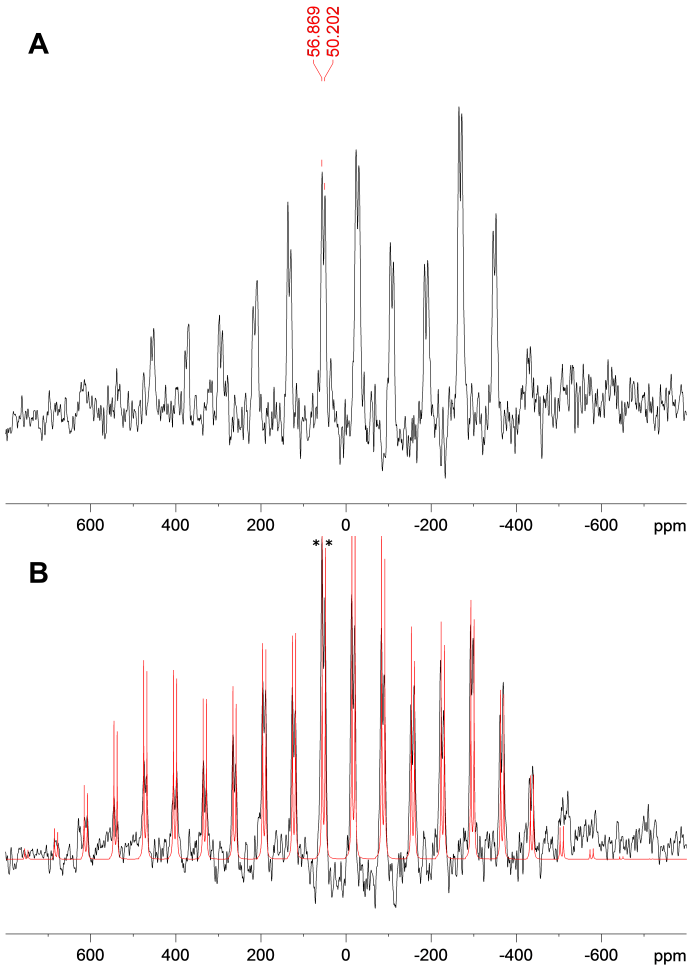

Figure 3.63: Solid State NMR spectra of compound **40**.

structure of compound (DIMPY)Sn **40** is further supported by the solid state ^{1}H-^{13}C CPMAS spectrum.

The heteroleptic germanium complexes DAMPYNHGeN(SiMe$_3$)$_2$ **36** and DAMPYNHGeCl **37** (Figure 3.64, Table 3.12) show a similar bonding motif and are related to the heteroleptic SAMPYGeN(SiMe$_3$)$_2$ **9**. Compound DAMPYNHGeN(SiMe$_3$)$_2$ **36** crystallizes in the triclinic space group P$\bar{1}$ containing two independent molecules in the unit cell. Complex **36** bears a trigonal pyramidal environment and the Ge atom is threefold coordinated by three nitrogen atoms. As in complex SAMPYGeN(SiMe$_3$)$_2$ **9**, compound DAMPYNHGeN(SiMe$_3$)$_2$ **36** possesses two covalent Ge - N bonds with a bond lengths of Ge - N1 with 1.923(1) Å and Ge - N4 with 1.948(2) Å. As expected, the donor-acceptor interaction Ge - N3 is elongated with 2.111(2) Å. The Ge - N distances are in good agreement with literature known Ge - N bonds and the

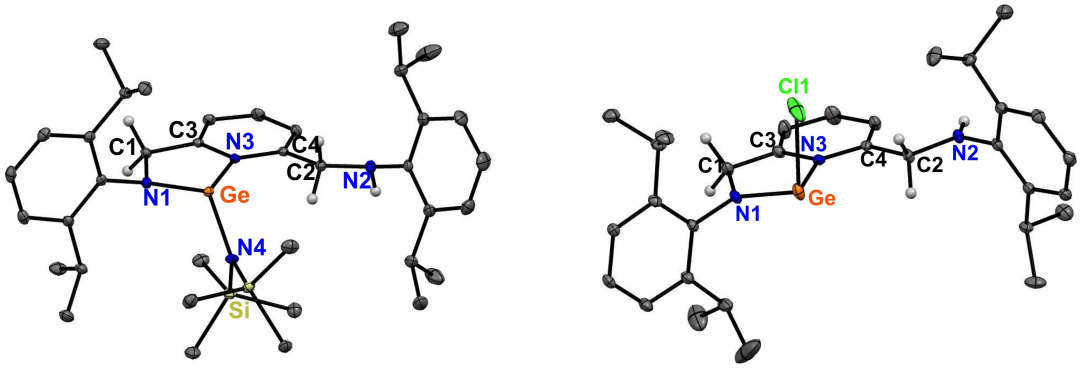

Figure 3.64: Solid state structures of compounds **36** and **37**. Anisotropic displacement parameters are depicted at the 50% probability level. Hydrogen atoms are omitted for clarity except at the CH_2 and the HC=N functionality.

SAMPYGeN$(SiMe_3)_2$ **9** ranging from 1.910 - 2.083 Å.[151] The angles observed in complex **36** are for N1-Ge-N4 with 106.85(7)° and N1-Ge-N3 with 79.72(7)° and are similar to the angles of complex SAMPYGeN$(SiMe_3)_2$ **9** as expected. Also the bond lengths of the coordinated DAMPY ligand are as expected for C1 - N1 with 1.441(3) Å and C1 - C3 with 1.497(3) Å. The comparison of the coordinated amino functionality with the uncoordinated amino functionality within the complex DAMPYNHGeN$(SiMe_3)_2$ **36** shows that the C1 - N1 is slightly shortened in case of the uncoordinated C2 - N2 distance with 1.409(3) Å and the C2 - C4 distance is slightly elongated with 1.500(3) Å.

Complex DAMPYNHGeCl **37** crystallizes in the monoclinic space group Pc and bears a trigonal pyramidal environment. The Ge atom is threefold coordinated by two nitrogen atoms and by one chlorine atom. The Ge - N distances reveal a similar trend as discussed for complex DAMPYNHGeN$(SiMe_3)_2$ **36** bearing a covalent Ge - N1 with 1.861(2) Å and a donor-acceptor interaction Ge - N3 with 2.077(2) Å. The angles observed in complex DAMPYNHGeCl **37** are N1-Ge-Cl with 88.69(7)° and N1-Ge-N3 with 80.96°. The N1-Ge-N3 angle agrees well with complex DAMPYNHGeN$(SiMe_3)_2$ **36**. Due to the similar bonding motif, the bond lengths of the ligand system shows the expected distances for the amide bond C1 - N1 with 1.446(4) Å and the slightly elongated uncoordinated amino bond with 1.462(3) Å. The back bone of the ligand system bears a C1 - C3 distance with 1.510(3) Å for the coordinated ligand site and a C2 - C4 with 1.511(3) Å for the uncoordinated ligand site.

Table 3.12: Comparison of the bond lengths [Å] and angles [°] of compounds DAMPYNHGeN(SiMe$_3$)$_2$ **36**, DAMPYNHGeCl **37**, (DIMPY)Ge **38** and **DIMPYGeCl$^+$ 29**.

Bond lengths and angles	**36**	**37**	**38**	**DIMPYGeCl$^+$ 29**
Ge – N1	1.923(1)	1.861(2)	1.935(1)	2.255(6)
Ge – N2	-	-	2.665(1)	2.314(6)
Ge – N3	2.111(2)	2.077(2)	1.945(1)	2.077(4)
Ge - N4/Cl1	1.948(2)	2.324(1)	-	2.228(2)
C1 – N1	1.441(3)	1.446(4)	1.347(2)	1.270(6)
C1 – C3	1.497(3)	1.510(3)	1.391(2)	1.473(8)
C2 – N2	1.409(3)	1.462(3)	1.297(2)	1.277(6)
C2 – C4	1.500(3)	1.511(3)	1.434(2)	1.464(8)
N1-Ge-N4/Cl1	106.85(7)	88.69(7)	-	85.99(1)
N1-Ge-N2	-	-	151.23(5)	146.42(2)
N1-Ge-N3	79.72(7)	80.96(1)	82.48(6)	73.84(2)

In Figure 3.65, the solid state structure of the germanium complex (DIMPY)Ge **38** is shown. In case of the previously discussed complexes DAMPYNHGeN(SiMe$_3$)$_2$ **36** and DAMPYNHGeCl **37**, a DAMPY ligand is coordinating a Ge^{II} atom. The ligand system changes significantly regarding the (DIMPY)Ge complex **38** where a DIMPY ligand system stabilizes a Ge atom in the formal oxidation state zero. During writing this PhD thesis, a related (MeDIMPY)Ge^0 complex[162] was published which bears a similar bonding motif compared to the (DIMPY)Ge complex **38**. Compound **38** crystallizes in the

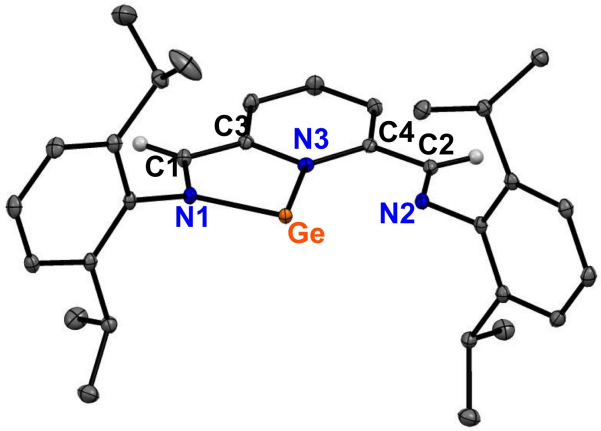

Figure 3.65: Solid state structure of compound **38**. Anisotropic displacement parameters are depicted at the 50% probability level. Hydrogen atoms are omitted for clarity except at the CH$_2$ and the HC=N functionality. The Ge atom is disordered but only one position is shown for clarity.

monoclinic space group $P2_1/c$ (Figure 3.65, Table 3.12). In case of compound **38** as well as the literature known (MeDIMPY)Ge^0 complex[162] the Ge atom within the complex bears a disorder which was solved by modeling another Ge atom in the plane of the DIMPY ligand. Hence, two different Ge - N_{im} distances are observed in complex (DIMPY)Ge **38** with Ge - N1 of 1.935(1) Å and Ge - N2 of 2.665(1) Å. These Ge - N_{im} distances differ more than in the (MeDIMPY)Ge^0 complex[162] with 2.047(7) Å and 2.306(7) Å. The Ge - N_{py} distance, Ge - N3, is 1.945(1) Å long and agrees well with the (MeDIMPY)Ge^0 complex[162] with a Ge - N_{py} of 1.899(18) Å. The donor-acceptor interactions of complex (DIMPY)Ge **38** are in case of Ge - N1 and Ge - N3 slightly shortened compared to the donor-acceptor interactions of the cation $[DIMPYGeCl]^+$ bearing distances ranging from 2.077(4) to 2.314(6) Å (Table 3.12). The N1-Ge-N2 angle is 151.23(5)° and is bigger than the N1-Ge-N2 angle of the cation $[DIMPYGeCl]^+$ with 146.42(2)°. This applies also for the N1-Ge-N3 angle with 82.48(6)° for complex (DIMPY)Ge **38** and with 73.84(2)° for the cation $[DIMPYGeCl]^+$ bearing an additional chlorine atom bonded towards the Ge center. The additional chlorine functionality bonded to the Ge atom is the reason for the differences within the complexes (DIMPY)Ge **38** and the cation $[DIMPYGeCl]^+$. Hence, it can be rationalized that the (DIMPY)Ge complex **38** bears the resonance structure **I**, **II** and **III** within the compound. A certain degree of a Ge^0 atom is present in the complex. Donor acceptor interactions of the ligand system stabilize the Ge^0 atom and the bond lengths are in good agreement with the (MeDIMPY)Ge^0 complex.[162] However, a slight asymmetry within complex **38** bears the resonance structures **II** and **III**, too. In the resonance structures **II** and **III**, the Ge atom remains in the oxidation state +2. Compared to the (MeDIMPY)Ge^0 complex[162] in literature, the unusual bonding situation in complex (DIMPY)Ge **38** is much more alike with resonance structure **I** than with the resonance structures **II** and **III**. Therefore, the (DIMPY)Ge complex **38** can be described as a neutral DIMPY ligand coordinating a Ge^0 atom *via* donor-acceptor interactions. Furthermore, a backbonding of the Ge^0 atom to the ligand is observed and has an additional stabilizing effect. This bonding situation will be further investigated *via* theoretical calculations and discussed later.

The heteroleptic bisstannylene DAMPY($Sn^{II}N(SiMe_3)_2)_2$ **39** crystallizes in the monoclinic crystal system C2/c (Figure 3.66, Table 3.13). The Sn1 atom is threefold coordinated by three N atoms. The three nitrogen atoms coordinate to the Sn1 atom with one donor-acceptor and two covalent interactions. The two covalent (DAMPY)-Sn bonds are Sn1 - N1 with 2.109(3) Å and Sn2 - N2 with 2.146(3) Å, and the Sn1 - N3 donor-acceptor interaction has a distance of 2.319(3) Å. The Sn2 atom faces away from the complex center and possesses two covalent Sn - N bonds (Sn2 - N2 2.059(3) Å and Sn2 - N5 2.099(3) Å). The covalent and the donor-acceptor Sn - N interactions in compound **39** agree well with those reported in literature.[40,165] Furthermore the C1-N1 bond distances conform to C - N single bonds of 1.445(4) and 1.462(4) Å in length. The N1-Sn1-N4 angle is 103.57(12)° and the five membered ring shows a N1-Sn1-N4 angle with 74.69(10)°.

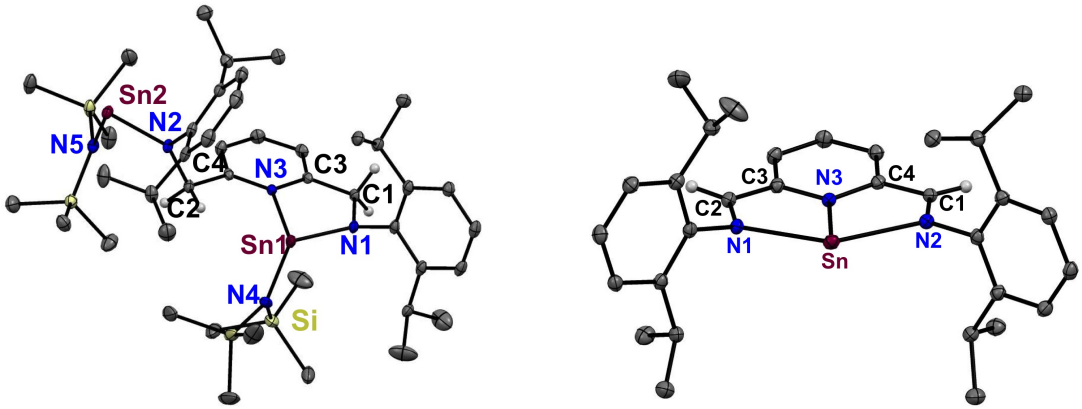

Figure 3.66: Solid state structures of compounds DAMPY($Sn^{II}N(SiMe_3)_2)_2$ **39** and (DIMPY)Sn **40**. Anisotropic displacement parameters are depicted at the 50% probability level. Hydrogen atoms are omitted for clarity except at the HC=N functionality.

Compound (DIMPY)Sn **40** crystallizes in the monoclinic space group $P2_1/c$ (Figure 3.66, Table 3.13). The most prominent characteristic of compound **40** is that the Sn atom is in a formal oxidation state of zero stabilized by donor-acceptor interactions from the DIMPY ligand. The nitrogen atoms of the DIMPY ligand coordinate to the Sn^0 center and hence form a planar complex creating two five-membered chelating rings. The Sn-N1 and Sn-N2 bond distances are 2.397(2) and 2.315(2) Å and agree well with those reported in literature for Sn -N_{py} bonds ranging from 2.286(2) to 2.6879(17) Å.[40,165] In the related compounds [MeDIMPY$Sn^{II}Cl]^+$ [$Sn^{II}Cl_3]^-$ ion pair[40] and complex [DIMPY$Sn^{II}Cl]^+$ [$Sn^{II}Cl_3]^-$ **31** a slight elongation of the Sn-N bond distances is

Table 3.13: Comparison of the bond lengths [Å] and angles [°] of compounds **DIMPYSnCl$^+$ 31**, DAMPY($Sn^{II}N(SiMe_3)_2)_2$ **39** and DIMPYSn **40**.

Bond lengths and angles	**DIMPYSnCl$^+$ 31**	**39**	**40**
Sn – N1	2.453(2)	2.109(3)	2.397(2)
Sn(2) – N2	2.414(2)	2.059(3)	2.315(2)
Sn – N3	2.303(2)	2.319(3)	2.122(2)
Sn(2) - N5/Cl1	2.452(7)	2.146(3)	-
C1 – N1	1.274(3)	1.445(4)	1.308(3)
C1 – C3	1.478(3)	1.498(4)	1.422(3)
C2 – N2	1.274(3)	1.462(4)	1.321(3)
C2 – C4	1.474(3)	1.520(4)	1.406(3)
N1-Sn-Cl1	85.30(5)	103.57(1)	-
N1-Sn-N2	68.74(6)	-	142.43(7)
N1-Sn-N3	136.70(6)	74.69(1)	70.50(7)

observed as compared to compound **40**. This is attributed to the smaller coordination number of Sn^0 since there are no interactions with a chlorine atom, solvent molecule, or the metal center of a neighboring molecule. Moreover, the unusual bonding situation in **40** is further substantiated by a significant shortening of the Sn - N_{py} bond (2.122(2) Å). This bond length is well below the range of Sn - N_{py} bonds for related species varying from 2.286(2) to 2.6879(17) Å.[40,102,165] In addition, the Sn-N3 distance is shorter compared to the Sn - N1 and Sn - N2 between the central tin atom and the imino groups (Table 3.14). Related complexes with the same bonding motif as compound **40**, such as the cationic $[DIMPYP]^+$,[36] $[DIMPYAs]^{+}$[37] and $[DIMPYTe]^{2+}$[41] complexes exhibit identical trends in the structural motifs with short N_{py}-E and longer N_{im}-E bonds.[36,37,41] In these complexes, the geometry of the ligand system is strictly constrained. To compensate for the constrained ligand system the element center N_{py} - E distance is shortened. The N1-Sn-N2 angle for compound **40**, which depends on the size of the element center, is 142.43(7)° and agrees well with the related complex.[36,37,40,41] In complex **40**, the N1 - C1 and N2 - C2 double bond lengths are 1.308(3) and 1.321(3) Å and are in the typical range compared to imino bond lengths of the related complexes.[36,37,40,41]

In Table 3.14 the solid state structures of the SIMPY ligand, the (SIMPY)Ge **12**, (DIMPY)Ge **38** and (DIMPY)Sn **40** are compared. As discussed for the complex (SIMPY)Ge **12** in chapter 3.2, two resonance structures describe this germanium complex. One considers a neutral SIMPY ligand coordinating a Ge^0 atom and the other displays a dianionic $SIMPY^{2-}$ ligand coordinating a Ge^{II} atom covalently in expense of the aromaticity in the pyridine ring. Regarding the solid state structures the bonding situation in the complexes can be analyzed for the solid state. For the (SIMPY)Ge complex a certain degree of a Ge^0 complex can be confirmed by theoretical calculations and with the solid state structure analysis the bonding motif more likely represents the dianionic $(SIMPY^{2-})Ge^{II}$ complex. This is confirmed by the C_{py} - C_{py} and C_{py} - N_{py} distances of the pyridine ring which differ significantly compared to the pyridine ring distances of the SIMPY ligand. When the aromaticity is intact bond lengths of C_{py} - C_{py} around 1.39 Å and of C_{py} - N_{py} around 1.34 Å are observed. The (SIMPY)Ge complex reveals C_{py} - C_{py} distances varying from 1.349(7) to 1.429(6) Å and elongated C_{py} - N_{py} bond lengths of 1.39 Å. In case of the (DIMPY)Ge complex

Table 3.14: Bond lengths [Å] and angles [°] of compounds **SIMPY**, (SIMPY)Ge **12**, (DIMPY)Ge **38** and (DIMPY)Sn **40**.

Bond lengths and angles	SIMPY	(SIMPY)Ge 12	38	40
E – N1	-	1.873(4)	1.935(1)	2.397(2)
E – N2	-	1.903(4)	2.665(1)	2.315(2)
E - N3	-	-	1.945(1)	2.122(2)
C1 - N1	1.270(2)	1.376(4)	1.347(2)	1.308(3)
C1 – C2	1.473(3)	1.374(5)	1.391(2)	1.422(3)
C2 - C3	1.390(3)	1.429(6)	1.406(2)	1.380(4)
C3 - C4	1.390(3)	1.351(6)	1.374(2)	1.394(4)
C4 - C5	1.378(3)	1.419(8)	1.405(2)	1.388(4)
C5 - C6	1.381(3)	1.349(7)	1.373(2)	1.395(4)
C6 - N2	1.333(3)	1.392(5)	1.399(2)	1.390(4)
N2 - C3	1.339(3)	1.397(6)	1.406(2)	1.393(4)

these differences are only slightly present. The C_{py} - C_{py} distances are ranging from 1.373(2) to 1.406(2) Å and the C_{py} - N_{py} bond lengths are still elongated around 1.39 Å due to coordination towards an element center. The aromaticity is only slightly disturbed and the (DIMPY)Ge complex is represented by a mixture of the resonance structure **I** a neutral DIMPY ligand coordinating a Ge^0 atom and the resonance structures **II** and **III** a dianionic $DIMPY^{2-}$ interacting with a Ge^{II} in the solid state. As discussed previously the (DIMPY)Ge

complex is much more alike with resonance structure **I** than with **II** and **III** compared to the (MeDIMPY)Ge^0 complex.[162] In case of the (DIMPY)Sn complex **40**, the aromaticity of the pyridine ring system is still intact. The C_{py} - C_{py} distances are around 1.39 Å as in the SIMPY ligand system and the C_{py} - N_{py} bond lengths are elongated around 1.39 Å which can be explained by the coordination environment of the Sn center. The (DIMPY)Sn complex is best described with the resonance structure **I** a neutral DIMPY ligand coordinating a Sn^0 atom. Another prominent bond length is the C_{im} - C_{py} in the backbone of the ligand system. In case of the SIMPY ligand the C_{im} - C_{py} is a typical single bond with 1.473(3) Å. In case of the (SIMPY)Ge complex the C_{im} - C_{py} bond length is shortened with 1.374(5) Å representing a delocalization in the five membered ring. For the (DIMPY)Ge complex the C_{im} - C_{py} bond length is slightly more elongated with 1.391(2) Å. In case of the (DIMPY)Sn complex **40** a much more elongated C_{im} - C_{py} distance is observed with 1.422(3) Å which is shortened compared to the SIMPY ligand due to the coordination towards an element center.

To obtain further insights into the (DIMPY)Sn^0 **40**, the electronic environment of the ^{119}Sn atom will be investigated by ^{119}Sn Mössbauer spectroscopy and is compared to typical related Sn^{II} complexes.[102] ^{119}Sn Mössbauer spectra of compounds (DIMPY)Sn^0 **40**, $[DIMPYSn^{II}Cl]^+$ $[Sn^{II}Cl_3]^-$ **31** and $DIMPYSnOTf_2$ **34** are presented in Figures 3.67 and 3.68 together with transmission integral fits.** The corresponding fitting parameters are listed in Table 3.15. All samples

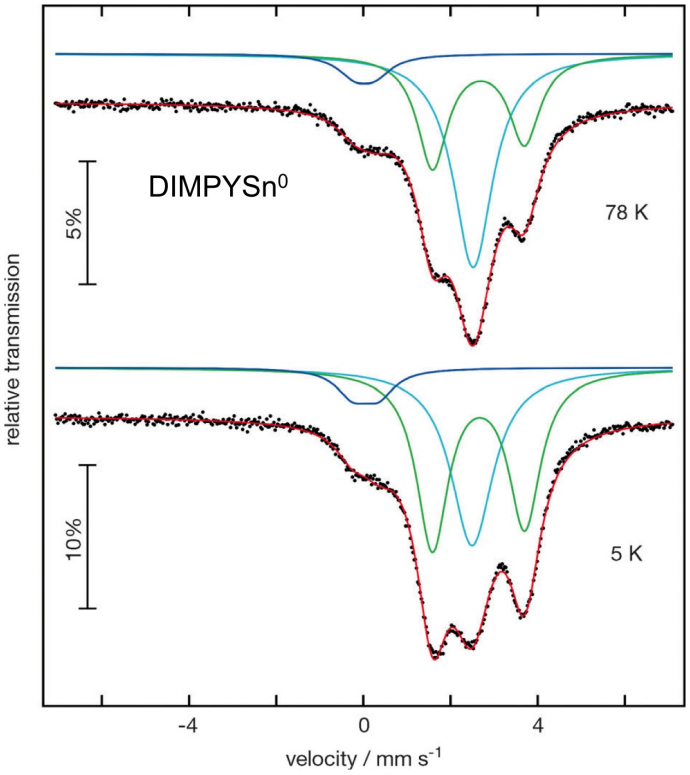

Figure 3.67: Experimental and simulated ^{119}Sn Mössbauer spectra of complex (DIMPY)Sn **40** at 78 and 5 K.[102]

show small contributions of a tetravalent tin species (isomers shifts around 0 mm s^{-1}), most likely due to hydrolysis of the sample and formation of SnO_2.[102] The complex ^{119}Sn spectrum of (DIMPY)Sn^0 **40** at 78 K was best reproduced by a superposition of three spectral components 1) the small SnO_2 contribution, 2) a quadrupole split signal at δ= 2.64 mm s^{-1}, and 3) a third signal without quadrupole splitting at δ= 2.52 mm s^{-1}. The latter arises from β-Sn, which forms upon decomposition of the complex.[102]

** ^{119}Sn Mössbauer spectra were recorded and analyzed by B. Gerke and R. Pöttgen from the Institut für Anorganische und Analytische Chemie, Westfälische Wilhelms Universität Münster.

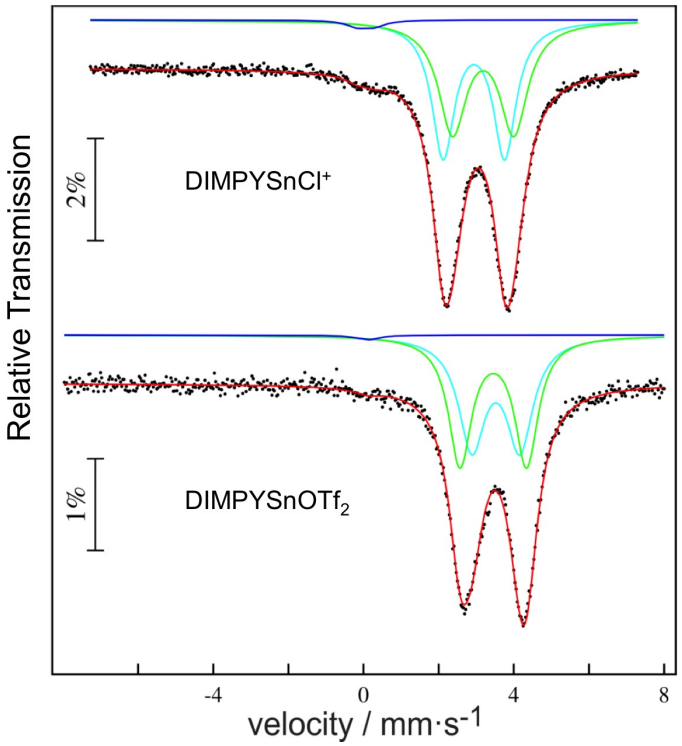

Figure 3.68: Experimental and simulated ^{119}Sn Mössbauer spectra of the complexes $[DIMPYSn^{II}Cl]^+$ $[Sn^{II}Cl_3]^-$ **31**[102] and $DIMPYSnOTf_2$ **34**.

Table 3.15: Fitting parameters of ^{119}Sn Mössbauer spectroscopic measurements at 78 K. δ= isomer shift, ΔE_Q= electric quadrupole splitting, Γ= experimental line width. Parameters marked with an asterisk were kept fixed during the fitting procedure.

Compound	δ **(mm s^{-1})**	ΔE_Q **(mm s^{-1})**	Γ **(mm s^{-1})**	ratio (%)
(DIMPY)Sn	2.52(1)	0*	1.10(2)	54(1)
at 78 K	2.64(1)	2.11(1)	0.84(1)	39(1)
	0.02(1)	0.46(5)	0.92(7)	8(1)
(DIMPY)Sn	2.50(1)	0*	1.18(2)	38(1)
at 5 K	2.64(1)	2.12(1)	0.89(1)	54(1))
	0.05(4)	0.59(2)	0.89(5)	8(1)
$DIMPYSnCl^+$	2.94(1)	1.64(1)	0.73(1)	49*
at 78 K	3.18(1)	1.63(1)	0.90(1)	49*
	0.05(4)	0.45(8)	0.7*	2.1(1)
$DIMPSnOTf_2$	3.52(1)	1.28(2)	0.86(2)	49(1)
at 78 K	3.45(1)	1.77(2)	0.75(1)	50*
	0.1(1)	0	0.75*	1(1)

The isomer shift of δ= 2.64 mm s^{-1} is in good agreement with that of neutral tin.[102] Compounds $[DIMPYSn^{II}Cl]^+$ $[Sn^{II}Cl_3]^-$ **31** and $DIMPYSnOTf_2$ **34** show

signals (besides the small SnO_2 contribution) which can be attributed to divalent tin within the complexes. In case of complex $[DIMPYSn^{II}Cl]^+$ $[Sn^{II}Cl_3]^-$ **31**, a second signal at δ= 3.18 mm s^{-1} can be assigned to the anion $[Sn^{II}Cl_3]^-$.[102] Hence, it can be concluded that the (DIMPY)Sn **40** bears a Sn^0 atom in an oxidation state of zero due to the differences observed in the ^{119}Sn Mössbauer spectra. The signals in case of (DIMPY)Sn **40** can be assigned to neutral tin.[102] Experimentally, the (DIMPY)Sn **40** was studied intensively. To gain a better understanding of the unusual bonding situation in the complex, a theoretical study was performed.

DFT investigations have been carried out to get a deeper insight into the electronic features of (DIMPY)Sn^0 **40**.[††] To contrast the unique bonding situation in (DIMPY)Sn^0 **40** from the one in typical stannylenes, additional calculations for a hypothetical stannylene complex (DAMPY)Sn^{II} were carried out (Figure 3.69). Therefore, the solid state structure of the (DIMPY)Sn^0 **40** complex was geometry optimized at a density functional level using the hybrid MPW1PW91 functional together with a double-zeta basis set (SDD).[102]

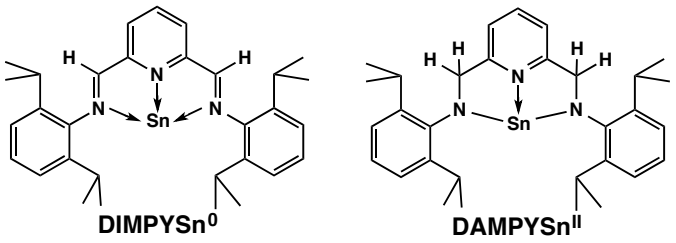

Figure 3.69: Compound (DIMPY)Sn **40** is compared theoretically to a hypothetical stannylene, the related (DAMPY)Sn^{II} complex.

Table 3.16: Comparison of the bond lengths [Å] and angles [°] of the experimental values of compound(DIMPY)Sn **40** with the theoretical values of the (DIMPY)Sn^0 and the hypothetical (DAMPY)Sn^{II} complex.

Bond lengths and angles	**DIMPYSn**$_{exp}$	**DIMPYSn**$_{calc}$	**(DAMPY)Sn^{II}**
Sn-N1	2.397(2)	2.376	2.181
Sn-N2	2.315(2)	2.361	2.181
Sn-N3	2.122(2)	2.152	2.4
N1-C1	1.308(3)	1.329	1.452
N2-C2	1.321(3)	1.331	1.452
N3-C3	1.390(3)	1.404	1.351
N3-C7	1.393(3)	1.403	1.351
C1-C7	1.422(4)	1.42	1.506
C2-C3	1.406((4)	1.418	1.506
N1-Sn-N2	142.43(7)	141.9	137.3
N1-Sn-N3	70.50(7)	70.9	68.7
N2-Sn-N3	72.15(7)	71.1	68.7

The optimized gas phase structure of (DIMPY)Sn^0 **40** closely resembles the molecular structure in the solid state as shown in Table 3.16. In Table 3.16 the most important bond lengths and angles of the calculated tin complexes are collected and compared to the molecular structure of (DIMPY)Sn^0 **40**. In the

[††] Theoretical studies in collaboration with M. Flock. Institute of Inorganic Chemistry, TU Graz

calculated (DAMPY)Sn^{II} complex two of the Sn-N bonds are rather short indicating covalent interactions, while the third interaction with the pyridine ring (Sn - N3) is weak. The exact contrary bonding behavior is observed in (DIMPY)Sn^0 complex. According to the short Sn-N_{py} distance both atoms seem to interact strongly.

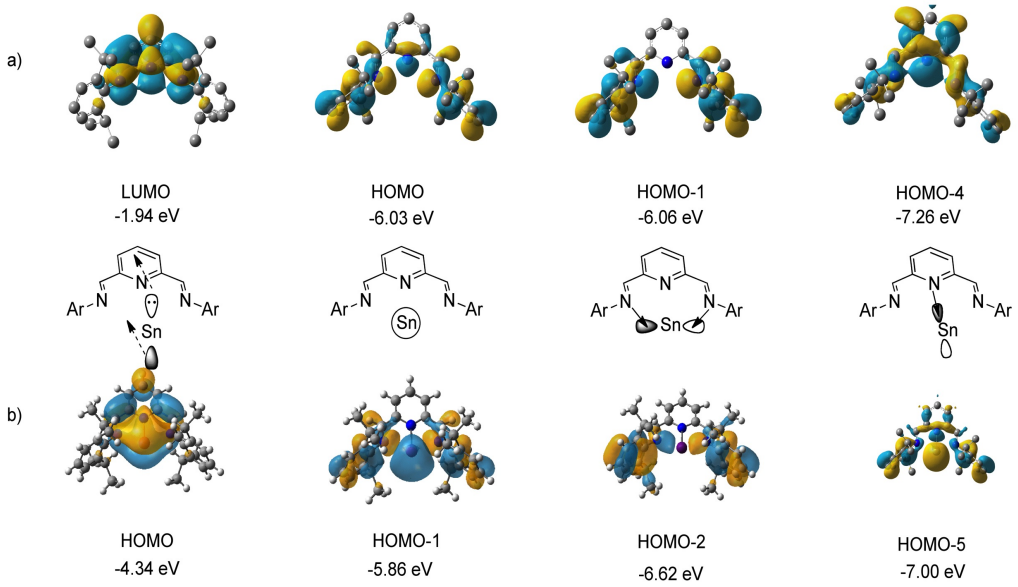

Figure 3.70: Frontier orbitals of the DIMPY ligand and the DIMPYSn complex **40**.[102]

To gain a better understanding of the bonding situation within the (DIMPY)Sn^0 complex, the frontier orbitals of the DIMPY ligand were calculated and compared to the frontier orbitals of the (DIMPY)Sn^0 complex (Figure 3.70).[102] Interaction between the ligand orbitals HOMO-4 and HOMO-1 with in-plane p-orbitals of the Sn atom result in the orbitals HOMO-2 and HOMO-5 of complex (DIMPY)Sn^0 **40**. The HOMO-1 in (DIMPY)Sn^0 complex **40** has essentially s-electron character at the Sn atom. Most significant, however, is the nature of the HOMO in the (DIMPY)Sn^0 complex **40**. It originates from a backbonding interaction between the filled, out of plane p-orbital at Sn π type LUMO of the uncomplexed ligand. Therefore, the contribution of backdonation of electron density from the low oxidation state Sn center to the DIMPY ligand is crucial for the bonding situation in the (DIMPY)Sn^0 complex **40**. Hence, the backdonation results in a short pyridenyl N_{py} - E (E= Ge, Sn) distance as discussed in the solid state structure analysis for the (DIMPY)Ge^0 and (DIMPY)Sn^0 complexes.[102]

A topological analysis of the electron density of (DIMPY)Sn^0 by QTAIM[166] calculations shows bond critical points for all three Sn-N interactions (Figure 3.71). The existence of bond critical points and especially the Laplacians of the

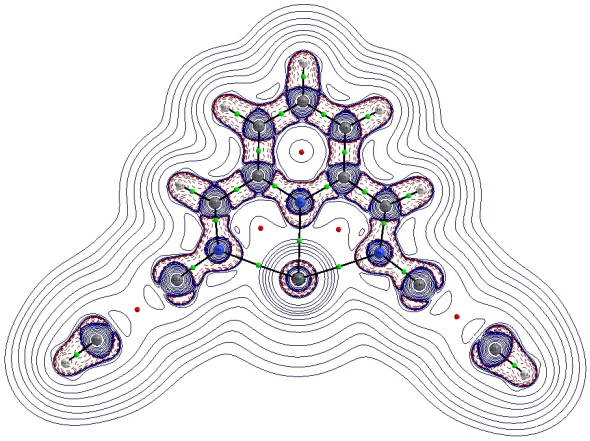

Figure 3.71: Plot of the Laplacian of the electron density, $\nabla 2\rho$, of (DIMPY)Sn^0 in the molecular Sn-N-N-N plane. Bond and ring critical points are also included.

electron density ($\nabla 2\rho$) together with the total energy density H_b at these critical points are used to categorize the interatomic interactions. In case of covalent interactions a $\nabla 2\rho < 0$ is found, while $\nabla 2\rho > 0$ point to electrostatic (closed-shell) interactions. Additionally, the sign of the total energy density H_b at the bond critical point (BCP) assigns wether the interaction between two atoms is electrostatic dominant ($H_b > 0$) or covalent ($H_b < 0$) dominant. The respective electron density ρ at the bond critical points between Sn-N1 and Sn-N2 are 0.056 a.u. and 0.058 a.u. For Sn-N3 a value of 0.088 a.u. is found confirming in all three cases weak interactions. The $\nabla 2\rho$ values are +0.15, +0.15, and +0.24, respectively. The H_b values are -0.013, -0.014, and -0.031. The combination of all these BCP parameters point to typical metal bonding and are comparable in size to those found for metallocenes.[166] Figure 3.71 shows charge concentrations in the molecular plane corresponding to the lone pairs of the three nitrogen atoms pointing towards the Sn atom. Furthermore, anagostic interactions with the C-H bonds of the diisopropylphenyl ligands stabilize the tin center in the ligand framework. Formally an oxidation state of zero can be ascribed to the tin atom in (DIMPY)Sn^0 while the (DAMPY)Sn^{II} should involve a Sn^{II} atom. The calculated atomic Sn charges originating from Mulliken, natural population, and from the QTAIM analyses are inconclusive. The values range

between 0.54 and 0.96 for (DIMPY)Sn^0 and 0.73 and 1.24 for the (DAMPY)Sn^{II} complex.

The orbitals of both complexes differ in several respects as shown in Figure 3.72. Most prominently, the (DIMPY)Sn^0 HOMO is of a π type orbital involving all three nitrogens and the Sn atom. A similar π orbital consisting mostly of interactions between N1, N2 and Sn is the HOMO-2 in the (DAMPY)Sn^{II} complex. The σ type orbital identified as a lone pair MO on the Sn atom is the HOMO-1 in both cases. The HOMO-LUMO gap is considerably higher (3.99 eV) for (DAMPY)Sn^{II} than for (DIMPY)Sn^0 complex (2.35 eV).

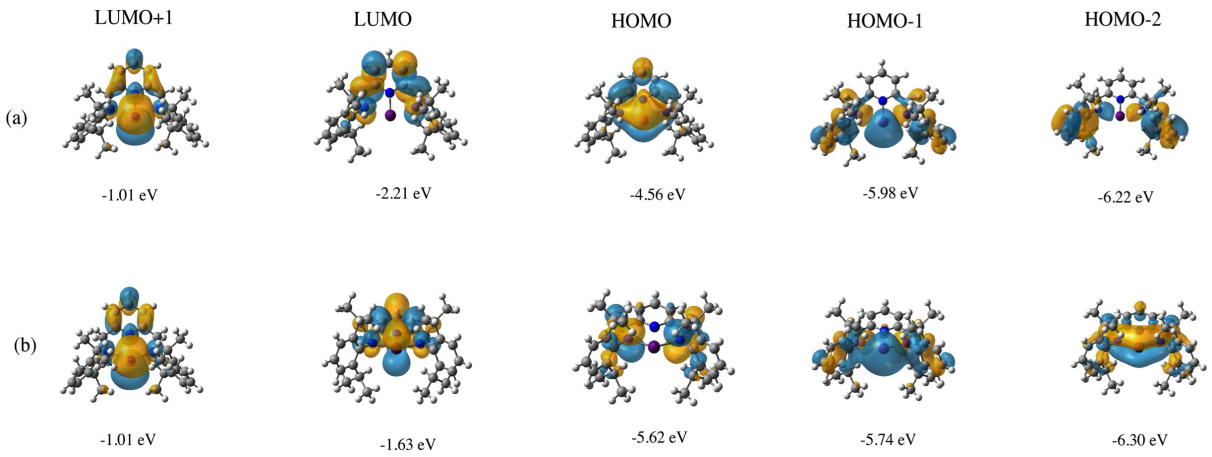

Figure 3.72: Compound (DIMPY)Sn^0 **40** is compared theoretically to a hypothetical stannylene, the related (DAMPY)Sn^{II} complex.

Due to the differences in the frontier orbitals of compound (DIMPY)Sn^0 **40** and in (DAMPY)Sn^{II} a difference in the chemical reactivity is expected. Frenking et al. used first and second proton affinities (PA) to identify divalent E^0 compounds.[103–108] The HOMO and the $HOMO^{-1}$ of the (DIMPY)Sn^0 complex act as a Lewis base in contrast to the DAMPYSn^{II} complex which act as Lewis base ($HOMO^{-1}$) and as Lewis acid (LUMO). Hence, the (DIMPY)Sn^0 complex can interact with it's two lone pairs with other molecules or protons. The DAMPYSn^{II} complex can act as Lewis base and as Lewis acid, but is limited due to the fact that only one lone pair can interact with another molecule or proton. Therefore, the first PAs shouldn't differ strongly, but the second PA should be considerably higher in case of oxidation state zero complexes due to the second lone pair which can interact with the proton as discussed

in chapter 2. Accordingly, we find only small differences between the first PA of (DIMPY)Sn^0, and (DAMPY)Sn^{II} (233.6 kcal/mol vs. 225.8 kcal/mol). There is however, a striking difference on the proton site (Figure 3.73).[103–108] In (DAMPY)Sn^{II} protonation occurs at the σ lone pair coplanar to the N1-Sn-

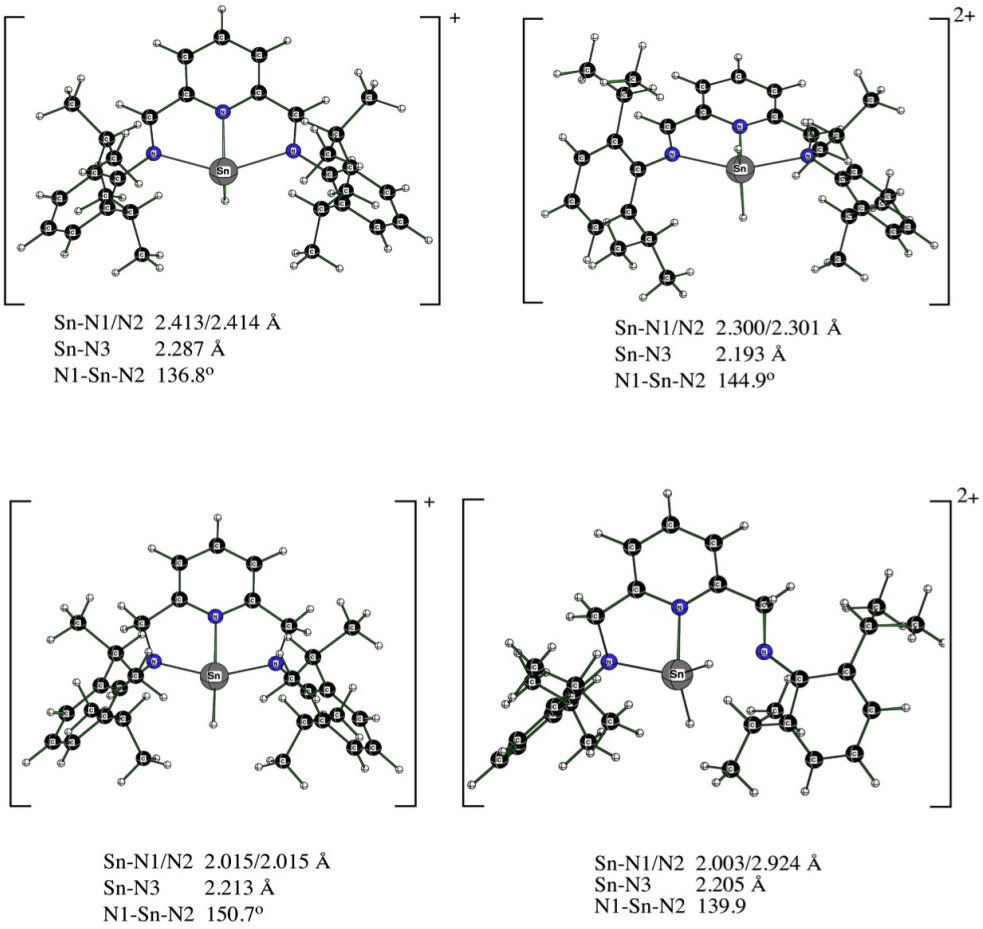

Figure 3.73: MPW1PW91/SDD optimized structures of mono- and diprotonated (DIMPY)Sn^0 (above) and (DAMPY)Sn^{II} (below) complexes.

N2 plane. The π orbital is the protonation site in the (DIMPY)Sn^0 complex, decreasing the N1-Sn-N2 angle to 136.8° and increasing the Sn-N3 bond length to 2.2867 Å. The second PA of (DIMPY)Sn^0 is with 152.3 kcal/mol and 36.6 kcal/mol higher than the 2. PA of (DAMPY)Sn^{II} (115.8 kcal/mol). These protonation energies coincide with the results of Frenking et al. for complexes with Sn^0 character.

E^0 complexes are rare in literature and therefore their reactivity is unknown in contrast to E^{II} compounds - tetrylenes. The reactivity of tetrylenes should differ from the reactivity of tetrylones - E^0 species. This can be explained by the fact that a tetrylene possesses one lone pair of electrons and a vacant π orbital. In case of tetrylones - E^0 complexes - only donor-acceptor interactions are stabilizing the group 14 element center. Hence, two lone pairs of electrons remain at the group 14 element. The E^0 complex possesses therefore mainly π donor properties and act as Lewis base in contrast to E^{II} compounds which can act as σ donor and as π acceptor and act as Lewis base and Lewis acid. As discussed in chapter 2, the activation of small molecules is dependent on the presence of open coordination sites and valence orbitals separated by modest energies ($\leq$4 eV).[28] In case of the (DIMPY)Sn^0 complex the HOMO-LUMO gap is with 2.35 eV considerably lower than for the for hypothetical (DAMPY)Sn^{II} with 3.99 eV. This indicates that the (DIMPY)Sn^0 complex is very reactive and could activate small molecules. However, the fact that open coordination sites are less developed than in the E^0 compound could be problematic. Still, a different reaction behavior should be investigated due to the difference in the frontier orbitals. Therefore the reactivity of the (DIMPY)Sn^0 complex **40** was investigated towards small molecules as H_2, CO_2, P_4 and transition metal complexes. As shown in Figure 3.74, the (DIMPY)Sn^0 complex **40** was reacted with

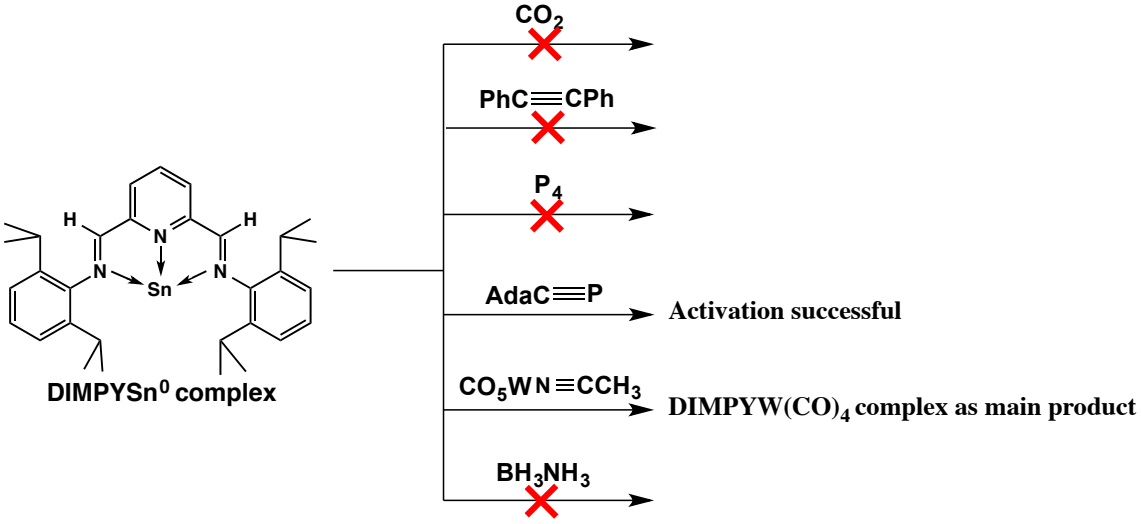

Figure 3.74: The activation of small molecules by the (DIMPY)Sn^0 complex **40**.

ammonia-borane BH_3NH_3 (H_2 source), CO_2, PhC≡CPh, P_4 and AdaC≡P in etheric solvents at room temperature. The reaction solutions were stirred at

room temperature for several days, as well were treated with heating and ultrasonication. However, no activation of small molecules was observed in case of the reaction with BH_3NH_3 (H_2 source), CO_2, PhC≡CPh and P_4. Presumably the (DIMPY)Sn^0 complex **40** cannot accept the electrons of the small molecules. In literature, E≡E species activate H_2 by following steps as discussed in chapter 2: The π HOMO orbital of the E≡E species donates electrons into the σ* orbital of H_2 and then a electron donation of the σ orbital of H_2 follows into the π*-LUMO of ArE≡EAr. This interaction enables the oxidative addition of H_2 due to the weakening of the H-H bond.[145] If the π*-LUMO orbital of the (DIMPY)Sn^0 cannot interact with the σ orbital of H_2, no activation can take place. Another explanation could be the stability of the complex forming two ring fragments with delocalized π cyclization. A change in the stabilized aromatic molecule is thermodynamically not favored.

The reaction with adamantyl phosphalkyne was successful. In literature, the reaction of tetrylenes with C≡P species was investigated.[167–169] Examples are

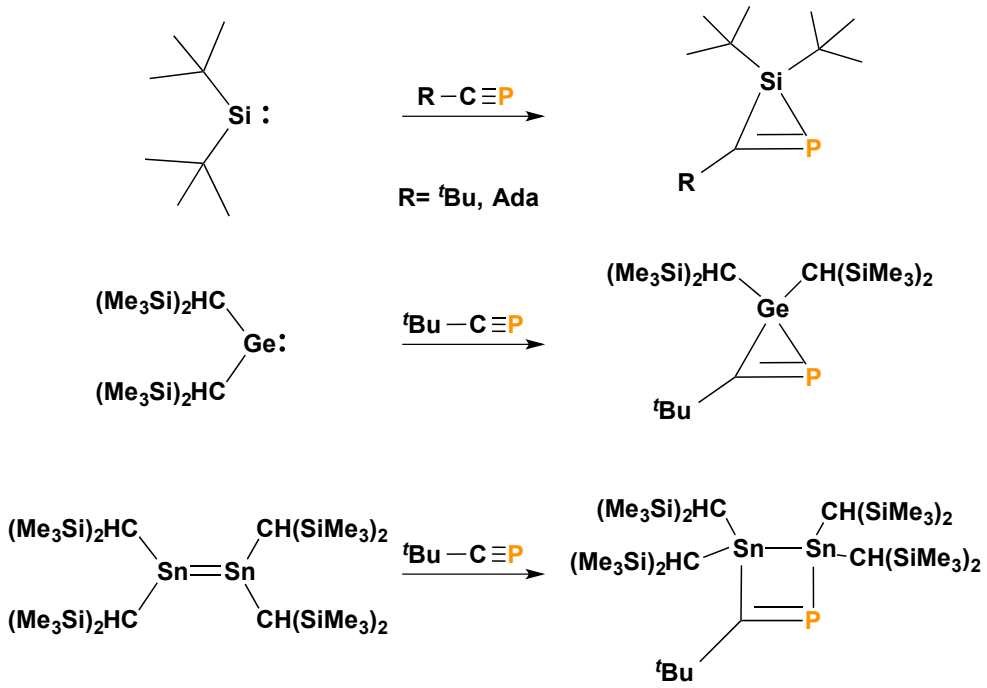

Figure 3.75: The activation of phosphalkynes by tetrylenes - E^{II} complexes. The tetrylene reacts *via* insertion into the C≡P triple bond and a ring systems containing the group 14 element in the oxidation state of +4 are observed.[167–169]

shown in Figure 3.75.[167–169] The tetrylene reacts with the phosphalkyne by inserting into the C≡P triple bond forming three or four membered rings. In the

ring system, the group 14 element does not possess the oxidation state of +2. Instead, an oxidation state of +4 is observed. The reaction of the (DIMPY)Sn^0 complex with adamantyl phosphalkyne (Ada C≡P) leads to a highly interesting Sn^{II} species. The (DIMPY)Sn^0 complex **40** reacts with two equivalents

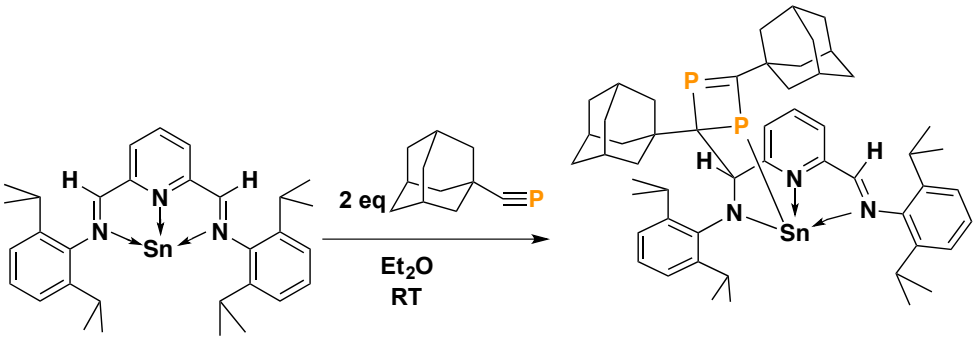

Figure 3.76: The activation of adamantyl phosphalkyne by the (DIMPY)Sn^0 complex **40**.

of Ada-C≡P in diethyl ether at room temperature. A color change was immediate when the reaction solution turned from dark purple to dark red. After stirring for 48 hours at room temperature, all volatile components were removed *in vacuo* and a dark red powder was obtained. The dark red powder was recrystallized in Et_2O at -30°C and dark red cubic crystals of the DIMPYSn(AdaCP)$_2$ **42** were used for X-ray diffraction methods. As shown in Figure 3.76, a four membered adamantyl P-C-P=C ring coordinates towards the DIMPYSn complex. The (DIMPY)Sn^0 complex changed significantly and the DIMPYSn(AdaCP)$_2$ **42** bears a Sn atom in the oxidation state of +2 where the Sn atom is coordinated by a P atom and a N atom covalently. The reaction mechanism is presumably that the Ada-C≡P species coordinates the Sn atom forming a covalent Sn - P bond. Then the formation of a covalent Sn - N bond follows to stabilize the low valent group 14 element. Hence, the imino bond C=N of the ligand system changed due to the coordination forming an amino bond. The reactive C_{am} at the back bone of the ligand system reacts with the C of the coordinating Ada-C≡P species and forms a highly reactive intermediate. This highly reactive intermediates reacts with a second Ada-C≡P to the four membered adamantyl P-C-P=C ring. The reaction of the (DIMPY)Sn^0 complex **40** with Ada-C≡P is untypical and different from the literature known reactions of tetrylenes with phosphaalkynes.[167–169] The reaction of E^0 species do differ strongly from E^{II} complexes as demonstrated. In case of the reaction of

the (DIMPY)Sn^0 complex with Ada-C≡P, a product is formed bearing a low valent Sn^{II} atom. In literature as shown in Figure 3.75, the E^{II} complexes reacted with phosphaalkynes to give E^{IV} ring systems. The DIMPYSn(AdaCP)$_2$ **42** was fully characterized by heteronuclear NMR and solid state structure analysis. In the ^{31} P NMR two different signals are observed. For the C=**P** group a low field shift at 317 ppm is investigated as expected and for the C - **P** fragment a signal in the high field at 30 ppm is observed which is expected for a phosphorus atom coordinated to a C atom *via* a single bond. Both signals are doublets due to the $^2J_{P-P}$ coupling of the two phosphorus atoms with a coupling constant of 39.2 Hz. These findings are conclusive with the ^{1}H and ^{119}Sn NMR spectra. The ^{119}Sn NMR displays a signal at -37 ppm with a $^1J_{P-Sn}$ coupling of 681 Hz. In Figure 3.77, the solid state structure of complex DIMPYSn(AdaCP)$_2$ **42**

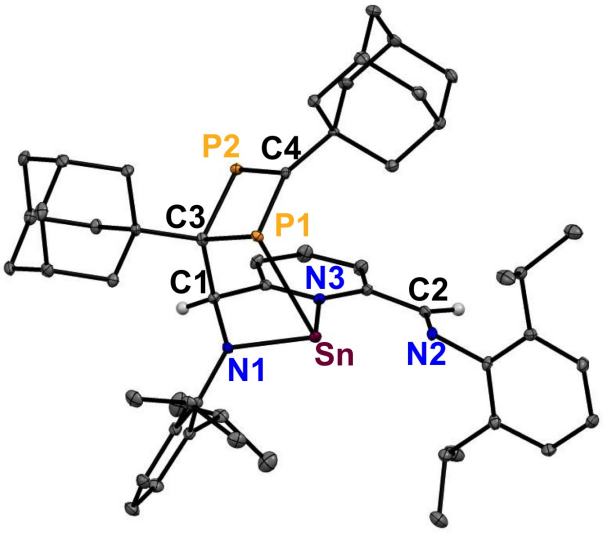

Figure 3.77: Solid state structures of compound DIMPYSn(AdaCP)$_2$ **42**. Anisotropic displacement parameters are depicted at the 50% probability level. Hydrogen atoms are omitted for clarity except at the HC-N and HC=N functionalities. Selected bond lengths [Å] and angles [°] : Sn - N1, 2.124(2); Sn - N2, 2.960(2), Sn - N3, 2.305(2); Sn - P1, 2.684(8); N1 - C1, 1.468(3); N2 - C2, 1.265(4); C1 - C3, 1.563(4); P1 - C3, 1.894(3); P2 - C4, 1.705(3); N1-Sn-N3, 75.60(8); N1-Sn-P1, 84.85(6).

is displayed. Compound DIMPYSn(AdaCP)$_2$ **42** crystallizes in the monoclinic crystal system $P2_1/n$ and bears a trigonal pyramidal environment within the complex. The Sn atom is coordinated by three N atoms and one P atom. Two Sn - N bonds are covalently coordinated with bond lengths of Sn - N1 with 2.124(2) Å and Sn - N3 with 2.305(2) Å. The Sn - N2 distance is a very elongated donor-acceptor interaction with 2.960(2) Å. The Sn - N distances agree well

with literature known complexes[40,165] and with the Sn complexes discussed previously in this PhD thesis. The covalent Sn - P1 single bond is 2.684(8) Å long and agrees with Sn - P single bonds known in literature ranging from 2.5526(7) Å to 2.6612(12) Å.[170] The angles observed in the complex are N1-Sn-N3 with 75.60(8)° and N1-Sn-P1 with 84.85(6)°. As discussed previously, is the N1 - C1 an amide bond with 1.468(3) Å and elongated in contrast to the imino bond N2 - C2 with 1.265(4) Å. The P1 - C3 distance is a single bond with 1.894(3) Å compared to the P2 - C4 double bond with 1.705(3) Å in the four membered ring.

Another reaction was performed to investigate the reaction behavior of the (DIMPY)Sn^0 complex towards Lewis acids. A Lewis acid is for example the tungsten complex $(CO)_5WN{\equiv}CCH_3$ due to the fact that the transition metal complex accepts electrons. The (DIMPY)Sn^0 complex possesses two lone pairs of electrons and act as a Lewis base. Investigating the reaction of the (DIMPY)Sn^0 complex with the tungsten complex $(CO)_5WN{\equiv}CCH_3$ can demonstrate interesting coordination modes of the unknown E^0 species. The equimolar reaction of the (DIMPY)Sn^0 complex and the tungsten complex $(CO)_5WN{\equiv}CCH_3$ was performed in diethyl ether at room temperature as shown in Figure 3.78. A color change was immediate when the reaction solution turned from dark purple to dark red. After stirring for 48 hours at room temperature, all volatile components were removed *in vacuo* and the dark red powder was recrystallized in Et_2O at -30°C. Dark red cubic crystals were obtained and characterized as the DIMPYW$(CO)_4$ complex **43**. Unfortunately, not only was the dark red powder obtained. Tin metal precipitated out of the reaction solution. This lead to the formation of the DIMPYW$(CO)_4$ complex **43** and not to a desired DIMPYSn - W$(CO)_5$ complex. This can be presumably explained by the fact that the (DIMPY)Sn^0 complex is very labile in presence of a strong Lewis acid. The (DIMPY)Sn^0 complex decomposes and the free DIMPY ligand coordinates towards the $(CO)_5WN{\equiv}CCH_3$ compound and forms the DIMPYW$(CO)_4$ complex **43**. In Figure 3.79, the solid state structure of complex DIMPYW$(CO)_4$ complex **43** is shown. Compound DIMPYW$(CO)_4$ complex **43** crystallizes in the monoclinic crystal system $P2_1/n$ and bears an octahedral environment. The W atom is sixfold coordinated by two N atoms and four C atoms. The W - N distances bear a covalent W - N1 bond with 2.200(5) Å and an elongated donor-acceptor interaction with 2.307(5) Å as expected. Two CO

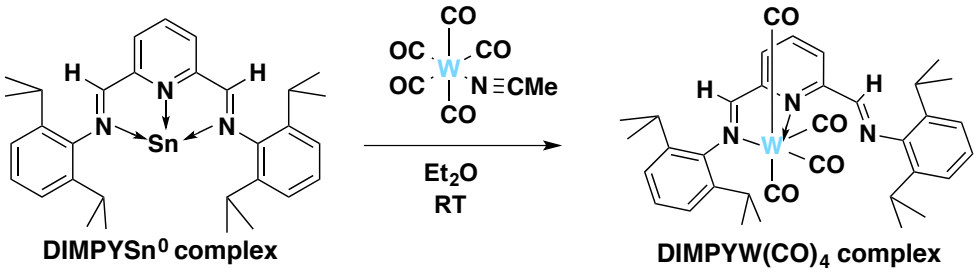

Figure 3.78: The reaction of the (DIMPY)Sn^0 complex **40** with $(CO)_5WN{\equiv}CCH_3$ leads not to the desired DIMPYSn - $W(CO)_5$ complex. Instead, the DIMPYW$(CO)_4$ complex **43** is formed.

groups are located in the plane of the DIMPY ligand fragment and two are perpendicular to this plane with an angle of N1-W-O1, 97.3(2)°. The angle N1-W-N3 is 72.2(2)°. The imino bond N1 - C1 is 1.294(8) Å long and the second imino bond which is turned away from the molecule center is elongated with N2 - C2 of 1.329(9) Å and in typical range of a C=N double bond.

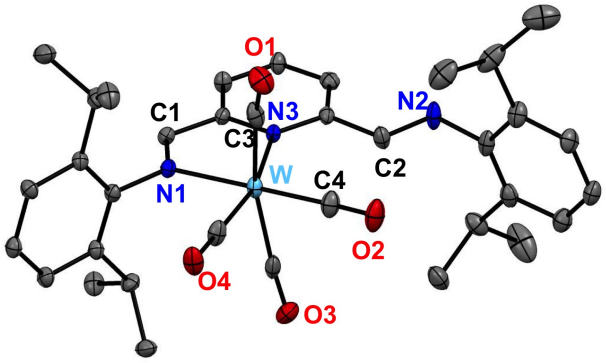

Figure 3.79: Solid state structures of compound DIMPYW$(CO)_4$ complex **43**. Anisotropic displacement parameters are depicted at the 50% probability level. Hydrogen atoms are omitted for clarity except at the HC=N functionality. Selected bond lengths [Å] and angles [°] : W - N1, 2.200(5); W - N3, 2.307(5); W - C3, 2.055(7); W - C4, 1.946(7); N1 - C1, 1.294(8); N2 - C2, 1.329(9); C3 - O1, 1.144(8)); C4 - O2, 1.191(8); N1-W-N3, 72.2(2); N1-W-O1, 97.3(2).

3.5 Synthesis of Low Valent Group 14 Complexes Using Phosphaethenylpyridine Ligands (PAPY)

P-based ligands show an impressive richness of applications in coordination chemistry, homogeneous catalysis, new molecular and polymeric P-containing materials mainly in context of transition metal chemistry.[75] The phosphaethenyl pyridine ligand system (PAPY) was used to stabilize transition metal complexes only.[69–73] For the PAPY ligand system no main group complex is known so far. Related species are, for example, various phosphorus NHC analog systems such as 1,3-diphospha-2-metallapentanes [ML_n(P(Ph)C_6H_4PPh)] [L_n= rac-SnR_2 or $SnMe_2$].[82] Similar compounds were synthesized for Si, Ge and Sn.[83] Furthermore a 1-sila-2,5- diphosphacyclopent-3-ene was reported.[84] Regarding the reactivity of the imino ligand systems with group 14 elements, a different reactivity is expected for phosphaalkene based ligand systems as discussed in chapter 2. To investigate the different reaction behavior of imino and phosphaalkene based ligand systems, the PAPY ligand was reacted with group 14 precursors as EX_2 salts (E= Ge, Sn; X= Cl, OTf) and $E(N(SiMe_3)_2)_2$ (E= Ge, Sn, Pb). In chapter 3.3, these reactions were also performed for the related nitrogen based imino ligand system SIMPY. In case of the reaction with EX_2 salts (E= Ge, Sn; X= Cl, OTf), loose donor-acceptor complexes SIMPYEX_2 were isolated in high yields. The reaction with $E(N(SiMe_3)_2)_2$ (E= Ge, Sn, Pb) yielded $SIMPY_2E$ complexes due to the intramolecular elimination of the H atom at the backbone of the ligand system and forming $HN(SiMe_3)_2$.

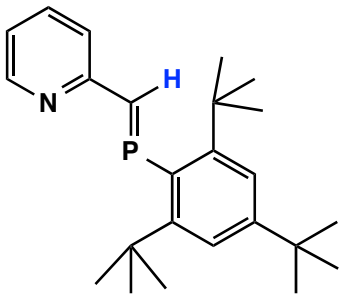

Figure 3.80: The phosphaethenylpyridine ligand system PAPY.

The phosphaethenyl pyridine ligand system PAPY was reacted with $GeCl_2$*dioxane, $SnCl_2$ and $SnOTf_2$ in CH_2Cl_2 or $CHCl_3$ at room temperature as shown in Figure 3.81. The yellow cloudy reaction solution was stirred over night. The solvent was removed *in vacuo* and a yellow powder was obtained. The yellow powder could be analyzed as the (PAPY)$GeCl_2$ complex **44**, the (PAPY)$SnCl_2$ complex **45** and the (PAPY)$SnOTf_2$ **46** *via* heteronuclear NMR spectroscopy and elemental analysis. The choice of the solvent is crucial for the formation of the desired products. If an etheric solvent as THF is used to obtain the complexes (PAPY)$GeCl_2$ complex **44**, the (PAPY)$SnCl_2$ **45** and the (PAPY)$SnOTf_2$ **46**, the compounds are not formed. Etheric solvents are stronger donors than the PAPY ligand and coordinate the EX_2 salts. Therefore, the loose donor-acceptor complexes (PAPY)$GeCl_2$ complex **44**, the (PAPY)$SnCl_2$ **45** and the (PAPY)$SnOTf_2$ **46** are only obtained in less polar solvents such as CH_2Cl_2 or $CHCl_3$. The complexes (PAPY)$GeCl_2$ **44**, (PAPY)$SnCl_2$ **45** and (PAPY)$SnOTf_2$

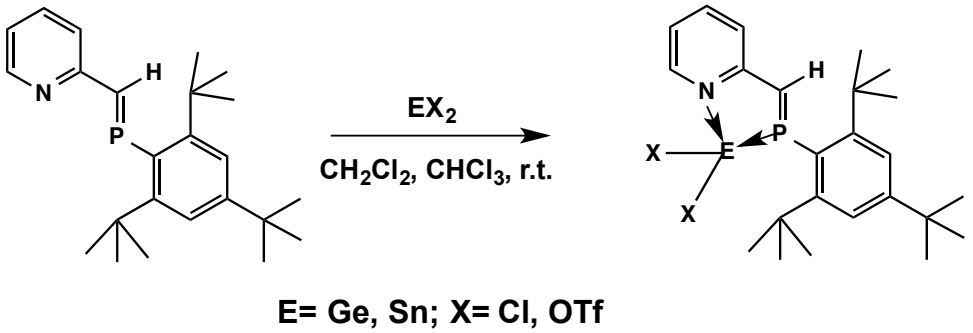

Figure 3.81: The equimolar reaction of the PAPY ligand with EX_2 salts (E= Ge, Sn; X= Cl. OTf), affords the complexes (PAPY)$GeCl_2$ complex **44**, the (PAPY)$SnCl_2$ **45** and the (PAPY)$SnOTf_2$ **46** in high yields.

46 were characterized *via* heteronuclear NMR spectroscopy and by elemental analysis. Unfortunately no solid state structures could be isolated.

The PAPY ligand system displays a signal at 283.3 ppm in the ^{31}P NMR spectrum. The signal splits into a doublet by measuring a coupled ^{31}P NMR spectrum with a $^{2}J_{P-H}$ coupling constant of 25 Hz due to the presence of a H atom at the backbone of the ligand system. The neutral PAPY ligand coordinates a group 14 element within the complexes (PAPY)$GeCl_2$ complex **44**, the (PAPY)$SnCl_2$ **45** and the (PAPY)$SnOTf_2$ **46** *via* donor-acceptor interactions. Due to the coordination towards a group 14 element, the ^{31} P NMR signal is

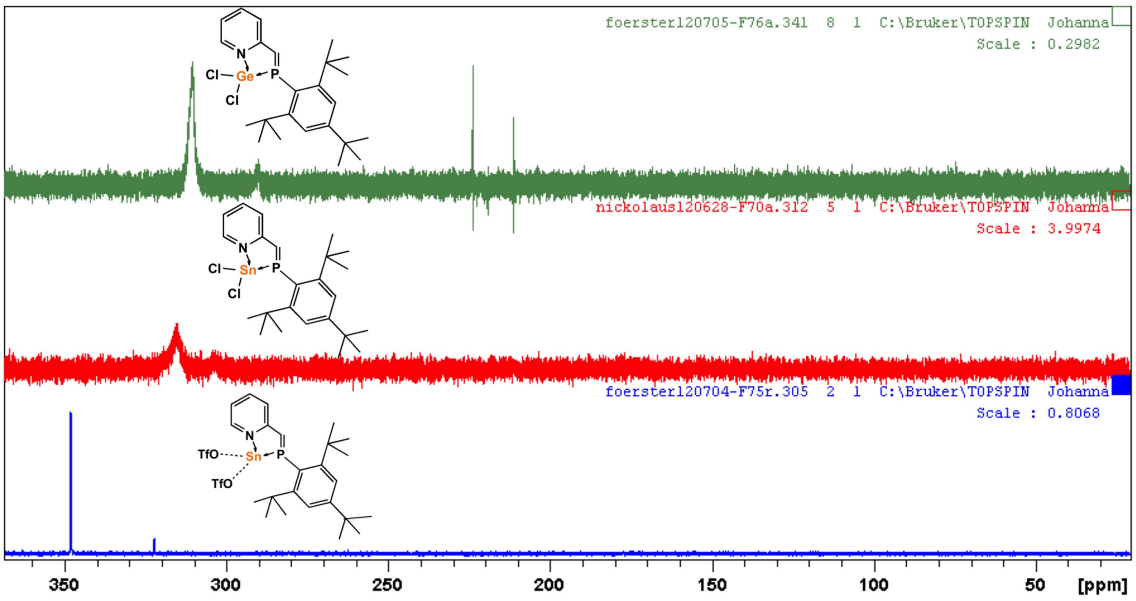

Figure 3.82: The ^{31}P NMR of the complexes (PAPY)$GeCl_2$ complex **44**, the (PAPY)$SnCl_2$ **45** and the (PAPY)$SnOTf_2$ **46** show a significant signal in the low field.

shifted towards low field as shown in Figure 3.82. For complex (PAPY)$GeCl_2$ complex **44** a low field shift at 311.2 ppm is observed which is broadened. In case of the (PAPY)$SnCl_2$ **45** a broadened signal was observed too at 313.0 ppm. The broadened signals are presumably obtained due to thermodynamical processes in solution. Perhaps, a second PAPY ligand interacts with the formed complexes or the (PAPY)EX_2 complexes interact with each other and therefore the signals reveal broadened. In case of the (PAPY)$SnOTf_2$ complex **46**, a sharp signal is observed at 347.8 ppm. The ^{1}H and ^{13}C NMR spectra confirm the fact that the PAPY ligand system donates EX_2 salts (E= Ge, Sn; X= Cl, OTf). Hence, it can be concluded that the phosphaethenyl pyridine ligand system forms loose donor-acceptor complexes (PAPY)EX_2 (E= Ge, Sn; X= Cl, OTf) too as the lighter congener SIMPY. The main difference is that less polar solvents have to be used to synthesize the (PAPY)EX_2 compounds. This can be explained by the fact that the C=P bond is less polar than the C=N bond. Therefore, the C=N functionality represents better donor properties than the C=P group and provides much more stable SIMPYEX_2 complexes.

The reaction of the PAPY ligand system with $E(N(SiMe_3)_2)_2$ (E= Ge, Sn, Pb) differs notably from the reactions with the SIMPY ligand system. The reaction of the SIMPY ligand with $E(N(SiMe_3)_2)_2$ (E= Ge, Sn, Pb) afforded $SIMPY_2E$ compounds no matter in which ratio the starting materials were reacted. Furthermore no matter which group 14 element was involved, the main product was always the $SIMPY_2E$ complexes. Only the reaction time was increased regarding the element starting from Ge (complete conversion) to Pb (always starting materials present). In case of the reaction of the PAPY ligand system with $E(N(SiMe_3)_2)_2$ (E= Ge, Sn, Pb) the main products vary completely depending on the group 14 element.

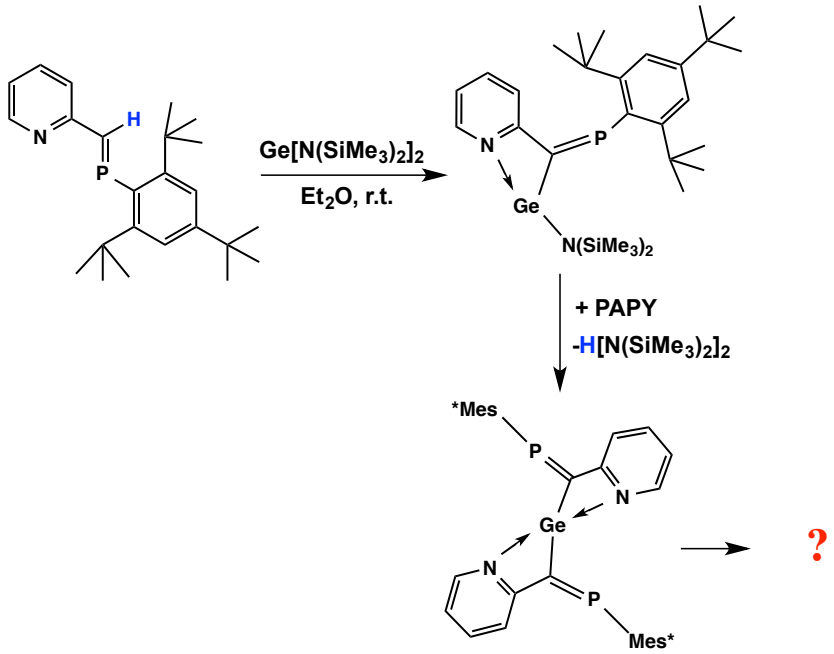

Figure 3.83: The reaction of the PAPY ligand with $Ge(N(SiMe_3)_2)_2$ affords the complexes (PAPY)GeN(SiMe$_3$)$_2$ **47**, the $PAPY_2Ge$ **48** and an unidentified (PAPY)Ge species **49**.

The PAPY ligand was reacted with one equivalent of $E(N(SiMe_3)_2)_2$ (E= Ge, Sn, Pb) to investigate if the $PAPY_2E$ complexes are formed although an excess of $E(N(SiMe_3)_2)_2$ (E= Ge, Sn, Pb) is present. In case of the reaction with the SIMPY ligand system, $SIMPY_2E$ complexes are formed no matter in which ratio the starting materials were present in reaction solution. In case of the reaction with the PAPY ligand, different complexes were observed. The PAPY ligand was dissolved in diethyl ether and $Ge(N(SiMe_3)_2)_2$ was added at room temperature. Furthermore, traces of $KN(SiMe_3)_2$ were added to accelerate the

conversion. The addition of $KN(SiMe_3)_2$ was performed for all reaction carried out with the PAPY ligand to decrease reaction time and afford a full conversion. Traces of $KN(SiMe_3)_2$ react with the H atom at the backbone of the ligand system to eliminate $HN(SiMe_3)_2$ and to give the potassium salt of the PAPY ligand. Then the group 14 element precursor react with the potassium PAPY salt to give the PAPY group 14 complexes and $KN(SiMe_3)_2$. Hence, $KN(SiMe_3)_2$ acts as catalyst for the reaction. The reaction solution was stirred for 48 hours and the color of the reaction solution changed from slightly orange to a dark red. NMR studies were performed out of the reaction solution and reveal that several products are formed. In Figure 3.83, the possible products are shown. In the first step, a heteroleptic (PAPY)GeN$(SiMe_3)_2$ complex **47** is formed *via* elimination of the H atom at the backbone of the ligand system and the formation of $HN(SiMe_3)_2$ which was observed *via* NMR spectroscopy. In the next step, a homoleptic $PAPY_2Ge$ complex **48** is observed by an additional elimination of a H atom at the backbone of a second PAPY ligand and the formation of a second equivalent of $HN(SiMe_3)_2$. Further reaction leads to an unidentified germanium complex (PAPY)Ge **49**.

In case of the reaction with the PAPY ligand and $Sn(N(SiMe_3)_2)_2$ a different product is observed as shown in Figure 3.84. The PAPY ligand was re-

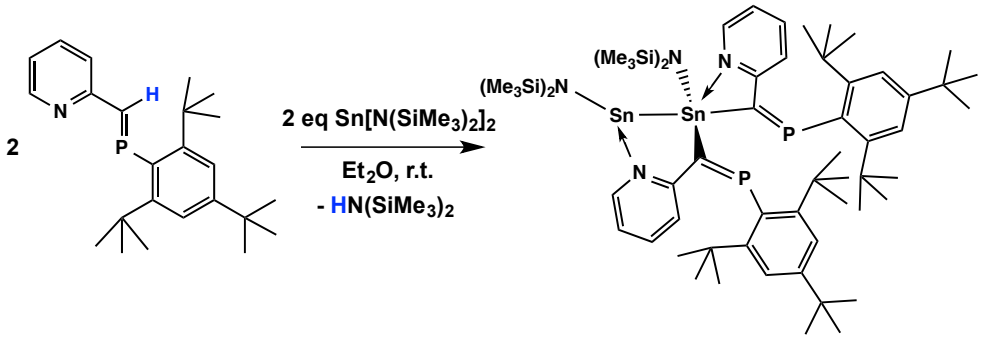

Figure 3.84: The equimolar reaction of the PAPY ligand with $Sn(N(SiMe_3)_2)_2$ gives the rare stannyl-stannylene complex $PAPY_2(N(SiMe_3)_2)SnSnN(SiMe_3)_2$ **50**.

acted with $Sn(N(SiMe_3)_2)_2$ in diethyl ether at room temperature and stirred for severals days. The reaction time was increased compared to the reaction with $Ge(N(SiMe_3)_2)_2$. The same trend was investigated for the reaction of $E(N(SiMe_3)_2)_2$ (E= Ge, Sn, Pb) with the SIMPY ligand. The heavier the group 14 element, the longer does the conversion to products

need. After several days stirring, a dark red solution was observed. All volatile components were removed *in vacuo* and a dark red powder was obtained which was recrystallized in diethyl ether at -30°C. Dark red cubic crystals were collected and a solid state structure of a rare stannyl-stannylene complex $PAPY_2(N(SiMe_3)_2)SnSnN(SiMe_3)_2$ **50** was investigated. The possible reaction pathway is displayed in Figure 3.85. The reaction of the PAPY ligand with $Sn(N(SiMe_3)_2)_2$ yields in the first step the heteroleptic $(PAPY)SnN(SiMe_3)_2$ complex. The second step involves a dimerization of two equivalents of the heteroleptic $(PAPY)SnN(SiMe_3)_2$ complex forming the intermediate $[(PAPY)SnN(SiMe_3)_2]_2$. Then a ligand exchange reaction takes place affording the rare stannyl-stannylene complex $PAPY_2(N(SiMe_3)_2)SnSnN(SiMe_3)_2$ **50**. These dimetallic compounds bear a di-

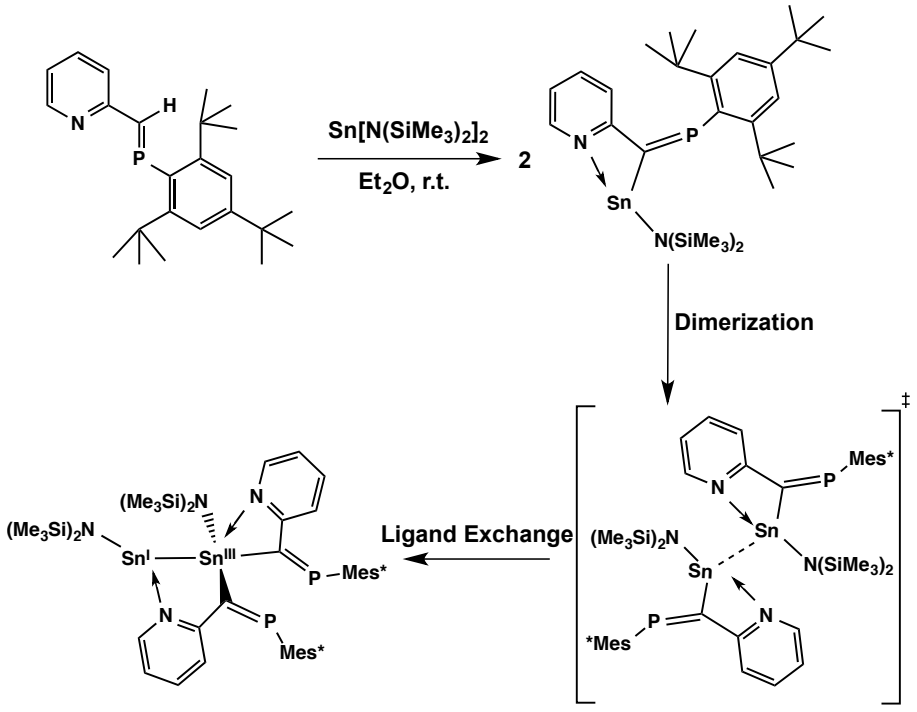

Figure 3.85: The presumed reaction mechanism of the formation of the rare stannyl-stannylene complex $PAPY_2(N(SiMe_3)_2)SnSnN(SiMe_3)_2$ **50**.

valent and a tetravalent heavier group 14 element with direct metal to metal bonding. These compounds were only existing as unstable intermediates of (e.g.) dimetallenes and verified through trapping reactions.[133–136] Until now only a few stable compounds have been isolated.[129,131,132,137–139,141] The first structurally characterized compound with a $RSn\text{-}SnR_3$ bonding mo-

tif was synthesized via the reaction of a halogenated Sn^{II} precursor [$(Sn_2$-$(Me_3Si)_2C$-$C_5H_4N)Cl$] with [$Li(THF)_3Sn$-$2(SiMe_3)_3$] in Et_2O. Further examples were synthesized,[129,138,139] but a rearrangement reaction as shown in Figure 3.85 was not investigated. In literature, the rearrangement of dimeric dimetallenes $R_2E{=}ER_2$[26,95] to corresponding RE-ER_3 species in solution was investigated by NMR studies.[139] However, due to large substituents of the dimeric dimetallenes $R_2E{=}ER_2$, structure RE-ER_3 is thermodynamically disfavored. This can be explained by the fact that three large substituents have to coordinate towards one E atom. If one of the two organic substituents at each E atom is relatively small, movement of that substituent to the other E atom is possible.[139] This is also the fact for the observed stannylstannylene complex $PAPY_2(N(SiMe_3)_2)SnSnN(SiMe_3)_2$ **50**. The PAPY ligand and the $N(SiMe_3)_2$ functionalities are small enough to rearrange and yield the complex $PAPY_2(N(SiMe_3)_2)SnSnN(SiMe_3)_2$ **50**.

The reaction of the PAPY ligand with $Pb(N(SiMe_3)_2)_2$ afforded one product the heteroleptic (PAPY)$PbN(SiMe_3)_2$ complex **51** as shown in Figure 3.86. The PAPY ligand was reacted with one equivalent $Pb(N(SiMe_3)_2)_2$ in diethyl ether at room temperature. $KN(SiMe_3)_2$ was added as catalyst and driving force as in

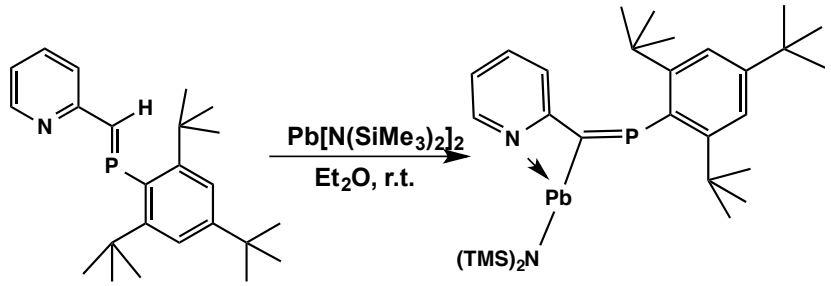

Figure 3.86: The equimolar reaction of the PAPY ligand with $Pb(N(SiMe_3)_2)_2$ yields the heteroleptic complex (PAPY)$PbN(SiMe_3)_2$ **51**.

the reactions before. However, no full conversion was observed for the reaction of PAPY ligand with $Pb(N(SiMe_3)_2)_2$ although the reaction solution was stirred for weeks. A color change was observed from orange to a dark red. The complex (PAPY)$PbN(SiMe_3)_2$ **51** was characterized *via* heteronuclear NMR studies.

In Figure 3.87, the comparison of the ^{31}P NMR spectra for the reaction of the PAPY ligand with E(N(SiMe$_3$)$_2$)$_2$ (E= Ge, Sn, Pb) is shown. The PAPY ligand

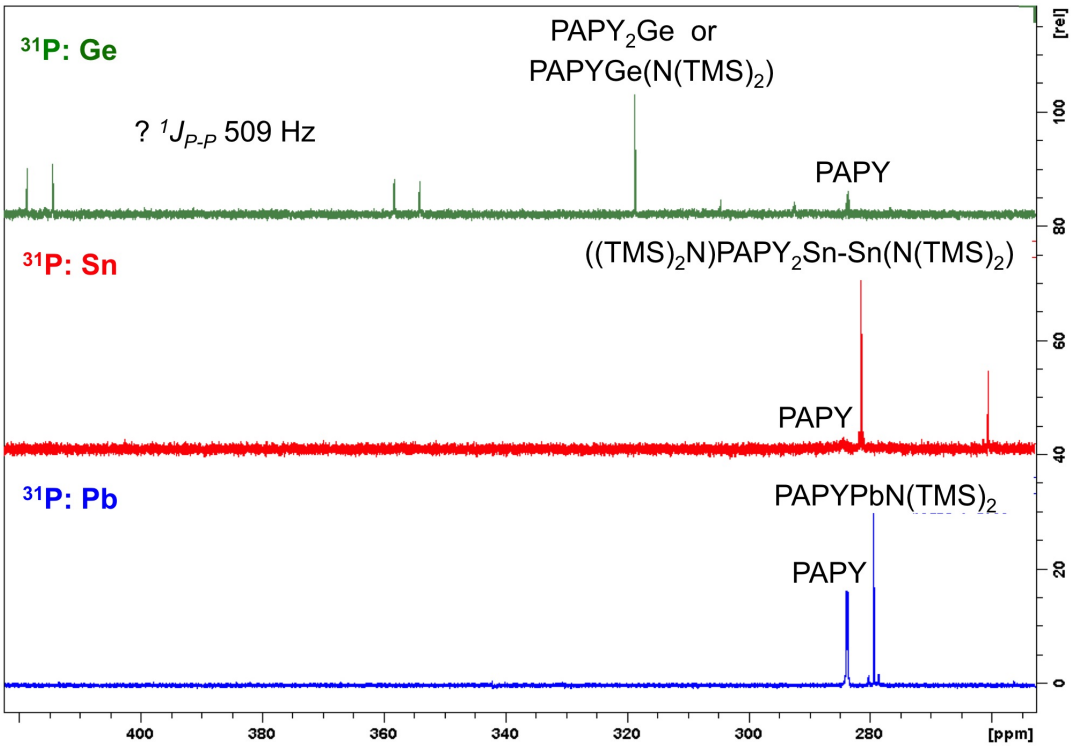

Figure 3.87: The ^{31}P NMR spectra of the reaction of the PAPY ligand with E(N(SiMe$_3$)$_2$)$_2$ (E= Ge, Sn, Pb).

is present in traces in the reaction solution in case of E= Ge and Sn. However in case of E= Pb, two-thirds of the starting material is left. As mentioned, an unidentified (PAPY)Ge complex is formed reacting the PAPY ligand with Ge(N(SiMe$_3$)$_2$)$_2$. The unidentified species reveals a set of two doublets around 418 ppm and 356 ppm with a large coupling constant of 509 Hz as shown in Figure 3.88. The PAPY ligand bears a signal at 283.3 ppm in the ^{31}P NMR spectrum. The signal splits into a doublet by measuring a coupled ^{31}P NMR spectrum with a $^{2}J_{P-H}$ coupling constant of 25 Hz due to the presence of a H atom at the backbone of the ligand system. In case of the observed low field shifts of the unidentified species, no $^{2}J_{P-H}$ coupling is found. Hence, the H atom at the backbone is eliminated. The large coupling constant of 509 Hz can be assigned to a $^{1}J_{P-P}$ coupling with a direct P-P bond. In literature, compounds with a symmetrical C=P-P=C bonding motif show a signal at 390 ppm with a $^{1}J_{P-P}$ coupling of 337 Hz.[171] Other possible compounds which reveal similar ^{31}P shifts are compounds bearing a P=P fragment. The P=P fragment displays

signals ranging from 400 ppm to 600 ppm with $^{1}J_{P-P}$ coupling constant around 500 to 700 Hz.[171] Therefore, the unidentified species reveals an unsaturated

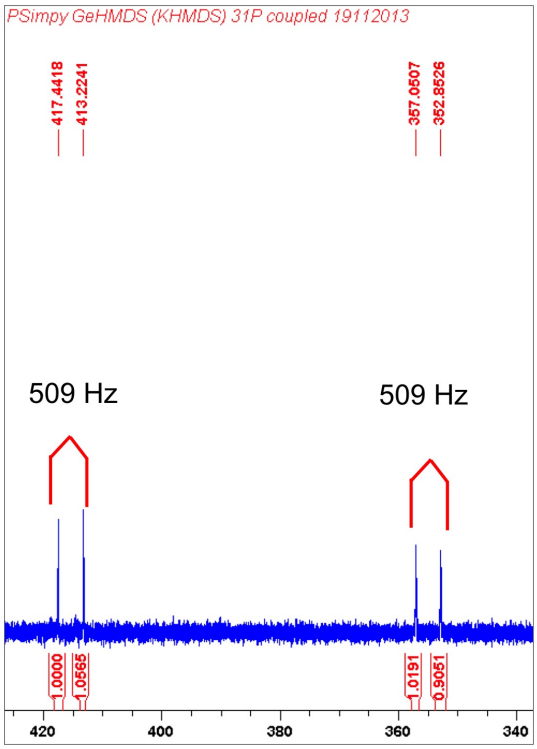

Figure 3.88: The ^{31}P NMR spectra of the unidentified (PAPY)Ge species **49**.

bonding motif with presumably a -C=P-P=C- fragment or a P=P fragment due to the low field shifting. This formation of this unidentified species could presumably be the result of a C-C coupling reaction (and further rearrangments) as observed in the reduction reaction of (SIMPY)$GeCl_2$ with alkali metals in chapter 3.3. The other complex which is present in the reaction solution is either the heteroleptic complex (PAPY)$GeN(SiMe_3)_2$ **47** or the homoleptic complex $PAPY_2Ge$ **48**. In the ^{31}P NMR spectrum a low field shift is observed at 320 ppm without any coupling to other nuclei. The ^{1}H, ^{13}C and ^{29}Si NMR spectra show several signals which indicates the formation of these products and a complex reaction pathway. In case of the reaction with the PAPY ligand and $Sn(N(SiMe_3)_2)_2$, one signal at 281 ppm with a $^{2}J_{P-^{117}Sn}$ coupling constant of 80 Hz and a $^{2}J_{P-^{119}Sn}$ coupling constant of 76 Hz. Another signal is high field shifted at 261 ppm with a broadened $^{2}J_{P-Sn}$ coupling constant of 195 Hz. In the ^{29}Si NMR spectra two signals are observed at -2.26 and -2.98 ppm. The ^{1}H and ^{13}C NMR spectra confirm the structure of the rare stannyl-stannylene complex $PAPY_2(N(SiMe_3)_2)SnSnN(SiMe_3)_2$ **50**. In the ^{119}Sn NMR two signals are inves-

tigated at -106 and 348 ppm. These two signals do not show a $^{1}J_{Sn-Sn}$ coupling. This can be explained by the fact that in solution the stannyl-stannylene complex $PAPY_2(N(SiMe_3)_2)SnSnN(SiMe_3)_2$ **50** is dissociated or the Sn - Sn bond is very elongated and therefore no $^{1}J_{Sn-Sn}$ coupling is observed. For the reaction with the PAPY ligand and $Pb(N(SiMe_3)_2)_2$ one new ^{31}P signal is observed in the ^{31}P NMR spectrum. This signal can be assigned to the heteroleptic complex $(PAPY)PbN(SiMe_3)_2$ **51** with a signal at 279 ppm and a $^{2}J_{P-^{207}Pb}$ coupling constant of 203 Hz. In the ^{29}Si NMR spectrum a signal at -4.82 ppm is observed. The ^{1}H and ^{13}C NMR spectra confirm the structure of the heteroleptic complex $(PAPY)PbN(SiMe_3)_2$ **51**.

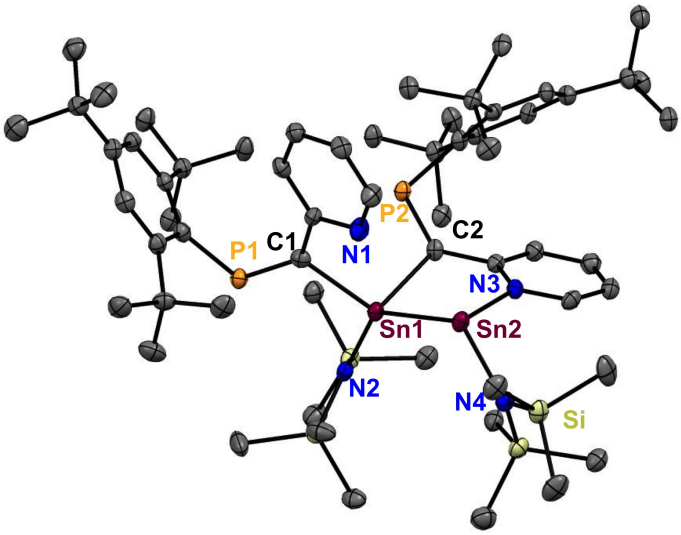

Figure 3.89: Solid state structure of the compound stannyl-stannylene $PAPY_2(N(SiMe_3)_2)SnSnN(SiMe_3)_2$ **50**. Anisotropic displacement parameters are depicted at the 50% probability level. Hydrogen atoms are omitted for clarity. Selected bond lengths [Å] and angles [°] : Sn1 - Sn2, 2.895(6); Sn1 - C1, 2.214(8); Sn1 - C2, 2.476(6); Sn1 - N1, 3.010(6); Sn1 - N2, 2.103(4); Sn2 - N3, 2.359(4), Sn2 - N4 2.148(6); P1 - C1, 1.683(6); P2 - C2, 1.679(8); Sn2-Sn1-C1, 116.4(2); Sn2-Sn1-C2, 86.9(2); C1-Sn1-C2, 116.4(2).

The solid state structure of the rare stannyl-stannylene complex $PAPY_2(N(SiMe_3)_2)SnSnN(SiMe_3)_2$ **50** is displayed in Figure 3.89. Compound **50** crystallizes in the triclinic crystal system $P\bar{1}$. The Sn1 atom is fivefold coordinated by two C atoms, two N atoms and one Sn atom. The Sn1 - Sn 2 distance is 2.895(6) Å and agrees well with Sn-Sn distance of bimetallic $RSn\text{-}SnR_3$ ranging from 2.8508(4) to 2.8909(2).[131,137] The Sn - C distances are covalent bonds with a Sn1 - C1 bond length of 2.214(8) Å and a slightly elongated Sn1 - C2 bond length of 2.476(6) Å and are in good agreement with literature known Sn1 - C

bonds..[131] The Sn1 - N1 bond length is a very weak donor-acceptor interaction with 3.010(6) Å and the Sn1 - N2 distances is a covalent bond with 2.103(4) Å. The Sn2 atom in contrast is only threefold coordinated by two N atoms and the Sn1 atom. The Sn2 - N3 distance is a typical donor-acceptor interaction with a bond length of 2.359(4) Å and the pyridenyl N_{py} is stabilizing the Sn2 atom although the PAPY ligand is covalently bonded towards the Sn1 atom. The shortened Sn2 - N4 distance is a covalent bond with 2.148(6) Å and is in good agreement with literature known Sn - N distances ranging from 2.121 to 2.397 Å.[151] The P1 - C1 distance with 1.683(6) Å and the P2 - C2 with 1.679(8) Å are typical P=C double bonds. The angles observed within compound **50** are the Sn2-Sn1-C1 angle with 116.4(2)°, the Sn2-Sn1-C2 angle with 86.9(2)° and the C1-Sn1-C2 with 116.4(2)°. This solid state structure is a rare example of a bimetallic compound with the bonding motif RSn-SnR_3.

To gain further insights in the reaction chemistry, a theoretical study was performed.‡‡ Therefore, the solid state structure of the $PAPY_2(N(SiMe_3)_2)SnSnN(SiMe_3)_2$ **50** as well as the presumed heteroleptic $(PAPY)EN(SiMe_3)_2$ complexes and the homoleptic $PAPY_2E$ (E = Ge, Sn, Pb) compounds were geometry optimized at a density functional level using the hybrid MPW1PW91 functional together with a double-zeta basis set (SDD) and pseudopotentials on Sn and Pb.

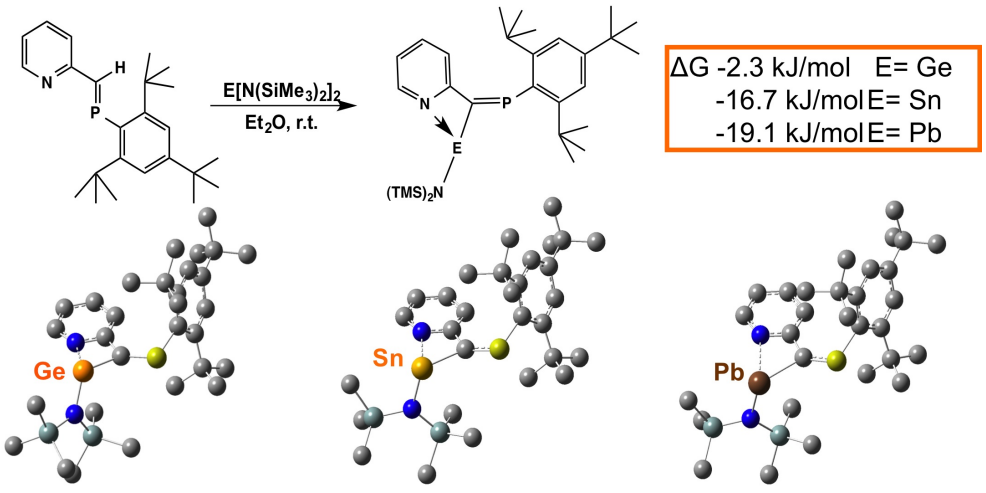

Figure 3.90: The calculated reaction enthalpies of the heteroleptic complexes $(PAPY)EN(SiMe_3)_2$ (E = Ge, Sn, Pb).

‡‡ Theoretical studies in collaboration with M. Flock. Institute of Inorganic Chemistry, TU Graz

Figure 3.90 displays the geometry optimized heteroleptic complexes (PAPY)EN(SiMe$_3$)$_2$ (E = Ge, Sn, Pb). The reaction enthalpies were calculated for the equimolar reaction of the PAPY ligand with E(N(SiMe$_3$)$_2$)$_2$ by elimination of the H atom at the backbone of the ligand system and the formation of hexamethyldisilazane. As shown in Figure 3.90 the calculated reaction enthalpies ΔG are for E= Ge -2.3 kJ/mol, for E= Sn -16.7 kJ/mol and for E= Pb 19.1 kJ/mol. This confirms that the heteroleptic (PAPY)PbN(SiMe$_3$)$_2$ complex is a thermodynamically very favored and stable product. Hence, it explains the fact that it is the only product observed experimentally. In case of E= Sn the reaction is favored too, but in case of E= Ge, the heteroleptic (PAPY)GeN(SiMe$_3$)$_2$ complex is not thermodynamically favored which leads to further reactions with a second PAPY molecule and the investigation of different products compared to the reaction with E= Pb.

Figure 3.91 presents the results of the calculation of the geometry optimized homoleptic PAPY$_2$E complexes (E = Ge, Sn, Pb). In this case the trend is reversed compared to the geometry optimized heteroleptic (PAPY)EN(SiMe$_3$)$_2$ complexes (E = Ge, Sn, Pb). Hence, the germanium complex is thermodynamically favored with ΔG of -16.3 kJ/mol. The tin complex reveals a ΔG of -9.4 kJ/mol and the homoleptic lead complex is thermodynamically unfavored with a reaction enthalpy ΔG of -6.4 kJ/mol.

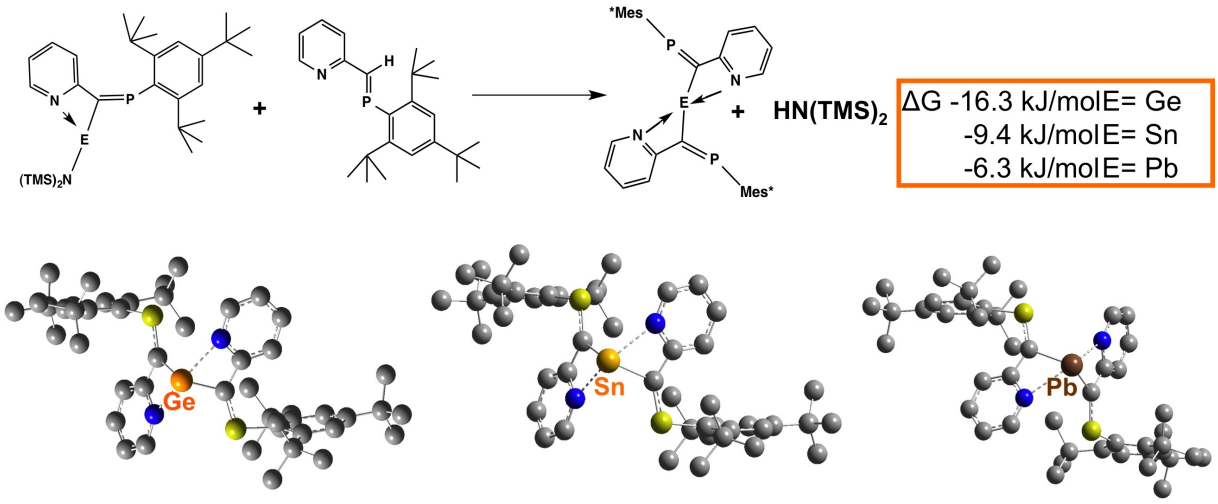

Figure 3.91: The calculated reaction enthalpies of the homoleptic complexes PAPY$_2$E (E = Ge, Sn, Pb).

In Figure 3.92, the results of the geometry optimized RE-ER$_3$ complexes are shown. Two equivalents of the PAPY ligand reacted with two equivalents of E(N(SiMe$_3$)$_2$)$_2$ *via* the elimination of the H atom at the ligand backbone to form hexamethyldisilazane and the rare RE-ER$_3$ complexes. In general, the forma-

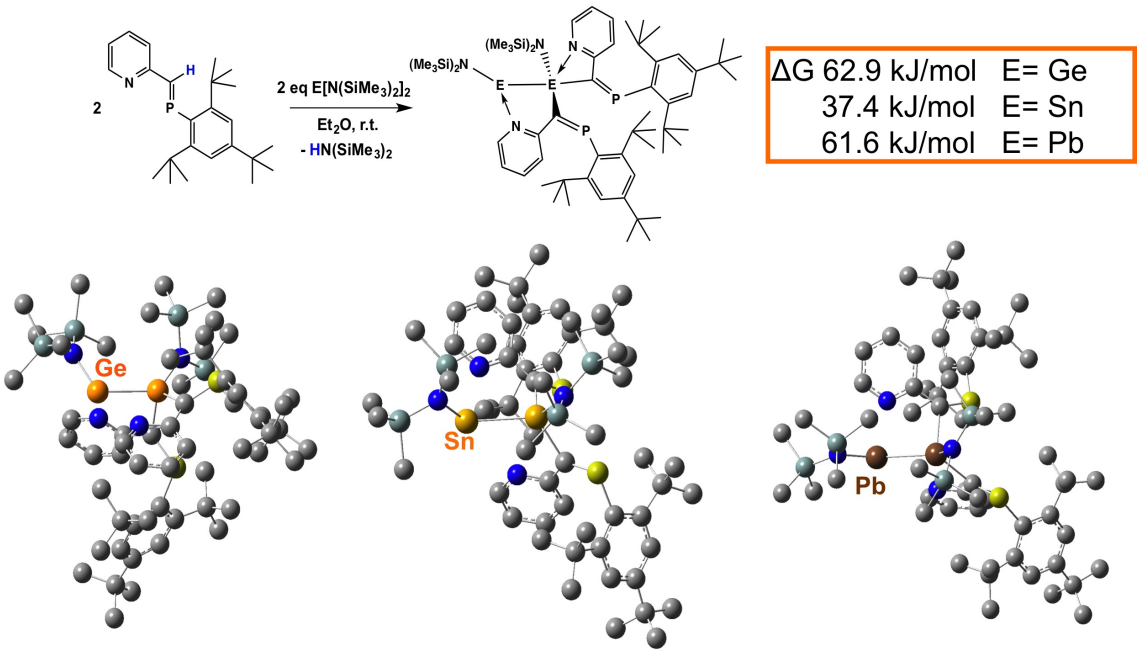

Figure 3.92: The calculated reaction enthalpies of the PAPY$_2$(N(SiMe$_3$)$_2$)E-EN(SiMe$_3$)$_2$ (E = Ge, Sn, Pb) complexes.

tion of the rare RE-ER$_3$ complexes is an endothermic reaction which implies the input of energy into the system. Interestingly, the formation of the germanium and lead RE-ER$_3$ complexes are much less favored with ΔG of 62.9 kJ/mol and ΔG of 61.6 kJ/mol, respectivley, than the RSn-SnR$_3$ complex. In case of the RSn-SnR$_3$ complex, a reaction enthalpy ΔG of 37.4 kJ/mol was calculated. This results confirm the experimental observations that in case of E= Sn a rare stannyl stannylene RSn-SnR$_3$ complex is formed in contrast to the reactions with E= Ge and Pb.

This interesting results confirm the expectations that the phosphaalkene based ligand system PAPY reveals a different reaction chemistry than the imino based ligand system SIMPY. Depending on the group 14 element different products were observed reacting them with the PAPY ligand. Furthermore, a very rare example of a stannyl stannylene complex PAPY$_2$(N(SiMe$_3$)$_2$)SnSnN(SiMe$_3$)$_2$ **50** could be isolated and fully character-

ized. The observed PAPY-group 14 complexes represent the first examples of the PAPY ligand coordinating main group elements and give new insights in the exciting and versatile chemistry of main group elements.

Chapter 4

Experimental Section

4.1 General Methods

All manipulations were carried out using modified Schlenk techniques or in a mBRAUN UNIlab drybox under an inert atmosphere. Solvents were dried using an Innovative Technologies column solvent purification system. Chemicals were purchased from Aldrich and used as received. The ligands SAMPY,[66] SAMPYLi,[153] SIMPY,[59] $SIMPY_2Na$,[25] PSIMPY,[172] DAMPY,[60] $DAMPYLi_2$,[63] DIMPY,[9] (Me)DIMPY[9] and $E[N(SiMe_3)_2]_2$, E(II)bis[bis(trimethylsilyl) amide] (E=Ge, Sn, Pb),[96] $SnOTf_2$,[173] adamantyl phosphalkine[174] were synthesized according to literature. ^{1}H, ^{13}C, ^{29}Si, ^{31}P and ^{119}Sn spectroscopic data was recorded on a Varian Mercury 300 MHz spectrometer (operating at 300.22 MHz for ^{1}H, 75.50 MHz for ^{13}C, 59.64 MHz for ^{29}Si, 121.54 MHz for ^{31}P and 112.17 MHz for ^{119}Sn). NMR spectra were referenced to deuterated benzene and chloroform which were dried either over potassium metal or phosphor pentoxide and destilled, and were recorded at 25°C. EPR spectra were recorded using the MiniScope MS300 (Magnettech, Germany) X-band spectrometer at ambient temperature and at 77 K. The g factor was calibrated with the use of an external DPPH standard. UV-Vis data was recorded on a Perkin Elmer (Lambda 35) spectrometer an the FT-IR spectroscopy on a Perkin-Elmer 883. Elemental analysis was performed on a Elementar Vario EL III spectrometer and the FT-IR spectroscopy on a Perkin-Elmer 883. Decomposition regions were determined using a Buechi 535 instrument.

4.1.1 X-ray Crystallography

All crystals suitable for single crystal X-ray diffractometry were removed from a Schlenk flask under a stream of N_2 and immediately covered with a layer of silicone oil. A single crystal was selected, mounted on a glass rod on a copper pin, and placed in the cold N_2 stream provided by an Oxford Cryosystems cryometer. XRD data collection was performed on a BRUKER APEX II diffractometer with use of Mo Kα radiation (λ= 0.71073 Å) and a CDD area detector. Empirical absorption corrections were applied using SADABS.[175,176] The structures were solved with use of either direct methods or the Patterson option in SHELXS and refined by the full-matrix least-squares procedures in SHELXL.[176–178] The space group assignments and structural solutions were evaluated using PLATON.[179] Non-hydrogen atoms were refined anisotropically. Hydrogen atoms were located in calculated positions corresponding to standard bond lengths and angles.

4.2 Synthesis of Group 1 Complexes Using IMPY Ligands

4.2.1 SIMPY$_2$Li (1)

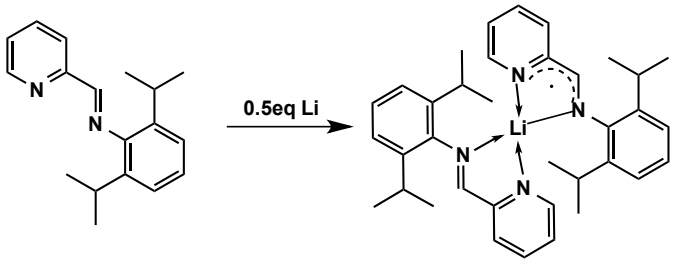

The SIMPY ligand (1.0 g, 3.75 mmol, 1 eq) was dissolved in 20 ml diethyl ether and the lithium metal (0.013 g, 1.88 mmol, 0.5eq) was added. The lithium metal reacts immediately with the SIMPY ligand and the solution turns redish due to a total consumption of Li metal. After stirring over night, the solution turned dark red. The solvent was removed and a dark red powder was obtained. Dark red cubic crystals suitable for X-ray analysis were obtained after recrystallizing in diethyl ether storing at -30°C. Yield: 91%. mp: 68.7 - 70.3°C. UV-VIS (in benzene, THF or heptane): 795, 693, 493 nm. $g = 2.0031 \pm 0.0001$ Elemental analysis (%) calcd for $C_{36}H_{44}N_4Li$ (539.72): C, 80.12; H, 8.22; N, 10.38 found: C, 79.98; H, 8.07; N, 9.61.

4.2.2 SIMPY$_2$Na (2)

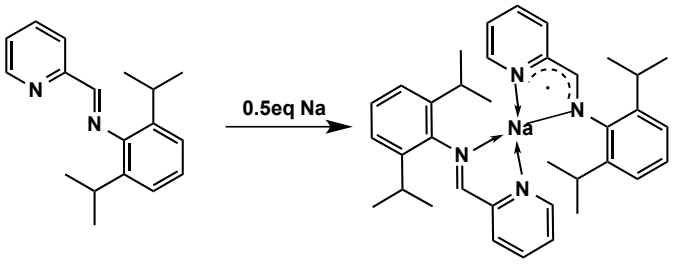

Procedure as described in 4.2.1, SIMPY ligand (400 mg, 1.50 mmol, 2eq) was dissolved in 20 mL benzene and sodium metal (17 mg, 0.75 mmol, 1 eq) was added. Dark red needle like crystals suitable for X-ray analysis were obtained

after recrystallizing in benzene storing at -30°C. Yield: 88%. mp: 139.1 - 139.9°C. $g = 2.0031 \pm 0.0001$ Elemental analysis (%) calcd for $C_{36}H_{44}N_4Na$ (555.77): C, 77.80; H, 7.98; N, 10.08; found: C, 77.96; H, 7.78; N, 8.81.

4.2.3 SIMPY$_2$K (3)

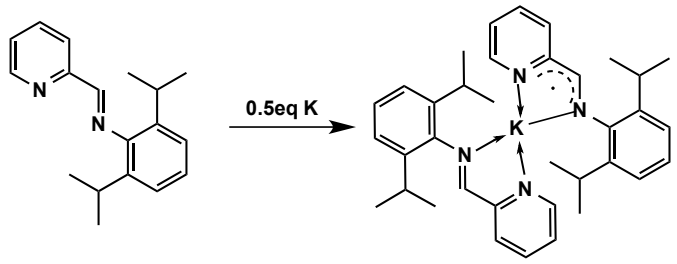

Procedure as described in 4.2.1, but instead of diethyl ether benzene was used as solvent. Yield: 86%. mp: 143.4 - 145.2°C. $g = 2.0031 \pm 0.0001$ UV-VIS (benzene): 611, 571, 410 nm. Elemental analysis (%) calcd for $C_{36}H_{44}N_4K$ (571.87): C, 75.61; H, 7.76; N, 9.80; found: C, 73.49; H, 6.95; N, 8.20.

4.2.4 DIMPYLi (4)

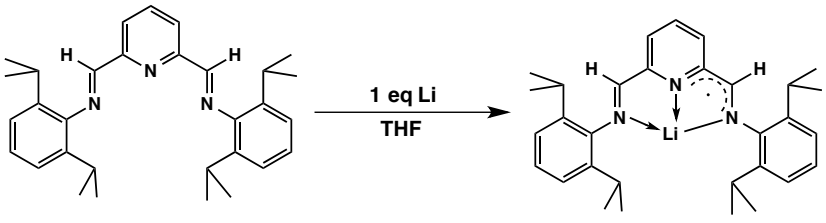

The DIMPY ligand (400 mg, 0.88 mmol, 1 eq) was dissolved in 6 mL THF and Li metal (6 mg, 0.88 mmol, 1 eq) was added. After stirring over night, the solution turned dark red and a total consumption of Li metal was observed. The solvent was removed and a dark red powder was obtained. Yield: 84%. UV-VIS (THF): 790, 560, 493 nm. Elemental Analysis calcd for $C_{31}H_{39}N_3Li$ (461.62): C, 80.66; H, 8.73; N, 9.10; found: C, 78.35; H, 8.71; N, 8.04.

4.2.5 DIMPYNa (5)

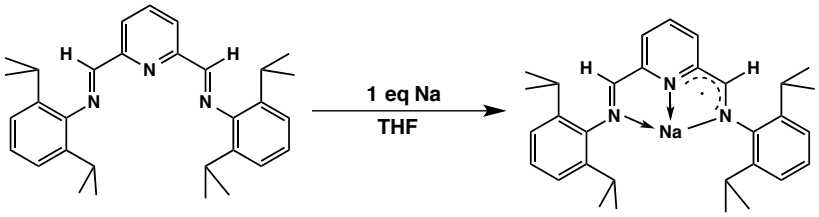

The DIMPY ligand (100 mg, 0.22 mmol, 1 eq) was dissolved in 6 mL THF and Na metal (5.07 mg, 0.22 mmol, 1 eq) was added. After stirring over night, the solution turned dark red and a total consumption of Na metal was observed. The solvent was removed and a dark red powder was obtained. Yield: 84%. UV-VIS (THF): 684, 577, 504 nm. Elemental Analysis calcd for $C_{31}H_{39}N_3Na$ (477,67): C, 77.95; H, 8.44; N, 8.80; found: C, 76.82; H, 8.13; N, 8.45.

4.2.6 DIMPYK (6)

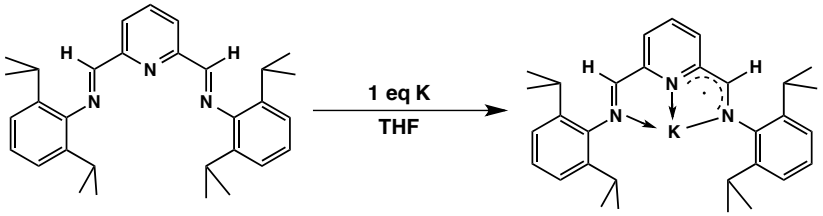

The DIMPY ligand (100 mg, 0.22 mmol, 1 eq) was dissolved in 6 mL THF and K metal (8.62 mg, 0.22 mmol, 1 eq) was added. After stirring over night, the solution turned dark red and a total consumption of K metal was observed. The solvent was removed and a dark red powder was obtained. Dark red needle like crystals suitable for X-ray analysis were obtained after recrystallizing in THF storing at RT. Yield: 84%. mp: 183.7-185.2°C. UV-VIS (THF): 732, 588, 490 nm. Elemental Analysis calcd for $C_{31}H_{39}N_3K$ (492.77): C, 75.56; H, 7.98; N, 8.53; found: C, 74.86; H, 7.90; N, 8.44.

4.2.7 DIMPYRb (7)

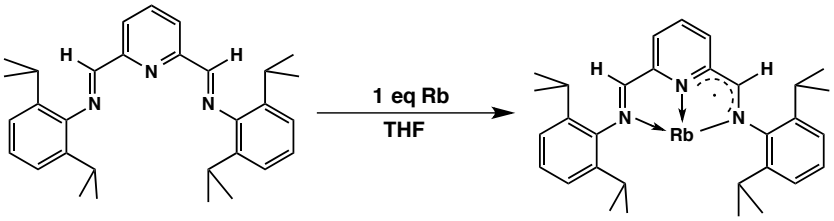

The DIMPY ligand (500 mg, 1.1 mmol, 1 eq) was dissolved in 6 mL THF and Cs metal (132 mg, 1.1 mmol, 1 eq) was added. After stirring over night, the solution turned dark red and a total consumption of Rb metal was observed. The solvent was removed and a dark red powder was obtained. Dark red crystalline blocks suitable for X-ray analysis were obtained after recrystallizing in THF storing at RT. Yield: 84%. decomposition: 133.5-136.7°C. UV-VIS (THF): 733, 613, 482 nm. Elemental Analysis calcd for $C_{31}H_{39}N_3Cs$ (587.59): C, 63.37; H, 6.86; N, 7.15; found: C, 64.53; H, 7.49; N, 7.00.

4.2.8 DIMPYCs (8)

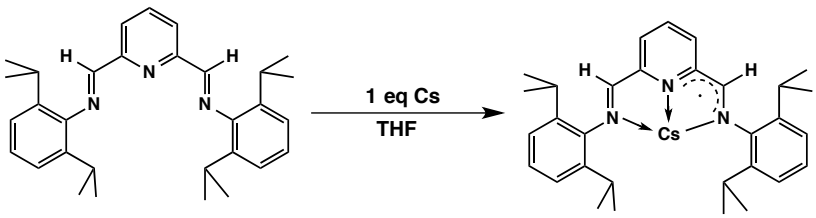

The DIMPY ligand (500 mg, 1.1 mmol, 1 eq) was dissolved in 6 mL THF and Cs metal (147 mg, 1.1 mmol, 1 eq) was added. After stirring over night, the solution turned dark red and a total consumption of Cs metal was observed. The solvent was removed and a dark red powder was obtained. Dark red needle like crystals suitable for X-ray analysis were obtained after recrystallizing in THF storing at RT. Yield: 83%. mp: 167.8 - 171.3°C. UV-VIS (THF): 709, 579, 481 nm. Elemental Analysis calcd for $C_{31}H_{39}N_3Cs$ (587.59): C, 63.37; H, 6.86; N, 7.15; found: C, 63.37; H, 7.04; N, 6.40.

4.3 Synthesis of low valent Main Group Complexes Using the SAMPY Ligand

4.3.1 SAMPYGeN(SiMe$_3$)$_2$ (9)

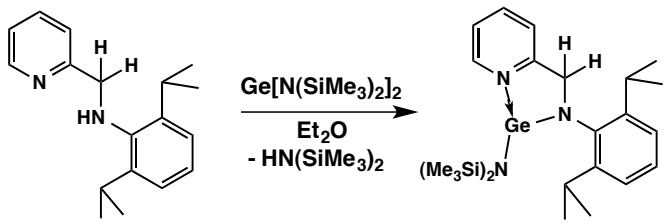

Ge[N(SiMe$_3$)$_2$]$_2$ (293 mg, 0.75 mmol, 1 eq) was dissolved in 4 mL Et$_2$O and the SAMPY ligand 2-[ArN=CH$_2$](NC$_5$H$_3$) (Ar= C$_6$H$_3$-2-Pr$^i_2$) (200 mg, 0.75 mmol, 1eq) was added at room temperature. After 5 days stirring all volatile components were removed via vacuum. A yellow powder was obtained and the product was extracted with cold pentane (5 mL) from the starting material. The pentane solution was concentrated and yellow needles were obtained by storing the solution at -30°C. Yield: 24%. mp: 149.5 - 151.2°C. ^{1}H NMR (300.22 MHz, C$_6$D$_6$): δ 8.05 (d, 1H, PyH), 7.21 (m, 3H, CH arom), 6.64 (t, 1H, PyH), 6.31 (d, 1H, PyH), 6.25 (t, 1H, CH arom), 4.82 (s, CH$_2$), 3.67 (sept, 2H, CH^{i}Pr), 1.34 (dd, 12H, CH$_3{}^i$Pr), 0.24 (s, 18H, [CH$_3$SiN]$_2$N). ^{13}C NMR (75.50 MHz, C$_6$D$_6$): δ 162.48 (ArH), 149.23 (ArH), 145.51 (ArH), 143.32 (ArH), 138.35 (ArH), 126.95 (ArH), 125.22 (ArH), 123.90 (ArH), 122.55 (ArH), 120.60 (ArH), 64.73 (CH$_2$), 28.19 (CH^{i}Pr), 25.35 (CH$_3{}^i$Pr) 5.69 ([CH$_3$SiN]$_2$N).
^{29}Si (59.64 MHz, C$_6$D$_6$): δ -2.46.
Elemental analysis (%) calcd for C$_{25}$H$_{44}$N$_3$Si$_2$Ge (515.45): C, 58.26; H,8.60; N, 8.15; found: C,57.35; H, 8.23; N, 7.86.

4.3.2 SAMPYSnN(SiMe$_3$)$_2$ (10)

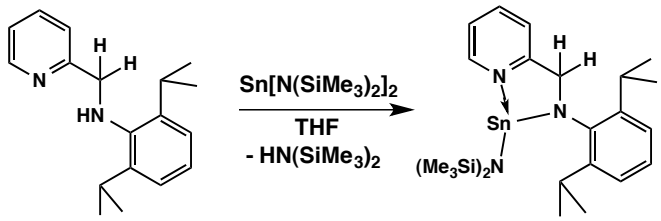

Sn[N(SiMe$_3$)$_2$]$_2$ (326 mg, 0.75 mmol, 1 eq) was dissolved in 4 mL THF and the SAMPY ligand 2-[ArN=CH$_2$](NC$_5$H$_3$) (Ar= C$_6$H$_3$-2,6-Pr$^i_2$) (200 mg, 0.75 mmol, 1eq) was added at room temperature. After 24 hours stirring at room temperature all volatile components were removed in vacuo. A yellow greenish powder was obtained and recrystallized in Et$_2$O to give yellow greenish needles while storing at -30°C. Yield: 43%. mp: 141.8 - 142.7°C. ^{1}H NMR (300.22 MHz, C$_6$D$_6$): δ 7.84 (d, 1H, PyH), 7.15 (m, 3H, CH arom), 6.62 (dt, 1H, PyH), 6.33 (d, 1H, PyH), 6.22 (t, 1H, CH arom), 4.94 (broad s, CH$_2$), 3.65 (broad sept, 2H, CH^{i}Pr), 1.27 (dd broad signal, 12H, CH$_3{}^i$Pr), 0.19 (broad s, 18H, [CH$_3$SiN]$_2$N). ^{13}C NMR (75.50 MHz, C$_6$D$_6$): δ 165.72 (ArH), 151.23 (ArH), 147.93 (ArH), 144.69 (ArH), 138.20 (ArH), 127.01 (ArH), 124.52 (ArH), 123.64 (ArH), 122.23 (ArH), 121.28 (ArH), 65.91 (CH$_2$), 28.01 (CH^{i}Pr), 25.40 (CH$_3{}^i$Pr) 6.22 ([CH$_3$SiN]$_2$N).
^{29}Si (59.64 MHz, C$_6$D$_6$): δ -2.91. ^{119}Sn NMR (112.17 MHz, C$_6$D$_6$): δ 79.78.
Elemental analysis (%) calcd for C$_{25}$H$_{44}$N$_3$Si$_2$Sn (561.53): C, 53.47; H,7.90; N, 7.48; found: C,52.58; H, 7.07; N, 7.63.

4.3.3 SAMPYPbN(SiMe$_3$)$_2$ (11)

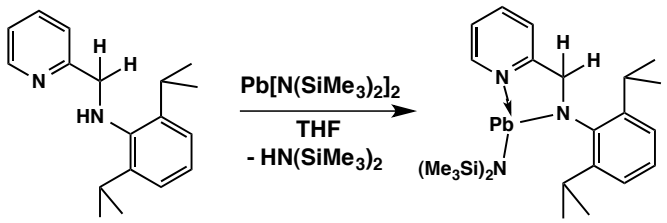

Pb[N(SiMe$_3$)$_2$]$_2$ (392 mg, 0.75 mmol, 1 eq) was dissolved in 4 mL THF and the SAMPY ligand 2-[ArN=CH$_2$](NC$_5$H$_3$) (Ar= C$_6$H$_3$-2,6-Pr$^i_2$) (200 mg, 0.75 mmol, 1eq) was added at room temperature. After 24 hours stirring at room temperature all volatile components were removed in vacuo. A yellow greenish powder was obtained and recrystallized in Et$_2$O to give yellow greenish needles while storing at -30°C. Yield: 31%. mp: 126.4 - 127.6°C. ^{1}H NMR (300.22 MHz, C$_6$D$_6$): δ 7.14 (m, 3H, CH arom), 7.11 (t, 1H, PyH), 6.81 (d, 1H, PyH), 6.64 (d, 1H, PyH), 6.31 (t, 1H, PyH), 6.01 (broad s, CH$_2$), 4.10 (broad sept, 2H, CH^{i}Pr), 1.38 (d broad signal, 12H, CH$_3^i$Pr), 0.29 (broad s, 18H, [CH$_3$SiN]$_2$N). ^{13}C NMR (75.50 MHz, C$_6$D$_6$): δ 166.21 (ArH), 163.59 (ArH), 152.76 (ArH), 149.55 (ArH), 146.20 (ArH), 135.76 (ArH), 123.17 (ArH), 123.13 (ArH), 122.71 (ArH), 120.98 (ArH), 120.19 (ArH), 65.43 (CH$_2$), 27.41 (CH^{i}Pr), 26.45 (CH$_3^i$Pr) 2.23 ([CH$_3$SiN]$_2$N). ^{29}Si (59.64 MHz, C$_6$D$_6$): δ -4.96.

4.3.4 SIMPYGe (12)

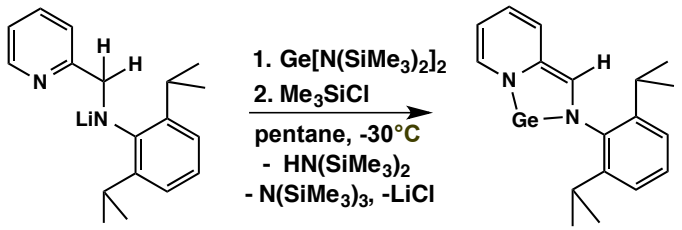

Ge[N(SiMe$_3$)$_2$]$_2$ (1.47 g, 3.73 mmol, 1 eq) was dissolved in 10 mL pentane and added to a suspension of the lithiated SAMPY ligand[153] (1.02 g, 3.73 mmol, 1 eq) in pentane at -30°C. After stirring for 1 hour at -30°C, the orange-brown solution was warmed up to room temperature and stirred for further 12 hours.

Then Me_3SiCl was reacted with the $LiN(SiMe_3)_2$ and the orange-brown solution was separated from the salts via a filter cannula. All volatile components were removed in vacuo and the product was obtained via recrystallization in pentane at -30°C. Yield: 62%. mp: 86.5 - 87.3°C. ^{1}H NMR (300.22 MHz, C_6D_6): δ 7.84 (d, 1H, PyH), 7.18 (m, 3H, CH arom), 6.84 (d, 1H, PyH), 6.78 (s, 1H, HC=N), 6.09 (dd, 1H, PyH), 5.46 (t, 1H, PyH), 2.77 (sept, 2H, CH^{i}Pr), 1.09 (dd, 12H, CH$_3{}^i$Pr). ^{13}C NMR (75.50 MHz, C_6D_6): δ 144.70 (ArH), 140.95 (ArH), 135.45 (ArH), 135.01 (ArH), 126.99 (ArH), 123.00 (ArH), 122.73 (ArH), 120.38 (ArH), 119.96 (ArH), 105.53 (ArH), 27.72 (CH^{i}Pr), 25.69 (CH$_3{}^i$Pr), 24.37 (CH$_3{}^i$Pr). Elemental analysis (%) calcd for $C_{18}H_{22}N_2Ge$ (339.02): C, 63.77; H,6.54; N, 8.26; found: C,62.46; H, 7.14; N, 7.76.

4.3.5 SAMPY$_2$Pb (13)

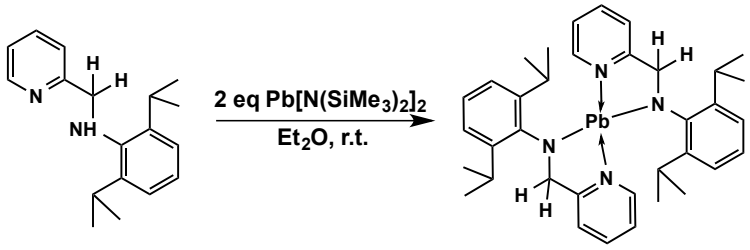

The Sampy ligand (200 mg, 0.75 mmol, 1 eq) was dissolved in 5 mL diethyl ether and $Pb[N(SiMe_3)_2]_2$ (196 mg, 0.37 mmol, 0.5 eq) was added dropwise. After 24 hours stirring at room temperature a yellow precipitate is formed. The yellow powder was filtrated and washed three times with 5 mL pentane. The powder was recrystallized in THF at -30°C. Yield: 72%. mp: 171.2-173.5°C. ^{1}H NMR (300.22 MHz, C_6D_6): δ 7,14 (m, 3H, CH arom), 6.82 (d, 2H, PyH), 6.78 (t, 2H, PyH), 6.63 (d, 2H, PyH), 6.30 (t, 2H, PyH), 5.93 (broad s, 4H, CH_2), 4.10 (broad sept, 4H, CH^{i}Pr), 1.38 (d broad signal, 24H, CH$_3{}^i$Pr). ^{13}C NMR (75.50 MHz, C_6D_6): δ 166.21 (ArH), 152.67 (ArH), 146.20 (ArH), 135.77 (ArH), 123.60 (ArH), 123.18 (ArH), 122.71 (ArH), 121.55 (ArH), 120.98 (ArH), 120.20 (ArH), 65.44 (CH_2), 27.49 (CH^{i}Pr), 26.41 (CH$_3{}^i$Pr), 24.10 (CH$_3{}^i$Pr). Elemental analysis (%) calcd for $C_{36}H_{46}N_4Pb$ (741.99): C, 58.28; H,6.25; N, 7.55; found: C,55.58; H, 6.08; N, 7.36.

4.3.6 Activation of Small Molecules with the SIMPYGe complex 12

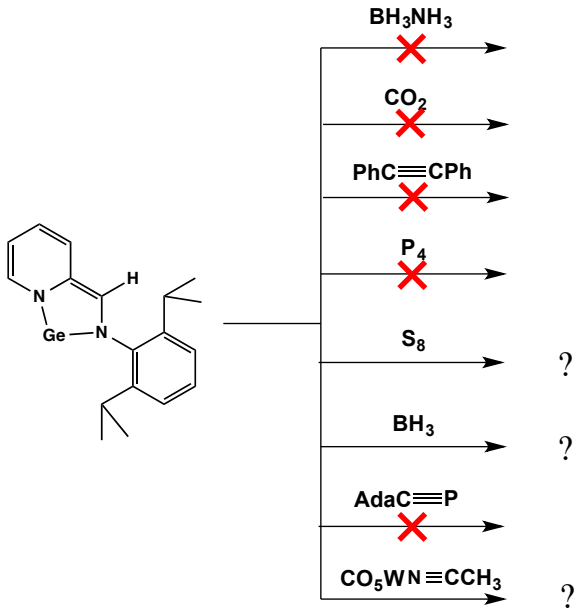

Various reactions of small molecules with the (SIMPY)Ge complex **12** were carried out in THF at room temperature. Surprisingly, the (SIMPY)Ge complex **12** is so stable that no reactions occur with NH_3BH_3, CO_2, PhC≡CPh, P_4 and AdaC≡P at all. The reaction solutions were stirred at room temperature for several days. Furthermore, heating and ultrasonication were performed, too. However, no activation of small molecules was observed. Further details are discussed in chapter 3.2.

4.3.7 SAMPYAlMe$_2$ (14)

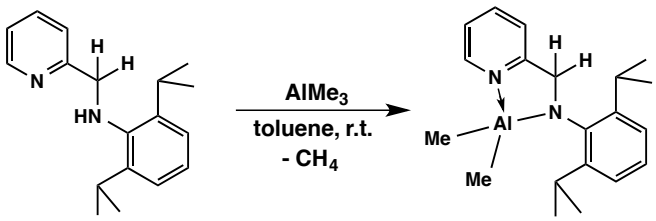

The SAMPY ligand (200 mg, 0.75 mmol, 1 eq) was dissolved in 6 mL toluene and $AlMe_3$ (0.75 mL, 1.0 M in toluene, 0.75 mmol, 1 eq) was added dropwise at room temperature. Color change was immediate as the solution went from clear transparent to a bright yellow green and a gas evolution was investigated. The solvent was removed and the solid then dried under vacuum. Suitable crystals for X-ray analysis were obtained after recrystallizing in toluene at -30°C. Yield: 99%. mp: 162 - 164°C. ^{1}H NMR (300.22 MHz, C_6D_6): δ 7.78 (d, 1H, PyH), 7.40 (s, 3H, CH arom), 7.28 (m, 3H, PyH), 4.58 (s, 2H, CH_2), 3.99 (sept, 2H, CH^{i}Pr), 1.49 (broad d, 12H, $CH_3{}^i$Pr). ^{13}C NMR (75.50 MHz, C_6D_6): δ 162.61 (ArH), 148.49 (ArH), 143.36 (ArH), 138.37 (ArH), 128.91 (ArH), 128.14 (ArH), 125.27 (ArH), 123.71 (ArH), 122.21 (ArH), 59.62 (CH^{i}Pr), 27.28 ($CH_3{}^i$Pr), 25.62 ($CH_3{}^i$Pr), 25.62 ($CH_3{}^i$Pr), 21.02 ((CH_3)$_2$Al). Elemental analysis (%) calcd for $C_{20}H_{29}N_2Al$ (324.45): C, 74.04; H, 9.01; N, 8.63; found: C, 69.15; H, 8.41; N, 7.80.

4.3.8 SAMPYAlI$_2$ (15)

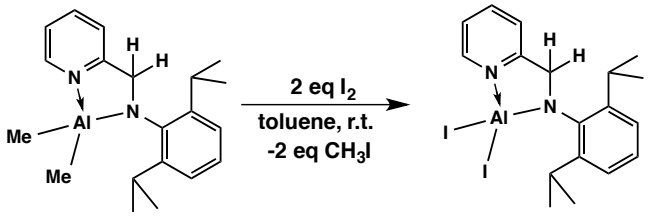

The SAMPYAlMe$_2$ complex (200 mg, 0.62 mmol, 1eq) was dissolved in 10 mL toluene and cooled to -30°C. Iodide (312 mg, 1.23 mmol, 2 eq) dissolved in 10 mL toluene was added dropwise. The solution turned from dark red to yellow-greenish. After 12 hours stirring all volatile components were reduced in vacuo. The yellow greenish powder was recrystallized in diethyl ether at -30°C. The ^{1}H and ^{13}C NMR spectra indicate that complex **15** was formed, but that byproducts were formed as well. Mixtures of the desired product **15** with a mixed species SAMPYAlMeI and a ligand exchange product SAMPY$_2$AlI **16** were observed. ^{1}H NMR (300.22 MHz, C_6D_6): δ 7.78 (d, 1H, PyH), 7.39 (m, 3H, CH arom.), 7.18 (d, 1H, PyH), 6.84 (t, 1H, PyH), 6.44 (d, 1H, PyH), 6.20 (t, 1H, PyH),4.58 (s, 1H, CH_2), 3.89 (sept, 2H, CH^{i}Pr), 1.45 (d, 12H, $CH_3{}^{i}$Pr). ^{13}C NMR (75.50 MHz, C_6D_6): δ 159.49 (ArH), 148.95 (ArH), 147.69 (ArH), 137.35 (ArH), 128.92 (ArH), 124.73 (ArH) , 122.43 (ArH), 120.58 (ArH), 57.69 (CH_2), 27.57(CH^{i}Pr), 26.58 ($CH_3{}^{i}$Pr), 25.84 ($CH_3{}^{i}$Pr) ppm.

4.3.9 SAMPY$_2$AlI (16)

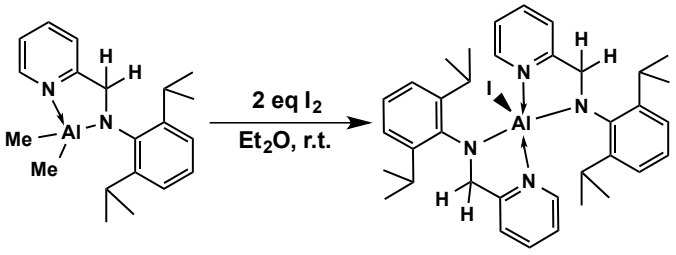

The SAMPYAlMe$_2$ complex (200 mg, 0.62 mmol, 1eq) was synthesized as described in 4.3.7. All volatile components were removed in vacuo. Then iodide

(312 mg, 1.23 mmol, 2 eq) dissolved in 10 mL toluene was added dropwise at -30°C. The solution turned from dark red to yellow-greenish. After 12 hours stirring all volatile components were reduced in vacuo. The yellow greenish powder was recrystallized in diethyl ether at -30°C. Light green cubic crystals were obtained. Yield: 36%. mp: 166.5 - 167.4°C. ^{1}H NMR (300.22 MHz, C_6D_6): δ 8.03 (d, 2H, PyH), 7.31 (d, 2H, CH arom), 7.05 (m, 4H, CH arom.), 6.87 (d, 1H, PyH), 6.63 (t, 2H, PyH), 6.39 (d, 1H, PyH), 6.20 (t, 2H, PyH),4.68 (s, 2H, CH_2), 4.64 (s, 2H, CH_2), 4.39 (sept, 2H, CH^iPr), 4.24 (sept, 2H, CH^iPr), 1.79 (d, 6H, $CH_3{}^iPr$), 1.34 (d, 12H, $CH_3{}^iPr$), 0.50 (d, 6H, $CH_3{}^iPr$). ^{13}C NMR (75.50 MHz, C_6D_6): δ 159.49 (ArH), 148.50 (ArH), 147.69 (ArH), 146.42 (ArH), 137.35 (ArH), 128.92 (ArH), 125.28 (ArH), 124.72 (ArH), 124.45 (ArH), 122.43 (ArH), 120.58 (ArH), 120.33 (ArH), 57.70 (CH^iPr), 27.57 ($CH_3{}^iPr$), 27.50 ($CH_3{}^iPr$), 27.11 ($CH_3{}^iPr$), 26.58 ($CH_3{}^iPr$). Elemental analysis (%) calcd for $C_{36}H_{46}N_4AlI$ (688.68): C, 62.79; H, 6.73; N, 8.14; found: C, 52.83; H, 6.09; N, 6.02.

4.3.10 SIMPY$_2$GaI (17)

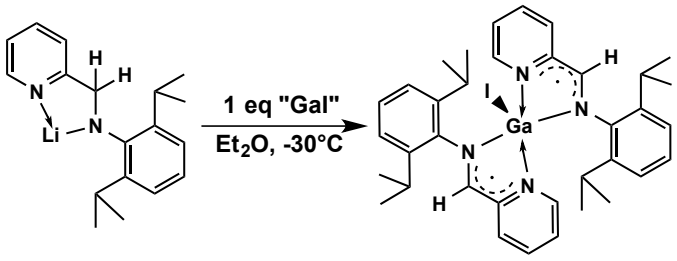

Diethyl ether was cooled to -30°C and the SAMPYLi (200 mg, 0.73 mmol, 1 eq) was added. A suspension of GaI (147 mg, 0.73 mmol, 1 eq) in diethyl ether was cooled to -30°C and added slowly to the lithiated ligand. A dark green solution was obtained after stirring 30 minutes at -30°C. All volatile components were removed in vacuo and the dark green powder was recrystallized in diethyl ether to obtain dark green cubic crystals. Yield: 38%. degradation: 143°C. g= 2.0027(1)

4.4 Synthesis of low valent Main Group Complexes Using the SIMPY Ligand

4.4.1 SIMPY$_2$Ge (18)

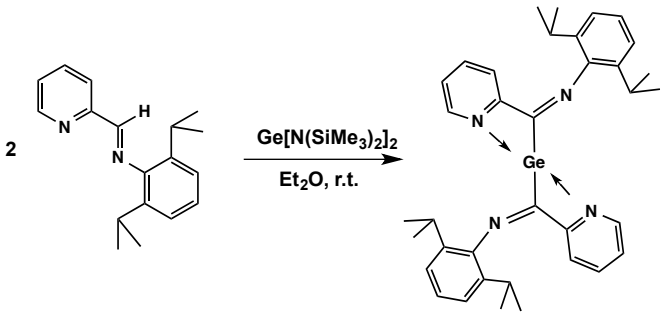

The SIMPY ligand (200 mg, 0.75 mmol, 1 eq) was dissolved in 5 mL of diethyl ether and of Ge[N(SiMe$_3$)$_2$]$_2$ (221 mg, 0.56 mmol, 0.75 eq) was added. After two weeks stirring at room temperature, volatile components were removed in vacuo. The dark red powder was recrystallized in diethyl ether. Yield: 51% ^{1}H NMR (300.22 MHz, C_6D_6): δ 8.52 (d, 2H, PyH), 8.21 (broad d, 2H, PyH), 7.18 (m, 8H, CH arom.), 6.71 (t, 2H, PyH), 3.14 (sept, 4H, CH^{i}Pr), 1.17 (d, 24H, CH$_3$^{i}Pr). ^{13}C NMR (75.50 MHz, C_6D_6): δ 163.62 (ArH), 149.64 (ArH), 137.11 (ArH), 136.06 (ArH), 124.70 (ArH), 123.11 (ArH), 119.32 (ArH), 28.03 (CH^{i}Pr), 23.23 (CH$_3$^{i}Pr).

4.4.2 SIMPY$_2$Sn (19)

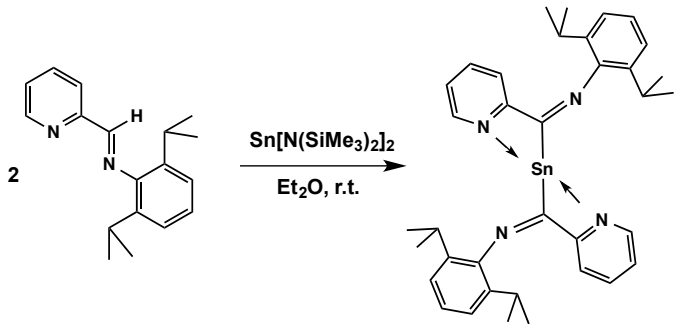

Procedure as described in 4.4.1. The SIMPY ligand (200 mg, 0.75 mmol, 1 eq) was dissolved in 5 mL of diethyl ether and of Sn[N(SiMe$_3$)$_2$]$_2$ (247 mg, 0.56 mmol, 0.75 eq) was added. The dark red brownish powder was recrystallized in diethyl ether. ^{1}H NMR (300.22 MHz, C_6D_6): δ 7.63 (d, 2H, PyH), 7.22 (m, 8H, CH arom.), 6.79 (broad t, 2H, PyH), 6.40 (broad t, 2H, PyH), 3.73 (broad sept, 4H, CH^{i}Pr), 1.21 (broad d, 24H, CH$_3{}^i$Pr). Yield: 23% ^{13}C NMR (75.50 MHz, C_6D_6): δ 147.36 (ArH), 136.47 (ArH), 135.91 (ArH), 124.75 (ArH), 124.62 (ArH), 123.00 (ArH), 122.86 (ArH), 120.52 (ArH), 117.86 (ArH), 28.07 (CH^{i}Pr), 23.17 (CH$_3{}^i$Pr), 22.00 (broad signal, CH$_3{}^i$Pr).

4.4.3 SIMPY$_2$Pb (20)

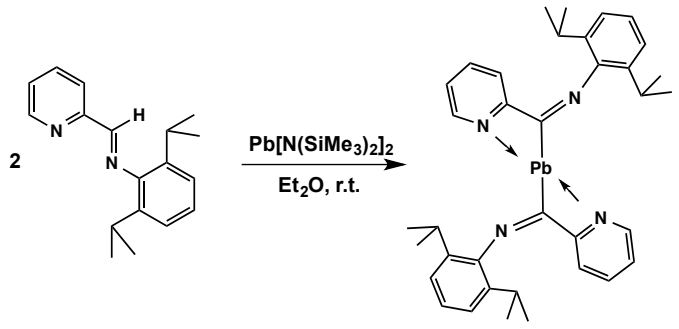

Procedure as described in 4.4.1. The SIMPY ligand (200 mg, 0.75 mmol, 1 eq) was dissolved in 5 mL of diethyl ether and of Pb[N(SiMe$_3$)$_2$]$_2$ (296 mg, 0.56 mmol, 0.75 eq) was added. The dark red brownish powder was recrystallized

in diethyl ether. Yield: 18% ^{1}H NMR (300.22 MHz, C_6D_6): δ 7.63 (d, 2H, PyH), 7.23 (t, 2H, PyH), 7.19 (m, 8H, CH arom.), 6.39 (t, 2H, PyH), 3.15 (sept, 4H, CH^{i}Pr), 0.95 (dd, 24H, CH$_3$^{i}Pr). ^{13}C NMR (75.50 MHz, C_6D_6): δ 171.72 (ArH), 164.19 (ArH), 154.60 (ArH), 148.88 (ArH), 147.35 (ArH), 136.48 (ArH), 128.17 (ArH), 124.30 (ArH), 123.49 (ArH), 123.49 (ArH) 122.87 (ArH), 28.81 (CH^{i}Pr), 23.03 (broad signal, CH$_3$^{i}Pr).

4.4.4 SIMPYGeCl$_2$ (21)

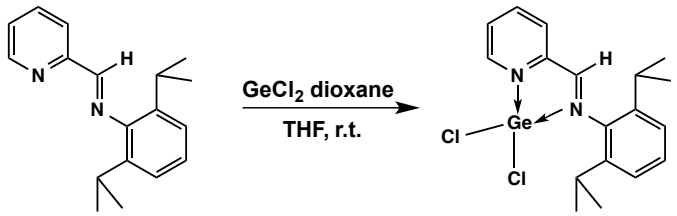

$GeCl_2$ dioxane (434 mg, 1.84 mmol, 1 eq) was dissolved in 4 mL THF and the SIMPY ligand 2-[ArN=CH](NC_5H_4) (Ar= C_6H_3-2-Pr$^{i}_2$) (500 mg, 1.84 mmol, 1eq) was added at room temperature. Color change was immediate as the solution went from clear transparent to a bright orange. The solvent was removed and the solid then dried in vacuo. Orange needle like crystals suitable for X-ray analysis were obtained by recrystallization in THF and storing at -30°C. Yield: 99%. mp: 153°C. ^{1}H NMR (300.22 MHz, C_6D_6): δ 8.84 (d, 1H, PyH), 8.65 (s, 1H, HC=N), 7.97 (d, 1H, PyH), 7.22 (m, 4H, CH arom), 6.83 (t, 1H, PyH), 3.18 (sept, 2H, CH^{i}Pr), 1.23 (d, 12H, CH$_3$^{i}Pr). ^{13}C NMR (75.50 MHz, C_6D_6): δ 163.87 (C=N, imine), 149.98 (ArH), 148.35 (ArH), 140.39 (ArH), 139.24 (ArH), 127.09 (ArH), 125.48 (ArH), 123.93(ArH), 123.10 (ArH), 28.47 (CH^{i}Pr), 24.07 (CH$_3$^{i}Pr). Elemental analysis (%) calcd for $C_{18}H_{22}Cl_2N_2Ge$ (409.92): C, 52.74; H, 5.41; N, 6.83; found: C, 51.51; H, 5.25; N, 6.49.

4.4.5 SIMPYGeBr$_2$ (22)

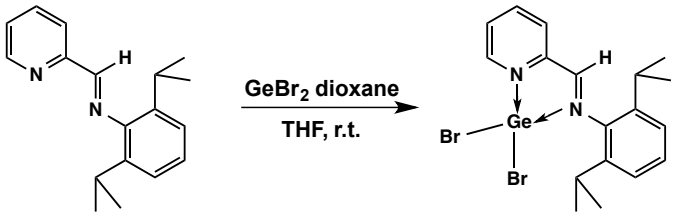

Procedure as described in 4.4.4. $GeBr_2$ dioxane (241 mg, 0.75 mmol, 1 eq) was dissolved in 4 mL THF and the SIMPY ligand (200 mg, 0.75 mmol, 1eq) was added at room temperature. Dark orange crystals were obtained after recrystallizing in a THF/benzene mixture (2:1) at room temperature. Yield: 99%. mp: 169.9 - 171.9°C. ^{1}H NMR (300.22 MHz, C_6D_6): δ 8.85 (d, 1H, PyH), 8.49 (s, 1H, HC=N), 7.87 (d, 1H, PyH), 7.21 (m, 4H, CH arom), 6.76 (t, 1H, PyH), 3.17 (sept, 2H, CH^{i}Pr), 1.22 (d, 12H, CH$_3{}^i$Pr). ^{13}C NMR (75.50 MHz, C_6D_6): δ 161.57 (C=N, imine), 150.67 (ArH), 148.50 (ArH), 139.54 (ArH), 138.17 (ArH), 126.48 (ArH), 126.15 (ArH), 124.46 (ArH), 123.59 (ArH), 28.28 (CH^{i}Pr), 23.73 (CH$_3{}^i$Pr). Elemental analysis (%) calcd for $C_{18}H_{22}Br_2N_2$ Ge (498.83): C, 43.34; H, 4.54; N, 5.62; found: C, 43.17; H, 4.44; N, 5.54.

4.4.6 SIMPYSnCl$_2$ (23)

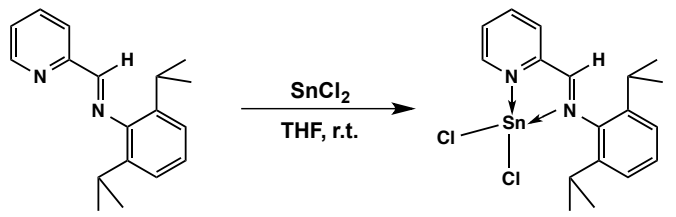

Procedure as described in 4.4.4. $SnCl_2$ (338 mg, 1.84 mmol, 1 eq) was dissolved in 4 mL THF and the SIMPY ligand (500 mg, 1.84 mmol, 1eq) was added at room temperature. Orange crystals were obtained after recrystallizing in THF at -30°C. Yield: 99%. mp: 205°C. ^{1}H NMR (300.22 MHz, D_2O capillary/THF)): δ 9.18 (d, 1H, PyH), 8.50 (s, 1H, HC=N), 8.32 (d, 1H, PyH), 8.11 (t, 1H, PyH), 7.68 (t, 1H, PyH), 7.26 (d, 1H, CH arom), 7.22 (t, 1H, CH arom), 3.13 (sept, 2H,

CH^iPr), 1.27 (d, 12H, $CH_3{}^iPr$). ^{13}C NMR (75.50 MHz, D_2O capillary/THF): δ 163.28 (C=N, imine), 149.94 (ArH), 137.87 (ArH), 137.49 (ArH), 126.09 (ArH), 124.78 (ArH), 123.27 (ArH), 122.97 (ArH), 27.99 (CH^iPr), 23.22 ($CH_3{}^iPr$). ^{119}Sn NMR (112.17 MHz, D_2O capillary/THF): δ -216.34. Elemental analysis (%) calcd for $C_{18}H_{22}Cl_2N_2Sn$ (456.00): C, 47.41; H, 4.86; N, 6.14; found: C, 45.87; H, 4.68; N, 5.91.

4.4.7 SIMPYSnBr$_2$ (24)

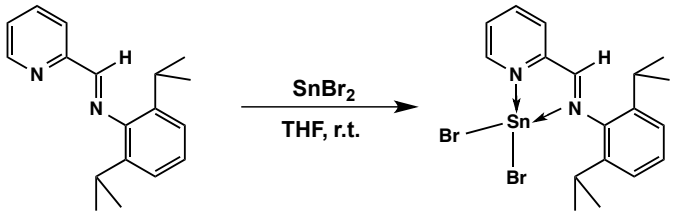

Procedure as described in 4.4.4. $SnBr_2$ (209 mg, 0.75 mmol, 1 eq) was dissolved in 4 mL THF and the SIMPY ligand (200 mg, 0.75 mmol, 1eq) was added at room temperature. Red cubic crystals were obtained after recrystallizing in a THF/benzene mixture (2:1) at room temperature. Yield: 99%. mp: 208°C. ^1H NMR (300.22 MHz, $CDCl_3$): δ 9.94 (d, 1H, PyH), 8.38 (s, 1H, HC=N), 8.18 (t, 1H, PyH), 7.95 (d, 1H, PyH), 7.74 (t, 1H, PyH), 7.18 (m, 3H, CH arom), 2.94 (sept, 2H, CH^iPr), 1.12 (d, 12H, $CH_3{}^iPr$). ^{13}C NMR (75.50 MHz, $CDCl_3$): δ 160.82 (C=N, imine), 151.77 (ArH), 149.24 (ArH), 141.18 (ArH), 138.85 (ArH), 128.17 (ArH), 126.85 (ArH), 123.84 (ArH), 123.26 (ArH), 28.41 (CH^iPr), 24.41 ($CH_3{}^iPr$). ^{119}Sn NMR (112.17 MHz, C_6D_6): δ -80.07. Elemental analysis (%) calcd for $C_{18}H_{22}Br_2N_2Sn$ (544.90): C, 39.68; H, 4.07; N, 5.14; found: C, 39.80; H, 4.02; N, 5.22.

4.4.8 SIMPYSnI$_2$ (25)

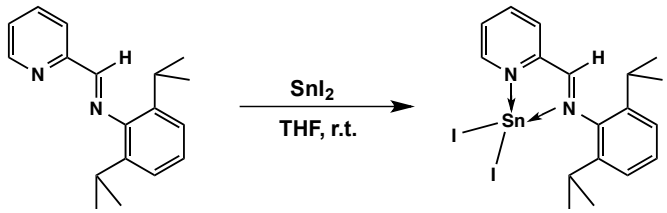

Procedure as described in 4.4.4. SnI_2 (932 mg, 2.50 mmol, 1 eq) was dissolved in 4 mL THF and the SIMPY ligand (400 mg, 2.50 mmol, 1eq) was added at room temperature. Dark red cubic crystals were obtained after recrystallizing in a THF/benzene mixture (2:1) at room temperature. Yield: 99%. mp: 191.4 - 192.3°C. ^{1}H NMR (300.22 MHz, C_6D_6): δ 9.21 (d, 1H, PyH), 8.37 (s, 1H, HC=N), 8.00 (d, 1H, PyH), 7.82 (t, 1H, PyH), 7.36 (t, 1H, PyH), 7.07 (m, 4H, CH arom), 3.00 (sept, 2H, CH^{i}Pr), 1.08 (d, 12H, CH$_3$^{i}Pr). ^{13}C NMR (75.50 MHz, C_6D_6): δ 163.16 (C=N, imine), 151.60 (ArH), 151.18 (ArH), 138.89 (ArH), 137.81 (ArH), 126.58 (ArH), 125.32 (ArH), 124.91 (ArH), 124.49 (ArH), 123.09 (ArH), 27.96 (CH^{i}Pr), 23.34 (CH$_3$^{i}Pr). ^{119}Sn NMR (112.17 MHz, C_6D_6): δ 317 ppm. Elemental analysis (%) calcd for $C_{18}H_{22}I_2N_2Sn$ (638.91): C, 33.84; H,3.41; N, 4.38; found: C 31.45,; H, 2.73; N, 3.84.

4.4.9 SIMPYSnOTf$_2$ (26)

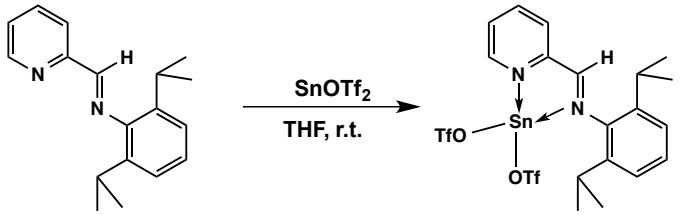

SIMPY ligand (0.5 g, 1.88 mmol, 1 eq) was dissolved in 5 mL THF and $SnOTf_2$ (0.78 g, 1.88 mmol, 1 eq) was added. The light yellow solution turned into a bright orange. All volatile components were removed via vacuo and a bright orange powder was obtained. Yield: 99%. mp: 67.5 - 68.6°C. ^{1}H NMR (300.22

MHz, C_6D_6): δ 9.43 (broad s, 1H, HC=N), 8.19 (broad d, 1H, PyH), 7.58 (broad s, 1H, PyH), 7.18 (m, 3H, CH arom), 2.65 (broad sept, 2H, CH^iPr), 1.24 (broad d, 12H, $CH_3{}^iPr$). ^{13}C NMR (75.50 MHz, C_6D_6): δ 167.22 (C=N, imine),150.72 (ArH), 147.77 (ArH), 144.97 (ArH), 142.17 (ArH), 141.02 (ArH), 129.51 (ArH), 124.34 (ArH), 122.29 (ArH), 118.06 (ArH), 28.16 (CH^iPr), 23.18 ($CH_3{}^iPr$), 23.14 ($CH_3{}^iPr$). ^{119}Sn NMR (112.17 MHz, C_6D_6/THF): δ -27.75.

4.4.10 $(SIMPYGeCl)_2$ (27)

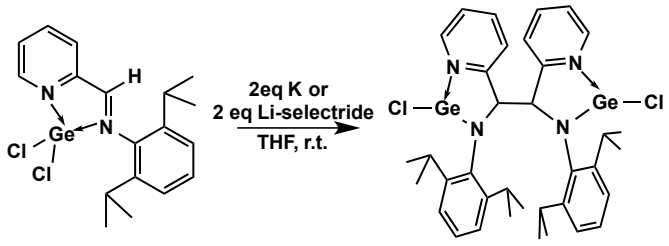

The SIMPY ligand (500 mg, 1.78 mmol, 1 eq) was dissolved in 5 mL THF and $GeCl_2$*dioxane (412 mg, 1.78 mmol, 1 eq) was added. After 15 min the potassium metal (140 mg, 3.56 mmol, 1 eq) or Li-selectride (1 M in THF) (3.6 mL, 3.56 mmol, 2 eq) was added and the solution stirred over night. A dark orange solution was obtained. All volatile components were reduced in vacuo. Toluene was added to seperate the product from KCl salt and then recrystallized at -30°C to obtain slightly yellow cubic crystals. Yield: 28%. ^1H NMR (300.22 MHz, C_6D_6): δ 8.76 (d, 2H, PyH), 7.85 (t, 2H, PyH), 7.51 (d, 2H, PyH), 7.38 (m, 2H, CH-arom.), 7.23(d, 4H, CH-arom.), 7.15 (t, 2H, PyH), 4.49 (s, 2H, CH), 3.64 (sept, 4H, CH^iPr), 1.39 (d, 24H, $CH_3{}^iPr$). ^{13}C NMR (75.50 MHz, C_6D_6): δ 159.50 (ArH), 149.27 (ArH), 143.86 (ArH), 142.76 (ArH), 136.32 (ArH), 123.67 (ArH), 123.23 (ArH), 122.02 (ArH), 121.86 (ArH), 67.16 (CH), 27.65 (CH^iPr), 23.94 ($CH_3{}^iPr$).

4.4.11 SIMPYSnCl$_2$ + reducing agents

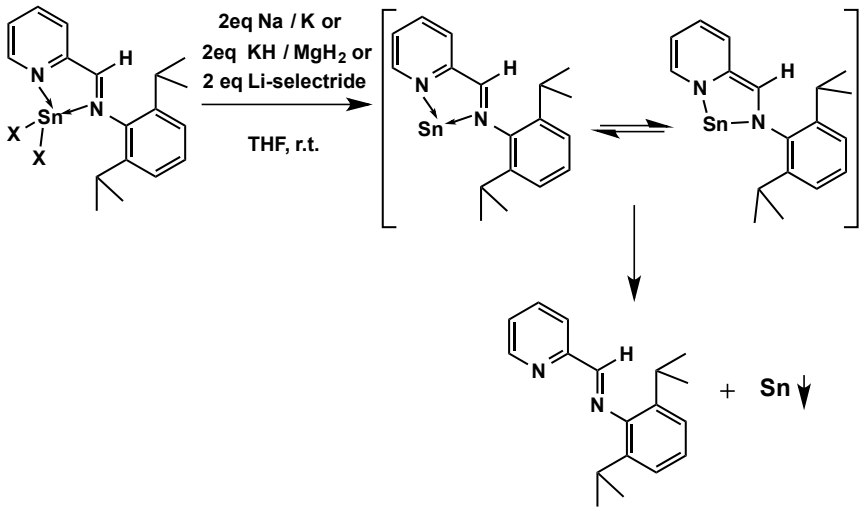

The reaction of the SIMPYSnX$_2$ complexes with reducing agents like Na, K, KH, MgH$_2$ and Li-selectride gives not the desired stannylene. Instead the SIMPY ligand is formed and Sn metal precipitates.

4.4.12 (SIMPYSiCl$_3$)$_2$ (28)

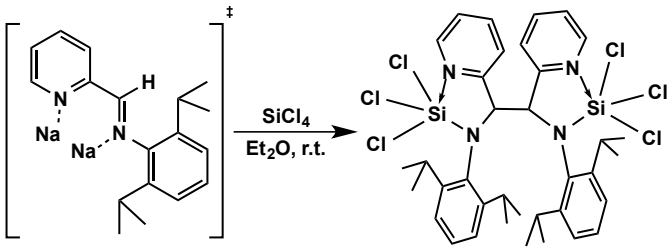

The SIMPYNa$_2$ complex (1.17 g, 3.75 mmol, 1 eq) was dissolved in diethyl ether and SiCl$_4$ (0.43 mL, 3.75 mmol, 1eq) was added dropwise. The dark red solution turned bright orange. After 24 hours stirring all volatile components were reduced in vacuo and the slightly orange powder was recrystallized in THF at -30°C to obtain clear cubic crystals. Yield: 41%. mp: 167.4-168.9°C. ^{1}H NMR (300.22 MHz, C_6D_6): δ 8.43 (d, 2H, PyH), 8.24 (d, 2H, PyH), 7.01 (m, 8H, CH arom.), 6.70 (t, 2H, PyH), 6.15 (t, 2H, PyH), 4.65 (S, 2H, CHCH), 3.77 (sept,

4H, CH^{i}Pr), 1.40 (d, 24H, CH$_3$^{i}Pr). ^{13}C NMR (75.50 MHz, C_6D_6): δ 145.62 (ArH), 141.44 (ArH), 141.22 (ArH), 137.73 (ArH), 135.40 (ArH), 133.46 (ArH), 131.77 (ArH), 126.70 (ArH), 125.59 (ArH), 124.51 (ArH), 121.05 (ArH), 120.65 (ArH), 120.60 (ArH), 120.45 (ArH), 65.91 (CHCH), 25.07 (CH^{i}Pr), 24.96 (CH^{i}Pr), 20.68 (CH$_3$^{i}Pr). ^{29}Si (59.64 MHz, C_6D_6): δ -19.09 ppm. Elemental analysis (%) calcd for $C_{36}H_{44}Cl_6N_4SiN_2$ (801.65): C, 53.94; H, 5.53; N, 6.99; found: C 54.32,; H, 6.01; N, 6.48.

4.4.13 (SIMPYNa$_2$) + ECl$_2$ (E= Sn, Pb)

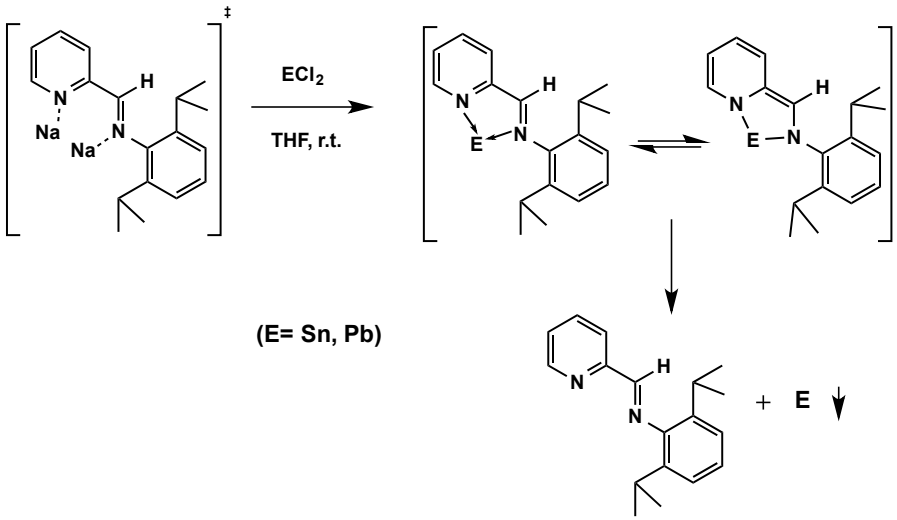

The reaction of the SIMPYNa$_2$ intermediate with SnCl$_2$ or PbCl$_2$ gives not the desired stannylene or plumbylene. Instead the SIMPY ligand is formed and Sn or Pb metal precipitates.

4.5 Synthesis of low valent Main Group Complexes Using the DIMPY Ligand

4.5.1 $[DIMPYGeCl]^{+}[GeCl_3]^{-}$ (29)

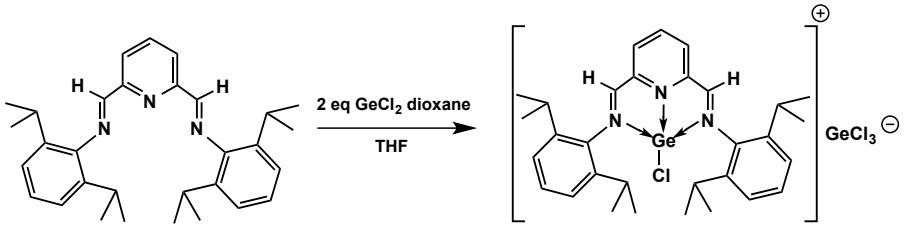

$GeCl_2$ dioxane (0,51 g, 2.20 mmol, 2 eq) was dissolved in 5 mL THF and the ligand DIMPY (0.50 g, 1.10 mmol, 1 eq) was added at room temperature. Color change was immediate as the solution went from clear transparent to orange. The solvent was reduced and the solid then dried in vacuo. Orange needle like crystals suitable for X-ray analysis were obtained by recrystallization in a mixture of THF/benzene at room temperature. Yield: 98%. Mp: 158.6 - 160.7°C. ^{1}H NMR (300.22 MHz, C_6D_6): δ 8.61(s, 1H, HC=N), 8.55 (s, 1H, HC=N), 8.44 (t, 1H, PyH), 8.30 (td, 1H, PyH), 7.15 (m, 6H, CH arom), 3.15 (broad sept, 4H, $CH^{i}Pr$), 1.25 (broad d, 12H, $CH_3{}^{i}Pr$), 1.16 (broad d, 12H, $CH_3{}^{i}Pr$). ^{13}C NMR (75.50 MHz, C_6D_6): δ 162.87 (C=N, imine), 159.75 (C=N, imine), 154.67 (ArH), 148.66 (ArH), 146.34 (ArH), 139.57 (ArH), 137.13 (ArH), 136.19 (ArH), 132.67 (ArH), 128.18 (ArH), 124.77 (ArH), 123.15 (ArH), 122.19 (ArH), 28.08 ($CH^{i}Pr$), 23.14 ($CH_3{}^{i}Pr$). Elemental analysis (%) calcd for $C_{31}H_{39}Cl_4N_3Ge_2$ (740.75): C, 50.26; H, 5.31; N, 5.67. found: C, 63.47; H, 6.66; N, 7.03.

4.5.2 [DIMPYGeBr]$^+$[GeBr$_3$]$^-$ (30)

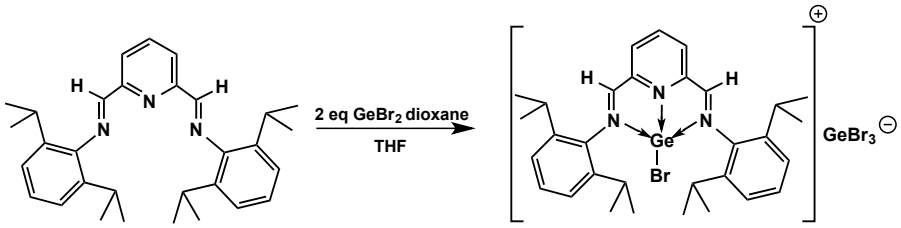

Procedure as described in 4.5.1. $GeBr_2$ (0,28 g, 0.88 mmol, 2 eq) was dissolved in 5 mL THF and the ligand DIMPY (0.20 g, 0.44 mmol, 1 eq) was added at room temperature. Orange needle like crystals suitable for X-ray analysis were obtained by recrystallization in a mixture of THF/benzene at room temperature. Yield: 98%. Mp: 171.7 - 172.5°C. ^{1}H NMR (300.22 MHz, C_6D_6): δ 8.61(s, 1H, HC=N), 8.55 (s, 1H, HC=N), 8.44 (t, 1H, PyH), 8.30 (td, 1H, PyH), 7.15 (m, 6H, CH arom), 3.15 (broad sept, 4H, CH^{i}Pr), 1.25 (broad d, 12H, CH$_3{}^i$Pr), 1.16 (broad d, 12H, CH$_3{}^i$Pr). ^{13}C NMR (75.50 MHz, C_6D_6/THF): δ 160.06 (C=N, imine), 148.41 (ArH), 146.34 (ArH), 141.71 (ArH), 140.28 (ArH), 139.58 (ArH), 132.43 (ArH), 129.45 (ArH), 128.16 (ArH), 124.48 (ArH), 124.27 (ArH), 30.02 (CH^{i}Pr), 28.64 (CH^{i}Pr).
Elemental analysis (%) calcd for $C_31H_{39}Cl_4N_3Ge_2$ (740.75): C, 50.26; H, 5.31; N, 5.67. found: C, 42.33; H, 4.59; N, 4.44.

4.5.3 [DIMPYSnCl]$^+$[SnCl$_3$]$^-$ (31)

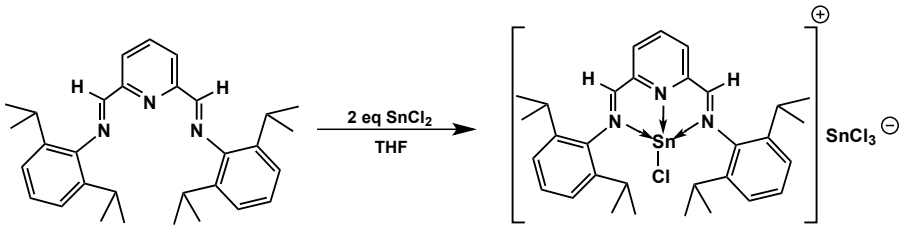

Procedure as described in 4.5.1. $SnCl_2$ (0,42 g, 2.20 mmol, 2 eq) was dissolved in 5 mL THF and the ligand DIMPY (0.50 g, 1.10 mmol, 1 eq) was added at room temperature. Orange needle like crystals suitable for X-ray analysis

were obtained by recrystallization in THF and storing at -30 °C for several days. Yield: 94%. Mp: 208-210°C . ^{1}H NMR (300.23 MHz, C_6D_6): δ 8.12 (s, 2H, HC=N), 7.58 (t, 1H, p-CH-Py), 7.35 (d, 2H, m-CH-Py), 6.82 (s, 6H, CH arom.), 3.12 (sept, 4H, CH^{i}Pr), 1.02 (d, 12H, CH$_3$^{i}Pr), 0.95 (d, 12H, CH$_3$^{i}Pr) ppm. ^{13}C NMR (75.50 MHz, C_6D_6): δ 162.37 (C=N, imine), 148.78 (Ar-CH), 144.29 (Ar-CH), 141.20 (Ar-CH), 140.56 (Ar-CH), 132.87 (Ar-CH), 128.06 (Ar-CH), 127.96 (Ar-CH), 127.64 (Ar-CH), 127.32 (Ar-CH), 124.33 (Ar-CH), 28.36 (CH^{i}Pr), 25.38 (CH$_3$^{i}Pr), 24.43 (CH$_3$^{i}Pr) ppm. ^{119}Sn NMR (111.92 MHz, C_6D_6): δ -57.9 ($SnCl_3$-anion), -445.2 (DimpySnCl) ppm. IR (KBr) ν/cm^{-1}: 3068 (w), 3032 (w), 2962 (s), 2920 (s), 1959 (w), 1642 (s), 1591 (s), 1385 (m), 1363 (m), 1324 (w), 1260 (s), 1163 (m), 1098 (s), 1043 (s), 1020 (s), 937 (w), 850 (w), 802 (s), 750 (w), 553 (m), 393 (w). Elemental analysis (%) calcd for $C_{31}H_{41}Cl_4N_3Sn_2$ (834.91): C, 44.60; H, 4.95; N, 5.03. found: C, 45.14; H, 5.14; N, 4.79.

4.5.4 [DIMPYSnBr]$^{+}$[SnBr$_3$]$^{-}$ (32)

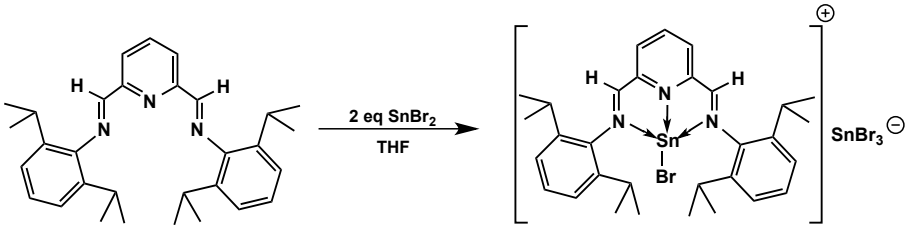

Procedure as described in 4.5.1. $SnBr_2$ (0,61 g, 2.20 mmol, 2 eq) was dissolved in 5 mL THF and the ligand DIMPY (0.50 g, 1.10 mmol, 1 eq) was added at room temperature. Dark orange needles were obtained after recrystallizing in a THF/benzene mixture (2:1) at room temperature. Yield: 98%. Mp: 196.6 - 197.8°C ^{1}H NMR (300.23 MHz,C_6D_6): δ 8.61 (s, 1H, HC=N), 8.48 (s, 1H, HC=N), 8.38 (d, 1H, PyH), 8.18 (t, 1H, PyH), 7.92 (d, 1H, PyH), 7.24 (m, 6H, CH arom.), 3.21 (broad sept, 4H, CH^{i}Pr), 1.33 (d, 12H, CH^{3i}Pr), 1.23 (d, 12H, CH$_3$^{i}Pr) ppm. ^{13}C NMR (75.50 MHz, C_6D_6): δ 162.83 (C=N, imine), 159.39 (C=N, imine),154.63 (Ar-CH), 148.12 (Ar-CH), 146.08 (Ar-CH), 140.30 (Ar-CH), 139.58 (Ar-CH), 137.00 (Ar-CH), 132.09 (Ar-CH), 128.31 (Ar-CH), 124.78 (Ar-CH), 124.37 (Ar-CH), 123.15 (Ar-CH), 122.23 (Ar-CH), 28.07 (CH^{i}Pr), 25.40 (CH$_3$^{i}Pr), 23.13 (CH$_3$^{i}Pr) ppm. ^{119}Sn NMR (111.92 MHz, C_6D_6): δ 98.18 (DimpySnBr), -405.84

($SnBr_3$-anion) ppm. Elemental analysis (%) calcd for $C_{31}H_{39}Br_4N_3Sn_2$ (1010.70): C, 36.84; H, 3.89; N, 4.16. found: C, 40.83; H, 4.25; N, 4.62.

4.5.5 $[DIMPYSnI]^+[SnI_3]^-$ (33)

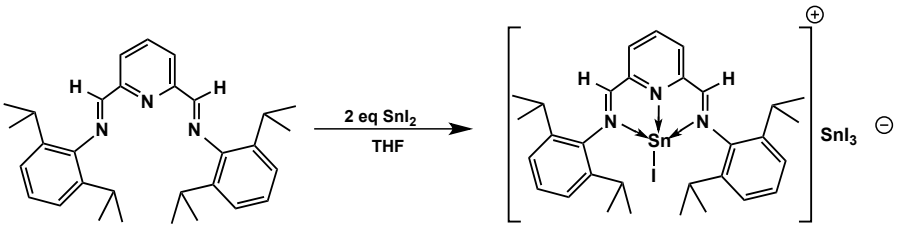

Procedure as described in 4.5.1. SnI_2 (0,82 g, 2.20 mmol, 2 eq) was dissolved in 5 mL THF and the ligand DIMPY (0.50 g, 1.10 mmol, 1 eq) was added at room temperature. Dark redish needles were obtained after recrystallizing in a THF/benzene mixture (2:1) at room temperature. Yield: 98%. Mp: 196.6 - 197.8°C ^{1}H NMR (300.23 MHz,C_6D_6): δ 9.24 (d, 1H, PyH), 8.40 (s, 1H, HC=N), 8.04 (d, 1H, PyH), 7.86 (t, 1H, PyH), 7.38 (t, 2H, CH arom.), 7.08 (m, 4H, CH arom.), 3.02 (broad sept, 4H, CH^iPr), 1.09 (d, 24H, $CH^{3i}Pr$) ppm. ^{13}C NMR (75.50 MHz, C_6D_6): δ 163.30 (C=N, imine), 162.82 (Ar-CH), 159.36 (Ar-CH), 151.03 (Ar-CH), 146.00 (Ar-CH), 139.58 (Ar-CH), 137.88 (Ar-CH), 132.76 (Ar-CH), 127.97 (Ar-CH), 126.87 (Ar-CH), 125.49 (Ar-CH), 123.16 (Ar-CH), 122.59 (Ar-CH), 27.98 (CH^iPr), 23.45 ($CH_3{}^iPr$) ppm. ^{119}Sn NMR (111.92 MHz, C_6D_6): δ (DimpySnI), (SnI_3-anion) ppm. Elemental analysis (%) calcd for $C_{33}H_{47}I_4N_3Sn_2$ (1230.80): C, 32.20; H, 3.85; N, 3.41;. found: C, 33.61; H, 3.77; N, 4.33;

4.5.6 DIMPYSnOTf$_2$ (34)

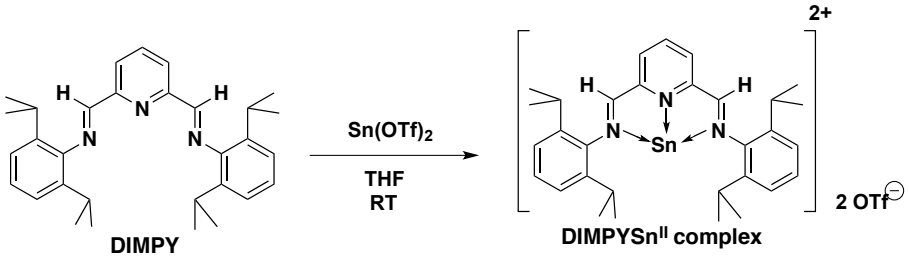

DIMPY ligand (0,5 g, 1,10 mmol, 1 eq) was dissolved in 5 mL THF and $SnOTf_2$ (0,46 g, 1,10 mmol, 1 eq) was added. The solvent was reduced in vacuo and an orange powder was obtained. Cubic orange crystals were obtained via recrystallizing in THF/benzene mixture at room temperature. Yield: 98%. Mp: 202.7 - 204.9°C ^{1}H NMR (300.23 MHz,C_6D_6): δ 8.18 (s, 2H, HC=N), 7.31 (t, 1H, PyH), 7.14 (m, 8H, CH arom.), 3.52 (broad sept, 4H, CH^{i}Pr), 1.27 (d, 24H, CH^{3i}Pr) ppm. ^{13}C NMR (75.50 MHz, C_6D_6): δ 163.48 (C=N, imine), 151.07 (Ar-CH), 144.48 (Ar-CH), 141.53 (Ar-CH), 131.03 (Ar-CH), 128.46 (Ar-CH), 124.79 (Ar-CH), 122.28 (Ar-CH), 118.05 (Ar-CH), 27.62 (CH^{i}Pr), 24.65 (CH$_3{}^i$Pr) ppm. ^{119}Sn NMR (111.92 MHz, C_6D_6): δ -46.43 ppm. Elemental analysis (%) calcd for $C_{39}H_{57}F_6N_3O_6S_2Sn$ (960.72): C, 48.76; H, 5.98; N, 4.37. found: C, 47.01; H, 4.93; N, 4.42.

4.5.7 Reduction of the [DIMPYGeX][GeX_3] precursors

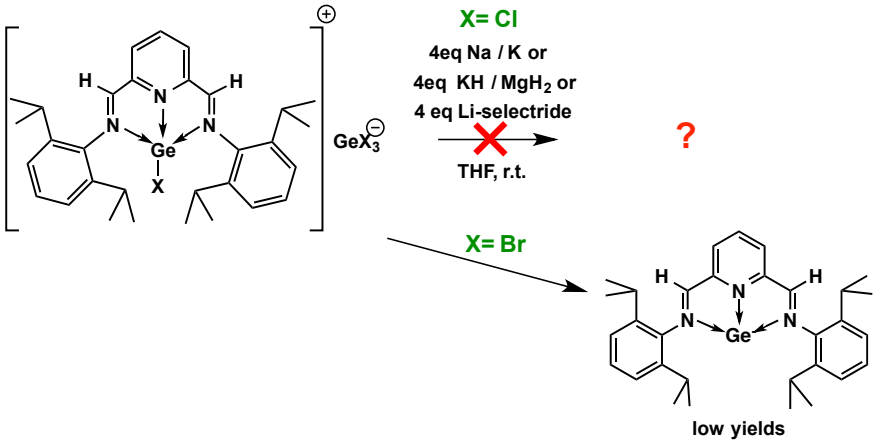

The [DIMPYGeX][GeX_3] complexes were reduced with Na, K, KH, MgH_2 and Li-selectride in THF at room temperature as well as at low temperatures of -30°C. The reduction reactions give only in case of X= Br the desired dark green (DIMPY)Ge complex, but in low yields. In case of the $[DIMPYGeCl]^+[GeCl_3]^-$ complex **29**, red solutions were obtained after warming up to room temperature and stirring over night. According to NMR studies several products are observed, which could not be characterized. No matter which reducing agent was used, no main product could be isolated. In case of the $[DIMPYGeBr]^+[GeBr_3]^-$ complex **30**, dark green solutions were obtained. Again several products were observed. However, it was possible to crystallize one product and characterize it as the desired dark green (DIMPY)Ge complex. Due to low yields, the synthetic route to give the (DIMPY)Ge complex was not satisfying.

4.5.8 Reduction of the [DIMPYSnX][SnX_3] precursors

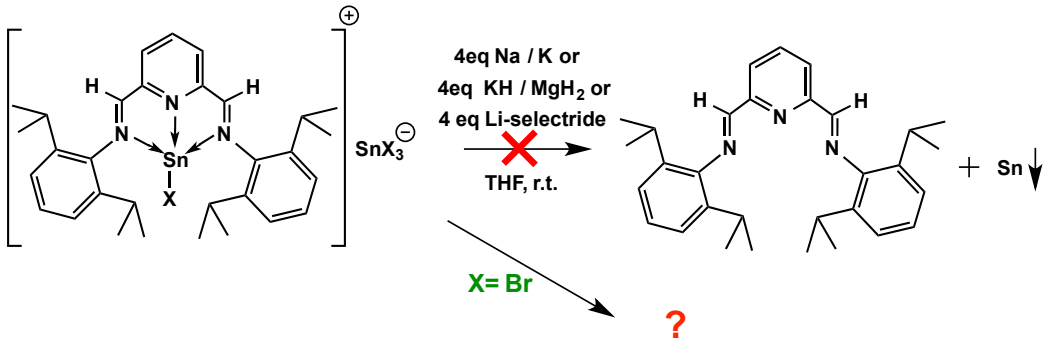

The reaction of the [DIMPYSnX][SnX_3] complexes with reducing agents like Na, K, KH, MgH_2 and Li-selectride gives not the desired DIMPYSn complex. Instead DIMPY ligand and Sn metal is formed. In case of the reduction with $[DIMPYSnBr]^+[SnBr_3]^-$ complex **32**, a dark green solution was obtained. The ^1H NMR did only show the DIMPY ligand in reaction solution, but no Sn metal was precipitated. Presumably, a radical species is formed. Unfortunately this species could not be isolated.

4.6 Synthesis of low valent Main Group Complexes Using the DAMPY Ligand

4.6.1 DAMPYNHGeN(SiMe$_3$)$_2$ (36)

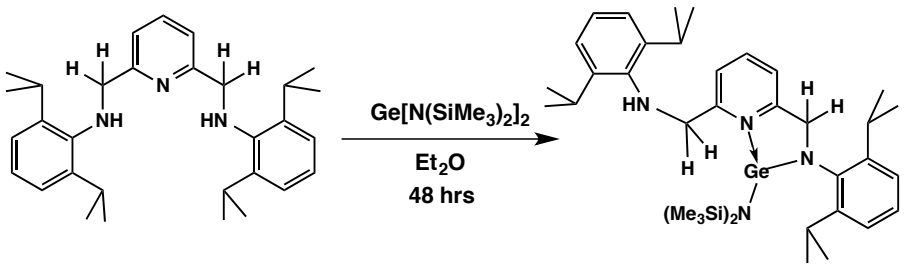

The DAMPY ligand (0.3 g, 0.65 mmol, 1 eq) was dissolved in diethyl ether and Ge[N(SiMe$_3$)$_2$]$_2$ (0.25 g, 0.65 mmol, 1 eq) was added slowly at room temperature. After 48 hours, a slightly greenish solution was obtained and the solution was concentrated. Light green cubic crystals were obtained by keeping the concentrated solution at -30°C. Yield: 16%. ^{1}H NMR (300.23 MHz, C_6D_6): δ 7.01 (s, 3H, arom.), 6.79 (m, 4H, arom.), 6.71(t, 1H, PyH), 6.61 (d, 1H, PyH), 4.78 (s, 2H, CH_2), 4.76 (s, 2H, CH_2), 3.65 (sept, 2H, CH^iPr), 3.26 (sept, 2H, CH^iPr), 1.34 (d, 12H, CH_3-^{i}Pr), 1.23 (d, 12H, CH_3-^{i}Pr) ppm. ^{13}C ^{1}H NMR (75.50 MHz, C_6D_6): δ 160.96 (ArH), 156.15 (ArH) 143.10 (ArH), 141.66 (ArH), 141.31 (ArH), 139.19 (ArH), 126.34 (ArH), 124.83 (ArH), 123.65 (ArH), 122.29 (ArH), 118.81 (ArH), 28.26 (CH^iPr), 27.67 ($CH_3{}^iPr$), 24.08 ($CH_3{}^iPr$) ppm.

4.6.2 DAMPYNHGeCl (37)

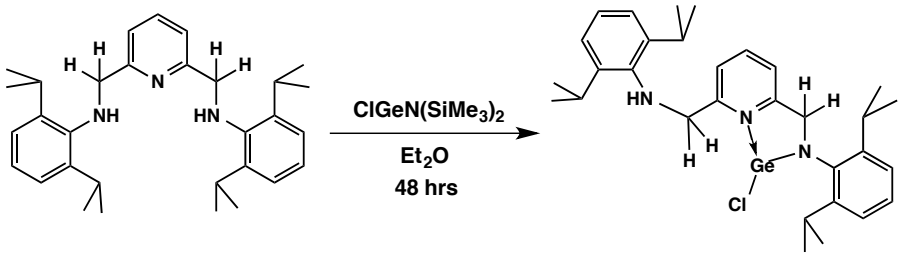

The DAMPY ligand was dissolved in diethyl ether and $ClGeN(SiMe_3)_2$ was added slowly at room temperature. After 48 hours, a slightly greenish solution was obtained and the solution was concentrated. Light green cubic crystals were obtained by keeping the concentrated solution at -30°C. Yield: 23%. Mp: 136.6 - 138.1 °C. ^{1}H NMR (300.23 MHz, C_6D_6): δ 7.08 (s, 2H, arom.), 7.02 (s, 4H, arom.), 6.69(m, 2H, PyH), 6.29 (d, 1H, PyH), 4.43 (broad s, 2H, CH_2), 4.19 (s, 2H, CH_2), 3.21 (sept, 2H, CH^iPr), 3.19 (sept, 2H, CH^iPr), 1.28 (d, 12H, CH_3-^{i}Pr), 1.10 (d, 12H, CH_3-^{i}Pr) ppm. ^{13}C ^{1}H NMR (75.50 MHz, C_6D_6): δ 160.96 (ArH), 156.15 (ArH) 143.10 (ArH), 141.66 (ArH), 141.31 (ArH), 139.19 (ArH), 126.34 (ArH), 124.83 (ArH), 123.65 (ArH), 122.29 (ArH), 118.81 (ArH), 28.26 (CH^iPr), 27.67 ($CH_3{}^iPr$), 24.08 ($CH_3{}^iPr$) ppm. Elemental analysis (%) calcd for $C_{33}H_{48}N_3ClGe$ (594.27): C, 66.63; H, 8.13; N, 7.06; found: C, 67.34; H, 8.08; N 7.17.

4.6.3 DIMPYGe (38)

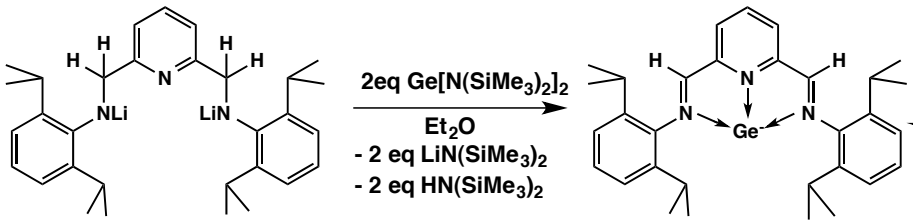

The DAMPY ligand (0.6 g, 1.31 mmol) was dissolved in 10 mL pentane and cooled to -78 °C. ^{n}BuLi (1.1 mL, 2.5 M, 2.62 mmol, 2 eq) was added dropwise to the solution and after 10 minutes reaction time a yellow precipitate was

formed. The solution was allowed to warm up to -20 °C for 10 minutes. The solution turned brownish and more yellow precipitate was formed. Then the solution got cooled down again to -78 °C and the solvent was removed via a cannula. Then $Ge[N(SiMe_3)_2]_2$ (1.0 g, 2.62 mmol, 2 eq) dissolved in 5 mL diethyl ether was added to the lithiated DAMPY ligand and after 30 minutes stirring at -78 °C warmed up to room temperature. The reaction mixture was stirred over night at room temperature. Me_3SiCl (0.53 mL, 3.7 mmol, 2.8 eq) was added to the reaction mixture to react with $LiN(SiMe_3)_2$. After 1 hour additional stirring, the solvent was removed and 10 mL pentane was added to separate the salt from the reaction solution via a filter cannula. The reaction mixture was stored at -30 °C to obtain dark green crystals. The crystals were isolated via filtration and washed three times with 1 mL pentane. Suitable crystalline material for examination by single-crystal X-ray diffraction was obtained by recrystallization in diethyl ether at -30 °C. Yield: 58%. Mp: 126.3 - 128.1 °C. ^{1}H NMR (300.23 MHz, C_6D_6): δ 7.78 (s, 2H, HC=N), 7.20 (m, 6H, arom.), 6.68 (d, 2H, m-CH-Py), 6.21 (t, 1H, p-CH-Py), 2.97 (sept, 4H, CH^iPr), 1.15 (dd, 24H, CH_3-^{i}Pr) ppm. ^{13}C ^{1}H NMR (75.50 MHz, C_6D_6): δ 160.58 (C=N, imine), 160.27 (C=N, imine) 152.92 (Ar-CH), 148.23 (Ar-CH), 144.56 (Ar-CH), 141.17 (Ar-CH), 138.66 (ArH), 137.34 (ArH), 136.94 (ArH), 126.28 (ArH), 125.80 (ArH), 125.30 (ArH), 123.76 (ArH), 123.76 (ArH), 122.99 (Ar-CH), 116.30 (Ar-CH), 28.02 (CH^iPr), 24.47 ($CH_3{}^iPr$), 24.14 ($CH_3{}^iPr$) ppm. UV (Et_2O): 629 + 601 (broad signals), 575, 425 nm. Elemental analysis (%) calcd for $C_{33}H_{47}N_3Ge$ (556.37): C, 71.24; H, 8.15; N, 7.55; found: C, 70.84; H, 8.06; N 7.63.

4.6.4 DAMPY[SnN(SiMe$_3$)$_2$]$_2$ (39)

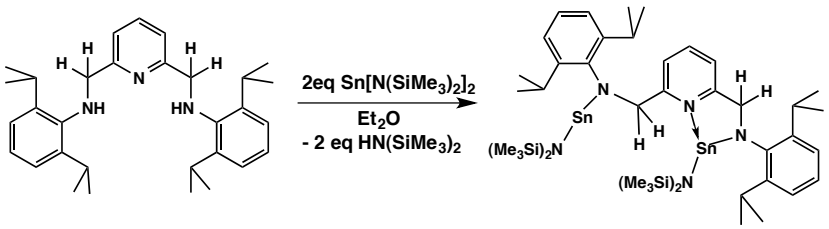

An excess of $Sn[N(SiMe_3)_2]_2$ (2.88 g, 0.66 mmol, 3eq) and the ligand DAMPY (0.1 g, 0.21 mmol, 1 eq) in 5 mL diethyl ether was stirred for 12 hours at room

temperature. All volatile components were removed under reduced pressure. The obtained yellow powder was washed three times with cold pentane. Crystalline material suitable for examination by single-crystal X-ray diffraction was obtained by recrystallization of the yellow powder in diethyl ether at -30 °C. Yield: 87%. Mp: 144-147°C. ^{1}H NMR (300.23 MHz, C6D6): δ 7.62 (d, 1H, Ar-CH), 7.25 (m, 4H, Ar-CH), 6.99 (t, 1H, Ar-CH), 6.51 (t, 1H, Ar-CH), , 6.51 (t, 1H, Ar-CH), 6.41 (d, 1H, Ar-CH), 5.70 (s, 1H, N-CH_2), 5.38 (s, 1H, N-CH_2), 5.01 (s, 1H, N-CH_2), 4.78 (s, 1H, N-CH_2), 4.07 (sept, 1H, CH^iPr)), 3.84 (sept, 1H, CH^iPr)), 3.42 (sept, 1H, CH^iPr)), 3.17 (sept, 1H, CH^iPr)), 1.37 (d, 6H, CH3^{i}Pr)), 1.21 (d, 12H, $CH_3{}^iPr$)), 1.08 (d, 6H, $CH_3{}^iPr$)), 0.31 (d, 36H, $[(CH_3)_3Si]_2N$) ppm. ^{13}C ^{1}H NMR (75.50 MHz, C_6D_6): δ 159.0 (Ar-CH), 157.48 (Ar-CH), 148.55 (Ar-CH), 147.67 (Ar-CH), 147.21 (Ar-CH), 138.33 (Ar-CH), 138.05 (Ar-CH), 125.97 (Ar-CH), 125.61 (Ar-CH), 125.18 (Ar-CH), 124.55 (Ar-CH), 123.73 (Ar-CH), 123.46 (Ar-CH), 123.17 (Ar-CH), 122.26 (Ar-CH), 119.82 (Ar-CH), 65.50 (N-CH_2), 62.60 (N-CH_2), 61.68 (N-CH_2), 29.81 (iPr), 28.07 (iPr), 27.80 (iPr), 27.68 (iPr), 26.96 (iPr), 26.61 (iPr), 25.10 (iPr), 24.48 (^{i}Pr), 24.07 (^{i}Pr), 23.65 (^{i}Pr), 23.13 (^{i}Pr), 22.48 (^{i}Pr), 5.379 ($[(CH_3)_3Si]_2N$) ppm. ^{29}Si NMR (59.64MHz, C_6D_6): δ -2.26 ppm. ^{119}Sn NMR (111.92 MHz, C_6D_6): δ 498.4 ($SnN(SiMe_3)_2$, not coordinated by N(py)), -195.7 (N(py)—$SnN(SiMe_3)_2$) ppm. IR (KBr) ?/cm-1: 3469 (w), 3376 (w), 3068 (w), 2964 (s), 2871 (m), 1593 (m), 1579 (m), 1452 (s), 1385 (m), 1359 (w), 1314 (w), 1259 (s), 1185 (m), 1099 (s), 1055 (s), 1017 (s), 932 (w), 869 (m), 831 (s), 802 (s), 753 (m), 679 (w), 568 (m), 531 (m). Elemental analysis (%) calcd for $C_{43}H_{77}N_5Si_4Sn_2$ (1013.87): C, 50.94; H, 7.65; N, 6.91. found: C, 50.14; H, 7.23; N, 6.88.

4.6.5 DIMPYSn (40)

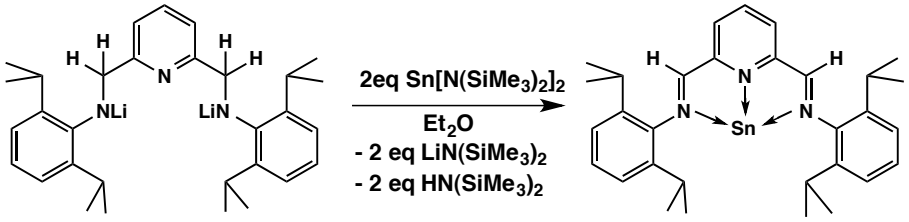

The DAMPY ligand (0.6 g, 1.31 mmol, 1 eq) was lithiated as described in 4.6.3. $Sn[N(SiMe_3)_2]_2$ (0.96 g, 2.62 mmol, 2 eq) dissolved in 5 mL diethyl ether was added to the lithiated DAMPY ligand and after 30 minutes stirring at -78 °C warmed up to room temperature. The reaction mixture was stirred over night at room temperature. Me_3SiCl (0.53 mL, 3.7 mmol, 2.8 eq) was added to the reaction mixture to react with $LiN(SiMe_3)_2$. After 1 hour additional stirring, the solvent was removed and 10 mL pentane was added to separate the salt from the reaction solution. The reaction mixture was stored at -30 °C to obtain purple cubic crystals. The crystals were isolated via filtration and washed three times with 1 mL pentane. Suitable crystalline material for examination by single-crystal X-ray diffraction was obtained by recrystallization in diethyl ether at -30 °C. Yield: 67%. Mp: 77-78 °C. ^{1}H NMR (300.23 MHz, C_6D_6): δ 8.49 (s, 2H, HC=N), 7.12 (m, 6H, arom.), 7.03 (d, 2H, m-CH-Py), 6.23 (t, 1H, p-CH-Py), 2.89 (sept, 4H, CH^{i}Pr), 1.15 (d, 12H, CH_3-^{i}Pr), 1.07 (d, 12H, CH_3-^{i}Pr) ppm. ^{13}C ^{1}H NMR (75.50 MHz, C_6D_6): δ 162.87 (C=N, imine), 145.42 (Ar-CH), 141.19 (Ar-CH), 137.11 (Ar-CH), 136.99 (Ar-CH), 123.13 (Ar-CH), 122.87 (Ar-CH), 28.08 (CH^{i}Pr), 25.14 (CH_3^{i}Pr), 24.54 (CH_3^{i}Pr) ppm. ^{119}Sn NMR (111.92 MHz, C_6D_6): δ 64 ppm (236 Hz). UV (Et_2O) nm: 325, 510, 830 (broad signal). IR (KBr) ?/cm^{-1}: 2963 (s), 2922 (w), 1645 (s), 1619 (w), 1448 (s), 1381 (m), 1315(w), 1262 (s), 1240 (m), 1095 (s), 1025 (s), 932 (w), 865 (w), 798 (s), 739 (w), 620 (m), 490 (w). Elemental analysis (%) calcd for $C_{33}H_{47}N_3Sn$ (604,46): C, 65.57; H, 7.84; N, 6.95; found: C, 64.44; H, 6.89; N 7.67.

4.6.6 Activation of Small Molecules by DIMPYSn^0

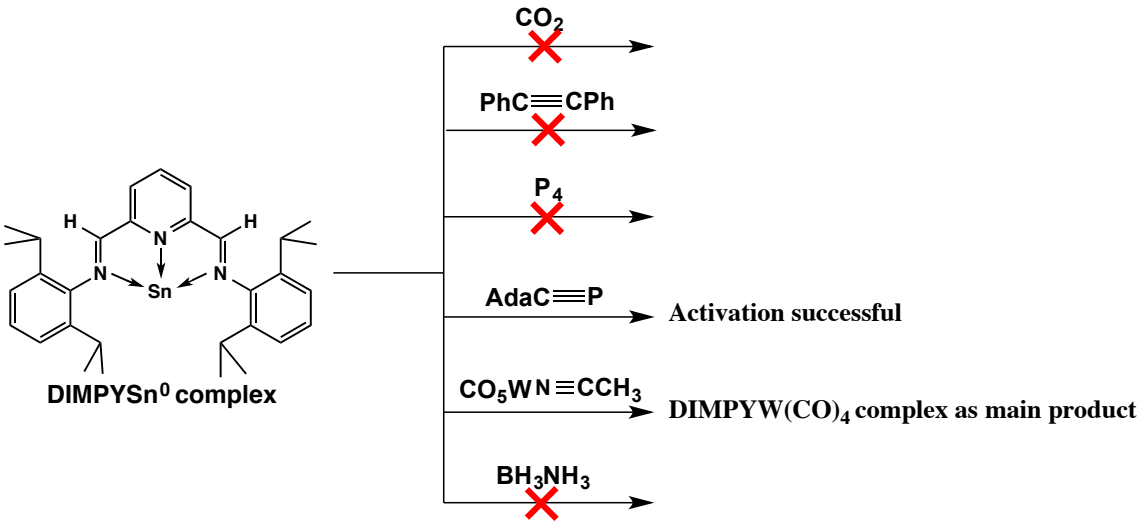

As shown in Figure 3.74, the DIMPYSn^0 complex **40** was reacted with ammonia-borane BH_3NH_3 (H_2 source), CO_2, PhC≡CPh, P_4 and AdaC≡P in etheric solvents at room temperature. The reaction solutions were stirred at room temperature for several days, as well were treated with heating and ultrasonication. However, no activation of small molecules was observed in case of the reaction with BH_3NH_3 (H_2 source), CO_2, PhC≡CPh and P_4. The reaction with adamantyl phosphalkyne was successful. Details are given in chapter 3.4.

4.6.7 DIMPYSn + Phosphalkyne (42)

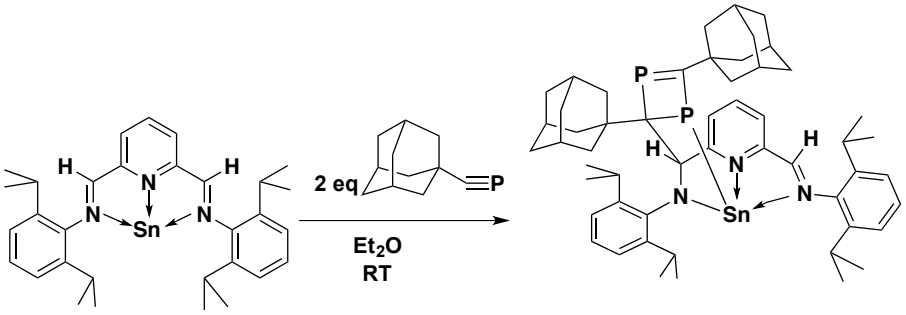

The DIMPYSn (100 mg, 0.15 mmol,1 eq) ligand was reacted with two equivalents of adamantly phosphaalkyne (54 mg, 0.30 mmol,2 eq) in 4 mL diethyl ether at room temperature. The purple solution turned dark red after 12 hours reaction time. All volatile components were reduced in vacuo. The dark red powder was recrystallized in diethyl ether at -30°C to give dark red cubic crystals. Yield: 43%. Mp: 86.3-87.5 °C. ^{1}H NMR (300.23 MHz, C_6D_6): δ 8.84 (s, 1H, HC=N), 8.25 (d, 1H, PyH), 8.02 (s, 1H, HC-N), 7.09 (m, 30 H, adamantyl), 7.04 (m, 6H, arom.), 6.23 (t, 1H, m-PyH), 5.57 (d, 1H, PyH), 3.03 (sept, 2H, CH^{i}Pr), 2.88 (sept, 2H, CH^{i}Pr), 1.09 (d, 12H, CH_3-^{i}Pr), 1.06 (d, 12H, CH_3-^{i}Pr) ppm. ^{13}C ^{1}H NMR (75.50 MHz, C_6D_6): The signals could not be assigned due to byproducts as DIMPY ligand and decomposition products. ^{119}Sn NMR (111.92 MHz, C_6D_6): δ -36.9 ppm(^{1}J-^{31}P 681.1 Hz).

4.7 Synthesis of low valent Main Group Complexes Using the PAPY Ligand

4.7.1 PAPY$GeCl_2$ (44)

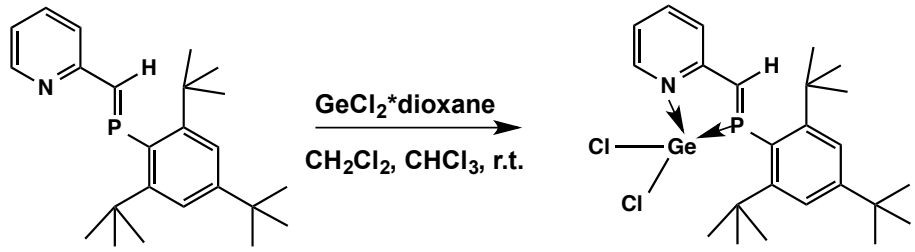

The PAPY ligand (0.1 g, 0.30 mmol, 1 eq) was reacted with $GeCl_2$*dioxane (0.061 g, 0.30 mmol, 1 eq) in 4 mL CH_2Cl_2 or $CHCl_3$ at room temperature. After 12 hours reaction time, a yellow cloudy solution was obtained and the solvent was removed in vacuo. A yellow powder was obtained in high yields which is very sensitive towards moisture. Yield: 73%. ^{1}H NMR (300.23 MHz, $CDCl_3$): δ 8.97 (d, 1H, PyH), 8.21 (d, 1H, HC=P), 7.74 (t, 1H, PyH), 7.68 (t, 1H, PyH), 7.19 (s, 2H, ArH), 1.20 (s, 18H, CH_3), 1.05 (s, 9H, CH_3). ^{13}C ^{1}H NMR (75.50 MHz, $CDCl_3$): δ 163.14 (C=P), 154.0 (ArH), 151.33 (ArH), 146.71 (ArH), 141.39 (ArH), 123.97 (ArH), 123.91 (ArH), 122.78 (ArH), 122.47 (ArH), 38.15 (CH_3), 34.17 (CH_3), 34.08 (CH_3), 31.27 (CH_3) ppm. ^{31}P NMR (121.54 MHz, $CDCl_3$): δ 320.02 ppm. Elemental analysis (%) calcd for $C_{25}H_{36}NPCl_2Ge$ (525.07): C, 57.19; H, 6.19; N, 2.67; found: C, 58.63; H, 6.59; N 2.38.

4.7.2 PAPY$SnCl_2$ (45)

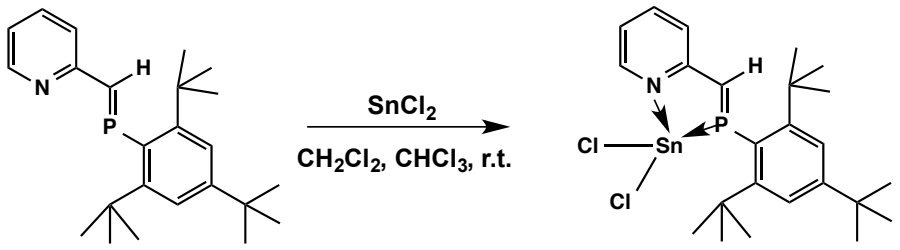

The PAPY ligand (0.1 g, 0.30 mmol, 1 eq) was reacted with $SnCl_2$ (0.050 g, 0.30 mmol, 1 eq) in 4 mL CH_2Cl_2 or $CHCl_3$ at room temperature. After 12

hours reaction time, a yellow cloudy solution was obtained and the solvent was removed in vacuo. A yellow powder was obtained in high yields which is very sensitive towards moisture. Yield: 76%. ^{1}H NMR (300.23 MHz, $CDCl_3$): δ 9.02 (d, 1H, PyH), 8.15 (d, 1H, HC=P), 7.86 (t, 1H, PyH), 7.80 (t, 1H, PyH), 7.41 (s, 2H, ArH), 1.45 (s, 18H, CH_3), 1.30 (s, 9H, CH_3). ^{13}C ^{1}H NMR (75.50 MHz, $CDCl_3$): δ 168.66 (C=P,), 156.52 (Ar-CH), 155.50 (Ar-CH), 153.91 (Ar-CH), 150.93 (Ar-CH), 140.41 (Ar-CH), 123.87 (Ar-CH), 122.20 (Ar-CH), 121.10 (Ar-CH), 38.06 (CH_3), 34.95 (CH_3), 34.04 (CH_3), 32.34 (CH_3), 31.17 (CH_3). ^{31}P NMR (121.54 MHz, $CDCl_3$): δ 312.98 ppm. Elemental analysis (%) calcd for $C_{25}H_{36}NPCl_2Sn$ (571.15): C, 52.57; H, 6.35; N, 2.45; found: C, 52.43; H, 6.24; N 2.58.

4.7.3 PAPYSnOTf$_2$ (46)

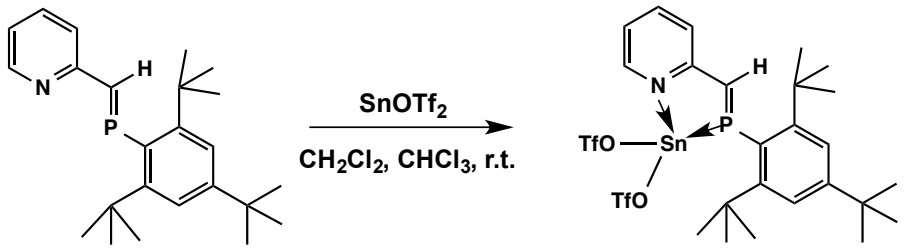

The PAPY ligand (0.05 g, 0.15 mmil, 1 eq) was reacted with $SnOTf_2$ (0.055 g, 0.15 mmol, 1 eq) in 4 mL CH_2Cl_2 or $CHCl_3$ at room temperature. After 12 hours reaction time, a bright yellow solution was obtained and the solvent was removed in vacuo. A yellow powder was obtained in high yields which is very sensitive towards moisture. Yield: 71%. ^{1}H NMR (300.23 MHz, $CDCl_3$): δ 8.56 (t, 1H, PyH), 8.48 (d, 1h, PyH), 8.26 (t, 1H, PyH), 8.03 (d,1H,HC=P), 7.65 (d,1H,PyH), 7.54 (s, 2H, CH arom), 1.419 (s, 9H, CH_3), 1.410 (s, 9H, CH_3), 1.377 (s, 9H, CH_3). ^{31}P NMR (121.54 MHz, $CDCl_3$): δ 324.73 ppm. Elemental analysis (%) calcd for $C_{26}H_{34}NPF_6O_6S_2Sn$ (784.35): C, 39.81; H,4.37; N, 1.79; found: C, 41.21; H, 4.26; N 1.89.

4.7.4 PAPY + GeN(SiMe$_3$)$_2$]$_2$ (47, 48 and 49)

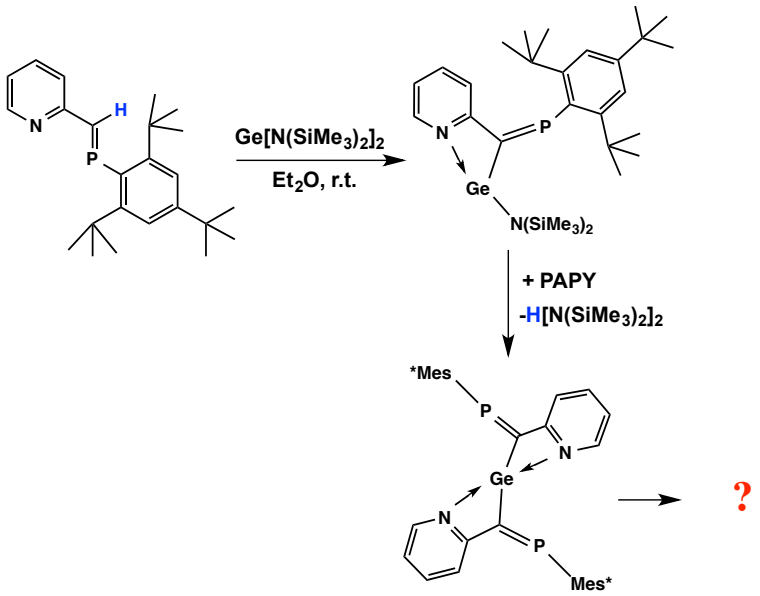

The phosphaalkene pyridine ligand (100 mg, 0.26 mmol, 1 eq) was dissolved in 5 mL diethyl ether and Ge[N(SiMe$_3$)$_2$]$_2$ (120 mg, 0.26 mmol, 1 eq) was added. 5 mg K[N(SiMe$_3$)$_2$]$_2$ was added as catalyst. After 48 hours stirring at room temperature, a dark red solution was formed. Volatile components were reduced in vacuo and a dark red powder was obtained. ^{1}H, ^{13}C and ^{31}P NMR studies were performed and a mixture of products, the complexes PAPYGeN(SiMe$_3$)$_2$ **47**, the PAPY$_2$Ge **48** and an unidentified (PAPY)Ge species **49**, was observed in reaction solution and could not be separated. Details are given in chapter 3.

4.7.5 $PAPY_2(N(SiMe_3)_2)SnSnN(SiMe_3)_2$ (50)

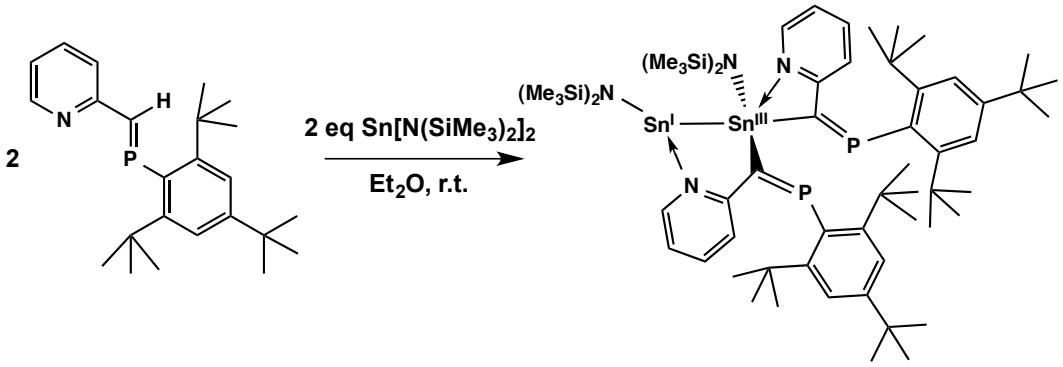

The phosphaalkene pyridine ligand (100 mg, 0.26 mmol, 1 eq) was dissolved in 5 mL diethyl ether and $Sn[N(SiMe_3)_2]_2$ (120 mg, 0.26 mmol, 1 eq) was added. $K[N(SiMe_3)_2]_2$ was added as catalyst. After 48 hours stirring at room temperature, a dark red solution was formed. Volatile components were reduced in vacuo and a dark red powder was obtained. Dark red cubic crystals suitable for X-ray analysis were obtained by recrystallization in diethyl ether at -30°C. Yield: 38%. ^{1}H NMR (300.23 MHz,C_6D_6): δ 8.35 (d, 1H, PyH), 7.49 (s, 4H, arom.), 7.45 (d, 1H, PyH), 7.42 (d, 1H, PyH), 6.86 (t, 2H, PyH), 6.39 (t, 2H, PyH), 5.01 (d, 1H, PyH), 1.55 (s, 18H, CCH_3) 1.42 (s, 36H, CCH_3), 0.312 (s, 18H, $(CH_3)_3SiN$), 0.309 (s, 18H, $(CH_3)_3SiN$) ppm. ^{13}C NMR (75.50 MHz, C_6D_6): δ 152.86 (Ar-CH), 152.60 (Ar-CH), 150.02 (Ar-CH), 149.98 (Ar-CH), 149.84 (Ar-CH), 149.50 (Ar-CH), 146.57 (Ar-CH), 144.51 (Ar-CH), 137.70 (Ar-CH), 136.01 (Ar-CH), 127.81 (Ar-CH), 127.74 (Ar-CH), 127.50 (Ar-CH), 127.13 (Ar-CH), 122.13 (Ar-CH), 121.83 (Ar-CH), 120.67 (Ar-CH) 37.95 (^{t}Bu), 37.69 (^{t}Bu), 34.72 (^{t}Bu), 34.69 (^{t}Bu), 32.69 (^{t}Bu), 32.76 (^{t}Bu), 31.41 (^{t}Bu), 31.27 (^{t}Bu), 5.41 ($(Me_3)_3$)SiN) ppm. ^{29}Si NMR (59.64 MHz, C_6D_6): δ -2.27, -2.98 ppm. ^{31}P NMR (121.54 MHz, C_6D_6): δ 281.67 (^2J-^{119}Sn 78.1 Hz, ^2J-^{117}Sn 98 Hz) , 260.78 (^2J-^{119}Sn 193.2 Hz) ppm. ^{119}Sn NMR (111.92 MHz, C_6D_6): δ 347.28, -107.10 ppm.

4.7.6 PAPYPbN(SiMe$_3$)$_2$ (51)

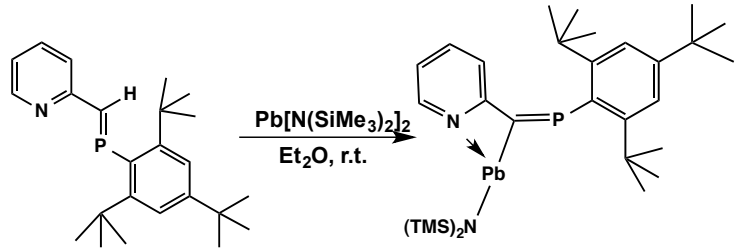

The phosphaalkene pyridine ligand (100 mg, 0.26 mmol, 1 eq) was dissolved in 5 mL diethyl ether and Pb[N(SiMe$_3$)$_2$]$_2$ (139 mg, 0.26 mmol, 1 eq) was added. After 48 hours stirring at room temperature, a dark red solution was formed. Volatile components were reduced in vacuo and a dark red powder was obtained. Dark red cubic crystals suitable for X-ray analysis were obtained by recrystallization in diethyl ether at -30°C. Yield: 33%. ^{1}H NMR (300.23 MHz,C$_6$D$_6$): δ 8.14 (d, 1H, PyH), 7.50 (s, 2H, arom.), 6.99 (t, 1H, PyH), 6.27 (t, 1H, PyH), 4.84 (d, 1H, PyH), 1.57 (s, 18H, CCH$_3$) 1.35 (s, 9H, CCH$_3$), 0.27 (s, 18H, (CH$_3$)$_3$SiN) ppm. ^{13}C NMR (75.50 MHz, C$_6$D$_6$): δ 162.47 (Ar-CH), 158.06 (Ar-CH), 152.63 (Ar-CH), 149.70 (Ar-CH), 149.63 (Ar-CH), 143.24 (Ar-CH), 140.24 (Ar-CH), 139.51 (Ar-CH), 136.48 (Ar-CH), 130.39 (Ar-CH), 122.15 (Ar-CH), 120.26 (Ar-CH), 120.18 (Ar-CH), 37.98 (^{t}Bu), 32.97 (^{t}Bu), 32.86 (^{t}Bu), 31.33 (^{t}Bu), 4.86 ((Me$_3$)$_3$)SiN) ppm. ^{29}Si NMR (59.64 MHz, C$_6$D$_6$): δ -4.82 ppm. ^{31}P NMR (121.54 MHz, C$_6$D$_6$): δ 279.32 (^2J-^{207}Pb 203 Hz).

Chapter 5

Conclusion

Low valent group 14 compounds featuring multiple bond species, e.g. the E≡E complexes (E= Si, Ge, Sn) and the heavier stable singlet carbene analogues (e.g. germylenes Ar_2Ge: (Ar= C_6H_3-2,6(C_6H_3-2,6-Pr^i_2)$_2$) activate small molecules such as H_2, NH_3, P_4 and olefins. Therefore, these low oxidation state compounds mimic transition metal centers and show potential for future catalytic applications. The ligand system is decisive for the catalytic behavior of the low valent group 14 complexes. The class of 'redox active' pyridine ligand systems gain more and more attention in modern transition metal chemistry.[1–3] However, this 'redox active' pyridine ligand systems are less applied in main group element chemistry although promising polymerization reactions were investigated for highly reactive transition metals.[1–10] In this PhD thesis the 'non innocent' imino ligand systems SIMPY, 2-[ArN=CH](NC_5H_4) (Ar= Dipp) and DIMPY, 2,6-[ArN=CH]$_2$(NC_5H_3) (Ar= Dipp) are applied to stabilize highly reactive group 1 and 14 elements. The synthesis and isolation of monoanionic 1^{st} row alkali salts yielded the monoanionic Li(SIMPY•)(SIMPY) complex as well as the dimeric Na(SIMPY•)(SIMPY) and K(SIMPY•)(SIMPY) complexes. Furthermore, monoanionic (DIMPY•)M salts were synthesized for the alkali metals M= Li, Na, K, Rb and Cs. In case of K, Rb and Cs dimeric (DIMPYM)$_2$ complexes were isolated. The SIMPY•$^-$ and DIMPY•$^-$ radical anions were investigated *via* EPR studies regarding the position of the electron stabilized within the SIMPY and DIMPY alkali metal complexes. It was proven that the alkali metals within the complexes influence the radical anion and an ion pairing phenomenon was observed in case of the SIMPY•$^-$ species.

The main work was focused on the synthesis of low valent group 14 complexes. Therefore, the diimino and monoimino pyridine ligand systems 2,6-$[ArN=CH]_2(NC_5H_3)$ (Ar= Dipp) (DIMPY) and 2-$[ArN=CH](NC_5H_4)$ (Ar= Dipp) (SIMPY) were used stabilizing heavier group 14 elements as well as their saturated amine analogs. A series of highly intersting low valent group 14 compounds in the low oxidation state of +2 were synthesized, isolated and fully characterized as the heteroleptic $SAMPYE^{II}N(SiMe_3)_2$ complexes (E= Ge, Sn, Pb), the $(SIMPY)EX_2$ salts or the ion pairs $[DIMPYEX]^+[EX_3]^-$ (E= Ge, Sn; X= Cl, Br, I). Reduction reactions of the $(SIMPY)EX_2$ salts and the ion pairs $[DIMPYEX]^+[EX_3]^-$ were performed resulting in surprising C-C coupling products (in case of Si and Ge), but were not successful in isolating desired SIMPYE and DIMPYE complexes (in case of E= Sn and Pb). Another synthetic route was implemented yielding the desired SIMPYGe and DIMPYE (E= Ge, Sn, Pb) complexes using the DAMPY ligand system 2,6-$[ArN\text{-}CH_2]_2(NC_5H_3)$ (Ar= Dipp). Unusual intramolecular eliminations of H atoms at the backbone of the ligand system lead to the highly interesting SIMPYGe and DIMPYE complexes bearing the group 14 element in the oxidation state of zero. In literature, E^0 species are rare and were very recently reported.[94,101,109,110,115–120] Furthermore the known E^0 complexes are exclusively coordinated by two N-heterocyclic carbene ligands or related donor molecules. Hence, the SIMPYGe and DIMPYE complexes represent the first examples of a neutral, mononuclear, group 14 complex with Ge, Sn and Pb in a formal oxidation state of zero stabilized by only one donor molecule. The complexes SIMPYGe, DIMPYGe and DIMPYSn were intensively studied *via* experimental and theoretical methods.

Furthermore, E^0 complexes are rare in literature and therefore their reactivity is unknown in contrast to E^{II} compounds.[26,27] Due to the fact that E^0 species possess two lone pairs of electrons, they formally act only as σ donors in contrast to E^{II} species which can act as σ donor and as π acceptor. Therefore the reactivity compared to oxidation state +2 compounds differs. These species can be compared to transition metals coordinated either in 16 electron or 18 electron complexes. In transition metal chemistry $16e^-$ and $18e^-$ compounds differ regarding their catalytic behavior. This was proven by the reaction of the $DIMPYSn^0$ complex with adamantyl phosphalkyne. An interesting compound was formed by the insertion of the $DIMPYSn^0$ into the P≡C triple bond form-

ing a five membered ring, which was so reactive that a second insertion into a P≡C triple bond took place. The DIMPYSn(AdaCP)$_2$ **42** bears a Sn atom in the oxidation state of +2 which differs from the literature known compounds bearing the group 14 element in the oxidation state +4 after reacting with a phosphalkyne.

The stabilization of low valent group 14 elements by related P-based ligands are barely known for group 14 elements. The monophosphaalkene ligand system 2-[ArP=CH](NC$_5$H$_4$) (Ar= Mes*) (PAPY) was therefore reacted with group 14 elements. Compared to the imino congener, the phosphaalkene pyridine ligand system shows a different reaction behavior. Thereby, a very rare example of a stannylstannylene RSn^{I}Sn^{III}PAPY$_2$R (R=N(SiMe$_3$)$_2$) species was isolated and fully characterized. In this respect, a new phenomenon was studied for the PAPY ligand system as well as for the SIMPY ligand regarding their reaction behavior to eliminate the H atom at the ligand backbone.

Investigating low valent group 14 complexes stabilized by redox active pyridine ligand systems involving imino, amino or phosphaalkene functionalities gave new and highly interesting insights in the promising field of low oxidation state main group chemistry.

List of Figures

List of Tables

Bibliography

[1] Luca, O. R.; Crabtree, R. H. *Chem. Soc. Rev.*, **2013**, *42*, 1440–1459.

[2] Praneeth, V. K. K.; Ringenberg, M. R.; Ward, T. R. *Angew. Chem. Int. Ed.*, **2013**, *51*, 10228–10234.

[3] Lyaskovskyy, V.; de Bruin, B. *ACS Catalysis*, **2012**, *2*(2), 270–279.

[4] Gibson, V. C.; Redshaw, C.; Solan, G. A. *Chem. Rev.*, **2007**, *107*, 1745–1776.

[5] Britovsek, G. J. P.; Bruce, M.; Gibson, V. C.; Kimberley, B. S.; Maddox, P. J.; Mastroianni, S.; McTavish, S. J.; Redshaw, C.; Solan, G. A.; Stromberg, S.; White, A. J. P.; Williams, D. J. *J. Am. Chem. Soc.*, **1999**, *121*, 8728–8740.

[6] Takeuchi, D.; Osakada, K. *Polymer*, **2008**, *49*, 4911–4924.

[7] Bianchini, C.; Mantovani, G.; Meli, A.; Migliacci, F.; Zanobini, F.; Laschi, F.; Sommazzi, A. *Eur. J. Inorg. Chem.*, **2003**, pp 1620–1631.

[8] Russell, S. K.; Darmon, J. M.; Lobkovsky, E.; Chirik, P. J. *Inorg. Chem.*, **2010**, *49*, 2782–2792.

[9] Britovsek, G. J. P.; Bruce, M.; Gibson, V. C.; Kimberleya, B. S.; Maddox, P. J.; Mastroianni, S.; McTavish, S. J.; Redshaw, C.; Solan, G. A.; Stromberg, S.; White, A. J. P.; Williams, D. J. *J. Am. Chem. Soc.*, **1999**, *121*, 8728–8740.

[10] Wallenhorst, C.; Kehr, G.; Luftmann, H.; Fröhlich, R.; Erker, G. *Organometallics*, **2008**, *27*, 6547–6556.

[11] Lu, Z.; Reeske, G.; Moore, J. A.; Cowley, A. H. *Chem. Commun.*, **2006**, pp 5060–5061.

[12] Blackmore, I. J.; Gibson, V. C.; Hitchcock, P. B.; Rees, C. W.; Williams, D. J.; White, A. J. P. *J. Am. Chem. Soc.*, **2005**, *127*, 6012–6020.

[13] Zimmermann, M.; Trnroos, K. W.; Anwander, R. *Angew. Chem. Int. Ed.*, **2007**, *46*, 3126 –3130.

[14] Knijnenburg, Q.; Smits, J. M. M.; Budzelaar, P. H. M. *Organometallics*, **2006**, *25*, 1036–1046.

[15] Scott, J.; Gambarotta, S.; Korobkov, I.; Knijnenburg, Q.; de Bruin, B.; Budzelaar, P. H. M. *J. Am. Chem. Soc.*, **2005**, *127*, 17204–17206.

[16] Budzelaar, P. H. M. *Eur. J. Inorg. Chem.*, **2012**, pp 530–534.

[17] Baker, R. J.; Jones, C.; Kloth, M.; Mills, D. P. *New. J. Chem.*, **2004**, *28*, 207–213.

[18] Myers, T. W.; Kazem, N.; Stoll, S.; Britt, R. D.; Shanmugam, M.; Berben, L. A. *J. Am. Chem. Soc.*, **2011**, *133*, 8662–8672.

[19] Myers, T. W.; Berben, L. A. *Inorg. Chem.*, **2012**, *51*, 1480–1488.

[20] Myers, T. W.; Berben, L. A. *J. Am. Chem. Soc.*, **2011**, *133*, 11865–11867.

[21] Cates, C. D.; Myers, T. W.; Berben, L. A. *Inorg. Chem.*, **2012**, *51*, 11891–11897.

[22] van Gastel, M.; Lu, C. C.; Wieghardt, K.; Lubitz, W. *Inorg. Chem.*, **2009**, *48*, 2626–2632.

[23] Lu, C. C.; Bill, E.; Weyhermüller, T.; Bothe, E.; Wieghardt, K. *J. AM. CHEM. SOC*, **2008**, *130*, 3181–3197.

[24] Trifonov, A. A. *Eur. J. Inorg. Chem.*, **2007**, pp 3151–3167.

[25] Nayek, H. P.; Arleth, N.; Trapp, I.; Löble, M.; Ona-Burgos, P.; Kuzdrowska, M.; Lan, Y.; Powell, A. K.; Breher, F.; Roesky, P. W. *Chem. Eur. J.*, **2011**, *17*, 10814 – 10819.

[26] Lee, V. Y.; Sekiguchi, A. *Organometallic compounds of low-coordinate Si, Ge, Sn and Pb*. John Wiley & Sons Ltd, 2010.

[27] Asay, M.; Jones, C.; Driess, M. *Chem. Rev.*, **2011**, *111*(354-396).

[28] Power, P. P. *Nature*, **2010**, *463*, 171–177.

[29] Martin, D.; Soleilhavoup, M.; Bertrand, G. *Chem. Sci.*, **2011**, *2*, 389–399.

[30] Darmon, J. M.; Turner, Z. R.; Lobkovsky, E.; Chirik, P. J. *Organometallics*, **2012**, *31*(6), 2275–2285.

[31] Enright, D.; Gambarotta, S.; Yap, G. P. A.; Budzelaar, P. H. M. *Angew. Chem. Int. Ed.*, **2002**, *41*, 3873–3876.

[32] Bart, S. C.; Lobkovsky, E.; Chirik, P. J. *Journal of the American Chemical Society*, **2004**, *126*(42), 13794–13807. PMID: 15493939.

[33] Bouwkamp, M. W.; Bowman, A. C.; Lobkovsky, E.; Chirik, P. J. *Journal of the American Chemical Society*, **2006**, *128*(41), 13340–13341. PMID: 17031930.

[34] Bart, S. C.; Lobkovsky, E.; Chirik, P. J. *Journal of the American Chemical Society*, **2004**, *126*(42), 13794–13807. PMID: 15493939.

[35] Tay, B.-Y.; Wang, C.; Chia, S.-C.; Stubbs, L. P.; Wong, P.-K.; van Meurs, M. *Organometallics*, **2011**, *30*, 6028–6033.

[36] Martin, C. D.; Ragogna, P. J. *Dalton Trans.*, **2011**, *40*, 11976–11980.

[37] Reeske, G.; Cowley, A. H. *Chem. Commun.*, **2006**, pp 1784–1786.

[38] Martin, C. D.; Le, C. M.; Ragogna, P. J. *J. Am. Chem. Soc.*, **2009**, *131*, 15126–15127.

[39] Jurca, T.; Lummiss, J.; Burchell, T. J.; Gorelsky, S. I.; Richeson, D. S. *J. Am. Chem. Soc.*, **2009**, *131*, 4608–4609.

[40] Singh, A. P.; Roesky, H. W.; Carl, E.; Stalke, D.; Demers, J.-P.; Lange, A. *J. Am. Chem. Soc.*, **2012**.

[41] Reeske, G.; Cowley, A. H. *Chem. Commun.*, **2006**, pp 4856–4858.

[42] Myers, T. W.; Berben, L. A. *Journal of the American Chemical Society*, **2013**, *135*(27), 9988–9990.

[43] Pedrido, R.; Romero, M. J.; Bermejo, M. R.; Gonzalez-Noya, A. M.; Maneiro, M.; Rodriguez, M. J.; Zaragoza, G. *Dalton Trans.*, **2006**, pp 5304–5314.

[44] Vlcek, A. J. *Coordination Chemistry Reviews*, **2002**, *230*, 225–242.

[45] v Knoten, G.; Vrieze, K. *Adv. Organomet. Chem.*, **1982**, *21*, 151/239.

[46] Schoeller, W. W.; Grigoleit, S. *J. Chem. Soc. Dalton Trans.*, **2002**, pp 405–409.

[47] Vrieze, K. *Journal of Organometallic Chemistry*, **1986**, *304*, 307–326.

[48] Zoet, R.; Vankoten, G.; Vrieze, K.; Duisenberg, A. J. M.; Spek, A. L. *Inorganica Chimica Acta*, **1988**, *148*, 71–84.

[49] Polm, L. H.; Vankoten, G.; Elsevier, C. J.; Vrieze, K.; Vansanten, B. F. K.; Stam, C. H. *Journal of Organometallic Chemistry*, **1986**, *304*, 353–370.

[50] Gao, Y.; Zhang, Y.; Qiu, C.; Zhao, J. *Applied Organometallic Chemistry*, **2011**, *25*, 54–60.

[51] Westerhausen, M.; Bollwein, T.; Makropoulos, N.; Schneiderbauer, S.; Suter, M.; Nöth, H.; Mayer, P.; Piotrowski, H.; Polborn, K.; Pfitzner, A. *Eur. J. Inorg. Chem.*, **2002**, pp 389–404.

[52] Summerscales, O. T.; Myers, T. W.; Berben, L. A. *Organometallics*, **2012**, *31*, 3463–3465.

[53] van Gastel, M.; Lu, C. C.; Wieghardt, K.; Lubitz, W. *Inorg. Chem.I*, **2009**, *48*, 2626–2632.

[54] Trifonov, A. A.; Shestakov, B. G.; Gudilenkov, I. D.; Fukin, G. K.; Giambastiani, G.; Bianchini, C.; Rossin, A.; Luconi, L.; Filippi, J.; Soracec, L. *Dalton Trans.*, **2011**, *40*, 10568–10575.

[55] Trifonov, A. A.; Fedorova, E. A.; Borovkov, I. A.; Fukin, G. K.; Baranov, E. V.; Larionova, J.; Druzhkov, N. O. *Journal of Organometallic Chemistry*, **2007**, *26*, 2488–2491.

[56] Trifonov, A. A.; Gudilenkov, I. D.; Larionova, J.; Luna, C.; Fukin, G. K.; Cherkasov, A. V.; Poddel'sky, A. I.; Druzhkov, N. O. *Organometallics*, **2009**, *28*, 6707–6713.

[57] Bouška, M.; Dostál, L.; Růžička, A.; Jambor, R. *Organometallics*, **2013**, *32*(6), 1995–1999.

[58] Ullah, F.; Oprea, A. I.; Kindermann, M. K.; Bajor, G.; Veszpremi, T.; Heinicke, J. *Journal of Organometallic Chemistry*, **2009**, *694*, 397–403.

[59] Benko, Z.; Burck, S.; Gudat, D.; Nieger, M.; Nyulaszi, L.; Shore, N. *Dalton Trans.*, **2008**, pp 4937–4945.

[60] Guerin, F.; McConville, D. H.; Vittal, J. J. *Organometallics*, **1996**, *15*, 5586–5590.

[61] Guérin, F.; McConville, D. H.; Vittal, J. J.; Yap, G. A. P. *Organometallics*, **1998**, *17*, 5172–5177.

[62] Guérin, F.; McConville, D. H.; Payne, N. C. *Organometallics*, **1996**, *15*, 5085–5089.

[63] Cruz, C. A.; Emslie, D. J. H.; Harrington, L. E.; Britten, J. F.; Robertson, C. M. *Organometallics*, **2007**, *26*, 692–701.

[64] Hahn, F. E.; Zabula, A. V.; Pape, T.; Hepp, A. *Eur. J. Inorg. Chem.*, **2007**, pp 2405–2408.

[65] Zabula, A. V.; Pape, T.; Hepp, A.; Schappacher, F. M.; Rodewald, U. C.; Pöttgen, R.; Hahn, F. E. *J. Am. Chem. Soc.*, **2008**, *130*, 5648–5649.

[66] Nienkemper, K.; Kehr, G.; Kehr, S.; Fröhlich, R.; Erker, G. *Journal of Organometallic Chemistry*, **2008**, *693*, 1572–1589.

[67] Lin, Y.-C.; Yu, K.-H.; Lin, Y.-F.; Lee, G.-H.; Wang, Y.; Liu, S.-T.; Chen, J.-T. *Dalton Trans.*, **2012**, *41*, 6661–6670.

[68] Zhang, S.; Katao, S.; Sun, W.-H.; Nomura, K. *Organometallics*, **2009**, *28*, 5925–5933.

[69] Floch, P. L. *Coordination Chemistry Reviews*, **2006**, *250*(5–6), 627 – 681. ¡ce:title¿17th Main Group Chemistry¡/ce:title¿.

[70] Weber, L. *Angew,. Chem.*, **1996**, *108*, 292–310.

[71] Yoshifuji, M. *Pure Appl. Chem.*, **2005**, *77*(12), 2011–2020.

[72] Ozawaa, F.; Yoshifuji, M. *Dalton Trans.*, **2006**, pp 4987–4995.

[73] van der Vlugt, J. I.; Reek, J. N. H. *Angew. Chem. Int. Ed.*, **2009**, *48*, 8832 – 8846.

[74] Cochran, B. M.; Michael, F. E. *J. Am. Chem. Soc.*, **2008**, *130*, 2786–2792.

[75] Mathey, F. *Angew. Chem., Int. Ed.*, **2003**, *42*, 1578–1604.

[76] Nakajima, Y.; Nakao, Y.; Sakaki, S.; Tamada, Y.; Ono, T.; Ozawa, F. *J. Am. Chem. Soc.*, **2010**, *132*, 9934–9936.

[77] Orthaber, A.; Belaj, F.; Pietschnig, R. *Inorganica Chimica Acta*, **2011**, *374*, 211–215.

[78] Brookhart, M.; Daugulis, O. Catalysts for olefin polymerization. Technical Report WO 03/076450 A1, E.I. Du Pont de Nemours and Company, 2003.

[79] Hayashi, A.; Ishiyama, T.; Okazaki, M.; Ozawa, F. *Organometallics*, **2007**, *26*, 3708–3712.

[80] Izod, K. *Coordination Chemistry Reviews*, **2002**, *227*, 153–173.

[81] Cheng, F.; Hector, A. L.; Levason, W.; Reid, G.; Webster, M.; Zhang, W. *Inorg. Chem.*, **2010**, *49*, 752–760.

[82] Bohra, R.; Hitchcock, P.; Lappert, M. F.; Leung, W.-P. *J. Chem. Soc., Chem. Commun.*, **1989**, pp 728–730.

[83] Issleib, K.; Leissring, E.; Riemer, M. *Z. anorg. allg. Chem.*, **1984**, *519*, 75–86.

[84] Sierra, M. L.; Maigrot, N.; Charrier, C.; Ricard, L.; Mathey, F. *Organometallics*, **1992**, *11*, 462–464.

[85] Schoeller, W. W.; Eisner, D. *Inorg. Chem.*, **2004**, *43*, 2585–2589.

[86] Zabula, A. V.; Hahn, F. E. *Eur. J. Inorg. Chem.*, **2008**, pp 5165–5179.

[87] Cotton, J. D.; Cundy, C. S.; Harris, D. H.; Hudson, A.; Lappert, M. F.; Lednor, P. W. *J. Chem. Soc., Chem. Commun.*, **1974**, pp 651–652.

[88] Harris, D. H.; Lappert, M. F. *J. Chem. Soc., Chem. Commun.*, **1974**, pp 895–896.

[89] Harris, D. H.; Lappert, M. F.; Pedley, J. B.; Sharp, G. J. *J. Chem. Soc., Dalton Trans*, **1976**, pp 945– 950.

[90] Nagendran, S.; Roesky, H. W. *Organometallics*, **2008**, *27*, 457–492.

[91] III, A. J. A.; Harlow, R. L.; Kline, M. K. *J. Am. Chem. Soc.*, **1991**, *113*, 361–363.

[92] Herrmann, W. A. *Angew. Chem. Int. Ed.*, **2002**, *41*(1290-1309).

[93] Hahn, F. E.; Jahnke, M. C. *Angew. Chem. Int. Ed.*, **2008**, *47*(3122-3172).

[94] Wang, Y.; Robinson, G. H. *Chem. Commun.*, **2009**, pp 5201–5213.

[95] Fischer, R. C.; Power, P. P. *Chem. Rev.*, **2010**, *110*, 3877–3923.

[96] Hitchcock, P. B.; Lappert, M. F.; Miles, S. J.; Thorne, A. J. *J. Chem. Soc., Chem. Commun.*, **1984**, pp 480–482.

[97] Snow, J. T.; Murakami, S.; Masamune, S.; Williams, D. J. *Tetrahedron Lett.*, **1984**, *25*, 4191–4194.

[98] Pu, L.; Twamley, B.; Power, P. P. *J. Am. Chem. Soc.*, **2000**, *122*, 3524–3525.

[99] Stender, M.; Phillips, A. D.; Wright, R. J.; Power, P. P. *Angew. Chem., Int. Ed.*, **2002**, *41*(1785-1787).

[100] Phillips, A. D.; Wright, R. J.; Olmstead, M. M.; Power, P. P. *J. Am. Chem. Soc.*, **2002**, *124*, 5930–5931.

[101] Wang, Y.; Xie, Y.; Wei, P.; King, R. B.; Schaefer, H. F.; von R. Schleyer, P.; Robinson, G. H. *Science*, **2008**, *321*, 1069–1071.

[102] Flock, J.; Suljanovic, A.; Torvisco, A.; Schoefberger, W.; Gerke, B.; Pöttgen, R.; Fischer, R. C.; Flock, M. *Chemistry – A European Journal*, **2013**, *19*(46), 15504–15517.

[103] Tonner, R.; Frenking, G. *Angew. Chem., Int. Ed.*, **2007**, *46*, 8695–9698.

[104] Klein, S.; Tonner, R.; Frenking, G. *Chem. Eur. J.*, **2010**, *16*, 10160–10170.

[105] Takagi, N.; Shimizu, T.; Frenking, G. *Chem. Eur. J.*, **2009**, *15*, 8593–8604.

[106] Tonner, R.; Frenking, G. *Chem. Eur. J.*, **2008**, *14*, 3260–3272.

[107] Tonner, R.; Frenking, G. *Chem. Eur. J.*, **2008**, *14*, 3273–3289.

[108] Tonner, R.; Frenking, G. *Pure Appl. Chem.*, **2009**, *81*, 597–614.

[109] Sidiropoulos, A.; Jones, C.; Stasch, A.; Klein, S.; Frenking, G. *Angew. Chem., Int. Ed.*, **2009**, *48*, 9701–9704.

[110] Jones, C.; Sidiropoulos, A.; Holzmann, N.; Frenking, G.; Stasch, A. *Chem. Commun.*, **2012**, *48*, 9855–9857.

[111] Dyker, C. A.; Lavallo, V.; Donnadieu, B.; Bertrand, G. *Angew. Chem. Int. Ed.*, **2008**, *47*, 3206–3209.

[112] Hofmann, M. A.; Bergstrßer, U.; Reiß, G. J.; Nyulaszi, L.; Regitz, M. *Angew,. Chem.*, **2000**, *39*, 1261–1263.

[113] Fürstner, A.; Alcarazo, M.; Goddard, R.; Lehmann, C. W. *Angew. Chem. Int. Ed.*, **2008**, *47*, 3210–3214.

[114] Alcarazo, M.; Lehmann, C. W.; Anoop, A.; Thiel, W.; Fürstner, A. *Nat. Chem.*, **2009**, *1*, 295–301.

[115] Ishida, S.; Iwamoto, T.; Kabuto, C.; Kira, M. *Nature*, **2003**, *421*, 725–727.

[116] Iwamoto, T.; Abe, T.; Kabuto, C.; Kira, M. *Chem. Commun.*, **2005**, pp 5190–5192.

[117] Iwamoto, T.; Abe, T.; Ishida, S.; Kabuto, C.; Kira, M. *J. Organomet. Chem.*, **2007**, *692*, 263–270.

[118] Iwamoto, T.; Masuda, H.; Kabuto, C.; Kira, M. *Organometallics*, **2004**, *23*, 197–199.

[119] Kira, M.; Iwamoto, T.; Ishida, S.; Masuda, H. *J. Am. Chem. Soc.*, **2009**, *131*, 17135–17144.

[120] Wiberg, N.; Lerner, H.-W.; Vasisht, S.-K.; Wagner, S.; Karaghiosoff, K.; Nöth, H.; Ponikwar, W. *Eur. J. Inorg. Chem.*, **1999**, pp 1211–1218.

[121] Schnepf, A.; Schnöckel, H. *Angew. Chem.*, **2002**, *114*, 3682–3704.

[122] Driess, M.; Nöth, H. *Molecular Clusters of the Main Group Elements*. Wiley-VCH, Weinheim, 2004.

[123] Mondal, K. H.; Roesky, H. W.; Schwarzer, M. C.; Frenking, G.; Niepötter, B.; Wolf, H.; Herbst-Irmer, R.; Stalke, D. *Angew. Chem.*, **2013**, *125*, 3036–3040.

[124] Xiong, Y.; Yao, S.; Tan, G.; Inoue, S.; Driess, M. *J. Am. Chem. Soc.*, **2013**, *135*, 5004–5007.

[125] Gans-Eichler, T.; Gudat, D.; Nieger, M. *Angew. Chem., Int. Ed.*, **2002**, *41*(11), 1888–1891.

[126] Gans-Eichler, T.; Gudat, D.; Nättingen, K.; Nieger, M. *Chem. Eur. J.*, **2006**, *12*, 1162–1173.

[127] Kircher, P.; Huttner, G.; Heinze, K.; Schiemenz, B.; Zsolnai, L.; Büchner, M.; Driess, A. *Eur. J. Inorg. Chem.*, **1998**, *1998*, 703–720.

[128] Drost, C.; Lonnecke, P.; Sieler, J. *Chem. Commun.*, **2012**, *48*, 3778–3780.

[129] Setaka, W.; Sakamoto, K.; Kira, M.; Power, P. P. *Organometallics*, **2001**, *20*(22), 4460–4462.

[130] Setaka, W.; Hirai, K.; Tomioka, H.; Sakamoto, K.; Kira, M. *Chem. Commun.*, **2008**, pp 6558–6560.

[131] Cardin, C. J.; Cardin, D. J.; Constantine, S. P.; Todd, A. K.; Teat, S. J.; Coles, S. *Organometallics*, **1998**, *17*(11), 2144–2146.

[132] Mehring, M.; Löw, C.; Schürmann, M.; Uhlig, F.; Jurkschat, K.; Mahieu, B. *Organometallics*, **2000**, *19*(22), 4613–4623.

[133] Dixon, C. E.; Liu, H. W.; Vander Kant, C. M.; Baines, K. M. *Organometallics*, **1996**, *15*(26), 5701–5705.

[134] Dixon, C. E.; Cooke, J. A.; Baines, K. M. *Organometallics*, **1997**, *16*(25), 5437–5440.

[135] Castel, A.; Escudie, J.; Riviere, P.; Satgé, J.; Bochkarev, M.; Maiorova, L.; Razuvaev, G. *Journal of Organometallic Chemistry*, **1981**, *210*(1), 37 – 42.

[136] Arp, H.; Baumgartner, J.; Marschner, C.; Müller, T. *Journal of the American Chemical Society*, **2011**, *133*(15), 5632–5635.

[137] Eichler, B. E.; Power, P. P. *Inorganic Chemistry*, **2000**, *39*(24), 5444–5449.

[138] Eichler, B. E.; Phillips, B. L.; Power, P. P.; Augustine, M. P. *Inorganic Chemistry*, **2000**, *39*(24), 5450–5453.

[139] Phillips, A. D.; Hino, S.; Power, P. P. *Journal of the American Chemical Society*, **2003**, *125*(25), 7520–7521.

[140] Hino, S.; Olmstead, M. M.; Power, P. P. *Organometallics*, **2005**, *24*(22), 5484–5486.

[141] Jurkschat, K.; Abicht, H.-P.; Tzschach, A.; Mahieu, B. *Journal of Organometallic Chemistry*, **1986**, *309*(3), C47 – C50.

[142] Brown, Z. D.; Power, P. P. *Inorg. Chem.*, **2013**, *52*, 6248–6259.

[143] Wiberg, N.; Vasisht, S. K.; Fischer, G.; Mayer, P. *Z. Anorg. Allg. Chem.*, **2004**, *630*, 1823–1828.

[144] Kinjo, R.; Ichinohe, M.; Sekiguchi, A.; Takagi, N.; Sumitomo, M.; Nagase, S. *J. Am. Chem. Soc.*, **2007**, *129*, 7766–7767.

[145] Spikes, G. H.; Fettinger, J. C.; Power, P. P. *J. Am. Chem. Soc.*, **2005**, *127*, 12232–12233.

[146] Wang, Y.; Ma, J. *Journal of Organometallic Chemistry*, **2009**, *694*, 2567–2575.

[147] Driess, M. *Organometallics*, **2011**, *30*, 1748–1767.

[148] Peng, Y.; Guo, J.-D.; Ellis, B. D.; Zhu, Z.; Fettinger, J. C.; Nagase, S.; Power, P. P. *J. Am. Chem. Soc.*, **2009**, *131*, 16272–16282.

[149] de Bruin, B.; Bill, E.; Bothe, E.; Weyhermüller, T.; Wieghardt, K. *Inorg. Chem.*, **2000**, *39*, 2936–2947.

[150] Sujanovic, A. *Design and Synthesis of Polysilazanes*. PhD thesis, TU Graz, 2011.

[151] Ding, Y.; Roesky, H. W.; Noltemeyer, M.; Schmidt, H.-G.; Power, P. P. *Organometallics*, **2001**, *20*(6), 1190–1194.

[152] Fjeldberg, T.; Hope, H.; Lappert, M. F.; Power, P. P.; Thorne, A. J. *J. Chem. Soc., Chem. Commun.*, **1983**, pp 639–641.

[153] Zhang, S.; Katao, S.; Sun, W.-H.; Nomura, K. *Organometallics*, **2009**, *28*, 5925–5933.

[154] Rao, M. S.; Roesky, H. W.; Anantharaman, G. *Journal of Organometallic Chemistry*, **2002**, *646*(1–2), 4 – 14.

[155] Cui, C.; Roesky, H. W.; Noltemeyer, M.; Lappert, M. F.; Schmidt, H.-G.; Hao, H. *Organometallics*, **1999**, *18*(11), 2256–2261.

[156] Qian, B.; Ward, D. L.; Smith, M. R. *Organometallics*, **1998**, *17*(14), 3070–3076.

[157] Cui, C.; Roesky, H. W.; Schmidt, H.-G.; Noltemeyer, M.; Hao, H.; Cimpoesu, F. *Angewandte Chemie International Edition*, **2000**, *39*(23), 4274–4276.

[158] Bordwell, F. G. *Acc. Chem. Res.*, **1988**, *21*, 456 – 463.

[159] Chai, Z.-Y.; Wang, Z.-X. *Dalton Trans.*, **2009**, pp 8005–8012.

[160] Chia, S.-P.; Xi, H.-W.; Li, Y.; Lim, K. H.; So, C.-W. *Angew. Chem. Int. Ed.*, **2013**, *52*, 6298–6301.

[161] Wrackmeyer, B. *Annual Reports on NMR Spectroscopy*, volume 16. Academic Press Inc. (London) Ltd., 1985.

[162] Chu, T.; Belding, L.; van der Est, A.; Dudding, T.; Korobkov, I.; Nikonov, G. I. *Angew. Chem. Int. Ed.*, **2014**, *53*(XX - XX).

[163] Knijnenburg, Q.; Hetterscheid, D.; Kooistra, T. M.; Budzelaar, P. H. M. *Eur. J. Inorg. Chem.*, **2004**, pp 1204 – 1211.

[164] Zhu, D.; Thapa, I.; Korobkov, I.; Gambarotta, S.; Budzelaar, P. H. M. *Inorg. Chem.*, **2011**, *50*, 9879 – 9887.

[165] Khan, S.; Michel, R.; Dieterich, J. M.; Mata, R. A.; Roesky, H. W.; Demers, J.-P.; Lange, A.; Stalke, D. *J. Am. Chem. Soc.*, **2011**, *133*, 17889 – 17894.

[166] Bader, R. F. W. *Accounts of Chemical Research*, **1985**, *18*, 9 – 15.

[167] Schaefer, A.; Weidenbruch, M.; Saak, W.; Pohl, S. *Angew. Chem. Int. Ed.*, **1987**, *99*, 806–807.

[168] Cowley, A. H.; Hall, S. W.; Nunn, C. M.; Power, J. M. *J. Chem. Soc., Chem. Commun.*, **1988**, pp 753 – 754.

[169] Cowley, A. H.; Hall, S. W.; Nunn, C. M.; Power, J. M. *Angew. Chem.*, **1988**, *100*, 874 – 875.

[170] Tam, E. C. Y.; Maynard, N. A.; Apperley, D. C.; Smith, J. D.; Coles, M. P.; Fulton, J. R. *Inorg. Chem.*, **2012**, *51*, 9403 – 9415.

[171] Berger, S.; Braun, S.; Kalinowski, H.-O. *NMR SPECTROSCOPY OF THE NON-METALLIC ELEMENTS*. JOHN WILEY & SONS (Chichester.New York.Weinheim.Brisbane.Singapore.Toronto), 1997.

[172] Jouaiti, A.; Geoffroy, M.; Bemardinelli, G. *Tetrahedron Lett.*, **1992**, *33*(35), 5071–5074.

[173] Macdonald, C. L. B.; Bandyopadhyay, R.; Cooper, B. F. T.; Friedl, W. W.; Rossini, A. J.; Schurko, R. W.; Eichhorn, H.; Herber, R. H. *J. Am. Chem. Soc.*, **2012**, *134*, 4332–4345.

[174] Allspach, T.; Regitz, M. *PAPERS*, **1986**, pp 31–36.

[175] Blessing, R. H. *Acta Crystallogr.*, **1995**, *A51*, 33 – 38.

[176] Sheldrick, G. M. *SADABS Version 2.10 Siemens Area Detector Correction*. Universitaet Goettingen, Germany, 2003.

[177] Sheldrick, G. M. *SHELXTL, Version 6.1*. Bruker AXS, Inc., , Madison, WI, 2002.

[178] Sheldrick, G. M. *SHELXS97 and SHELXL97*. Universitaet Goettingen, Goettingen, Germany, 2002.

[179] Spek, A. L. *J. Appl. Crystallogr.*, **2003**, *36*, 7 – 13.